UNITED STATES
DEPARTMENT OF THE INTERIOR
J. A. Krug, Secretary

BUREAU OF RECLAMATION
Michael W. Straus, Commissioner
Walker R. Young, Chief Engineer

BOULDER CANYON PROJECT
FINAL REPORTS

PART VI—HYDRAULIC INVESTIGATIONS

Bulletin 3

STUDIES OF CRESTS FOR OVERFALL DAMS

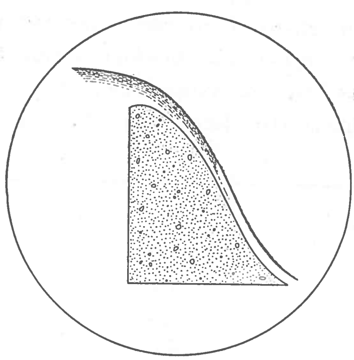

DENVER, COLORADO
1948

This bulletin is one of a series prepared to record the history of the Boulder Canyon Project, the results of technical studies and experimental investigations, and the more unusual features of design and construction. A list of the bulletins available and tentatively proposed for publication is given at the back of this report.

By joint resolution approved by the President April 30, 1947, the United States Congress changed the name of the dam theretofore known as *Boulder* Dam to *Hoover* Dam. This bulletin was too near completion on that date to permit making the appropriate changes in the drawings.

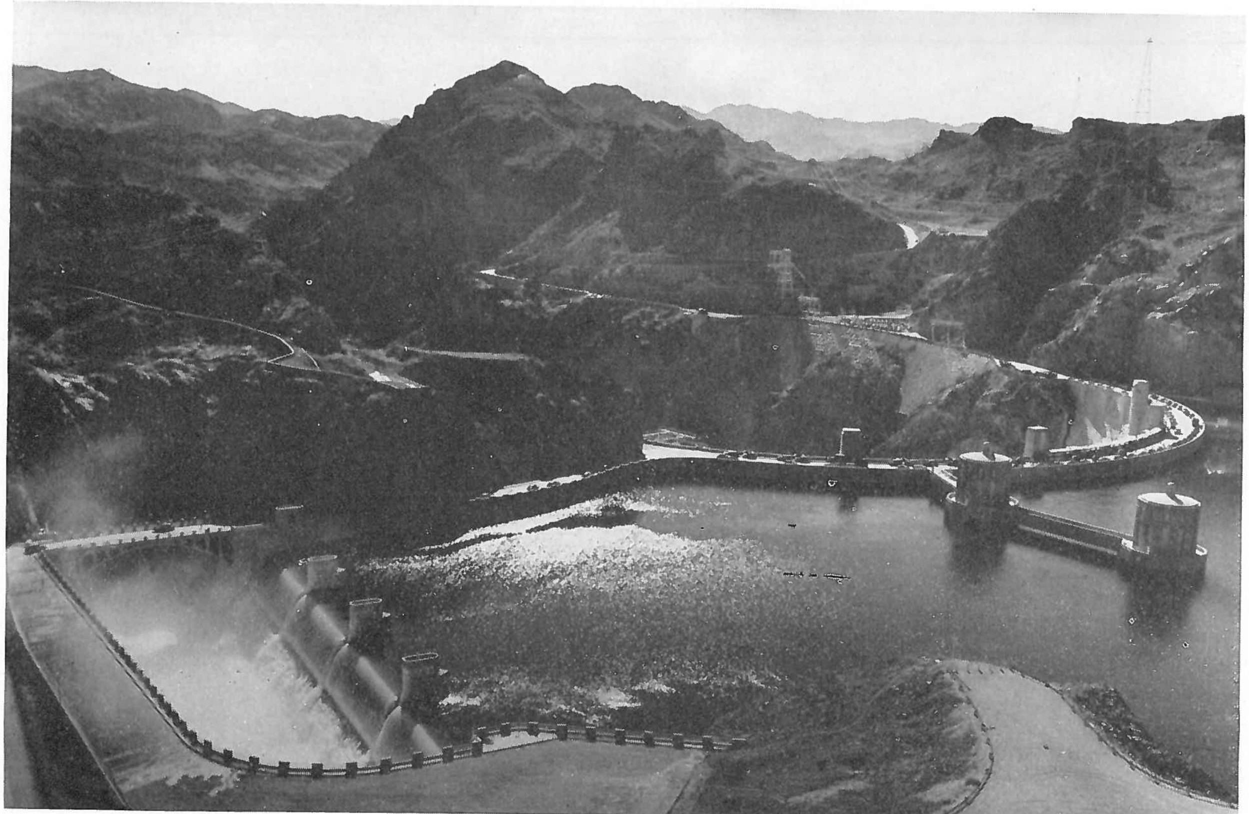

HOOVER DAM WITH ARIZONA SPILLWAY IN OPERATION.

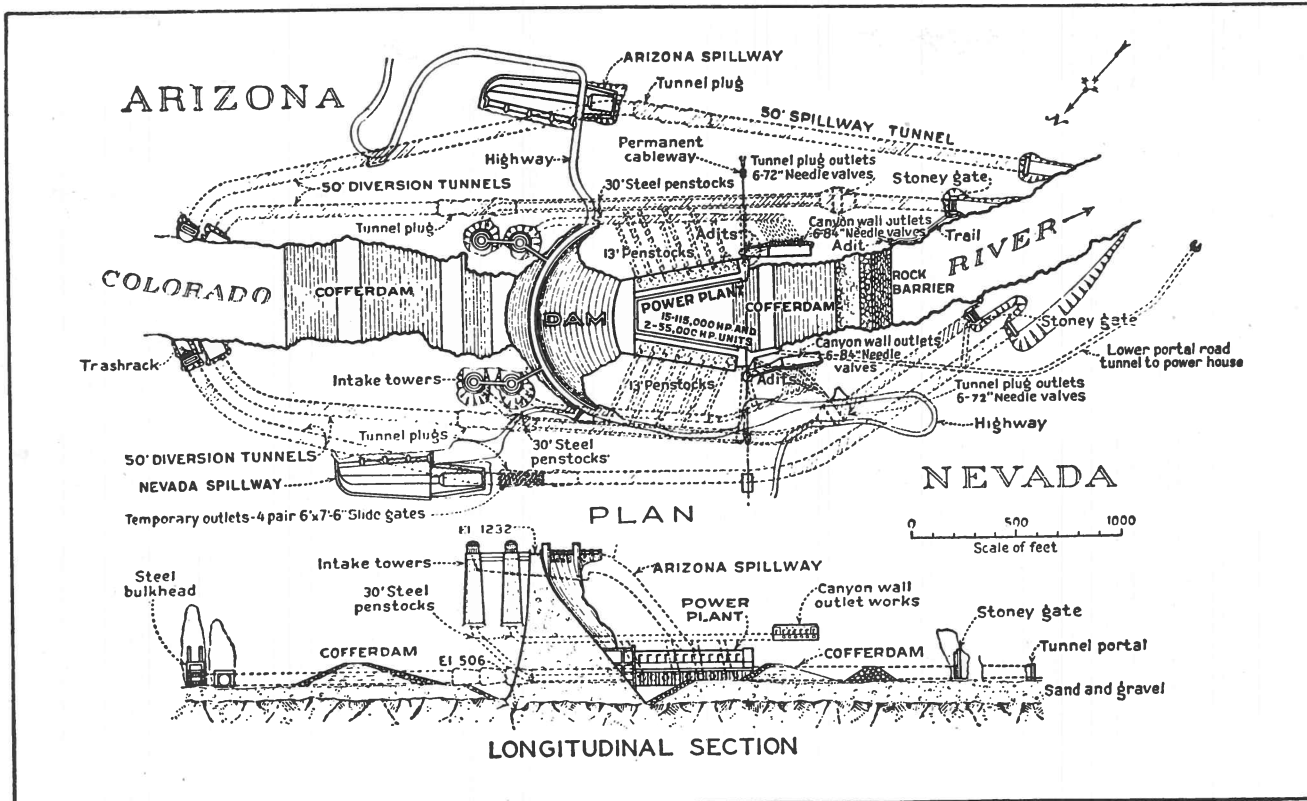

HOOVER DAM AND APPURTENANT WORKS.

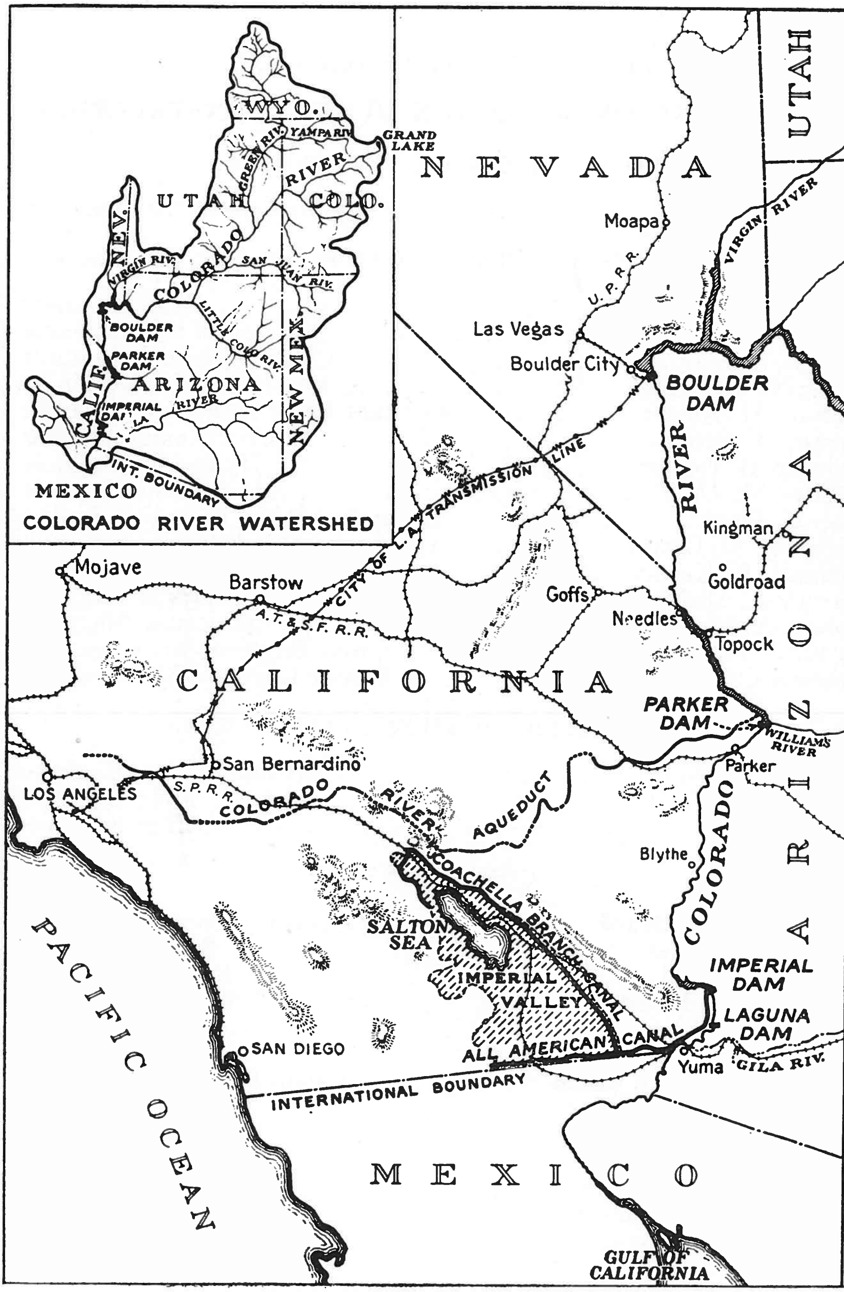

BOULDER CANYON PROJECT—LOCATION MAP.

BOULDER CANYON PROJECT

ENGINEERING ORGANIZATION DURING CONSTRUCTION

ADMINISTRATIVE OFFICE, WASHINGTON, D. C.

Elwood Mead*---------------------Commissioner of Reclamation

ENGINEERING AND EXECUTIVE OFFICE, DENVER, COLORADO

Raymond F. Walter*------------------------------Chief Engineer
Sinclair O. Harper----------------------Assistant Chief Engineer
John L. Savage------------------------Chief Designing Engineer
Leslie N. McClellan--------------------Chief Electrical Engineer
William H. Nalder-------------Assistant Chief Designing Engineer
Byram W. Steele---------------------------Civil Engineer-Dams
Erdman B. Debler---------------------------Hydraulic Engineer
Charles M. Day*-------------------------Mechanical Engineer
Ivan E. Houk-------------------Senior Engineer-Technical Studies
Harry R. McBirney-----------------------Civil Engineer-Canals
Kenneth B. Keener-----------------Assistant Civil Engineer-Dams
Harvey F. McPhail-------------------------Electrical Engineer
Robert A. Monroe--------------------------Structural Engineer
Porter J. Preston------------------Senior Engineer-Investigations
Howard C. Stetson-----------------Senior Engineer-Specifications

PROJECT OFFICE, BOULDER CITY, NEVADA

Walker R. Young--------------------------Construction Engineer
Ralph Lowry-------------------------------------Field Engineer
John C. Page-----------------------------------Office Engineer

CONSULTANTS

Colorado River Board---------------William L. Sibert,* Chairman
Charles P. Berkey--------------------------------Warren J. Mead
Daniel W. Mead-------------------------------Robert Ridgway*
Boulder Dam Board-----------------Andrew J. Wiley,* Chairman
William F. Durand------------------------------Arthur P. Davis*
David C. Henny*---------------------------------Louis C. Hill*
Concrete Research Board--------------Phaon H. Bates, Chairman
Franklin R. McMillan--------------------------Raymond E. Davis
Herbert J. Gilkey-------------------------------William K. Hatt
Special Consultants:
Harald M. Westergaard------------------------------Mechanics
Frederick L. Ransome*----------------------------------Geology
Gordon B. Kaufmann----------------------Architectural Features

PRINCIPAL CONTRACTORS

General Contractors-------------Six Companies, Inc., San Francisco
Penstock & Outlet Pipe-----The Babcock & Wilcox Co., New York

*Deceased.

FOREWORD

Colorado River, originating in the melting snows of the Wyoming and Colorado Rockies and augmented by rapid run-off from spasmodic rains and cloudbursts over a vast arid region, has menaced life and property in its descent to the Gulf of California since the days of the first covered wagon.

With increased population along the lower reaches of the river the problem of controlling the Colorado became more important. During recent years millions of dollars have been spent in mitigating the evils of silt deposition and in protecting the highly cultivated Imperial Valley lands from annual threats of inundation.

The need for a comprehensive plan of development to check the ravages of Colorado River, to regulate its flow, and to utilize a part of its enormous energy led, first, to investigations by the Reclamation Service of all water storage possibilities; next, to the Colorado River Compact, a mutual agreement for the protection of the seven basin States; and, finally, to the adoption of the Boulder Canyon project, as the initial development.

The Boulder Canyon Project Act, approved December 21, 1928, authorized a total appropriation of $165,000,000 for the various features involved. These include Hoover Dam and appurtenant works, the power plant, the reservoir, and the All-American Canal System. The purposes of the project are: (1) Flood and silt control for protection of lands along the lower river; (2) improvement of navigation; (3) river regulation and storage of water for irrigation and municipal use; and (4) development of electric power for domestic and industrial purposes. The project is self-liquidating, largely through contracts for disposal of electrical energy. It was constructed and is being operated under the supervision of the Bureau of Reclamation, United States Department of the Interior.

Hoover Dam is located on the Nevada-Arizona boundary near Las Vegas, Nev., at a place where Colorado River has carved a deep gorge between towering rock cliffs, known as Black Canyon. The dam is a concrete arched-gravity structure with a maximum height of 726 feet above foundation rock, a maximum base thickness of 660 feet, and a crest length of 1,244 feet. The dam and appurtenant works contain 4,400,000 cubic yards of concrete, of which 3,250,000 cubic yards were required in the dam.

During construction the river was diverted through four 50-foot diameter, concrete-lined tunnels, two on each side of the river. These tunnels were subsequently plugged near the upstream ends. The spillways, each of 200,000 second-feet capacity, are connected through inclined shafts to the two outer tunnels. A 30-foot diameter steel power penstock is installed in each of the inner tunnels. Discharge from the reservoir is controlled by cylinder gates in four intake towers, founded on the canyon walls near the upstream face of the dam. Four 30-foot steel penstocks, connected to the bases of the intake towers, conduct water to the power plant and to the outlet valves for release of flood, irrigation, and domestic water supply when the power plant discharge is insufficient for such purposes. The reservoir above the dam is 115 miles long and has a capacity of 30,500,000 acre-feet, the equivalent of 2 years' normal river flow.

The power plant is in a U-shaped, reinforced-concrete structure over 200 feet high and 1,500 feet long, located immediately downstream from the dam. The plant is designed for an ultimate installation of fifteen 115,000- and two 55,000-horsepower units, making a total installed capacity of 1,835,000 horsepower.

The All-American Canal, located near the Mexican border, will carry water to irrigate lands in the Imperial and Coachella Valleys. The canal proper, with a diversion capacity of 15,000 second-feet, is the largest ever constructed for irrigation purposes in America.

The entire Boulder Canyon project is characterized by the extraordinary. The height and base thickness of the dam, the size of the power units, the dimensions of the fusion-welded, plate-steel pipes, the novel system of artificially cooling the concrete, the speed and coordination of construction, and other major features of the project are without precedent. The magnitude of the undertaking introduced many new problems and intensified many usual ones, requiring investigations of an extensive and diversified character to insure structures representing the utmost in efficiency, safety, and economy of construction and operation.

The major credit for the conception of the project and the initiation of investigations leading to its adoption must be given to the late Arthur P. Davis, former Director of the Reclamation Service. Dr. Elwood Mead, Commissioner of Reclamation during the greater part of the construction period, passed away January 26, 1936, 4 months after the dedication of Hoover Dam. In commemoration of his untiring services on the Boulder Canyon project, the reservoir created by the construction of the dam has been officially named Lake Mead.

CONTENTS

CHAPTER IV—WEIRS SLOPING DOWNSTREAM

ANALYSIS OF EXPERIMENTAL RESULTS

APPLICATION OF EXPERIMENTAL RESULTS

CHAPTER V—WEIRS WITH UPSTREAM OVERHANG AND WEIRS WITH UPSTREAM OFFSETS AND RISERS

ANALYSIS OF EXPERIMENTAL RESULTS

APPLICATION OF EXPERIMENTAL RESULTS

CHAPTER VI—VERIFICATION OF EXPERIMENTAL DATA

PRESSURES ON DOWNSTREAM FACE OF OVERFLOW SECTIONS AND DISCHARGE COEFFICIENTS

CHAPTER VII—SUBMERGED FLOW STUDIES

DECREASE IN COEFFICIENT OF DISCHARGE PRODUCED BY SUBMERGED FLOW

CHAPTER VIII—OVERFLOW SECTIONS FOR HOOVER DAM SPILLWAYS

ANALYSIS OF DISCHARGE COEFFICIENTS

BIBLIOGRAPHY

LIST OF FIGURES

LIST OF TABLES

CHAPTER I—INTRODUCTION AND GENERAL DESCRIPTION OF LABORATORIES

INTRODUCTION

1. Scope of Bulletin.—Inasmuch as the Hoover Dam structures were of far greater magnitude than similar structures previously built, thorough studies were necessary to insure reliable designs. One of the more important of these studies was concentrated on the side-channel spillways, which were of unprecedented size for this type, involving velocities of approximately 175 feet per second. Bulletin 1 part VI, of this series contains the results of the majority of hydraulic model tests made on the Hoover Dam spillways. This bulletin is actually a sequel to the former bulletin but is confined entirely to the overflow crest section.

In the design of various preliminary forms of spillways proposed for Hoover Dam, many questions arose in connection with the overflow crest section concerning which reliable data were insufficient to permit dependable solutions. Therefore, a series of tests was instigated to provide more information on the design of the various overflow crest shapes proposed for the Hoover Dam spillways. As this field of study was extremely broad, only a very few of the experiments were completed previous to the actual construction of the spillways. The subject, however, was of such universal interest to dam designers that permission was obtained to continue this work during slack periods. As a result, the final program included a much broader and more thorough study than was originally anticipated.

Included in this bulletin, in addition to the results obtained experimentally by the Bureau of Reclamation, are references to all other available information on the subject. The combined information is now sufficient for design of the most common overflow sections. An attempt has been made to present this information from a practical standpoint for the use of designers.

With the trend in recent years toward higher dams and greater depths of flow over flood spillway crests, the importance of providing the correct profile has been materially increased. It has been the accepted practice for many years to design the crest of an overfall dam with the assumption that the space beneath the jet from a sharp-crested weir is filled with building material used in the dam. Despite all the studies previously made on the characteristics of flow over a weir, the undersurface of the nappe, being difficult to observe, has received a relatively small amount of attention.

A deficiency of section at any point under the nappe will result in the formation of a subatmospheric pressure between the downstream face of the dam and the nappe of water. With the formation of this vacuum, three undesirable conditions can develop:

1. The resultant force on the spillway section may be increased, due to the reduction of back pressure, which may detract from the stability of the dam against overturning and sliding.
2. The instability of the subatmospheric pressure, with its intermittent pressure change, can cause cavitation and localized disintegration of the boundary, known as pitting.
3. The intermittency of the subatmospheric pressure caused by the unstable condition prevailing beneath the flow sheet can cause a state of vibration in the dam. While the amplitude of this vibration may be exceedingly small, the accumulation of forces within the dam can produce secondary forces, particularly if the natural frequency of the structure bears a particular relation to that of the vibration of the nappe. This event is usually accompanied by undesirable rumblings and may even give rise to a movement resembling an earthquake in the proximity of the structure.

The under surface of the nappe as it leaves a weir crest rises slightly, gradually becomes horizontal, and finally falls, following a path approximating a parabola. To the uninitiated, the rise in this curve of travel is insignificant and scarely noticeable, but it constitutes an extremely important phase of the fundamentals of the contraction of a jet of flow over a sharp-edged control. While this shape has been the subject of considerable study in the past, the results in most cases have been based either entirely on theory or on rather meager experimental data.

2. History of Previous Experimental Work.—The first and most extensive studies of nappe shapes were those of Bazin,[1] made in 1886–88, in which he reduced his observations to unit head and constructed a base curve representing the results of his experiments. In the present studies on this subject, Bazin's results have been used for comparative purposes.

The term "nappe" as applied to the sheet of water flowing over a weir apparently originated with Bazin. In the translation of his works from the French to English, the translator's comment on the use of the word "nappe" is:

[1] Bazin, M., Recent Experiments on the Flow of Water Over Weirs, Annals des Ponts et Chaussées, October 1888 (translated by Arthur Marichal and John C. Trautwine, Jr., and published in the Proceedings of the Engineers' Club of Philadelphia, Vol. VII, No. 5, 1890, p. 259 and Vol. IX, No. 3, 1892, p. 231). Quotations reprinted by permission.

For want of a convenient English equivalent, we shall designate this sheet by its very appropriate French name, the nappe, a name applied primarily to a tablecloth, the form of which, as it passes from a horizontal to a vertical plane in passing over the edge of the table, is well imitated by the sheet of water passing over the weir.

Bazin, in discussing the subject, states:

The upper suface of the nappe has already been studied by certain experimenters, but the under surface, while less easy to observe, is perhaps of greater interest from a theoretical standpoint; for its form shows accurately the contraction at the crest. In forming this contraction, the under side of the nappe leaves the crest at a certain angle, rising at first, then becoming horizontal, and finally falling. This upward curve of the under side of the nappe, scarcely noticed until now, constitutes, nevertheless, one of the fundamental data of the phenomenon, and M. Boussinesq[2] has made it the basis of a new theory of the flow over weirs.

So far as is known, the first attempt recorded in American literature to develop the shape of an overfall dam to fit the overflowing sheet was that of Muller[3] in 1908. He attempted to extend a curve from the upper section of the lower nappe through Bazin's data. His expression for the curve shown in figure 1–A, in the terminology of this treatise, is

$$x^2-2.3\ h_s y=0 \tag{1}$$

for the thread of mean velocity, with the origin of coordinates at approximately 0.35 h_s above and 0.09 h_s downstream from the theoretical weir crest. He measured downward one-third the thickness of the nappe, normal to the thread of mean velocity, to locate the curve of the lower surface. Parker[4] reproduced Muller's curve and demonstrated that it does not fit well with Bazin's curve at the upper section. He attributed this difference to the fact that Bazin's curves were obtained with sharp-edged notches, under heads of 1.7 feet or less, and Muller applied them to thick notches, under heads of 5 or 10 feet.

Morrison and Brodie[5] offer the parabolic equation

$$x^2=1.80\ h_0 y \tag{2}$$

for the lower surface of the nappe, where h_0 is the head measured from the highest point of the lower nappe surface, see figure 1–A. The origin of the coordinates in this case is at the highest point of the lower nappe surface. As a factor of safety for dam design, they recommend that the equation be increased to

$$x^2=2.55\ h_0 y \tag{3}$$

[2] Boussinesq, M., Computes rendus de l'Académie des Sciences, July 4, 1887.

[3] Muller, R., Development of Practical Type of Concrete Spillway Dam, Eng. Rec., Vol. 58, October 24, 1908, p. 461.

[4] Parker, P. A. M., Form of the Downstream Face of Overflow Dams, The Control of Water, 1916, p. 399, D. Van Nostrand Co., New York.

[5] Morrison. E., and Brodie, O. L., Masonry Dam Design, 2nd, ed., 1916, pp. 120–133.

The equation $x^2=1.80\, h_0 y$ was used without any increase for factor of safety by the Miami Conservancy District in the design of their spillways. It can be shown that actually the lower nappe surface can be only approximately represented by a parabola.

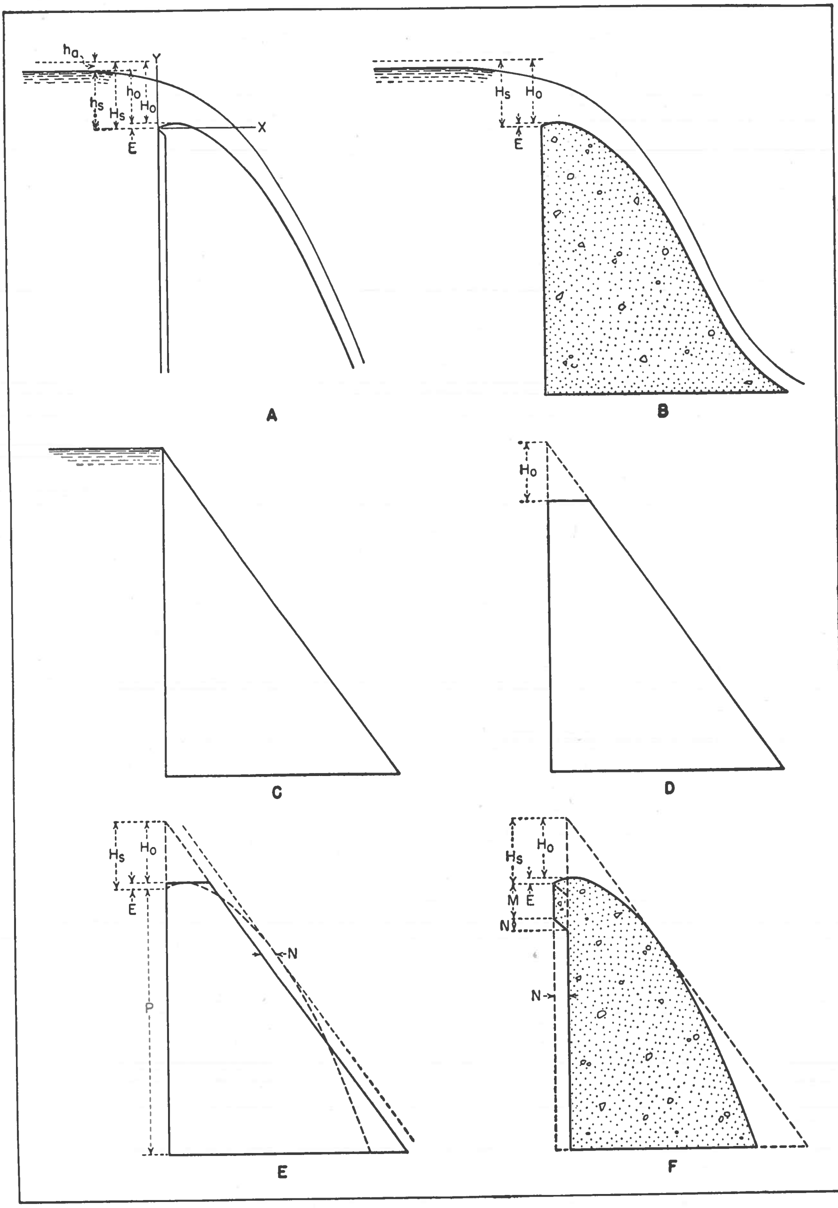

FIGURE 1.—DEVELOPMENT OF OGEE SECTION.

Woodward,[6] in the Miami Conservatory District report, says:

> The profiles of the ogee weirs were designed to conform approximately to the profile of the lower nappe of the overflow from a sharp-crested weir as determined by Bazin's experiments. The profiles as designed agree approximately in their upper portions with the formula $x^2=1.8\ H_0 y$, where x and y are horizontal and vertical coordinates measured from the crest of the (ogee) weir, * * *, and H_0 is the maximum effective head on the weir, including that due to velocity of approach (see figure 1–B). The discharge over the spillway weirs per foot of length was computed by the formula $q=3.8H_0^{3/2}$.

Creager [7] proposes an equation

$$x^2=2.732\ y \tag{4}$$

for the line of average velocity in the nappe, with the origin of coordinates 0.063 unit upstream from the face of the weir and 0.261 unit above the highest point of the lower nappe surface. Scimemi [8] shows that the equation given by Creager locates a line which will fall below even the lower surface if it is continued sufficiently far. This discrepancy, however, is less than the increase of cross section recommended by Creager as a factor of safety

Scimemi established an equation for a portion of the lower surface beyond $x=0.50$, which is

$$y=\frac{(x-0.10)^2}{1.55}+0.062x-0.186 \tag{5}$$

in which the origin of the coordinates is at the sharp crest of the weir. Unfortunately, this equation does not apply to the most important portion of the overflow section, namely, the portion between the spring point and the high point of the trajectory.

An empirical equation for the lower surface of the nappe, derived by R. R. Randolph, of the War Department, is

$$y=0.523H^{-0.882}x^{1.822} \tag{6}$$

with the origin of the coordinates at the highest point of the lower surface. A similar equation, with the same origin of coordinates, derived by H. L. Davis, of the Bureau of Reclamation, is

$$y=0.485H^{-0.875}x^{1.875} \tag{7}$$

Lamb [9] derived a set of parametric equations for the shape of the surface of a jet issuing from a sharp-edged orifice. With some modifications and the inclusion of the effect of gravity, equations might be derived to

---

[6] Woodward, S. M., Hydraulics of the Miami Flood Control Project, Technical Reports, Part VII, p. 223. Quotation reprinted by permission.

[7] Creager, W. P., Engineering for Masonry Dams, 1st ed., 1917, pp. 105–110.

[8] Scimemi, Ing. Prof. Ettore, Sulla forma delle vene tracimanti (On the Form of the Crest Streams), L'Energia Elettrica, April 1930.

[9] Lamb, H., Hydrodynamics, 5th ed., 1924, p. 95.

fit the observed data. With the additional experimental data now available, the development of such equations offers an opportunity for research to some engineer or mathematician.

In recent years it has been customary in the design of the overflow section of a spillway to use a vertical upstream face. The dam cross section was designed to fit exactly or to be slightly larger than the space beneath the lower nappe of a sharp-crested weir for a flow equal to the maximum discharge, as illustrated in figures 1–A and 1–B. The shape was, in most instances, computed in accordance with Bazin's classic experiments, which covered a variety of weirs; but the data for any particular shape were meager.

Recently, large dams having other than plain vertical upstream faces have been built, for which the data of Bazin are not applicable. In one form, the crest overhangs the upstream face of the dam, see figure 1–F. This type has been evolved as a result of its saving of material. The theoretical form of stable nonoverflow dam is a triangle with the water surface at the apex, as shown in figure 1–C. For an overflow dam, the corresponding shape would be approximately the trapezoid formed by removing the apex from the upper part of the triangle down to a distance equal to the design head on the crest, H_0, as shown in figure 1–D. With an overflow having a total head of H_0, however, the downstream side of the trapezoid does not have sufficient width, and the nappe would spring free of the dam, as shown in figure 1–E, and fall along a curve extending a maximum distance N outside the trapezoid. To insure freedom from undesirable vacuum effects, the space between the nappe and the dam should be filled with concrete. Concrete placed in this location, however, is not in position to resist most efficiently overturning of the dam. By moving the point corresponding to the weir crest upstream a distance N, the nappe can be brought tangent to the downstream face of the trapezoid. This results in a horizontal offset in the upper portion of the spillway section equal to the distance N. The upstream edge is commonly connected to the upstream face of the dam, either by a single inclined surface or by a short section of vertical face below which is an inclined face. The first form, outlined by the heavy broken diagonal line in figure I–F, was used on the Conowingo Dam on the Susquehanna River and the Rock Canyon barrier on the Arkansas River. The second form, shown by the solid lines in figure 1–F, was used for the Wilson Dam on the Tennessee River, the Safe Harbor Dam on the Susquehanna River, and the Bull Run Dam on the Bull Run River in Oregon. In this form, the concrete required under the nappe is placed where it is most effective in resisting overturning, which therefore results in a more economical dam. The projecting upstream portion of the dam usually alters the shape of the nappe and causes it to no longer follow the form which would result from a weir with a vertical upstream face.

The determination of the nappe shapes and the coefficients of discharge for such overhanging crests was one phase of the extensive series of experiments instigated by the Bureau of Reclamation.

3. Extent of Present Experimental Program.—In the design of various preliminary forms of spillways considered for Hoover Dam, there were many questions in connection with overflow crest shapes on which data were insufficient to permit exact solutions. During the course of the design work, experimental data were collected which proved of value in the preparation of the later designs of the side-channel spillways and which should be helpful in preparing future designs, not only of side-channel spillways but also of other forms employing overfall sections.

The principal phases of spillway design considered in the experiments by the Bureau of Reclamation were as follows:

1. Determination of the shape of dam required to best fit the lower nappe of the overfalling stream for any practical condition of design. Tests were made on sharp-crested weirs representing dam sections with vertical upstream faces, with sloping upstream faces, and also with overhangs and offsets in the upstream face.
2. A study of the deviations of the nappe shape due to velocity of approach. Bazin covered a portion of this field, but his experiments were not extensive enough to completely analyze this effect.
3. Determination of the coefficients of discharge for dams with vertical, sloping, overhanging, and offset upstream faces.
4. Determination of the reduction of pressure which occurs on the upstream face of a dam due to the increase of velocity at the crest. This effect, while slight, decreases the overturning moment of the dam and is conducive to a small reduction in section or can be used as a factor of safety.
5. Determination of the discharge coefficients for models of different shaped crests with and without control gates. These studies were to include the effects of adjacent terrain, piers, and position of drum gates.
6. In the case of supplementary tests on models of actual designs, the pressures on the crest and on the drum gates were observed to provide information for the use of the design department in computing stresses in the structural members.

4. Record of Present Experimental Program.—The laboratory tests on the above program were initiated in the hydraulic laboratory of the Colorado Agricultural Experiment Station at Fort Collins in 1932 as a means of providing urgently needed material for the completion of the spillway designs for Hoover Dam. Because of the routine nature of the studies, they were subject to considerable interruption by other work. These demands prevented the complete analysis of the results at the time they were made. In the following years, as time and personnel became available, the material was analyzed completely. A thorough study led to the conclusion that a large part of the data was inconsistent and much of the remainder was too meager. The inconsistencies were traced to errors made in the laboratory procedure and to the fact that an attempt was made to cover a large field with insufficient data. The principal difficulties encountered can be charged to lack of experience in planning a comprehensive study of this type; lack of a definitely planned program; lack of experienced laboratory assistants in the test work; and the deficiency of time and personnel with which to analyze the material coincident with the actual measurements. Testing of this nature requires extreme care and expert coordination, which can be maintained only with the very best of laboratory personnel.

Accordingly, in 1936, authority was sought and received to repeat certain portions of the original test program in order to provide a complete record. This new program was conducted in the hydraulic laboratory of the Bureau of Reclamation in the Customhouse, Denver, Colorado. Cognizance was taken of the shortcomings of the original tests to avoid a repetition of the failures; thus the mistakes were not repeated in the new laboratory. In full appreciation of the difficulties previously encountered, the repetition of the tests was preceded by a careful plan of procedure. As each set of measurements was completed, an analysis was made before proceeding to the next step. In that way inconsistent or irrelevant material was eliminated immediately. If the results of a particular test were not consistent, the test was repeated.

GENERAL DESCRIPTION OF LABORATORIES

5. Colorado Agricultural Experiment Station Hydraulic Laboratory.—The original experiments conducted by the Bureau of Reclamation on overfall dam shapes were performed in 1932 in the hydraulic laboratory of the Colorado Agricultural Experiment Station, Fort Collins, Colo. Figure 2 shows a general plan of the laboratory and the supply reservoir. The experimental apparatus was installed in the weir box within the laboratory building. A plan and section of the experimental flume are shown in figure 3. The experiments were conducted on weirs 2 feet in length, this being the greatest length over which a considerable head could be maintained with the available water supply. The approach to the weir and the channel downstream from the weir were both 2 feet wide, so that side contractions were suppressed. The interior of the channel was faced with 1-inch, finished, tongue-and-groove lumber. It was approximately 16 feet

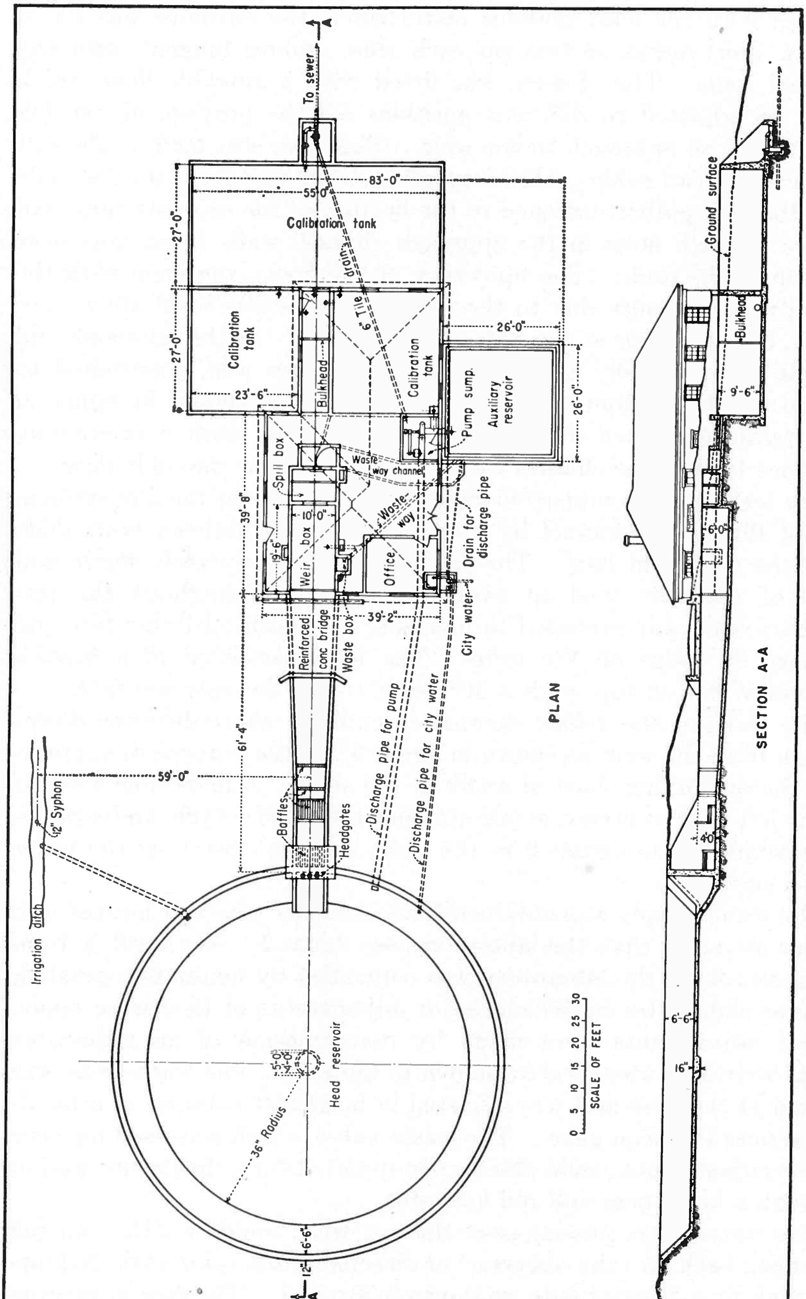

FIGURE 2.—HYDRAULIC LABORATORY AT COLORADO AGRICULTURAL EXPERIMENT STATION.

long and 7 feet deep. In order that the water might enter the 2-foot channel with the least possible disturbance, the entrance was flared with a short-raduis section on each side, ending tangent with the channel walls. The channel was fitted with a movable floor which could be adjusted to different positions for the purpose of varying the velocity of approach to the weir. This floor was held in place at each end by two cables, which extended downward from the movable floor through pulleys fastened to the bottom of the concrete tank and thence through holes in the approach channel walls to anchors near the top of the tank. The buoyancy of the floor, combined with the net upward pressure due to the difference in static head above and below, held the floor at the ends of taut cables. At the upstream end of this floating floor, a movable inclined ramp was constructed to extend to the bottom of the concrete tank, as shown in figure 3. This ramp, combined with the flaring side walls, made a converging entrance to the weir channel for all positions of the movable floor.

The test weir was supported on a vertical plate near the downstream end of the 2-foot channel by a splice plate and flathead bolts flush with the upstream face. The test weirs were accurately made and were of stainless steel to avoid corrosion. Throughout the test program, care was exercised to maintain a smooth upstream face and a sharp 90° edge on the weirs. The weirs consisted of a $\frac{1}{16}$-inch horizontal flat on top, with a 56° bevel to the downstream face.

The walls of the 2-foot channel extended a short distance downstream from the weir, as shown in figure 3, for the purpose of suppressing the overfalling sheet of water at the sides. A large hole was cut in the left wall to permit aeration under the lower nappe, and a plate-glass window was installed in the right wall for observing the lower nappe surface.

The water supply was obtained from a storage reservoir located at a higher elevation than the laboratory, see figure 2. The outflow from the reservoir to the laboratory was controlled by manually operated, circular slide gates by which major adjustments of flow were made. Minor adjustments were made by manipulation of an adjustable waste weir or a waste valve, shown in figure 3. The waste weir was hinged at the base and was adjusted in height by rotation of a handwheel near the head gage. The waste valve, which was used for very minor adjustments, could also be manipulated from the gaging station through a bevel gear and rod assembly.

The water, after passing over the test weir, could be either wasted (pumped back into the reservoir) or directed into a volumetric measuring tank by a diverter gate, as shown in figure 3. The flow measuring operation usually took only a small amount of time as compared with that required for the other measurements; therefore, the water flowed into the waste tank during the larger portion of the time.

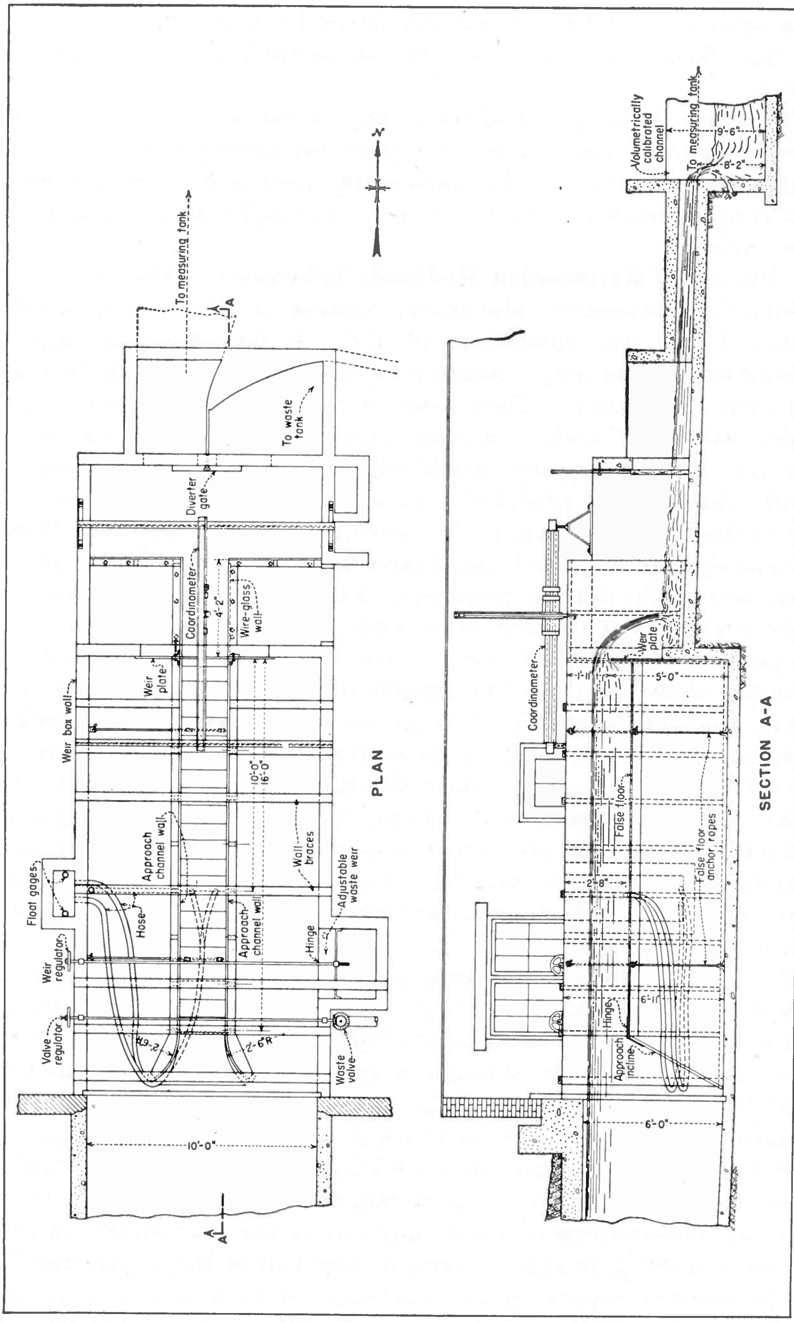

FIGURE 3.—WEIR-BOX INSTALLATION—COLORADO AGRICULTURAL EXPERIMENT STATION.

The head on the weir was measured by float or hook gages operating in an open well. The well was connected by heavy rubber hose to two taps flush with the surface of the movable floor, as shown in figure 3.

The shapes of the upper and lower nappe surfaces were measured with a coordinometer located above the weir, see figures 3, 4, and 5. A point was used to traverse the upper surface, see figure 6, while a hook, protruding through the sheet of water, was employed to traverse the lower surface.

6. Bureau of Reclamation Hydraulic Laboratory.—The Bureau of Reclamation hydraulic laboratory, located in the Customhouse, Denver, Colo., was completed in 1937. A repetition and also a continuation of the weir studies previously made were commenced soon after occupancy. These tests were made during lulls in the regular laboratory work. In other words, they were made at times when the laboratory pumps would otherwise have been idle; consequently the program extended over a period of some five years. A plan of the Denver laboratory is shown in figure 7. The weir flume was supplied by a 12-inch centrifugal pump with a capacity of 10 second-feet. The pump is powered by a 90-horsepower variable-speed slip-ring motor. A constant-level tank is used in conjunction with this pump to regulate the head on the line. A short distance from the outlet of the tank, the line branches into an 8-inch and a 12-inch pipe in which are located Venturi meters for measuring the discharge. Immediately downstream from the meters are hydraulically operated gate valves which are used for throttling the flow. This is the terminus of the permanent equipment. From this point temporary piping conducts the water to the various models. All bleeders, gages, and hydraulic and electric controls have been concentrated on one central board, see figure 8–A, for this particular portion of the laboratory system.

The equipment on the opposite s de of the laboratory consists of an 8-inch pump with a capacity of 5 second-feet and a 6-inch pump with a capacity of 2.5 second-feet, both driven at constant speeds. These pumps discharge through a bank of three Venturi meters installed in 4-, 6-, and 8-inch lines, as shown in figure 8-B. A 3-inch line also parallels this bank, in which a variable orifice meter can be employed to measure small discharges down to a few gallons of water per minute. The system is so arranged that, by means of three three-way motor-operated cocks, any one of the four meters can be connected directly to either pump, or any two of the meters can be used to measure separately the discharges of both pumps operating simultaneously. This system is very flexible, and all controls are centrally located on the gage board. The small buttons at the top

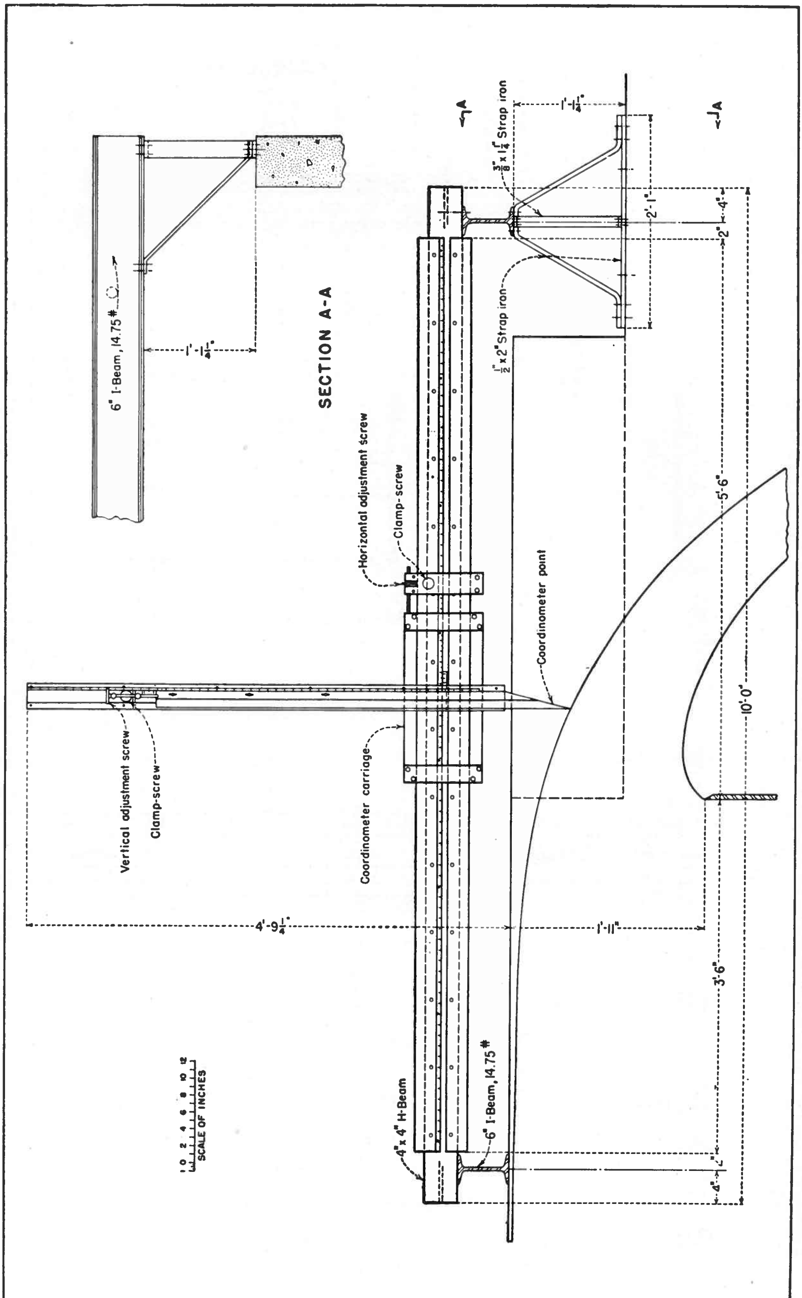

FIGURE 4.—ASSEMBLY OF UPPER NAPPE COORDINOMETER.

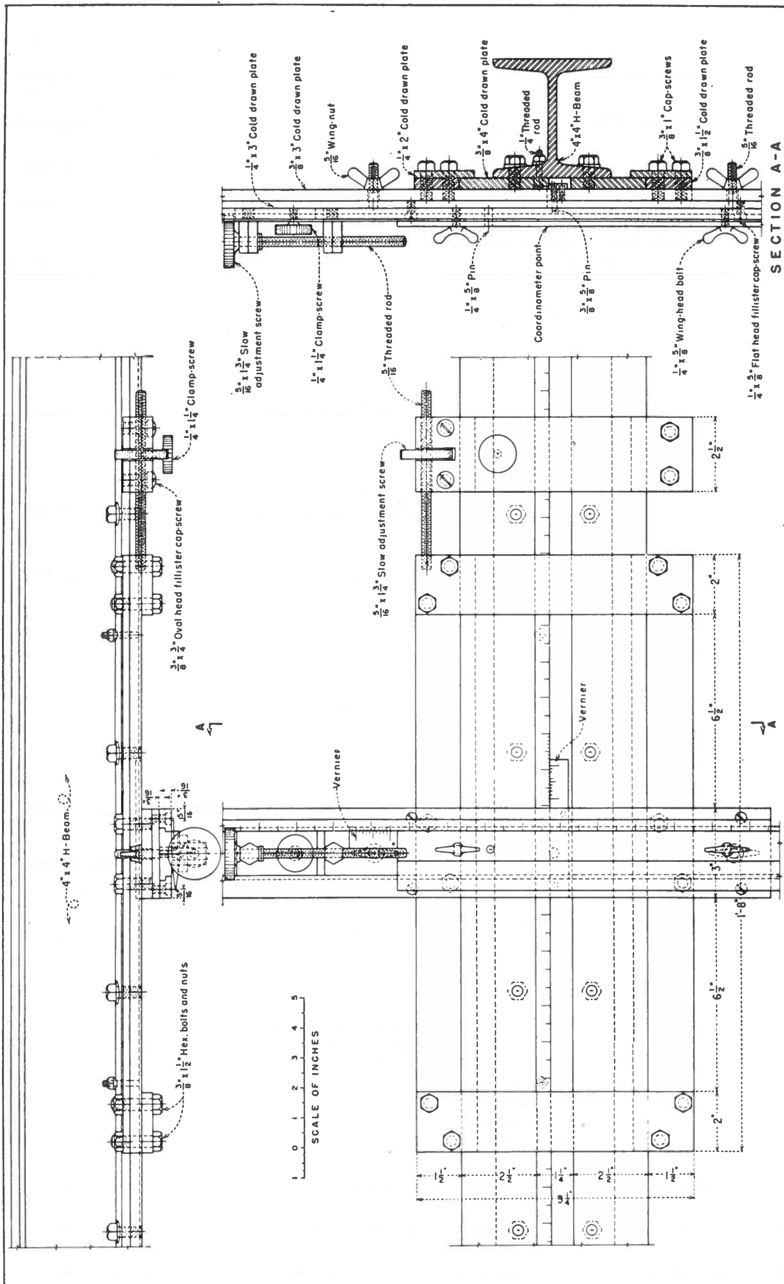

FIGURE 5.—DETAILS OF COORDINOMETER CARRIAGE.

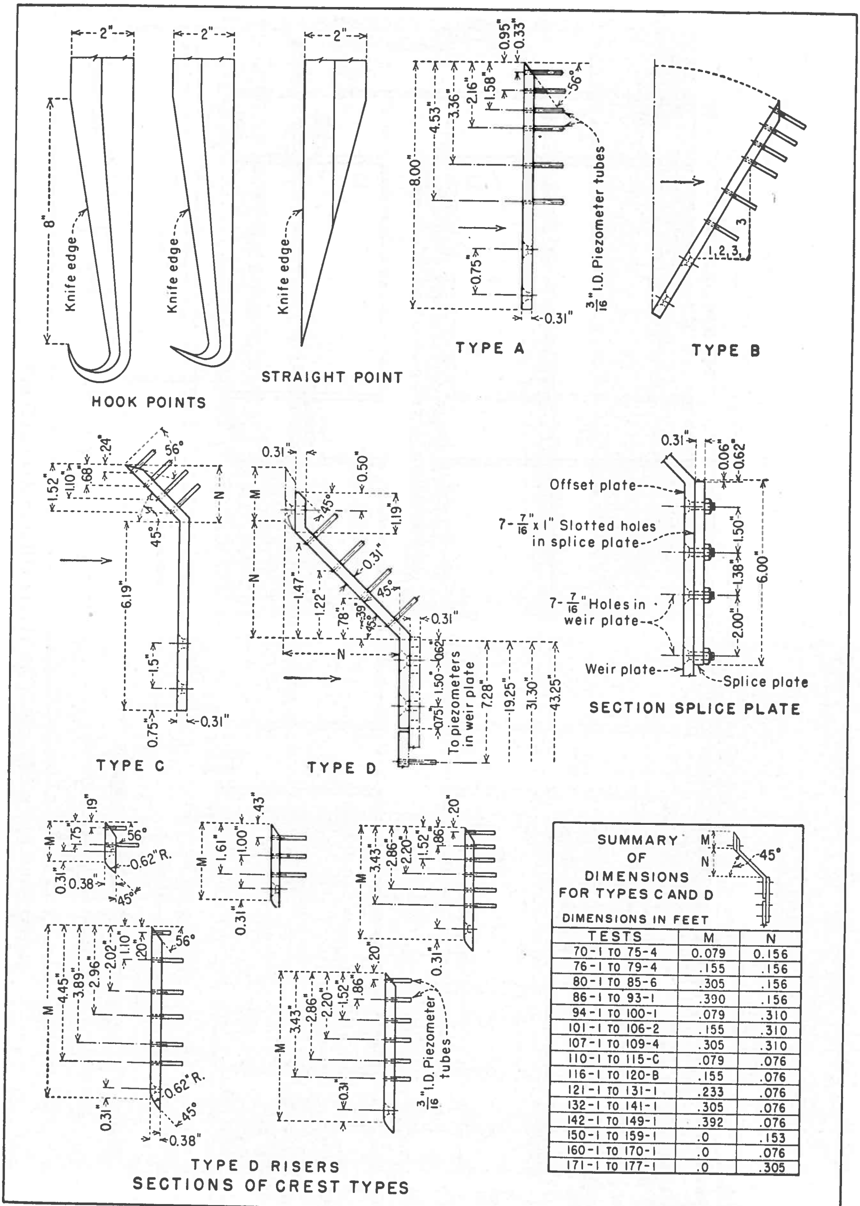

SUMMARY OF DIMENSIONS FOR TYPES C AND D

DIMENSIONS IN FEET

TESTS	M	N
70-1 TO 75-4	0.079	0.156
76-1 TO 79-4	.155	.156
80-1 TO 85-6	.305	.156
86-1 TO 93-1	.390	.156
94-1 TO 100-1	.079	.310
101-1 TO 106-2	.155	.310
107-1 TO 109-4	.305	.310
110-1 TO 115-C	.079	.076
116-1 TO 120-B	.155	.076
121-1 TO 131-1	.233	.076
132-1 TO 141-1	.305	.076
142-1 TO 149-1	.392	.076
150-1 TO 159-1	.0	.153
160-1 TO 170-1	.0	.076
171-1 TO 177-1	.0	.305

FIGURE 6.—DETAILS OF WEIR PLATES AND UPPER COORDINOMETER POINTS.

of the board indicate the positions of the three three-way cocks. Another innovation which adds to the flexibility of this system is a series connection leading from the discharge side of the 12-inch pump to the suction side of the 8-inch pump, see figure 7. This makes it possible to use the 8-inch pump as a booster whereby a head of approximately 200 feet can be developed.

A third and smaller system is located in the far end of the laboratory, see figure 7. This consists of an 8-inch vertical pump with a capacity of 3 second-feet, which discharges through either a 1.5-inch flow nozzle or a 6.5-inch modified Venturi meter. All controls are located in close proximity to a third gage board similar to the other two. Each meter in the laboratory is connected directly to a separate mercury manometer gage. By this arrangement, leakage from valves, cocks, and bypasses is eliminated, thus adding to the reliability of the system. It can also be noted from figure 7 that each of the three supply systems are interconnected. In other words, any one of the four pumps can supply water to any point in the laboratory. These interconnected lines also lead to the laboratory calibration tank, see figures 7 and 9, by which all meters in the laboratory are calibrated and checked at definite intervals.

The volumetric calibration tank, shown in figure 9–A, has a capacity of approximately 400 cubic feet. The size was limited by the area of the laboratory reservoir, consisting of channels under the floor, see figure 7. This limitation resulted from the fact that withdrawing 400 cubic feet of water caused the water surface in the channels to drop approximately 0.3 foot. This in turn produced a slight change in flow because of a change in head. The limited size of the tank, however, is compensated for by a reliable and extremely accurate timing device. The source of the time signals is a pendulum clock equipped with a photoelectric cell. The signals are transmitted by wire to a chronometer located near the calibration tank, which, by means of a magnetic pen, registers a line on a roll of paper for each impulse or second. The chronometer is shown in figure 9–C. A synchronous motor and a set of gears move the paper at various speeds, depending on the accuracy desired. A second magnetic pen, energized from a mercury switch on the swing spout, records a dash on the paper at the beginning and the end of each run. The chronometer makes it possible to measure time within one-hundredth of a second. Incorporated in the chronometer is a magnetic counter which records full seconds of time. This can be cut in or out of the circuit at any time, thus making it necessary to use the pens only at the beginning and end of a run to record fractions of seconds. The swing spout on the volumetric tank is actuated by a pneumatic cylinder which can be moved at any desired constant rate of speed,

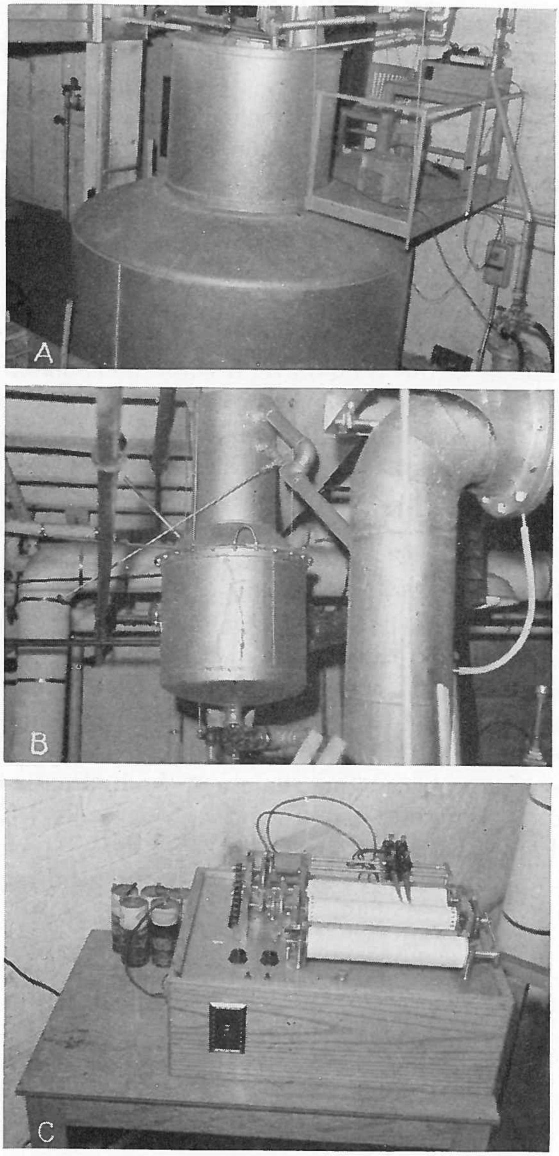

FIGURE 9.—LABORATORY CALIBRATION EQUIPMENT.

thus adding to the accuracy of the timing scheme. If greater accuracy is desired, the chronometer can be replaced by an oscillograph which will record time to one-thousandth of a second.

A small pipette tank, shown in figure 9–B, was used to calibrate the larger volumetric tank. The pipette tank consists of two compartments, one having a volume of about 1.5 cubic feet and the other a volume of approximately 7 cubic feet. Calibration of the volumetric tank is accomplished by repeatedly filling the pipette tank with water and emptying it into the larger one. The pipette tank in turn can be removed from the position shown and calibrated by weight, with the aid of a sensitive 500-pound scale. The net weight of the water is about 450 pounds and the tare 300 pounds.

7. Personnel.—The hydraulic research program was begun under the general supervision of E. W. Lane and completed under the direction of J. E. Warnock. J. N. Bradley planned the Denver laboratory program, directed the execution of the testing, and prepared this bulletin.

As the material in this bulletin represents the cooperative efforts of many individuals who assisted in the design, construction, and operation of the equipment, and in the analysis of the data, it is desired to acknowledge the assistance of W. M. Borland, W. H. Price, J. W. Ball, C. W. Thomas, D. J. Hebert, H. G. Dewey, Jr., T. G. Owen, W. J. Colson, D. C. Weed, D. M. Lancaster, R. A. Goodpasture, R. C. Besel, F. Locher, F. C. Lowe, R. R. Pomeroy, J. L. Lindsey, K. B. Florance, J A. Langendorf, Keith Jones, R. C. Edge, W. O. Parker, A. D. Wilson, F. L. Kelley, H. F. Doud, and H. A. Merz. Special credit is due A. N. Smith, who conducted the majority of the tests, compiled the data, and assisted in analyzing the results.

It is further desired to acknowledge the cooperation of the faculty of the Colorado State College and the staff of the Bureau of Agricultural Engineering in permitting the use of the hydraulic laboratory of the Colorado Agricultural Experiment Station in Fort Collins, where a portion of the testing was performed.

The text was edited by E. H. Larson and the drawings adapted to publication by R. H. Williams.

CHAPTER II—EXPERIMENTAL EQUIPMENT AND TEST PROCEDURE

EXPERIMENTAL EQUIPMENT

8. Experimental Flume.—The arrangement of the apparatus used in repeating the nappe-shape measurements in the Denver laboratory was similar to that used in the original experiments, except for refinements. A channel 33 feet long by 9.4 feet deep by 2 feet wide was constructed for these experiments, see figure 10. Water was supplied by the 12-inch pump, measured through the 8-inch or 12-inch Venturi meter, and discharged into the upper end of the 2-foot channel through a 12-inch pipe fitted at the end with a gradually expanding cone. Gravel baffles at the upstream end distributed the flow uniformly across the channel. The head on the weir was measured by a hook gage operating in an open well which was connected by a rubber hose to a piezometer flush with the top surface of the movable floor.

The movable floor was similar to that of the Fort Collins layout but different in that it was covered with sheet metal and sealed to the side walls and weir plate by strips of flexible packing rubber. This prevented all inflow except for the main stream. The floor in the original experiments consisted of tongue-and-groove lumber laid normal to the flow. The corners of these boards eventually warped, offering considerable resistance to the flow. In addition, no seals were provided between the walls and floor or weir and floor, with the result that considerable inflow occurred, especially up the face of the weir plate, due to the static pressure under the floor being greater than that above it. This latter was a source of error in the coefficients of discharge and in the nappe shapes obtained from the Fort Collins data. The error was not a constant but increased as the floor was elevated.

9. Weir Shapes Tested.—The weir blades used in the Denver experiments were of stainless steel, machined at an angle of 50° to a knife edge, as shown in figure 6. The same blades had been used in the Fort Collins experiments, except that they had been machined with a 90° edge and a 1/16-inch horizontal flat on top. It was observed in the earlier tests that the lower nappe did not spring from the 90° upstream corner but had a tendency to cling to the flat top of the weir. The point at which the nappe sprung free of the weir was not constant but varied with flow conditions. The phenomenon is principally a

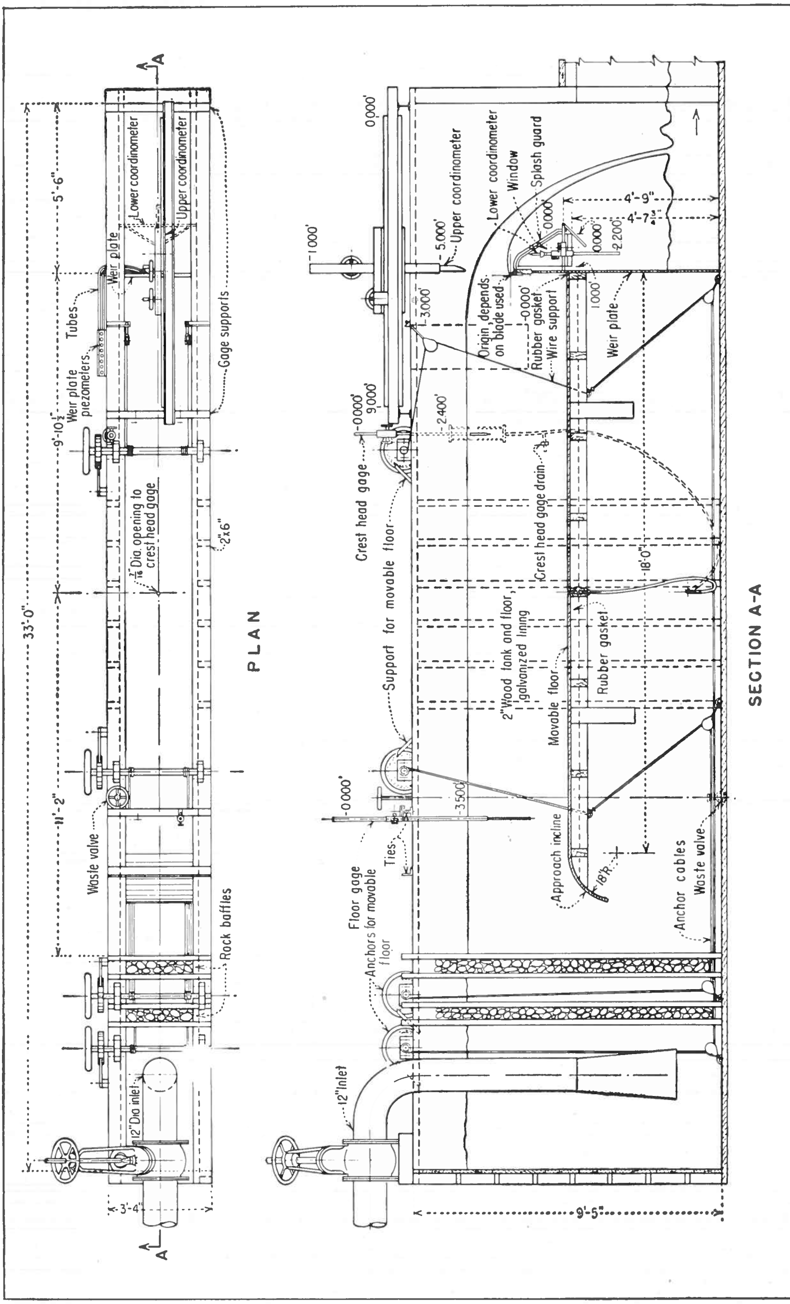

FIGURE 10.—PLAN AND SECTION OF EXPERIMENTAL FLUME.

surface-tension effect. Rouse and Reid,[10] at the Massachusetts Institute of Technology, had observed the same occurrence on a small weir that they had tested. The attempt made to eliminate this variable in the Denver experiments by grinding the weirs to a knife edge proved effective. Photographs of the vertical-face weir are shown in figure 11.

Figure 6 shows the various weir shapes tested. Type A represents a dam with vertical upstream face, and type B is applicable to a dam with sloping upstream face. Type C represents a dam with an overhang on the upstream face. Weirs of three sizes in type C were tested, all making an angle of 45 degrees with the vertical, as tabulated in figure 6. Type D is applicable to dams with a 45° offset on the upstream face. Three offsets were tested with five interchangeable riser heights, as shown in figure 6.

Piezometers, as shown in figure 6, were installed in all of the weir blades for the purpose of measuring pressures on the upstream face of the weir.

10. The Coordinometers.—The profiles of the nappe shapes were measured by specially constructed instruments known as coordinometers. The instrument by which the upper surface was measured is shown in detail in figures 4 and 5. It consisted essentially of a 4-inch horizontal H-beam, mounted over the weir channel parallel to the direction of flow, upon which was mounted an adjustable vertical bar having at its lower end a point to contact the water surface. The instrument was supported at its ends by two I-beams spanning the test channel normal to the direction of flow. The beams were made sufficiently heavy to support a live load of several hundred pounds without a measurable deflection. The carriage supporting the vertical beam was connected through a horizontal slow-motion screw to a clamp on the horizontal H-beam, by which arrangement fine adjustments of the horizontal position could be made. The vertical bar moved in a groove in the vertical beam and was fitted with a clamp, slow-motion screw, and vernier. Both horizontal and vertical scales could be read to 0.001 foot. The lower part of the vertical bar was constructed to accommodate points or hooks of different styles, such as shown in figure 6. The point was used to survey the upper nappe and the hooks were used to point-gage a downstream portion of the lower surface. In beginning the survey of the upper surface, the coordinometer carriage was set at a horizontal position, and the tip of the point was lowered until it touched the water surface. The horizontal and vertical readings were recorded, the carriage moved to a new position, and the process repeated until the entire upper nappe was traversed.

[10] Rouse, Hunter, and Lincoln Reid, Model Research on Spillway Crests, Civ. Eng., Vol. 5, January 1935, p. 10.

angles and could be placed in position either sloping toward or away from the weir. A neon glow lamp was connected by a single insulated wire to a setscrew on the point, which was electrically insulated from its mounting. By connecting the neon glow lamp to the ungrounded side of a 110-volt electrical circuit, the lamp was made to glow as the coordinometer point contacted the under side of the overflow sheet. This lamp was especially useful in traversing the lower nappe during fluctuations when the quantity of flow was large and the velocity of approach great. Since water tended to run down the point as it moved upward into contact with the water surface, a drip cup was placed at the base of the point, see figures 11 and 12, to prevent short-circuiting across the insulated mounting. It was found that the water discharging from this cup, if sufficiently steady, would cause a slight shock to the hand or arm of the operator; so a length of rubber hose was placed on the outlet from the cup to render the instrument harmless.

The under nappe was traversed in from three to five steps. Using a bent point in the lower coordinometer, with the slope of the point upstream, the under side of the jet was carefully surveyed from the crest of the weir to a random point near the vena contracta. The bent point was then replaced by the straight point, and observations were continued in a downstream direction to an arbitrary point where the nappe assumed a falling characteristic. The straight point was then replaced by a bent point with the slope downstream, and the observations continued to the limit of either the horizontal or vertical scale, depending on the trajectory. Simultaneously the coordinates of the upper nappe surface were obtained by another operator using the upper coordinometer equipped with one of the hooks and points shown in figure 6.

The resulting observations were recorded on suitable form sheets. Six observers were required to make a complete set of observations: Two to operate and record the observations of the lower coordinometer; two to operate and record the observations of the upper coordinometer; one to read and record the head on the weir and the pressures on the upstream face of the weir; and one to observe the differential head on the Venturi measuring device.

The upper coordinometer shown in figures 4 and 5 was used in the Fort Collins tests to traverse both the upper and lower nappes. It was not entirely satisfactory, particularly for the section of the lower nappe between the sharp crest of the test weir and the vena contracta, which is the critical portion of the nappe. If that portion of the spillway does not fit the lower surface of the sheet of water within a reasonable degree of accuracy, the entire shape of the lower nappe will change, which usually results in subatmospheric pressures on the dam face. This was proven in a series of studies on a model of one of the proposed crests for the Hoover Dam side-channel spillways. A profile developed from the original nappe studies, when incorporated into a crest, fitted satisfactorily beyond the vena contracta, but produced negative pressures between the spring line and the peak. Numerous trials failed to produce a completely satisfactory pressure distribution. The difficulty was finally traced to a combination of two causes: First, as previously mentioned, the water would cling to the flat top of the test weir and produce erroneous results; and second, the original coordinometer was not adapted to the exceedingly careful measurements needed in the critical region. In the Denver laboratory the first difficulty was remedied by grinding the top of the test weir to a knife edge, and the second by constructing the new coordinometer for measuring the lower nappe shape.

TEST PROCEDURE

11. Explanation of Symbols.—The following is a complete list of symbols as used throughout this bulletin. Reference is made to figures 13, 20, 30, and 44.

Q=total discharge, second-feet.

q=discharge per foot of crest, second-feet.

W=width of test channel at gaging section, feet.

L=length of test weir, feet.

A=area of flow cross section at gaging section, square feet.

V_a=average velocity of approach, feet per second.

h_a=average velocity head of approach, feet.

h_s=observed head above sharp crest of weir measured at gaging station, feet.

$H_s=h_s+h_a$=total design head above sharp crest of weir, feet.

E=maximum distance lower nappe rises above sharp crest of weir, feet.

h_o=observed head above high point on lower nappe, feet.

$H_o=h_o+h_a$=total design head above high point on lower nappe, feet.

H=any total head above high point of lower nappe, feet.

P=depth of approach floor below sharp crest of weir, feet.

P_2=depth of downstream floor below sharp crest of weir, feet.

d=depth of piezometer below sharp crest of weir, or depth of flow downstream from submerged dam, feet.

$\bar{d}$=vertical distance from centroid of pressure-reduction area to sharp crest of weir.

h_p=observed pressures on piezometers located in upstream face of weir referenced to sharp crest of weir, feet.

N=horizontal or vertical displacement on offset and overhanging weirs, feet.

M=height of riser on offset weirs, feet.

C=coefficient of discharge for ogee section, not coefficient of discharge as customarily computed for weir with sharp crest, $=\frac{Q}{LH_o^{3/2}}$ or $\frac{Q}{LH^{3/2}}$

h_d=total effective head on submerged dam.

The origin of X and Y coordinates was taken at the sharp crest of the weir. Horizontal measurements taken upstream from the weir are negative while those taken downstream are positive. Vertical measurements above the sharp crest of the weir are positive while those below are negative.

An attempt has been made throughout the bulletin to express the above symbols as dimensionless ratios wherever possible.

12. Relation of Gages to Weir Crest.—It was not practicable to make the zero of the scales on the coordinometers, head gage, and piezometer board coincide with the crest of the weir, as the position of the crest changed for each test arrangement. Prior to and at the conclusion of each test the coordinometer points, head gage, and piezometer board were referenced to the sharp crest of the weir. Some twenty weir set-ups were made; thus it was necessary to keep a clear and accurate record of all gage zeros, or reference settings.

13. Test Procedure.—To keep the number of tests at a minimum and still investigate a wide range of conditions, it was necessary to formulate a comprehensive program and adhere to it as closely as possible. Each weir was tested for various combinations of approach depth and discharge, which were selected with the object of obtaining definite desired values of $\frac{h_a}{H_s}$. This ratio was used as a criterion for combining the runs. A run was started by setting the floor and discharge for the value of $\frac{h_a}{H_s}$ desired. When the flow had stabilized throughout the system, traverses of the upper and lower nappe shapes were made, which required about 20 minutes. Simultaneously, readings were taken every minute on the head gage and the discharge manometer. Three pressure readings were recorded for each piezometer on the upstream face of the weir during this period. At one time, velocity traverses of the approach channel were made with a small current meter. These were later discontinued, as the velocity distribution was considered satisfactory.

CHAPTER III—WEIR WITH VERTICAL UPSTREAM FACE

ANALYSIS OF EXPERIMENTAL RESULTS

14. Compilation of Test Results.—The principal purpose of these experiments was to determine the effect of the velocity of approach on the profile of the lower nappe. Various combinations of velocity of approach and discharge were obtained by varying the depth of the movable floor and the pump discharge. Coefficients of discharge for the corresponding ogee sections were computed and profiles for the nappe shapes obtained. The terminology used in compiling the results is explained in figure 13 and in section 11. A summary of the test results on the weir with vertical upstream face is shown in table 1. Nappe traverses were not made on the entire series, as some runs were made solely to obtain discharge coefficients. Complete runs are indicated with asterisks in column 20, table 1.

The figures in column 1 indicate the test and run number, respectively. A change in test number indicates a shift of the movable floor. A change in run number indicates a different discharge. Columns 2 to 5, inclusive, are self-explanatory, see figure 13. The symbol A in column 6 represents the actual water cross section at the gaging station, or

$$A = W(P + h_s). \tag{8}$$

Column 7 is the velocity of approach, or

$$V_a = \frac{Q}{A}. \tag{9}$$

Column 8 is the average velocity head in the moving water, or

$$h_a = \frac{V_a^2}{2g}, \tag{10}$$

with no correction for unequal velocity distribution. It appeared from current-meter measurements that this correction would have been small in the majority of runs. To obtain velocity head corrections accurately would have required a separate study. The rise of the lower nappe above the sharp crest of the weir, designated as E in column 9, was obtained from the coordinometer traverse of the lower nappe. The total head above the high point of the lower nappe, H_o, column 10, is expressed by the equation

$$H_0 = (h_s + h_a) - E. \tag{11}$$

Columns 11, 12, and 13 are steps in the computation of the coefficient of discharge for the overfall crest, C, column 14. Column 16 is the ratio of the total head, H_o, to the approach depth below the overfall crest, $P+E$, column 15. The total head on the sharp-crested weir, H_s, column 17, was obtained by adding h_s and h_a. The dimensionless ratios $\frac{h_a}{H_s}$ in column 18 and $\frac{E}{H_s}$ in column 19 are self-explanatory.

15. Method of Combining Nappe Profiles.—The upper- and lower-nappe traverse measurements, as observed from the coordinometers,

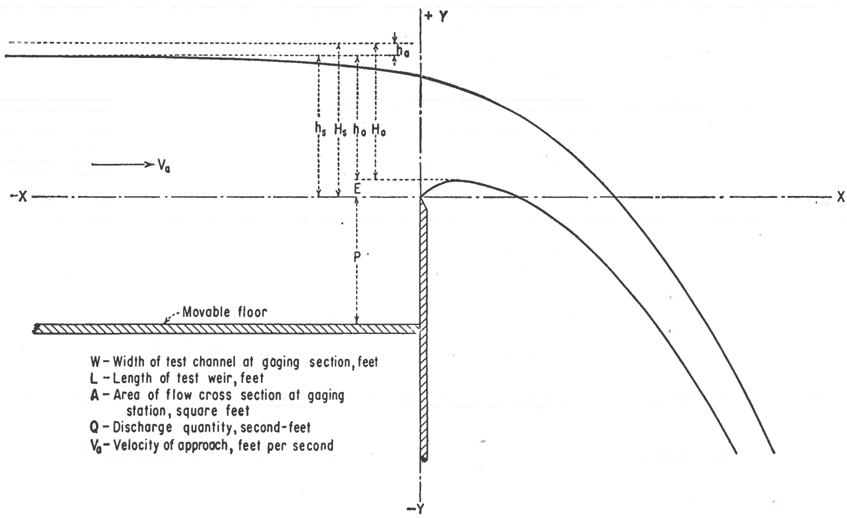

FIGURE 13.—PRINCIPAL ELEMENTS OF OVERFLOW CREST FOR VERTICAL-FACE DAM.

were related to the rectangular coordinates X and Y with the origin at the sharp crest of the weir, see figure 13, by subtracting the reference values, or zero readings. The results thus obtained, still considered as original data, are compiled in tables for both the upper and lower nappe shapes, which are on file in the hydraulic laboratory of the Bureau of Reclamation, Denver, Colorado. The tests so recorded are those indicated by asterisks in column 20 of table 1.

If these nappe shapes were plotted and superimposed one on another, there is a possibility that no two of them would be alike; however, they can be combined according to the laws of similitude. It has long been recognized that the nappe of water flowing freely over a sharp-crested weir has a similar shape for different heads. This was demonstrated by Bazin, who reduced all his experiments to the same basis

TABLE 1.—SUMMARY OF TESTS ON WEIR WITH VERTICAL UPSTREAM FACE

1 TEST	2 P, FEET	3 Q, SECOND-FEET	4 W, FEET	5 h_s, FEET	6 A, SQUARE FEET	7 V_a, FEET PER SECOND	8 h_a, FEET	9 E, FEET	10 H_o, FEET
				BUREAU OF RECLAMATION DATA					
1-1	5.000	0.350	2.019	0.139	10.376	0.034	0.0000	0.014	0.1250
1-2		0.780		0.257	10.574	0.074	0.0001	0.027	0.2101
1-3		1.570		0.382	10.866	0.144	0.0003	0.044	0.3383
1-4		1.900		0.434	10.971	0.173	0.0004	0.050	0.3844
1-5		2.600		0.540	11.185	0.232	0.0008	0.066	0.4748
1-6		3.140		0.605	11.316	0.277	0.0012	0.071	0.5352
1-7		3.830		0.691	11.490	0.333	0.0017	0.077	0.6157
1-8		4.070		0.719	11.547	0.352	0.0019	0.080	0.6409
1-9		4.805		0.802	11.714	0.410	0.0026	0.088	0.7166
1-10		5.100		0.834	11.779	0.433	0.0029	0.093	0.7439
1-11		5.680		0.395	11.902	0.477	0.0035	0.097	0.8015
1-12		6.395		0.967	12.047	0.531	0.0044	0.105	0.8664
1-13		7.450		1.067	12.249	0.608	0.0058	0.118	0.9548
1-14		8.830		1.193	12.504	0.706	0.0077	0.126	1.0747
1-15		9.600		1.260	12.639	0.760	0.0090	0.137	1.1320
2-1	4.596	2.060		0.458	10.204	0.202	0.0006	0.053	0.4056
2-2		2.908		0.576	10.442	0.278	0.0012	0.064	0.5132
2-3		3.080		0.598	10.487	0.294	0.0013	0.069	0.5303
2-4		3.633		0.667	10.626	0.342	0.0018	0.078	0.5908
2-5		4.700		0.790	10.874	0.432	0.0029	0.086	0.7069
2-6		4.797		0.801	10.897	0.440	0.0030	0.091	0.7130
2-7		5.640		0.891	11.078	0.509	0.0040	0.101	0.7940
2-8		6.775		1.004	11.306	0.599	0.0056	0.112	0.8976
2-9		7.500		1.072	11.444	0.655	0.0067	0.120	0.9587
2-10		8.480		1.162	11.625	0.729	0.0083	0.133	1.0373
2-11		9.495		1.251	11.805	0.804	0.0100	0.143	1.1180
3-1	3.497	0.340		0.137	7.337	0.046	0.0000	0.015	0.1220
3-2		0.730		0.230	7.525	0.097	0.0002	0.026	0.2042
3-3		1.546		0.378	7.824	0.198	0.0006	0.045	0.3336
3-4		2.430		0.511	8.092	0.300	0.0014	0.059	0.4534
3-5		4.103		0.723	8.520	0.482	0.0036	0.086	0.6406
3-6		5.670		0.894	8.865	0.640	0.0064	0.103	0.7974
3-7		7.735		1.094	9.269	0.835	0.0109	0.125	0.9799
3-8		9.200		1.225	9.534	0.965	0.0144	0.141	1.0984
4-1	2.497	0.360		0.141	5.326	0.068	0.0001	0.015	0.1261
4-2		1.105		0.300	5.647	0.196	0.0006	0.035	0.2656
4-3		1.695		0.400	5.849	0.290	0.0013	0.044	0.3573
4-4		2.500		0.518	6.087	0.411	0.0026	0.060	0.4606
4-5		3.516		0.650	6.354	0.553	0.0048	0.075	0.5798
4-6		4.730		0.790	6.636	0.713	0.0079	0.087	0.7109
4-7		6.125		0.935	6.929	0.884	0.0121	0.105	0.8421
4-8		8.200		1.127	7.317	1.121	0.0195	0.124	1.0225
4-9		9.560		1.247	7.559	1.265	0.0249	0.137	1.1349
5-1	2.001	0.800		0.243	4.531	0.176	0.0005	0.026	0.2175
5-2		1.760		0.408	4.864	0.362	0.0020	0.047	0.3630
5-3		3.510		0.644	5.340	0.657	0.0067	0.073	0.5777
5-4		4.670		0.779	5.613	0.832	0.0108	0.086	0.7038
5-5		5.850		0.897	5.851	1.000	0.0155	0.100	0.8125
5-6		7.110		1.015	6.089	1.168	0.0212	0.111	0.9252
5-7		9.120		1.194	6.451	1.414	0.0311	0.128	1.0971
6-1	1.500	1.000		0.280	3.594	0.278	0.0012	0.033	0.2482
6-2		1.480		0.363	3.761	0.394	0.0024	0.040	0.3254
6-3		2.410		0.502	4.042	0.596	0.0055	0.057	0.4505
6-4		3.215		0.606	4.252	0.756	0.0089	0.069	0.5459
6-5		4.895		0.795	4.634	1.056	0.0173	0.086	0.7263
6-6		6.180		0.914	4.874	1.268	0.0250	0.096	0.8430
6-7		7.060		1.003	5.054	1.397	0.0304	0.108	0.9254
6-8		7.860		1.073	5.195	1.513	0.0356	0.112	0.9966
6-9		9.400		1.200	5.451	1.724	0.0462	0.124	1.1222
7-1	1.010	0.850		0.250	2.544	0.334	0.0017	0.027	0.2247

TABLE 1.—SUMMARY OF TESTS ON WEIR WITH VERTICAL UPSTREAM FACE—Continued

1 TEST	11 $H_o^{\frac{3}{2}}$	12 L, FEET	13 $LH_o^{\frac{3}{2}}$	14 C	15 P+E, FEET	16 $\frac{H_o}{P+E}$	17 H_s, FEET	18 $\frac{h_a}{H_s}$	19 $\frac{E}{H_s}$	20 NAPPE PROFILES
				BUREAU OF RECLAMATION DATA						
1-1	0.0442	2.007	0.089	3.933	5.014	0.025	0.1390	0.0000	0.1007	
1-2	0.0963		0.193	4.041	5.027	0.042	0.2371	0.0004	0.1139	
1-3	0.1968		0.395	3.975	5.044	0.067	0.3823	0.0008	0.1151	
1-4	0.2384		0.478	3.975	5.050	0.076	0.4344	0.0009	0.1151	*
1-5	0.3272		0.657	3.957	5.066	0.094	0.5408	0.0015	0.1220	
1-6	0.3915		0.786	3.995	5.071	0.106	0.6062	0.0020	0.1171	*
1-7	0.4831		0.970	3.948	5.077	0.121	0.6927	0.0024	0.1112	
1-8	0.5131		1.030	3.951	5.080	0.126	0.7209	0.0026	0.1110	*
1-9	0.6066		1.217	3.948	5.088	0.141	0.8046	0.0032	0.1094	*
1-10	0.6416		1.288	3.960	5.093	0.146	0.8369	0.0035	0.1111	
1-11	0.7176		1.440	3.944	5.097	0.157	0.8985	0.0039	0.1080	*
1-12	0.8065		1.619	3.950	5.105	0.170	0.9714	0.0045	0.1081	
1-13	0.9330		1.873	3.978	5.118	0.187	1.0728	0.0054	0.1100	*
1-14	1.1141		2.236	3.949	5.126	0.210	1.2007	0.0064	0.1049	
1-15	1.2044		2.417	3.972	5.137	0.220	1.2690	0.0071	0.1080	*
2-1	0.2583		0.518	3.977	4.649	0.087	0.4586	0.0013	0.1156	*
2-2	0.3676		0.738	3.940	4.660	0.110	0.5772	0.0021	0.1109	
2-3	0.3861		0.775	3.974	4.665	0.114	0.5993	0.0022	0.1151	*
2-4	0.4542		0.912	3.984	4.674	0.126	0.6688	0.0027	0.1166	
2-5	0.5944		1.193	3.940	4.682	0.151	0.7929	0.0037	0.1085	
2-6	0.6020		1.208	3.971	4.687	0.152	0.8040	0.0037	0.1132	*
2-7	0.7075		1.420	3.972	4.697	0.169	0.8950	0.0045	0.1128	*
2-8	0.8504		1.707	3.969	4.708	0.191	1.0096	0.0055	0.1109	
2-9	0.9387		1.884	3.981	4.716	0.203	1.0787	0.0062	0.1112	*
2-10	1.0565		2.120	4.000	4.729	0.219	1.1703	0.0071	0.1136	
2-11	1.1821		2.372	4.003	4.739	0.236	1.2610	0.0079	0.1134	*
3-1	0.0426		0.085	4.000	3.512	0.035	0.1370	0.0000	0.1095	
3-2	0.0922		0.185	3.946	3.523	0.058	0.2302	0.0009	0.1129	
3-3	0.1927		0.387	3.995	3.542	0.094	0.3786	0.0016	0.1189	
3-4	0.3053		0.613	3.964	3.556	0.128	0.5124	0.0027	0.1151	
3-5	0.5127		1.029	3.987	3.583	0.179	0.7266	0.0049	0.1184	*
3-6	0.7121		1.429	3.968	3.600	0.222	0.9004	0.0071	0.1144	
3-7	0.9700		1.947	3.973	3.622	0.271	1.1049	0.0099	0.1131	*
3-8	1.1511		2.310	3.982	3.638	0.302	1.2394	0.0116	0.1138	
4-1	0.0448		0.090	4.004	2.512	0.050	0.1411	0.0007	0.1063	
4-2	0.1369		0.275	4.021	2.532	0.105	0.3006	0.0020	0.1164	
4-3	0.2136		0.429	3.954	2.541	0.141	0.4013	0.0032	0.1096	
4-4	0.3126		0.627	3.985	2.557	0.180	0.5206	0.0050	0.1153	*
4-5	0.4415		0.886	3.968	2.572	0.225	0.6548	0.0073	0.1145	
4-6	0.5994		1.203	3.932	2.584	0.275	0.7979	0.0099	0.1090	*
4-7	0.7727		1.551	3.949	2.602	0.324	0.9471	0.0128	0.1109	
4-8	1.0340		2.075	3.951	2.621	0.390	1.1465	0.0170	0.1082	
4-9	1.2090		2.426	3.940	2.634	0.431	1.2719	0.0196	0.1077	*
5-1	0.1014		0.203	3.931	2.027	0.107	0.2435	0.0021	0.1068	
5-2	0.2187		0.439	4.010	2.048	0.177	0.4100	0.0049	0.1146	*
5-3	0.4391		0.881	3.983	2.074	0.278	0.6507	0.0103	0.1122	*
5-4	0.5904		1.185	3.941	2.087	0.337	0.7898	0.0137	0.1089	
5-5	0.7324		1.470	3.980	2.101	0.387	0.9125	0.0170	0.1096	
5-6	0.8899		1.786	3.981	2.112	0.438	1.0362	0.0205	0.1071	*
5-7	1.1492		2.306	3.955	2.129	0.515	1.2251	0.0254	0.1045	
6-1	0.1237		0.248	4.032	1.533	0.162	0.2812	0.0043	0.1174	
6-2	0.1856		0.372	3.978	1.540	0.211	0.3654	0.0066	0.1095	
6-3	0.3024		0.607	3.970	1.557	0.289	0.5075	0.0108	0.1123	*
6-4	0.4034		0.810	3.969	1.569	0.348	0.6149	0.0145	0.1122	
6-5	0.6190		1.242	3.941	1.586	0.458	0.8123	0.0213	0.1059	*
6-6	0.7740		1.553	3.979	1.596	0.528	0.9390	0.0266	0.1022	
6-7	0.8902		1.787	3.952	1.608	0.575	1.0334	0.0294	0.1045	*
6-8	0.9949		1.997	3.936	1.612	0.618	1.1086	0.0321	0.1010	
6-9	1.1888		2.386	3.940	1.624	0.691	1.2462	0.0371	0.0995	
7-1	0.1065		0.214	3.972	1.037	0.217	2.2517	0.0068	0.1073	

* RUNS IN WHICH NAPPE PROFILES WERE MEASURED.

TABLE 1.—SUMMARY OF TESTS ON WEIR WITH VERTICAL UPSTREAM FACE—Continued

1 TEST	2 P, FEET	3 Q, SECOND-FEET	4 W, FEET	5 h_s, FEET	6 A, SQUARE FEET	7 V_a, FEET PER SECOND	8 h_a, FEET	9 E, FEET	10 H_o, FEET
BUREAU OF RECLAMATION DATA									
7-2	1.010	1.730	2.019	0.401	2.849	0.607	0.0057	0.044	0.3627
7-3		2.700		0.536	3.121	0.865	0.0116	0.058	0.4896
7-4		3.900		0.679	3.410	1.144	0.0204	0.072	0.6274
7-5		4.670		0.761	3.576	1.306	0.0265	0.082	0.7055
7-6		5.500		0.842	3.739	1.471	0.0337	0.087	0.7887
7-7		6.580		0.937	3.931	1.674	0.0436	0.095	0.8856
7-8		7.890		1.048	4.155	1.899	0.0560	0.105	0.9990
7-9		9.630		1.184	4.430	2.174	0.0735	0.116	1.1415
8-1	0.647	2.000		0.439	2.193	0.912	0.0130	0.047	0.4050
8-2	0.632	2.880		0.547	2.380	1.210	0.0228	0.057	0.5128
8-3	0.624	3.568		0.647	2.566	1.390	0.0300	0.064	0.6130
8-4	0.618	4.870		0.757	2.776	1.754	0.0478	0.075	0.7298
8-5	0.613	5.925		0.852	2.958	2.003	0.0624	0.083	0.8314
8-6	0.607	6.360		0.898	3.039	2.093	0.0681	0.085	0.8811
8-7	0.576	8.090		1.022	3.226	2.508	0.0978	0.092	1.0278
8-8	0.574	9.325		1.113	3.406	2.738	0.1165	0.100	1.1295
9-1	0.412	1.715		0.396	1.631	1.052	0.0172	0.038	0.3752
9-2	0.408	2.040		0.430	1.692	1.206	0.0226	0.039	0.4136
9-3	0.408	2.565		0.503	1.839	1.395	0.0303	0.046	0.4873
9-4	0.403	3.500		0.602	2.029	1.725	0.0463	0.054	0.5943
9-5	0.397	4.160		0.653	2.120	1.962	0.0598	0.058	0.6548
9-6	0.387	4.740		0.720	2.235	2.121	0.0700	0.062	0.7280
9-7	0.376	5.150		0.758	2.290	2.249	0.0786	0.065	0.7716
9-8	0.354	6.385		0.857	2.445	2.611	0.1060	0.070	0.8930
9-9	0.332	7.640		0.947	2.582	2.959	0.1361	0.073	1.0101
9-10	0.317	9.150		1.042	2.744	3.335	0.1729	0.080	1.1349
10-1	0.145	1.635		0.353	1.005	1.627	0.0412	0.027	0.3672
10-2	0.145	2.260		0.434	1.169	1.933	0.0581	0.032	0.4601
10-3	0.144	3.170		0.533	1.367	2.319	0.0836	0.039	0.5776
10-4	0.143	3.830		0.592	1.484	2.581	0.1036	0.041	0.6546
10-5	0.140	4.400		0.642	1.579	2.787	0.1207	0.041	0.7217
10-6	0.134	7.395		0.886	2.059	3.592	0.2006	0.059	1.0276
11-1	0.092	1.640		0.337	0.888	1.847	0.0530	0.024	0.366
11-2	0.094	2.280		0.413	1.049	2.173	0.0734	0.029	0.457
11-3	0.098	3.000		0.488	1.212	2.475	0.0952	0.032	0.551
11-4	0.101	3.790		0.560	1.368	2.770	0.1193	0.038	0.641
11-5	0.083	4.540		0.628	1.471	3.086	0.1480	0.040	0.736
11-6	0.082	4.890		0.660	1.535	3.186	0.1578	0.044	0.774
11-7	0.078	5.060		0.710	1.630	3.104	0.1498	0.050	0.810
BAZIN DATA (TYPICAL)									
2-10	3.724	4.149	3.284	0.516	13.924	0.298	0.0014	0.058	0.460
2-14		5.494		0.621	14.269	0.385	0.0023	0.070	0.554
2-18		7.054		0.732	14.634	0.482	0.0036	0.082	0.654
2-22		8.321		0.820	14.922	0.558	0.0049	0.092	0.733
2-26		10.300		0.942	15.323	0.672	0.0070	0.106	0.844
2-30		11.912		1.039	15.642	0.762	0.0090	0.116	0.932
2-34		14.977		1.208	16.197	0.925	0.0133	0.135	1.086
2-38		17.479		1.339	16.627	1.051	0.0171	0.150	1.206
9-1	1.145	3.739	6.555	0.299	9.465	0.395	0.0025	0.030	0.272
9-4		5.510		0.388	10.049	0.548	0.0047	0.039	0.354
9-8		7.761		0.481	10.658	0.728	0.0083	0.048	0.441
9-12		11.077		0.609	11.497	0.964	0.0144	0.061	0.562
9-16		14.655		0.723	12.245	1.197	0.0223	0.072	0.673
9-20		18.013		0.823	12.900	1.396	0.0304	0.082	0.771
9-24		21.153		0.914	13.497	1.567	0.0381	0.091	0.861
9-28		24.652		1.009	14.119	1.746	0.0473	0.101	0.955
9-32		28.194		1.095	14.683	1.920	0.0573	0.106	1.046
9-36		32.456		1.193	15.326	2.118	0.0698	0.116	1.147
9-40		37.218		1.301	16.034	2.321	0.0838	0.126	1.259

758318°—48——4

TABLE 1.—SUMMARY OF TESTS ON WEIR WITH VERTICAL UPSTREAM FACE—Continued

1 TEST	11 $H_o^{\frac{3}{2}}$	12 L, FEET	13 $LH_o^{\frac{3}{2}}$	14 C	15 $P+E$, FEET	16 $\frac{H_o}{P+E}$	17 H_s, FEET	18 $\frac{h_a}{H_s}$	19 $\frac{E}{H_s}$	20 NAPPE PROFILES
					BUREAU OF RECLAMATION DATA					
7-2	0.2184	2.007	0.438	3.950	1.054	0.344	0.4067	0.0140	0.1082	
7-3	0.3426		0.688	3.924	1.068	0.458	0.5476	0.0212	0.1059	*
7-4	0.4970		0.997	3.912	1.082	0.580	0.6994	0.0292	0.1029	*
7-5	0.5925		1.189	3.928	1.092	0.646	0.7875	0.0337	0.1041	
7-6	0.7004		1.406	3.912	1.097	0.719	0.8757	0.0385	0.0993	*
7-7	0.8334		1.673	3.933	1.105	0.801	0.9806	0.0445	0.0969	
7-8	0.9985		2.004	3.937	1.115	0.896	1.1040	0.0507	0.0951	*
7-9	1.2196		2.448	3.934	1.126	1.014	1.2575	0.0585	0.0922	
8-1	0.2578		0.517	3.868	0.694	0.584	0.4520	0.0288	0.1040	*
8-2	0.3672		0.737	3.908	0.689	0.744	0.5698	0.0400	0.1000	*
8-3	0.4799		0.963	3.705	0.688	0.891	0.6770	0.0443	0.0945	*
8-4	0.6234		1.251	3.893	0.693	1.053	0.8048	0.0594	0.0932	*
8-5	0.7581		1.522	3.893	0.696	1.195	0.9144	0.0682	0.0908	*
8-6	0.8270		1.660	3.831	0.692	1.273	0.9661	0.0705	0.0880	*
8-7	1.0420		2.091	3.869	0.668	1.539	1.1198	0.0873	0.0822	*
8-8	1.2004		2.409	3.871	0.674	1.676	1.2295	0.0948	0.0813	
9-1	0.2298		0.461	3.720	0.450	0.834	0.4132	0.0416	0.0920	*
9-2	0.2660		0.534	3.820	0.447	0.925	0.4526	0.0499	0.0862	*
9-3	0.3402		0.683	3.755	0.454	1.073	0.5333	0.0568	0.0863	*
9-4	0.4582		0.920	3.804	0.457	1.300	0.6483	0.0714	0.0833	*
9-5	0.5299		1.064	3.910	0.455	1.439	0.7128	0.0839	0.0814	*
9-6	0.6212		1.247	3.801	0.449	1.621	0.7900	0.0886	0.0785	*
9-7	0.6778		1.360	3.787	0.441	1.750	0.8366	0.0940	0.0777	*
9-8	0.8439		1.694	3.769	0.424	2.106	0.9630	0.1101	0.0727	*
9-9	1.0152		2.038	3.749	0.405	2.494	1.0831	0.1257	0.0674	*
9-10	1.2090		2.426	3.772	0.397	2.859	1.2149	0.1423	0.0658	*
10-1	0.2225		0.447	3.658	0.172	2.135	0.3942	0.1045	0.0685	*
10-2	0.3121		0.626	3.610	0.177	2.599	0.4921	0.1181	0.0650	*
10-3	0.4390		0.881	3.598	0.183	3.156	0.6166	0.1356	0.0633	*
10-4	0.5296		1.063	3.603	0.184	3.558	0.6956	0.1489	0.0589	*
10-5	0.6131		1.230	3.577	0.181	3.987	0.7627	0.1583	0.0538	*
10-6	1.0417		2.091	3.537	0.193	5.324	1.0866	0.1846	0.0543	*
11-1	0.221		0.443	3.702	0.116	3.155	0.390	0.1359	0.062	*
11-2	0.309		0.620	3.677	0.123	3.715	0.486	0.1510	0.060	*
11-3	0.409		0.820	3.659	0.130	4.238	0.583	0.1633	0.055	*
11-4	0.513		1.029	3.683	0.139	4.612	0.679	0.1757	0.056	*
11-5	0.631		1.266	3.586	0.123	5.984	0.776	0.1907	0.052	
11-6	0.681		1.366	3.580	0.126	6.143	0.818	0.1929	0.054	
11-7	0.729		1.462	3.461	0.128	6.528	0.860	0.1742	0.058	
					BAZIN DATA (TYPICAL)					
2-10	0.312	3.284	1.023	4.055	3.782	0.122	0.517	0.0027	0.1117	
2-14	0.412		1.353	4.062	3.794	0.146	0.623	0.0037	0.1117	
2-18	0.528		1.735	4.067	3.806	0.172	0.736	0.0049	0.1115	
2-22	0.628		2.062	4.036	3.816	0.192	0.825	0.0059	0.1113	
2-26	0.775		2.544	4.049	3.830	0.220	0.949	0.0074	0.1112	
2-30	0.899		2.951	4.036	3.840	0.243	1.048	0.0086	0.1111	
2-34	1.132		3.716	4.030	3.859	0.281	1.221	0.0109	0.1108	
2-38	1.325		4.350	4.018	3.874	0.311	1.356	0.0126	0.1106	
9-1	0.141	6.555	0.926	4.040	1.175	0.231	0.302	0.0083	0.0992	
9-4	0.210		1.380	3.993	1.184	0.299	0.393	0.0120	0.0988	
9-8	0.293		1.921	4.039	1.193	0.370	0.489	0.0170	0.0983	
9-12	0.422		2.765	4.006	1.206	0.466	0.623	0.0231	0.0977	
9-16	0.552		3.619	4.049	1.217	0.553	0.745	0.0299	0.0970	
9-20	0.677		4.439	4.058	1.227	0.628	0.853	0.0356	0.0964	
9-24	0.798		5.234	4.041	1.236	0.696	0.952	0.0400	0.0960	
9-28	0.934		6.122	4.027	1.246	0.767	1.056	0.0448	0.0955	
9-32	1.070		7.014	4.020	1.251	0.836	1.152	0.0497	0.0922	
9-36	1.229		8.054	4.030	1.261	0.910	1.263	0.0553	0.0916	
9-40	1.412		9.256	4.021	1.271	0.990	1.385	0.0605	0.0911	

* RUNS IN WHICH NAPPE PROFILES WERE MEASURED.

by expressing the dimensions in terms of the head on the weir. When this is done the results are in dimensionless terms equally applicable to any system of units. For two assumed conditions of flow, (1) a flow with a large head and great depth of approach, and (2) a flow with a small head and small depth of approach, the nappe shapes will be similar if the ratio of the head to the depth of approach is the same in each case. If the X and Y coordinates are expressed with respect to the head on the weir crest in each case, the $\frac{X}{H_s}$ and $\frac{Y}{H_s}$ profiles should coincide. Dividing the X and Y coordinates by H_s actually reduces all cases to the same head, usually denoted as unit head. This was the method used in combining the results of table 1 into table 2.

The X and Y coordinates of the lower nappe for each run were plotted to a large scale and a smooth curve drawn through them. This procedure removed irregularities that were naturally present due to fluctuations of the nappe surface, which fluctuations increased as the depth of approach decreased. Coordinates were then read from the smooth curve for each run and divided by H_s, the total head on the experimental weir for each particular run. Thus the coordinates for all runs were reduced to unit head. The coordinates in the unit-head form were then combined, the relation $\frac{h_a}{H_s}$ being used as the criterion. From column 18, table 1, it will be observed that the value of $\frac{h_a}{H_s}$ ranged from 0 to 0.193. The runs were grouped in table 2 according to their value of $\frac{h_a}{H_s}$ and plotted, with as many as five runs in a group. The curves in any one group were superimposed on each other and an average line drawn through them. The average lines from the individual groups were then combined into a final set of nappe profiles, expressed in terms of unit head, for values of $\frac{h_a}{H_s}$ ranging from 0.002 to 0.200. This adjustment was of necessity performed on a scale too large to reproduce in this bulletin. However, figure 14 gives some idea as to its character. As the velocity of approach increases (or as $\frac{h_a}{H_s}$ increases), the nappe profile for unit head flattens and crosses the profiles for the smaller values of $\frac{h_a}{H_s}$. The greatest deviation occurs close to the weir, which verifies the previous statement that the correct design of this portion of an ogee crest is important. In place of showing the final adjustment curves, the $\frac{X}{H_s}$ and $\frac{Y}{H_s}$ values have been tabulated for various values of $\frac{h_a}{H_s}$ in table 12.

TABLE 2.—METHOD OF COMBINING NAPPE SHAPES FOR VERTICAL-FACE WEIR

TEST	H_s, FEET	P, FEET	ACTUAL h_a/H_s	PLOTTED h_a/H_s
1-4	0.4344	5.00	0.0009	0.0020
1-6	0.6062	5.00	0.0020	0.0020
1-8	0.7209	5.00	0.0026	0.0020
1-9	0.8046	5.00	0.0032	0.0020
2-1	0.4586	4.60	0.0013	0.0020
2-3	0.5993	4.60	0.0022	0.0020
2-11	1.2610	4.60	0.0079	0.0100
3-7	1.1049	3.50	0.0099	0.0100
4-6	0.7979	2.50	0.0099	0.0100
5-3	0.6507	2.00	0.0103	0.0100
6-3	0.5075	1.50	0.0108	0.0100
4-9	1.2719	2.50	0.0196	0.0200
5-6	1.0362	2.00	0.0205	0.0200
6-5	0.8123	1.50	0.0213	0.0200
7-3	0.5476	1.01	0.0212	0.0200
6-7	1.0334	1.50	0.0294	0.0300
7-4	0.6994	1.01	0.0292	0.0300
8-1	0.4520	0.647	0.0287	0.0300
7-6	0.8757	1.010	0.0384	0.0400
8-2	0.5698	0.632	0.0400	0.0400
8-3	0.6770	0.624	0.0443	0.0400
9-1	0.4132	0.412	0.0416	0.0400
7-8	1.1040	1.010	0.0507	0.0500
9-2	0.4526	0.408	0.0499	0.0500
8-4	0.8048	0.618	0.0593	0.0600
9-3	0.5333	0.408	0.0568	0.0600
8-5	0.9144	0.613	0.0682	0.0700
8-6	0.9661	0.607	0.0704	0.0700
9-4	0.6483	0.403	0.0714	0.0700
9-5	0.7128	0.397	0.0838	0.0800
8-7	1.1198	0.576	0.0873	0.0900
9-6	0.7900	0.387	0.0886	0.0900
9-7	0.8366	0.376	0.0939	0.0900
9-8	0.9630	0.354	0.1101	0.1000
10-1	0.3942	0.145	0.1045	0.1000
9-9	1.0831	0.332	0.1257	0.1200
10-2	0.4921	0.145	0.1181	0.1200
9-10	1.2149	0.317	0.1423	0.1400
10-3	0.6166	0.144	0.1356	0.1400
11-1	0.3900	0.092	0.1359	0.1400
10-5	0.7627	0.140	0.1583	0.1600
11-3	0.5830	0.098	0.1633	0.1600
10-6	1.0866	0.134	0.1846	0.1800
11-4	0.6790	0.101	0.1757	0.1800

The X and Y coordinates for the upper nappe surfaces were treated in the same manner as for the lower profiles, and the final $\frac{X}{H_s}$ and $\frac{Y}{H_s}$ coordinates are listed in table 18 for different values of $\frac{h_a}{H_s}$. These coordinates are not as dependable as those for the lower nappe surface, since special factors may alter them. The upper surface of a sheet of water flowing over a dam is exposed to the atmosphere and may be altered by wind, air currents, or by the absorption of surrounding air. When flowing water, exposed to air, reaches a velocity of approxi-

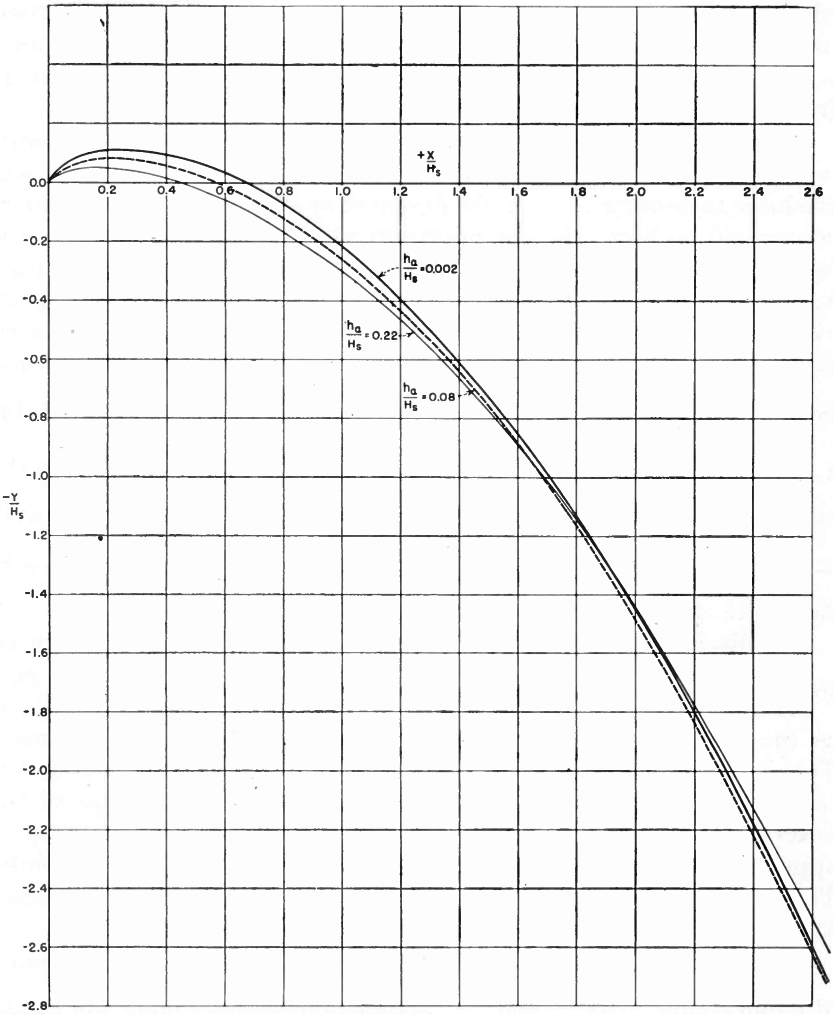

FIGURE 14.—TYPICAL LOWER NAPPE SHAPES SHOWING EFFECT OF VELOCITY OF APPROACH.

mately 20 feet per second, it begins to insufflate air. As the velocity increases, the penetration becomes more pronounced and the air actually mixes with the water. Thomas [11] found that water flowing at a depth of approximately 8 feet and a velocity of 80 feet per second absorbed 50 percent air by volume from the atmosphere. The upper-nappe-shape coordinates in table 18 therefore represent only the ideal case, where air plays little or no part. These coordinates, however, may be used as a starting point from which the area of a sheet of water may be estimated at various sections. The fact cannot be overem-

[11] Thomas, C. W., Progress Report on Studies of the Flow of Water in Open Channels with High Gradients, Bur. of Recl. Hyd. Lab. Report 35 (unpublished), July 27, 1938.

phasized that the profile of the upper surface depends largely on existing conditions. A common mistake is to design spillways and chutes with insufficient freeboard, which, in the end, usually proves costly from the standpoint of maintenance.

16. Relation of E to Velocity of Approach.—These experiments were made on a sharp-crested weir on which the observed head, h_s, was the basic measurement. In the design of an overflow section it is more convenient to begin the computations with the total head above the ogee crest, H_o. It is therefore desirable to be able to transfer from h_s to H_o or vice versa, see figure 13. This has been made possible by evaluating the maximum rise of the lower nappe above the sharp crest, E, and the velocity head of approach, h_a, each in terms of the total head on the sharp crest, H_s. With the ratio $\frac{h_a}{H_s}$ in column 18, table 1, as the abscissa, and the ratio $\frac{E}{H_s}$ in column 19 as the ordinate, the curve shown on figure 15–A was plotted. By entering this curve with a given value of $\frac{h_a}{H_s}$ the value of E can be obtained. As $H_s=H_o+E$, the curve affords a method for interchanging the various heads.

17. Discharge Coefficients.—The curve in figure 15–B was plotted from columns 14 and 16, table 1, with the dimensionless ratio $\frac{H_o}{P+E}$ as the abscissa and the coefficient of discharge C as the ordinate. This is not the coefficient of discharge for the sharp-crested weir, but rather for the equivalent ogee section outlined by the shape of the lower nappe. As the value of $P+E$ decreases, or as the velocity of approach increases, the coefficient of discharge decreases rapidly. This is further demonstrated in figure 16, where the observed head, h_s, is plotted with respect to the discharge over the weir.

The relationships shown in figure 15 have been carried to the limits of applicability. As $\frac{h_a}{H_s}$ and $\frac{H_o}{P+E}$ approach zero as a limit, the values of $\frac{E}{H_s}$ and C become constants for all practical purposes. The average value of $\frac{E}{H_s}$ is 0.115 for negligible velocity of approach, and C becomes 3.98 for the same condition. As the depth of approach is decreased and the velocity of approach increased, the values of $\frac{E}{H_s}$ and C decrease. Eventually values of $\frac{h_a}{H_s}$ and $\frac{H_o}{P+E}$ are approached where the relations are no longer valid. This limit is near the critical depth of flow. King[12] defines critical depth as (*a*) *the depth at which, for a given*

[12] King, H. W., Handbook of Hydraulics, 3d ed., 1939, p. 371, McGraw-Hill Book Co. Quotations reprinted by permission.

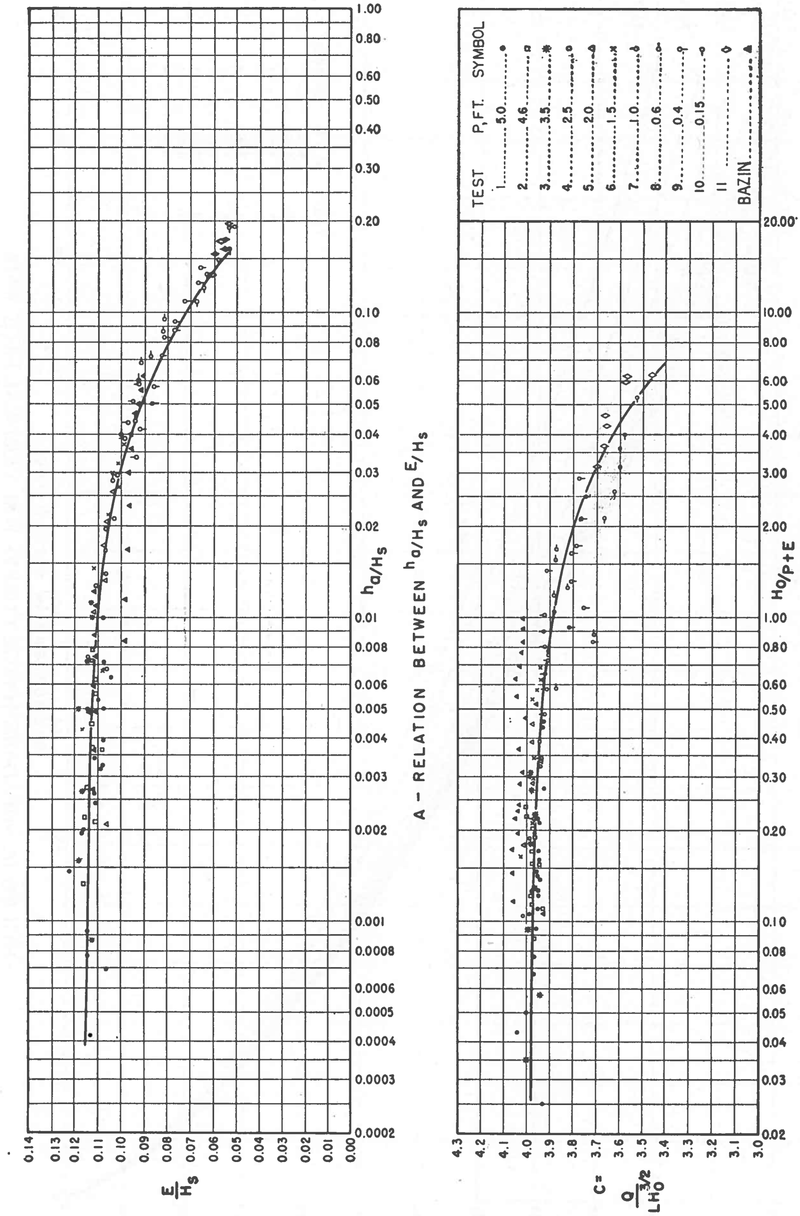

FIGURE 15.—VALUES OF E AND C FOR VERTICAL-FACE WEIR.

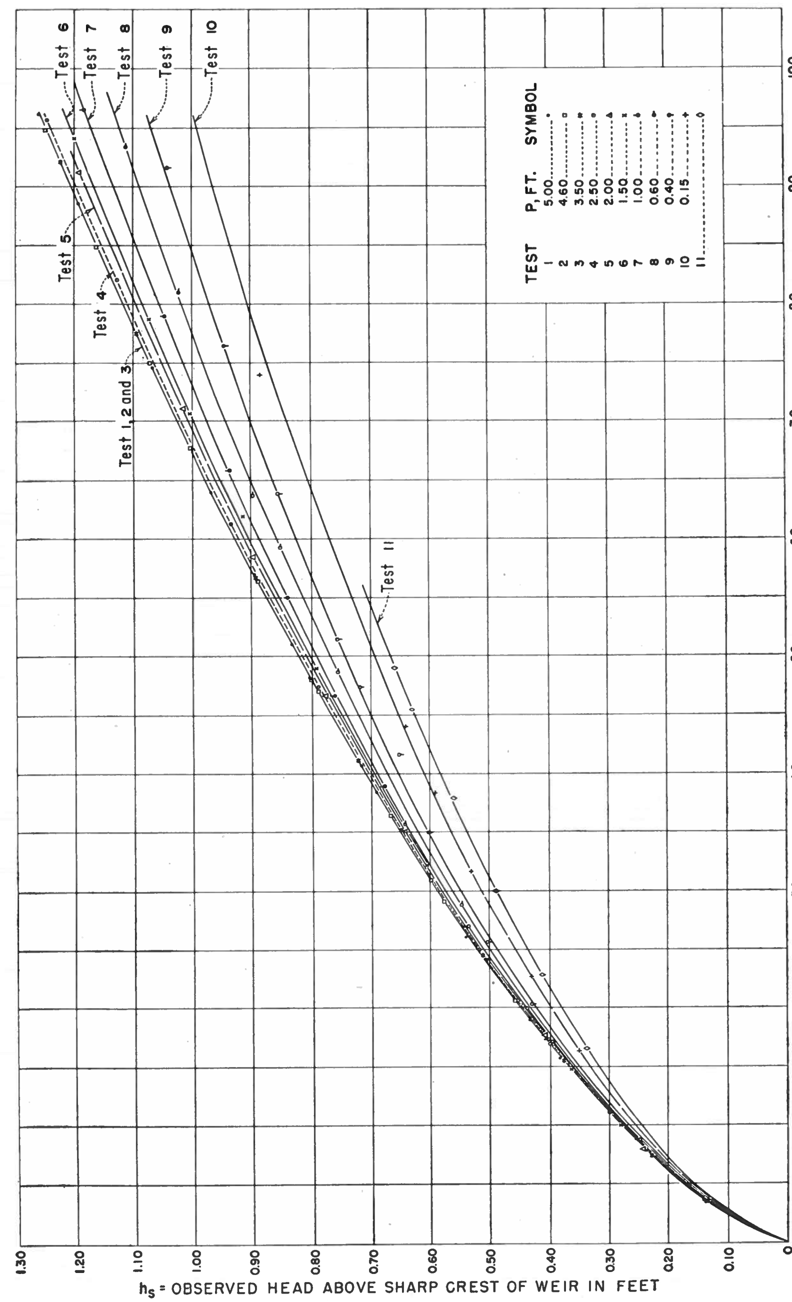

FIGURE 16.—HEAD-DISCHARGE CURVES FOR VERTICAL-FACE WEIR.

energy content of the water in the channel maximum discharge occurs; or (b) the depth at which in a given channel a given quantity of water flows with the minimum content of energy. In his discussion of critical depth, he says:

> It will be observed from both of the figures (fig. 91 and 92, King's Handbook of Hydraulics) that at or near critical depth a relatively large change in depth corresponds to a relatively small change in energy. Flow in this region is therefore rather unstable, as is usually indicated by characteristic water-surface undulations.

This limit was obvious in the test flume and was manifested by quite unstable surface undulations, as described by King. As the test data were analyzed, this limit became apparent from the inconsistency of the results beyond a certain value of $\frac{h_a}{H_s}$. In both figures 15–A and 15–B the curves drop rapidly at the right, and it was not possible from the tests to determine the characteristics of these curves beyond the values shown, as waves in the channel produced erroneous head measurements. Friction of the floor and side walls of the channel had a dominating influence on the behavior of the flow. For this reason, values of $\frac{h_a}{H_s}$ above 0.20 and values of $\frac{H_o}{P+E}$ above 7.00 have no value in this study and consequently are not recommended for prototype design.

18. Minor Factors Affecting Nappe Profiles.—Some doubt existed as to the possible effect produced by surface tension on the shape of the nappe profiles under small heads. Harris [13] recommends a molecular correction amounting to as much as 10 percent for coefficients of discharge. He recommends additive molecular correction at heads as low as 0.15 foot. He states:

> The molecular effect seldom exceeds three percent in the range of engineering application. * * * Weirs of large physical dimension need no correction and the smallest ones need most. * * *
>
> The predominating element contributing to the production of excessive flow in the smaller weirs, is the existence of molecular forces deforming the stream lines. This deformation being gradual and the deforming forces static in their nature, the deformation does not appreciably change the energy efficiency. It affects only the area and therefore appears directly in the quantity of flow. The deformation is too slight to modify appreciably the law by which the static forces influence the dynamic stream lines.

In other words, the molecular effect for heads of 0.5 foot or greater, which amounts to 3 percent or less, is not sufficient to be noticeable in the nappe profiles. Runs made by the Bureau of Reclamation on heads as low as 0.3 foot, see table 1, show no material deviation in the

[13] Harris, Chas. W., An Analysis of the Weir Coefficient for Suppressed Weirs, Univ. of Wash. Eng. Exp. Sta. Bull. No. 22, 1923. Quotation reprinted by permission.

nappe shape from others made at higher heads with the same value of $\frac{h_a}{H_s}$. The discharge coefficients for these low heads differ very little from those for the larger ones, as can be observed from table 1.

There is a noticeable surface-tension effect at very low heads; but it is difficult to define its limits, as the sharpness of the weir crest or a small amount of oil on the weir can cause a marked change in the intensity. In the case of weirs sloping downstream, the effect of friction on the water flowing over a flat, sloping surface is very noticeable for low heads. In an effort to eliminate surface-tension effects, few runs were made at heads less than 0.4 foot, see table 1. In addition, the weirs were machined to a knife edge to prevent the lower nappe from springing from a point other than the sharp edge. It is believed that viscous effects were of a negligible character in these tests.

19. Comparison of Results with Bazin.—Bazin performed a series of similar experiments in France during the years 1886 to 1888 on vertical weirs varying from 1 to 2 meters in length, but his investigation included only two positions of the approach floor. This limited his range of $\frac{h_a}{H_s}$ values from 0.002 to 0.070, which is insufficient for the majority of dam designs encountered in practice. Bazin performed numerous tests on vertical-face weirs of which a few representative runs are summarized at the bottom of table 1. The Bureau of Reclamation nappe shapes agree favorably with those of Bazin, but the comparison has not been included, due to the difficulty of reproduction. However, Bazin's values of $\frac{E}{H_s}$ in figure 15–A agree sufficiently well with the Bureau's values to verify the above statement.

The agreement is not as satisfactory for the coefficients of discharge shown in figure 15–B. Bazin's coefficients are consistently higher than those obtained by the Bureau. His weirs consisted of wood planking topped with a brass plate which, according to Bazin's report, had a sharp 90° upstream edge. As judged from the results of other more recent experimenters on sharp-crested weirs, Bazin's values are high. Schoder[14] attempted to check Bazin's discharge coefficients by performing minor changes in the approach channel to the weir, but invariably obtained coefficients smaller than those of Bazin. Not until the sharp edge of the weir was removed with a file did his values approach Bazin's. As a result, Professor Schoder concluded that Bazin's weirs did not have truly sharp crests. If this conclusion was true, Bazin would naturally have obtained a greater discharge for a given head than did recent experimenters. Whether Bazin's weirs

[14] Schoder, E. W., and K. B. Turner, Precise Weir Measurements, Trans. A. S. C. E., Vol. 93, 1929, p. 1053.

did or did not have true sharp 90° corners is now only a matter of conjecture. There is no existing proof pro or con.

Another possibility is that Bazin's weirs may have been sharp according to present standards, but an error could have been made in the calibration of his first weir, which was used to calibrate all others. A small error in discharge is magnified in the coefficient of discharge. It would probably be impossible to detect small differences in discharge from the nappe-shape measurements, as discharge is used merely to determine the velocity head of approach in this computation.

No attempt will be made to compare Schoder's and numerous other experimenters' work on weirs in this study, as the material is voluminous and most of the experimenters did not measure the value of E.

A mathematical analysis of the behavior of the sheet of water flowing over a sharp crest, for the various conditions encountered in practice, is suggested for further study. Vitols [15] attempted such a solution, taking into account the velocity of approach based to a large extent on the results of Bazin's experiments. An analysis of the new data for higher approach velocities and the additional overfall dam shapes, using this method or preferably a simpler one, offers an interesting problem for a mathematically adept student or engineer who has the time to pursue such a study. It was with this in mind that tables of the original upper- and lower-nappe-shape coordinates have been filed for future reference.

20. Reduction of Pressure on Upstream Face of Vertical Weir.— Another phase of this study was the determination of the reduction of pressure on the upstream face of the weir due to the conversion of static to kinetic energy as the water flowed over the crest. Piezometers were installed in the upstream face of each weir, as shown in figures 6 and 11, and connected to manometer tubes. Pressures were recorded during each test and the results as digested are shown plotted in figure 17. The extent of the pressure reduction in feet of water, measured downward from the sharp crest, is plotted in terms of the total head on the weir, H_s for different approach velocities. The actual elevation of the water surface in the manometer tubes, related to the weir crest, is h_p, and the vertical distance downward from the weir crest to the point at which the pressure was measured is d, as shown by the diagram in figure 17. The pressure reduction is greatest for the lower approach velocities.

The trapezoidal pressure diagram, $CBOE$, in figure 18, represents the conventional method used in computing pressures on the upstream face of a dam, with the resultant pressure, R_1, acting at the centroid of the trapezoidal area. The pressures indicated by this method are

[15] Vitols, A., Beitrag zur Frage des Vacuumlosen Dammprofiles (Vacuumless Dam Profiles), Wasserkraft und Wasserwirtschaft, Vol. 31, 1936, p. 207. Translated by Edward F. Wilsey in Bur. of Recl. Hyd. Lab. Report 22 (unpublished).

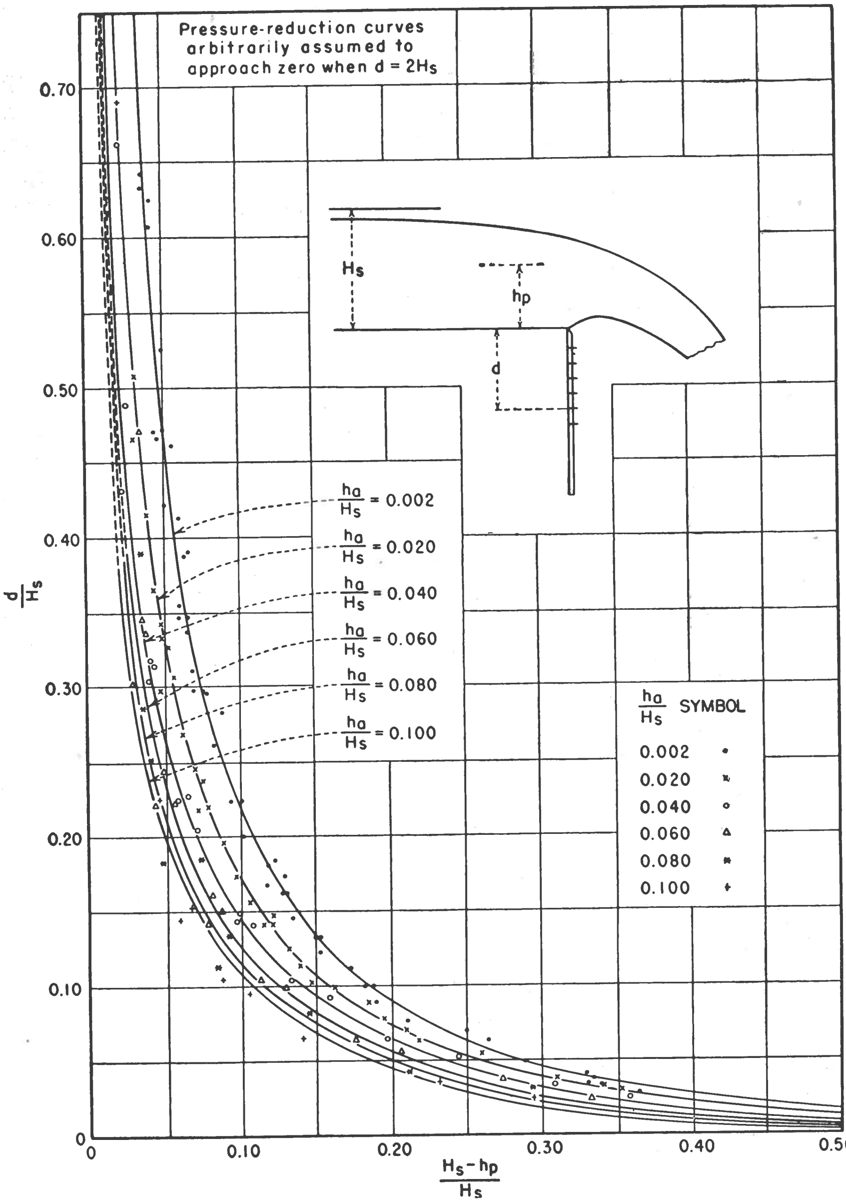

FIGURE 17.—REDUCTION OF PRESSURE ON UPSTREAM FACE OF VERTICAL WEIR.

larger than those which actually exist on overflow dams, as flow over the dam produces a reduction in pressure, *CBO*, which is greatest in the vicinity of the crest. By planimetering the areas enclosed by each individual curve and the axes in figure 17, the magnitude of the pressure reduction, R_2, for the weir with vertical upstream face is obtained.

The results are expressed by a single curve in figure 18–A (p. 46). The area *OBC*, expresses as $\frac{ft.^2}{H_s^2}$, is plotted for six values of $\frac{h_a}{H_s}$. With the coordinates in dimensionless terms, this curve is applicable to all dams of this type, regardless of size. It was assumed in the computations for the above curves that the ogee section of the dam would fit the lower nappe of the sheet of water flowing over it. Should this not be true, the resulting pressure reduction would be altered. To obtain the total pressure reduction in pounds for a given value of $\frac{h_a}{H_s}$, it is necessary to multiply the corresponding value of $\frac{ft.^2}{H_s^2}$, in figure 18–A, by the length of the dam, by H_s^2, and by the unit weight of water, w.

The position of the resultant, R_2, of the pressure-reduction area can be obtained from figure 18–B. The location of the resultant, measured downward from the sharp crest, and expressed in terms of unit head, is plotted with respect to $\frac{h_a}{H_s}$. The distance $\bar{d}$, from the sharp crest to the resultant R_2, for a given value of $\frac{h_a}{H_s}$, is obtained directly from this curve.

It is evident that the overturning moment as customarily computed for overflow dams is too large. The actual reduction in pressure is not appreciable; but where the moment arm is long, as in high dams, the effect on stability may be worth considering. The nominal method of analysis is not incorrect, but a factor of safety exists of which the designer may be unaware. It may be feasible to effect a reduction in other factors which are usually overdesigned for the sake of safety. The extent to which this information is useful, however, depends on the particular problem. The pressure reduction would be negligible for low dams but may be significant for high dams with large heads over the crest. C. W. Harris [16] has also developed a theoretical as well as an experimental treatment for the computation of pressure reduction on the upstream face of a vertical weir.

APPLICATION OF EXPERIMENTAL RESULTS

21. Design of an Overflow Dam Section with Vertical Upstream Face.—An overflow dam with vertical upstream face can now be designed for practically any field condition. In the following example, the dam will be so designed that, for the maximum designed head on the spillway, the face of the overflow section will fit the lower profile of the overflowing sheet of water with little or no negative pressure between the sheet of water and the face of the spillway.

[16] See footnote 13 in sec. 18.

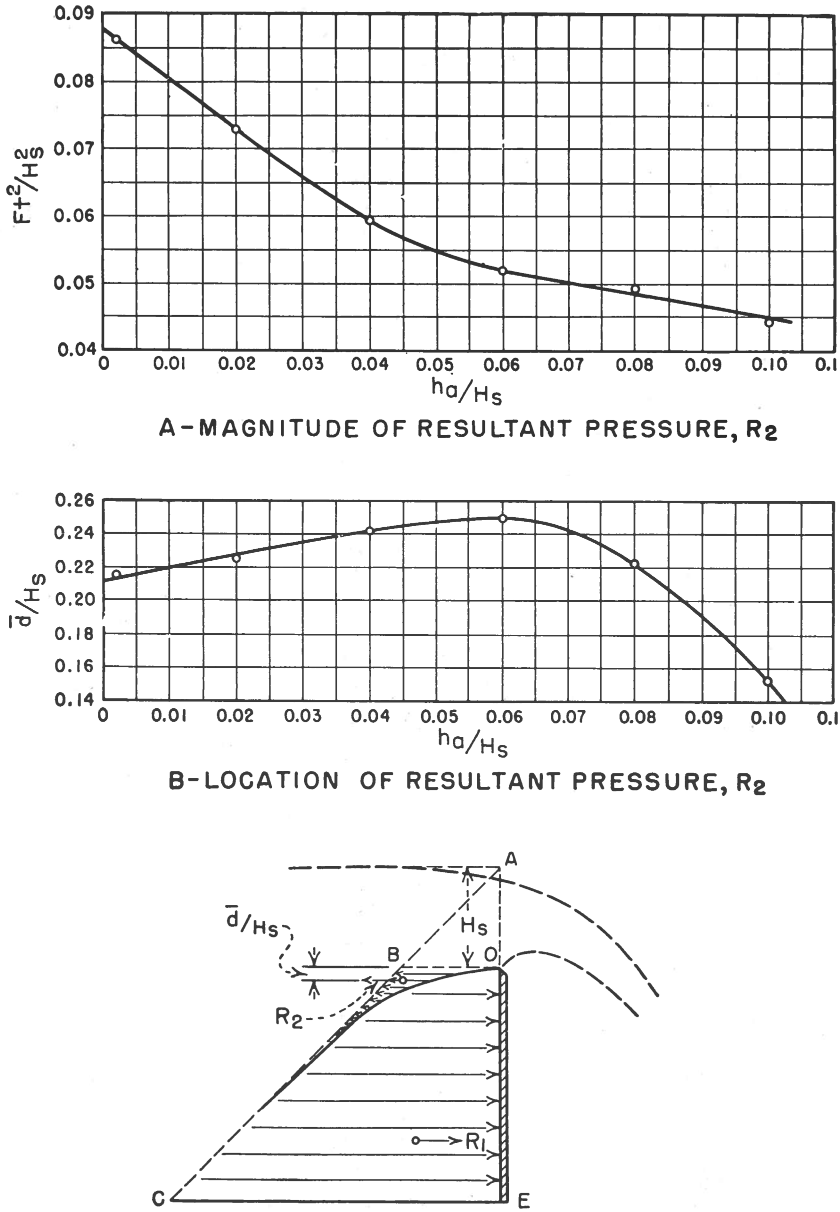

FIGURE 18.—RESULTANT OF PRESSURE-REDUCTION AREA—VERTICAL-FACE WEIR.

Example 1.—Given a maximum water surface at elevation 1,000.0 for a total discharge of 75,000 second-feet, with the average approach floor at elevation 880.0. Determine the crest elevation and coordinates for the shape of an overflow section with a crest length of 250 feet.

The solution is by successive approximations. First, assume a coefficient of discharge $C=3.75$. From the expression

$$Q=CLH_o^{3/2} \tag{12}$$

$$H_o^{3/2}=\frac{75{,}000}{3.75\times 250}=80.00$$

and

$$H_o=18.57 \text{ feet.}$$

Then

$$P+E=120.00-18.57=101.43 \text{ feet,}$$

$$\frac{H_o}{P+E}=\frac{18.57}{101.43}=0.183, \text{ and from figure 15–B, } C=3.96.$$

With this new value of C,

$$H_o^{3/2}=\frac{75{,}000}{3.96\times 250}=75.76,$$

and

$$H_o=17.90 \text{ feet.}$$

Then

$$P+E=120.00-17.90=102.10 \text{ feet,}$$

$$\frac{H_o}{P+E}=\frac{17.90}{102.10}=0.175, \text{ and from figure 15–B, } C=3.96.$$

It has now been established that the value of H_o is 17.90 and the coefficient of discharge, C, is 3.96. The crest of the spillway is then at 1,000−17.90, or elevation 982.10.

To determine H_s and $\frac{h_a}{H_s}$, first assume $H_s=H_o=17.90$ feet. Then the approximate value of h_a is computed as follows:

$$H_s+P=120.00 \text{ feet (approximate depth of approach).}$$

$$q=\frac{75{,}000}{250}=300 \text{ second-feet per foot of width,}$$

$$V_a=\frac{300}{120}=2.50 \text{ feet per second (velocity of approach),}$$

and

$$h_a=\frac{V_a^2}{2g}=0.097 \text{ feet and } \frac{h_a}{H_s}=\frac{0.097}{17.90}=0.0054.$$

From figure 15–A, $\frac{E}{H_s}=0.1125$.

Now,

$$H_o+E=H_s, \tag{13}$$

or

$$17.90+0.1125H_s=H_s$$

Then

$$H_s=\frac{17.90}{0.8875}=20.17 \text{ feet (first approximation).}$$

To obtain a more accurate value of V_a, the approach depth h_s+P should be used, which is also H_s+P-h_a, or $120.00-0.097=119.90$.

$$V_a=\frac{300}{119.90}=2.51 \text{ feet per second.}$$

Hence,

$$h_a=0.098 \text{ and } \frac{h_a}{H_s}=\frac{0.098}{20.17}=0.0049.$$

From figure 15–A,

$$\frac{E}{H_s}=0.113,$$

and

$$H_o+E=H_s \text{ or } 17.90+0.113\ H_s=H_s,$$

or

$$H_s=\frac{17.90}{0.887}=20.18 \text{ feet.}$$

Now $\frac{h_a}{H_s}=\frac{0.098}{20.18}=0.0049$, which agrees with the previous step. The final values are

$$\frac{h_a}{H_s}=0.0049 \text{ and } H_s=20.18.$$

In cases where the depth $P+E$ is small, see figure 15, more approximations will be needed to reach the final value of $\frac{h_a}{H_s}$ and H_s.

From the experimental results on lower nappe shapes for vertical weirs, table 12, values of $\frac{X}{H_s}$ are chosen, depending on the point spacing desired. These are tabulated in column 1 of table 3 and corresponding values of $\frac{Y}{H_s}$ are tabulated in column 2 for $\frac{h_a}{H_s}=0.0049$. By solving for X and Y from the values in columns 1 and 2, respectively, the coordinates for the overflow section, columns 3 and 4, are obtained. Column 5 expresses the values of Y in feet of elevation. The points are shown plotted in figure 19.

TABLE 3.—COORDINATES FOR OVERFLOW SECTION—EXAMPLE 1

$\frac{X}{H_s}$ 1	$\frac{Y}{H_s}$ 2	X, feet 3	Y, feet 4	Y, elevation, feet 5
0. 000	0. 0000	0. 00	0. 00	979. 86
0. 050	0. 0569	1. 01	1. 15	981. 01
0. 100	0. 0852	2. 02	1. 72	981. 58
0. 150	0. 1014	3. 03	2. 05	981. 91
0. 200	0. 1093	4. 04	2. 21	982. 07
0. 250	0. 1109	5. 05	2. 24	982. 10
0. 300	0. 1091	6. 05	2. 20	982. 06
0. 350	0. 1045	7. 06	2. 11	981. 97
0. 400	0. 0954	8. 07	1. 93	981. 79
0. 450	0. 0829	9. 08	1. 67	981. 53
0. 500	0. 069	10. 09	1. 39	981. 25
0. 600	0. 031	12. 11	0. 63	980. 49
0. 700	−0. 018	14. 13	−0. 36	979. 50
0. 800	−0. 075	16. 14	−1. 51	978. 55
0. 900	−0. 140	18. 18	−2. 83	977. 03
1. 000	−0. 215	20. 18	−4. 34	975. 52
1. 200	−0. 394	24. 22	−7. 95	971. 91
1. 400	−0. 607	28. 25	−12. 25	967. 61
1. 600	−0. 851	32. 29	−17. 17	962. 69
1. 800	−1. 133	36. 32	−22. 86	957. 00
2. 000	−1. 452	40. 36	−29. 30	950. 56
2. 200	−1. 799	44. 40	−36. 30	943. 56
2. 400	−2. 180	48. 43	−43. 99	935. 87
2. 600	−2. 603	52. 47	−52. 53	927. 33

The design of the straight portion of the spillway below the overflow section depends on the stability determinations and characteristics of the stilling pool at the toe of the spillway.

22. Determination of Wall Heights for Overflow Dam Section.— In designing spillway walls it is difficult, in some cases, to foresee the various factors which dictate the necessary height, such as diagonal waves propagated by piers, waves created at different gate openings, unsymmetrical flow produced by unequal approach conditions on the two sides of a spillway, unpredictable air currents, and waves created by unsymmetrical gate operation. The latter condition can be eliminated by operating the gates in a symmetrical manner; if all gates cannot be opened an equal amount, those that are opened should be chosen so as to produce a symmetrical pattern of flow. This procedure of gate operation is mandatory on Bureau projects. The extent of the effects of the remaining factors mentioned above, on the required wall height, can be determined satisfactorily only by a model study.

758318°—48——5

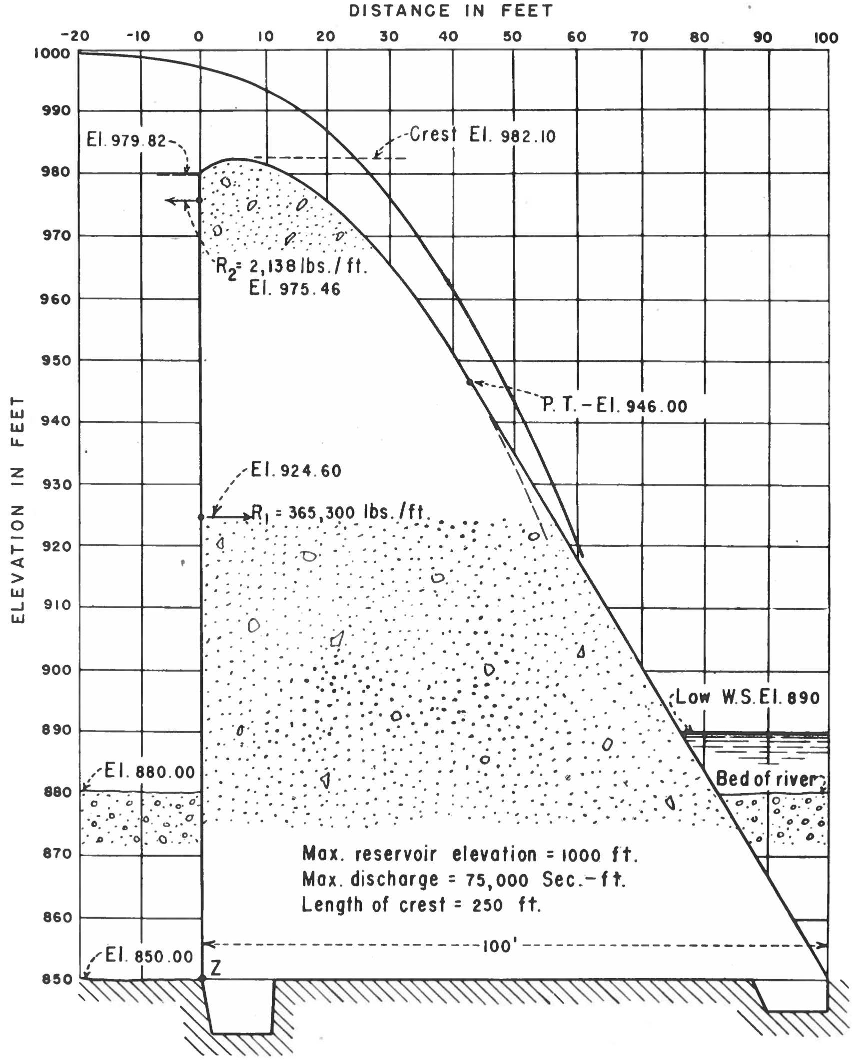

FIGURE 19.—RESULTS OF EXAMPLES 1, 2, AND 3—VERTICAL-FACE WEIR.

Example 2.—Determine the wall heights for the overflow dam section as designed in example 1.

As H_s and $\frac{h_a}{H_s}$ have been determined in example 1, it is necessary only to choose values of $\frac{X}{H_s}$ from the experimental upper-nappe results for vertical weirs, table 18, and record corresponding values of $\frac{Y}{H_s}$ for $\frac{h_a}{H_s}=0.0049$. The results are shown in column 1 and 2, table 4.

TABLE 4.—COORDINATES FOR UPPER SURFACE—EXAMPLE 2

$\frac{X}{H_s}$ 1	$\frac{Y}{H_s}$ 2	X, feet 3	Y, feet 4	Y, elevation, feet 5
−1. 000	0. 956	−20. 18	19. 29	999. 11
−0. 600	0. 928	−12. 11	18. 73	998. 55
−0. 300	0. 897	−6. 05	18. 10	997. 92
0. 000	0. 843	0. 00	17. 01	996. 83
0. 200	0. 788	4. 04	15. 90	995. 72
0. 400	0. 712	8. 07	14. 37	994. 19
0. 600	0. 617	12. 11	12. 45	992. 27
0. 800	0. 492	16. 14	9. 93	989. 75
1. 000	0. 342	20. 18	6. 90	986. 72
1. 200	0. 152	24. 22	3. 07	982. 89
1. 400	−0. 068	28. 25	−1. 37	978. 45
1. 600	−0. 318	32. 29	−6. 42	973. 40
1. 800	−0. 598	36. 32	−12. 07	967. 75
2. 000	−0. 905	40. 36	−18. 26	961. 56
2. 200	−1. 256	44. 40	−25. 35	954. 47
2. 400	−1. 653	48. 43	−33. 36	946. 46
2. 600	−2. 090	52. 47	−42. 18	937. 64
2. 800	−2. 553	56. 50	−51. 52	928. 30
3. 000	−3. 030	60. 54	−61. 15	918. 67

The values in column 3 and 4 were obtained by multiplying those in columns 1 and 2 by H_s, or 20.18. The points for the upper surface are also shown plotted in figure 19. This curve represents the actual water surface as obtained in the experiments, with near-perfect approach conditions and with little or no air absorption in the sheet of water. The amount of freeboard needed above this curve depends on the particular problem. Wave heights are difficult to predict. The expansion of the sheet of water due to air entrainment increases as the water accelerates, but it can be estimated with a reasonable degree of accuracy. In this connection, reference is made to a study by R. Ehrenberger,[17] to field observations by C. W. Thomas,[18] and to an analysis of the latter observations by V. L. Streeter.[19]

23. Determination of Pressure Reduction on Upstream Face of Dam.—

Example 3.—Determine the magnitude of the pressure reduction and the location of its resultant for the overflow section shown in figure 19.

[17] Enrenberger, R., Flow of Water in Steep Chutes with Special Reference to Self-Aeration. Osterreichischen Ingenieur und Architektenvereines No. 15/16 and 17/18, 1926. Translated by E. F. Wilsey in Bur. of Recl. Hyd. Lab. Report 29 (unpublished), October 1937.

[18] See footnote 11 in sec. 15.

[19] Streeter, V. L., Second Progress Report on Studies of the Flow of Water in Open Channels with High Gradients, Bur. Rec. Hyd. Lab. Report 40 (unpublished), October 13, 1938.

From the previous examples, $H_s=20.18$ feet and $\frac{h_a}{H_s}=0.0049$. Entering figure 18–A with the latter value, the pressure-reduction area *CBO*, expressed in terms of H_s^2, is found equal to 0.084.

The actual area is therefore $0.084\times(20.18)^2=34.2$ square feet, or 34.2 cubic feet of water per foot of dam. This is equal to a pressure reduction of $R_2=34.2\times62.5=2{,}138$ pounds per foot of dam length.

The position of the resultant of this negative force is located by entering figure 18–B with the same value of $\frac{h_a}{H_s}$. A value of $\frac{\bar{d}}{H_s}$ equal to 0.216 is obtained, which is the vertical distance from the point *O* to the centroid of the area *CBO*, expressed in terms of unit head. The position of the resultant pressure-reduction force, R_2, which acts in an upstream direction, is $\bar{d}=0.216\times20.18=4.36$ feet below point *O*, see figure 19.

This completes the solution to the above problem; however, as a matter of interest, the extent to which this small force reduces the overturning moment due to hydrostatic pressure acting on the upstream face of the dam will be investigated. If it is assumed that low water level downstream from the dam is elevation 890, see figure 19, it is not necessary to consider any hydrostatic forces below this point. The area *CBOE* in figure 18, considering the base at elevation 890, is equal to $\frac{20.18+110.0}{2}\times(110.0-20.18)=5{,}846$ square feet, and the hydrostatic pressure is $5{,}846\times62.5=365{,}375$ pounds per linear foot of dam.

The resultant of the force, designated as R_1, acts at the centroid of the area *CBOE*, elevation 924.6, shown in figure 19. The magnitude and location of the force R_2 are known from the above problem.

By taking moments about the base of the dam, point *Z* in figure 19, the reduction in the overturning moment, produced by the force R_2, is found equal to $\frac{2{,}138\times125.46}{365{,}375\times74.6}=0.00984$, or approximately 1 percent.

The relative importance of the force R_2 varies with the individual problem.

CHAPTER IV—WEIRS SLOPING DOWNSTREAM

ANALYSIS OF EXPERIMENTAL RESULTS

24. Weir Shapes Tested.—In continuation of the experimental study, three weirs with downstream slopes were tested to represent overflow dams with sloping upstream face, such as Imperial Dam on the Colorado River. (See Part IV, Bulletin 9, of this series.) The same weir plate was used as in the previous tests, except that it was placed on slopes of 1:3, 2:3, and 3:3, making angles with the vertical of 18.43°, 33.69°, and 45.0°, respectively, see figure 20. The knife edge was maintained on this weir for all three slopes. The experimental flume and the instrumentation were the same as for the vertical-weir tests, except that it was necessary to shift the lower coordinometer and shorten or lengthen the movable floor, depending on the weir.

25. Compilation of Nappe-Shape Results.—The test procedure and the compilation of the results for the three sloping weirs, shown in figure 20, were handled in the same manner as for the vertical weir. The material was prepared and the results were expressed for each weir in the same form as for the vertical weir. No additions nor changes in the terminology were necessary.

A summary of the tests made on the 1:3 sloping weir is shown in table 5, together with a compilation of all of Bazin's data on a weir having the same slope. The form is the same as that used for table 1. Nappe profiles were recorded for all runs shown in this table.

The X and Y coordinates for each run shown in table 5 were plotted to a large scale and smooth curves drawn through the points. Coordinate points were then read from the smooth curve for each run and divided by their respective values of H_s, thereby reducing all coordinates to unit head on the weir. The coordinates, in unit-head form, were then grouped as shown in table 6 and plotted, the relation $\frac{h_a}{H_s}$ being used as the criterion. An attempt was made to combine at least three runs made under different conditions of head and approach depth. The average line from each group was combined into a final set of nappe profiles for values of $\frac{h_a}{H_s}$ ranging from 0.002 to 0.20. The coordinates $\frac{X}{H_s}$ and $\frac{Y}{H_s}$ for the final lower-nappe-shape curves are tabulated for different values of $\frac{h_a}{H_s}$ in table 13. The coordinates

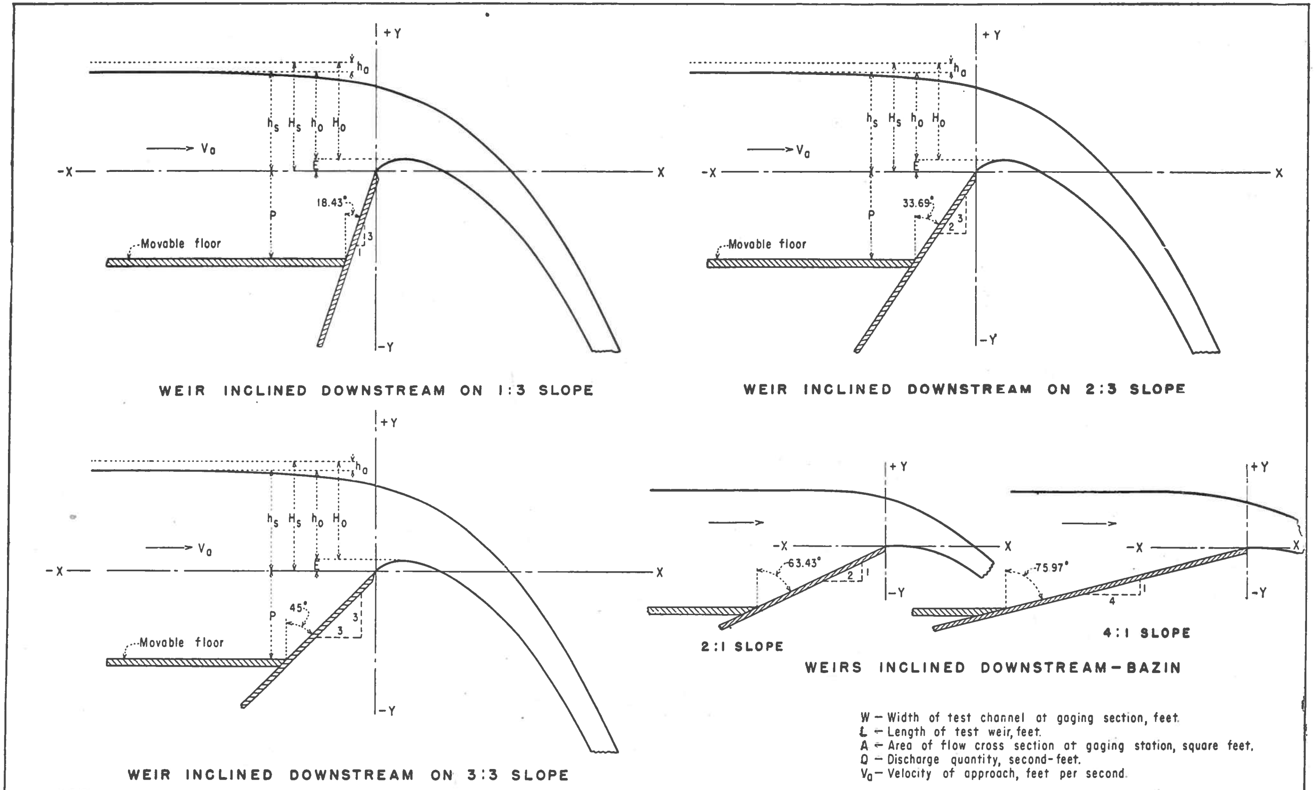

FIGURE 20.—PRINCIPAL ELEMENTS OF THE OVERFALL CREST FOR WEIR INCLINED DOWNSTREAM.

TABLE 5.—SUMMARY OF TESTS ON WEIR INCLINED DOWNSTREAM ON 1:3 SLOPE

1 TEST	2 P, FEET	3 Q, SECOND-FEET	4 W, FEET	5 h_s, FEET	6 A, SQUARE FEET	7 V, FEET PER SECOND	8 h_a, FEET	9 E, FEET	10 H_o, FEET
BUREAU OF RECLAMATION DATA									
13-1	5.08	4.118	2.069	0.698	11.955	0.344	0.0020	0.060	0.640
13-2	5.08	3.148		0.586	11.723	0.269	0.0010	0.052	0.535
13-3	5.08	2.700		0.528	11.603	0.233	0.0010	0.045	0.484
14-1	3.27	8.520		1.145	9.135	0.933	0.0135	0.098	1.061
15-1	2.51	4.725		0.763	6.772	0.698	0.0076	0.063	0.708
15-2	2.51	9.790		1.220	7.717	1.269	0.0251	0.105	1.140
15-3	2.49	9.925		1.239	7.715	1.286	0.0257	0.106	1.159
16-1	2.01	3.370		0.611	5.423	0.621	0.0060	0.050	0.567
16-2	2.01	6.805		0.960	6.145	1.107	0.0191	0.079	0.900
17-1	1.51	4.810		0.762	4.701	1.023	0.0163	0.063	0.715
17-2	1.49	9.863		1.204	5.574	1.769	0.0486	0.100	1.153
18-1	0.997	5.735		0.840	3.801	1.509	0.0354	0.070	0.805
18-2	0.992	9.980		1.185	4.504	2.216	0.0763	0.094	1.167
19-1	0.630	2.925		0.532	2.404	1.217	0.0230	0.047	0.508
19-2	0.630	5.000		0.751	2.857	1.750	0.0476	0.062	0.737
19-3	0.628	8.045		1.006	3.381	2.379	0.0880	0.073	1.021
20-1	0.554	9.690		1.115	3.453	2.806	0.1224	0.082	1.115
20-2	0.546	6.510		0.879	2.948	2.208	0.0758	0.068	0.887
21-1	0.397	2.665		0.496	1.848	1.442	0.0323	0.038	0.490
21-2	0.396	4.085		0.642	2.148	1.902	0.0562	0.050	0.648
21-3	0.393	6.350		0.840	2.551	2.489	0.0963	0.060	0.876
22-1	0.353	7.260		0.901	2.595	2.798	0.1217	0.062	0.961
23-1	0.320	4.400		0.660	2.028	2.170	0.0732	0.048	0.685
23-2	0.321	6.745		0.858	2.439	2.765	0.1189	0.060	0.917
24-1	0.266	6.490		0.822	2.251	2.883	0.1293	0.053	0.898
24-2	0.263	10.030		1.069	2.756	3.639	0.2059	0.064	1.211
25-1	0.232	2.810		0.495	1.504	1.868	0.0543	0.036	0.513
25-2	0.237	4.120		0.624	1.781	2.313	0.0832	0.040	0.667
25-3	0.234	6.000		0.778	2.094	2.865	0.1277	0.050	0.856
25-4	0.234	8.100		0.929	2.406	3.367	0.1763	0.057	1.048
26-1	0.171	7.680		0.886	2.187	3.512	0.1917	0.048	1.030
27-1	0.132	9.205		0.979	2.299	4.004	0.2492	0.046	1.182
27-2	0.141	6.335		0.780	1.906	3.324	0.1718	0.041	0.911
27-3	0.142	4.040		0.585	1.504	2.686	0.1122	0.035	0.662
27-4	0.146	2.940		0.486	1.308	2.248	0.0786	0.031	0.534
28-1	0.072	5.510		0.707	1.612	3.418	0.1816	0.024	0.865
28-2	0.076	3.035		0.484	1.159	2.619	0.1066	0.021	0.570
28-3	0.069	9.295		0.992	2.195	4.235	0.2789	0.023	1.248
BAZIN DATA (TYPICAL)									
14-1	3.717	6.392	3.281	0.666	14.382	0.444	0.0030	0.055	0.615
14-2	3.717	8.864		0.820	14.888	0.595	0.0056	0.075	0.751
14-3	3.717	11.583		0.981	15.415	0.751	0.0089	0.089	0.901
14-4	3.717	14.620		1.148	15.964	0.916	0.0131	0.101	1.060
14-5	3.717	17.657		1.306	16.481	1.072	0.0177	0.117	1.207
14-6	3.717	20.976		1.467	17.009	1.233	0.0236	0.136	1.355

TABLE 5.—SUMMARY OF TESTS ON WEIR INCLINED DOWNSTREAM ON 1:3 SLOPE—Continued

1 TEST	11 $H_o^{\frac{3}{2}}$	12 L, FEET	13 $LH_o^{\frac{3}{2}}$	14 C	15 $P+E$, FEET	16 $\frac{H_o}{P+E}$	17 H_s, FEET	18 $\frac{h_a}{H_s}$	19 $\frac{E}{H_s}$
		BUREAU OF RECLAMATION DATA							
13-1	0.512	2.017	1.033	3.986	5.140	0.125	0.700	0.0029	0.0857
13-2	0.391		0.789	3.990	5.132	0.104	0.587	0.0017	0.0886
13-3	0.337		0 680	3.971	5.125	0.094	0.529	0.0019	0.0851
14-1	1.093		2.205	3.864	3.368	0.315	1.1585	0.0117	0.0846
15-1	0.596		1.202	3.931	2.573	0.275	0.7706	0.0099	0.0818
15-2	1.217		2.455	3.988	2.615	0.436	1.2451	0.0201	0.0843
15-3	1.248		2.517	3.943	2.596	0.446	1.2647	0.0203	0.0838
16-1	0.427		0.861	3.914	2.060	0.275	0.6170	0.0097	0.0810
16-2	0.854		1.722	3.952	2.089	0.431	0.9791	0.0195	0.0807
17-1	0.605		1.220	3.943	1.573	0.455	0.7783	0.0209	0.0809
17-2	1.238		2.497	3.950	1.590	0.725	1.2526	0.0388	0.0798
18-1	0.7223		1.457	3.936	1.067	0.754	0.8754	0.0404	0.0800
18-2	1.2607		2.543	3.924	1.086	1.075	1.2613	0.0605	0.0745
19-1	0.3621		0.730	4.007	0.677	0.750	0.5550	0.0414	0.0847
19-2	0.6327		1.276	3.918	0.692	1.065	0.7986	0.0596	0.0776
19-3	1.0317		2.081	3.866	0.701	1.456	1.0940	0.0804	0.0667
20-1	1.2413		2.504	3.870	0.636	1.816	1.2374	0.0989	0.0663
20-2	0.8354		1.685	3.864	0.614	1.445	0.9548	0.0794	0.0712
21-1	0.3430		0.692	3.851	0.435	1.126	0.5283	0.0611	0.0719
21-2	0.5216		1.052	3.883	0.446	1.453	0.6982	0.0805	0.0716
21-3	0.8199		1.654	3.839	0.453	1.934	0.9363	0.1029	0.0641
22-1	0.9421		1.900	3.821	0.415	2.316	1.0227	0.1190	0.0606
23-1	0.5669		1.143	3.850	0.368	1.861	0.7332	0.0998	0.0655
23-2	0.8781		1.771	3.809	0.381	2.407	0.9769	0.1217	0.0614
24-1	0.8510		1.716	3.782	0.319	2.815	0.9513	0.1359	0.0557
24-2	1.3327		2 688	3 731	0.327	3.703	1 2749	0.1615	0.0502
25-1	0.3674		0.741	3.792	0.268	1.914	0.5493	0.0989	0.0655
25-2	0.5447		1.099	3.749	0.277	2.408	0.7072	0.1176	0.0566
25-3	0.7920		1 597	3.757	0.284	3.014	0.9057	0.1410	0.0552
25-4	1.0728		2.164	3.743	0.291	3.601	1.1053	0.1595	0.0516
26-1	1 0453		2.108	3.643	0.219	4.703	1.0777	0.1779	0.0445
27-1	1 2851		2 592	3.551	0.178	6.640	1.2282	0.2029	0.0375
27-2	0.8695		1.754	3.612	0.182	5.005	0.9518	0.1805	0.0431
27-3	0.5386		1.086	3.720	0.177	3.740	0.6972	0.1609	0.0502
27-4	0.3902		0.787	3.736	0.177	3.017	0.5646	0.1392	0.0549
28-1	0.8045		1.623	3.395	0.096	9.010	0.8886	0.2044	0.0270
28-2	0.4303		0.868	3.497	0.097	5.876	0.5906	0.1805	0.0356
28-3	1.3942		2.812	3.305	0.092	13.565	1.2709	0.2195	0.0181
		BAZIN DATA (TYPICAL)							
14-1	0.4821	3.281	1.582	4.046	3.772	0.163	0.6696	0.0044	0.0819
14-2	0.6502		2.133	4.162	3.792	0.198	0.8256	0.0068	0.0910
14-3	0.8557		2.808	4.122	3.806	0.237	0.9899	0.0090	0.0895
14-4	1.0913		3.581	4.084	3.818	0.278	1.1611	0.0113	0.0870
14-5	1.3254		4.349	4.059	3.834	0.315	1.3237	0.0134	0.0885
14-6	1.5765		5.172	4.057	3.853	0.352	1.4906	0.0159	0.0911

of the final upper-nappe-shape curves, which were obtained in the same manner, are listed in table 19.

The data for the 2:3 and 3:3 sloping weirs were treated in the same manner as those for the 1:3 sloping weir. Summaries of runs made on the 2:3 and 3:3 weirs are included as tables 7 and 8, respectively. The tables also include all of Bazin's work on weirs with these two slopes. The method of combining the nappe shape data for plotting from the 2:3 and 3:3 sloping weirs is shown in tables 9 and 10, respectively.

The final lower-nappe-shape coordinates, in terms of unit head, for the 2:3 and 3:3 sloping weirs are tabulated in tables 14 and 15, respectively. The final coordinates for the corresponding upper nappe shapes for various values of $\frac{h_a}{H_s}$ are listed in tables 20 and 21, respectively.

26. Bazin's Results on 2:1 and 4:1 Sloping Weirs.—In his experiments, Bazin included studies on weirs with downstream slopes of 2:1 and 4:1. These slopes were not included in this program, as they were not considered of sufficient importance to merit the expense involved. However, for the sake of completeness, Bazin's data have been included in table 11 for the 2:1 and 4:1 sloping weirs. Since only two approach depths were used, the data are meager. The maximum value of $\frac{h_a}{H_s}$ obtained by Bazin was 0.07, insufficient for the design of many low dams with moderate velocities of approach.

The X and Y coordinates, in terms of unit head, for the lower nappe shapes from Bazin's 2:1 and 4:1 downstream-sloping weirs are tabulated in tables 16 and 17, respectively. Similar coordinates for the 2:1 and 4:1 upper nappe shapes are listed in tables 22 and 23.

Tables 12, 13, 14, 15, 16, and 17, in which are tabulated lower coordinates for the vertical, 1:3, 2:3, 3:3, 2:1, and 4:1 weirs, have been grouped together to facilitate interpolation between tables. The same is true for tables 18, 19, 20, 21, 22, and 23, in which are tabulted coordinates of the upper nappe surface for the same weirs.

27. Relation of E to Velocity of Approach.—To facilitate interchange between the various heads, h_o, H_o, h_s, and H_s, the relation $\frac{E}{H_s}$ has been plotted with respect to $\frac{h_a}{H_s}$ in figure 21–A for the three sloping weirs tested. It is interesting to note that the value of E decreases as the angle of the weir is increased from the vertical, which means that the contraction at the under side of the jet decreases as the slope of the weir is flattened. The black triangles indicate Bazin's data on similar weirs. The agreement between these points and the recent data is quite satisfactory.

TABLE 6.—METHOD OF COMBINING NAPPE SHAPES FOR WEIR WITH 1:3 DOWNSTREAM SLOPE

TEST	H_s, FEET	P, FEET	ACTUAL h_a/H_s	PLOTTED h_a/H_s
13-1	0.700	5.08	0.0029	0.0020
13-2	0.587	5.08	0.0017	0.0020
13-3	0.529	5.08	0.0019	0.0020
14-1	1.1585	3.27	0.0117	0.0100
15-1	0.7706	2.51	0.0099	0.0100
16-1	0.6170	2.01	0.0097	0.0100
15-2	1.2451	2.51	0.0201	0.0200
15-3	1.2647	2.49	0.0203	0.0200
16-2	0.9791	2.01	0.0195	0.0200
17-1	0.7783	1.51	0.0209	0.0200
17-2	1.2526	1.49	0.0388	0.0400
18-1	0.8754	0.997	0.0404	0.0400
19-1	0.5550	0.630	0.0414	0.0400
18-2	1.2613	0.992	0.0605	0.0600
19-2	0.7986	0.630	0.0596	0.0600
21-1	0.5283	0.397	0.0611	0.0600
19-3	1.0940	0.628	0.0804	0.0800
20-2	0.9548	0.546	0.0794	0.0800
21-2	0.6982	0.396	0.0805	0.0800
20-1	1.2374	0.554	0.0989	0.1000
21-3	0.9363	0.393	0.1029	0.1000
23-1	0.7332	0.320	0.0998	0.1000
25-1	0.5493	0.232	0.0989	0.1000
22-1	1.0227	0.353	0.1190	0.1200
23-2	0.9769	0.321	0.1217	0.1200
25-2	0.7072	0.237	0.1176	0.1200
24-1	0.9513	0.266	0.1359	0.1400
25-3	0.9057	0.234	0.1410	0.1400
27-4	0.5646	0.146	0.1392	0.1400
24-2	1.2749	0.263	0.1615	0.1600
25-4	1.1053	0.234	0.1595	0.1600
27-3	0.6972	0.142	0.1609	0.1600
26-1	1.0777	0.171	0.1779	0.1800
27-2	0.9518	0.141	0.1805	0.1800
28-2	0.5906	0.076	0.1805	0.1800
27-1	1.2282	0.132	0.2029	0.2000
28-1	0.8886	0.072	0.2044	0.2000
28-3	1.2709	0.069	0.2195	0.2200

TABLE 7.—SUMMARY OF TESTS ON WEIR INCLINED DOWNSTREAM ON 2:3 SLOPE

1 TEST	2 P, FEET	3 Q, SECOND-FEET	4 W, FEET	5 h_s, FEET	6 A, SQUARE FEET	7 V, FEET PER SECOND	8 h_a, FEET	9 E, FEET	10 H_o, FEET	11 $H_o^{3/2}$	12 L, FEET	13 $LH_o^{3/2}$	14 C	15 P+E, FEET	16 $\frac{H_o}{P+E}$	17 H_s, FEET	18 $\frac{h_a}{H_s}$	19 $\frac{E}{H_s}$
									BUREAU OF RECLAMATION DATA									
29-1	4.724	4.410	2.069	0.714	11.2512	0.392	0.0024	0.044	0.6724	0.5514	2.000	1.1028	3.999	4.768	0.141	0.7164	0.0033	0.0614
29-2	4.721	3.330		0.597	11.0029	0.303	0.0014	0.037	0.5614	0.4206		0.8412	3.959	4.758	0.118	0.5984	0.0023	0.0618
29-3	4.721	2.730		0.523	10.8498	0.252	0.0010	0.033	0.4910	0.3441		0.6882	3.967	4.754	0.103	0.5240	0.0019	0.0630
30-1	2.482	9.510		1.181	7.5787	1.255	0.0245	0.068	1.1375	1.2132		2.4264	3.919	2.550	0.446	1.2055	0.0203	0.0564
31-1	2.007	6.750		0.942	6.1015	1.106	0.0190	0.057	0.9040	0.8595		1.7190	3.927	2.064	0.438	0.9610	0.0198	0.0593
32-1	1.511	4.405		0.705	4.5849	0.961	0.0143	0.042	0.6773	0.5574		1.1148	3.951	1.553	0.436	0.7193	0.0199	0.0584
33-1	0.885	8.005		1.012	3.9249	2.040	0.0647	0.058	1.0187	1.0282		2.0564	3.893	0.943	1.080	1.0767	0.0601	0.0539
34-1	0.635	4.785		0.715	2.7932	1.713	0.0457	0.044	0.7167	0.6067		1.2134	3.944	0.679	1.056	0.7607	0.0601	0.0578
35-1	0.476	7.490		0.933	2.9152	2.569	0.1026	0.051	0.9846	0.9770		1.9540	3.833	0.527	1.868	1.0356	0.0991	0.0492
36-1	0.405	2.455		0.457	1.7835	1.377	0.0295	0.027	0.4595	0.3115		0.6230	3.941	0.432	1.064	0.4865	0.0606	0.0555
36-2	0.406	6.010		0.801	2.4973	2.407	0.0901	0.047	0.8441	0.7755		1.5510	3.875	0.453	1.863	0.8911	0.1011	0.0527
37-1	0.328	4.180		0.630	1.9821	2.109	0.0691	0.031	0.6681	0.5461		1.0922	3.827	0.359	1.861	0.6991	0.0988	0.0443
38-1	0.278	6.800		0.834	2.3007	2.956	0.1358	0.042	0.9278	0.8937		1.7874	3.804	0.320	2.899	0.9698	0.1400	0.0433
39-1	0.239	7.610		0.878	2.3111	3.293	0.1686	0.044	1.0026	1.0039		2.0078	3.790	0.283	3.543	1.0466	0.1611	0.0420
40-1	0.238	5.600		0.731	2.0049	2.793	0.1213	0.033	0.8193	0.7416		1.4832	3.776	0.271	3.023	0.8523	0.1423	0.0387
41-1	0.175	5.050		0.670	1.7483	2.889	0.1297	0.026	0.7737	0.6805		1.3610	3.711	0.201	3.849	0.7997	0.1622	0.0325
41-2	0.174	6.515		0.779	1.9718	3.304	0.1697	0.035	0.9137	0.8734		1.7468	3.730	0.209	4.372	0.9487	0.1789	0.0369
42-1	0.151	3.050		0.493	1.3324	2.289	0.0814	0.022	0.5524	0.4105		0.8210	3.715	0.173	3.193	0.5744	0.1417	0.0383
42-2	0.151	4.040		0.582	1.5166	2.664	0.1103	0.025	0.6673	0.5451		1.0902	3.706	0.176	3.792	0.6923	0.1593	0.0361
43-1	0.127	4.150		0.580	1.4628	2.837	0.1251	0.019	0.6861	0.5683		1.1366	3.651	0.146	4.699	0.7051	0.1774	0.0269
43-2	0.128	6.255		0.748	1.8124	3.451	0.1851	0.028	0.9051	0.8611		1.7222	3.632	0.156	5.802	0.9331	0.1984	0.0300
44-1	0.086	3.005		0.476	1.1628	2.584	0.1038	0.011	0.5688	0.4291		0.8582	3.502	0.097	5.864	0.5798	0.1790	0.0190
44-2	0.084	4.705		0.626	1.4690	3.203	0.1595	0.013	0.7725	0.6790		1.3580	3.465	0.097	7.964	0.7855	0.2031	0.0165
									BAZIN DATA (TYPICAL)									
15-1	3.717	6.639	3.281	0.656	14.350	0.463	0.0033	0.040	0.619	0.487	3.281	1.598	4.155	3.757	0.165	0.6593	0.0050	0.0607
15-2	3.717	9.252		0.820	14.888	0.621	0.0059	0.049	0.777	0.685		2.247	4.117	3.766	0.206	0.8259	0.0072	0.0596
15-3	3.717	12.218		0.988	15.437	0.792	0.0098	0.062	0.936	0.906		2.973	4.110	3.779	0.248	0.9978	0.0099	0.0618
15-4	3.717	15.361		1.158	15.997	0.960	0.0144	0.069	1.104	1.160		3.806	4.036	3.786	0.292	1.1724	0.0123	0.0588
15-5	3.717	18.398		1.309	16.492	1.116	0.0194	0.082	1.246	1.391		4.564	4.031	3.799	0.328	1.3284	0.0146	0.0617
15-6	3.717	21.471		1.457	16.976	1.265	0.0249	0.089	1.393	1.644		5.394	3.981	3.806	0.366	1.4819	0.0168	0.0598

TABLE 8.—SUMMARY OF TESTS ON WEIR INCLINED DOWNSTREAM ON 3:3 SLOPE

1	2	3	4	5	6	7	8	9	10	11	12	13	14	15	16	17	18	19
TEST	P, FEET	Q, SECOND-FEET	W, FEET	h_s, FEET	A, SQUARE FEET	V, FEET PER SECOND	h_a, FEET	E, FEET	H_o, FEET	$H_o^{\frac{3}{2}}$	L, FEET	$LH_o^{\frac{3}{2}}$	C	$P+E$, FEET	$\frac{H_o}{P+E}$	H_s, FEET	$\frac{h_a}{H_s}$	$\frac{E}{H_s}$
							BUREAU OF RECLAMATION DATA											
45-1	4.221	4.015	2.069	0.665	10.1091	0.397	0.0025	0.029	0.6385	0.5102	2.000	1.0204	3.935	4.250	0.150	0.6675	0.0037	0.0434
45-2	4.222	2.990		0.549	9.8712	0.303	0.0014	0.023	0.5274	0.3830		0.7660	3.903	4.245	0.124	0.5504	0.0025	0.0418
45-3	4.224	2.820		0.527	9.8298	0.287	0.0013	0.021	0.5073	0.3613		0.7226	3.903	4.245	0.120	0.5283	0.0025	0.0398
46-1	2.484	8.905		1.118	7.4525	1.195	0.0222	0.048	1.0922	1.1414		2.2828	3.901	2.532	0.431	1.1402	0.0195	0.0421
47-1	2.017	6.950		0.950	6.1387	1.132	0.0200	0.041	0.9290	0.8954		1.7908	3.881	2.058	0.451	0.9700	0.0206	0.0423
48-1	1.522	4.510		0.706	4.6097	0.978	0.0148	0.033	0.6878	0.5704		1.1408	3.953	1.555	0.442	0.7208	0.0205	0.0458
49-1	0.884	7.635		0.969	3.8339	1.991	0.0617	0.042	0.9887	0.9831		1.9662	3.883	0.926	1.068	1.0307	0.0599	0.0407
50-1	0.626	4.465		0.676	2.6938	1.658	0.0427	0.029	0.6897	0.5728		1.1456	3.898	0.655	1.053	0.7187	0.0594	0.0404
51-1	0.468	7.010		0.880	2.7890	2.513	0.0982	0.038	0.9402	0.9117		1.8234	3.845	0.506	1.858	0.9782	0.1004	0.0388
52-1	0.384	5.405		0.737	2.3193	2.330	0.0844	0.031	0.7904	0.7027		1.4054	3.846	0.415	1.905	0.8214	0.1028	0.0377
52-2	0.387	2.255		0.431	1.6924	1.332	0.0276	0.019	0.4396	0.2915		0.5830	3.868	0.406	1.083	0.4586	0.0602	0.0414
53-1	0.317	3.925		0.598	1.8931	2.073	0.0668	0.023	0.6418	0.5142		1.0284	3.817	0.340	1.888	0.6648	0.1005	0.0346
54-1	0.273	6.290		0.784	2.1869	2.876	0.1286	0.030	0.8826	0.8291		1.6582	3.793	0.303	2.913	0.9126	0.1409	0.0329
55-1	0.259	7.565		0.870	2.3359	3.239	0.1631	0.034	0.9991	0.9987		1.9974	3.787	0.293	3.410	1.0331	0.1579	0.0329
56-1	0.235	6.250		0.771	2.0814	3.003	0.1402	0.031	0.8802	0.8258		1.6516	3.784	0.266	3.309	0.9112	0.1539	0.0340
57-1	0.179	4.340		0.596	1.6035	2.707	0.1139	0.023	0.6869	0.5693		1.1386	3.812	0.202	3.401	0.7099	0.1604	0.0324
57-2	0.170	6.035		0.734	1.8704	3.227	0.1619	0.028	0.8679	0.8086		1.6172	3.732	0.198	4.383	0.8959	0.1807	0.0313
58-1	0.150	2.665		0.443	1.2269	2.172	0.0733	0.015	0.5013	0.3549		0.7098	3.755	0.165	3.038	0.5163	0.1420	0.0291
58-2	0.151	3.520		0.521	1.3904	2.532	0.0997	0.018	0.6027	0.4679		0.9358	3.762	0.169	3.566	0.6207	0.1606	0.0290
58-3	0.151	4.860		0.631	1.6180	3.004	0.1403	0.022	0.7493	0.6486		1.2972	3.747	0.173	4.331	0.7713	0.1819	0.0285
59-1	0.132	5.310		0.659	1.6366	3.245	0.1637	0.022	0.8007	0.7165		1.4330	3.706	0.154	5.199	0.8227	0.1990	0.0267
60-1	0.080	2.110		0.370	0.9310	2.266	0.0798	0.010	0.4398	0.2917		0.5834	3.617	0.090	4.887	0.4498	0.1774	0.0222
60-2	0.079	3.150		0.473	1.1421	2.758	0.1182	0.014	0.5772	0.4385		0.8770	3.592	0.093	6.207	0.5912	0.1999	0.0237
							BAZIN DATA (TYPICAL)											
16-1	3.717	6.815	3.281	0.659	14.361	0.475	0.0036	0.026	0.6364	0.507	3.281	1.663	4.098	3.743	0.170	0.6626	0.0054	0.0396
16-2	3.717	9.676		0.830	14.920	0.649	0.0066	0.034	0.8031	0.720		2.362	4.097	3.750	0.214	0.8366	0.0078	0.0400
16-3	3.717	12.501		0.988	15.437	0.810	0.0102	0.041	0.9572	0.936		3.071	4.071	3.758	0.255	0.9982	0.0102	0.0411
16-4	3.717	15.679		1.155	15.986	0.981	0.0151	0.048	1.1219	1.188		3.898	4.022	3.765	0.298	1.1701	0.0129	0.0412
16-5	3.717	18.787		1.306	16.481	1.140	0.0203	0.057	1.2689	1.430		4.692	4.004	3.774	0.336	1.3263	0.0153	0.0433
16-6	3.717	21.365		1.431	16.890	1.265	0.0249	0.062	1.3936	1.646		5.401	3.956	3.779	0.369	1.4559	0.0171	0.0428
28-1	1.155	6.921		0.659	5.953	1.163	0.0210	0.028	0.6521	0.527		1.729	4.003	1.183	0.552	0.6800	0.0309	0.0410
28-2	1.155	13.101		0.991	7.040	1.861	0.0538	0.041	1.0038	1.006		3.301	3.969	1.196	0.839	1.0448	0.0515	0.0393
28-3	1.155	19.740		1.283	7.998	2.468	0.0948	0.053	1.3253	1.525		5.004	3.945	1.208	1.098	1.3778	0.0688	0.0381

TABLE 9.—METHOD OF COMBINING NAPPE SHAPES FOR WEIR WITH 2:3 DOWNSTREAM SLOPE

TEST	H_s, FEET	P, FEET	ACTUAL h_a/H_s	PLOTTED h_a/H_s
29-1	0.7164	4.724	0.0033	0.0020
29-2	0.5984	4.721	0.0023	0.0020
29-3	0.5240	4.721	0.0019	0.0020
30-1	1.2055	2.482	0.0203	0.0200
31-1	0.9610	2.007	0.0198	0.0200
32-1	0.7193	1.511	0.0199	0.0200
33-1	1.0767	0.885	0.0601	0.0600
34-1	0.7607	0.635	0.0601	0.0600
36-1	0.4865	0.405	0.0606	0.0600
35-1	1.0356	0.476	0.0991	0.1000
36-2	0.8911	0.406	0.1011	0.1000
37-1	0.6991	0.328	0.0988	0.1000
38-1	0.9698	0.278	0.1400	0.1400
40-1	0.8523	0.238	0.1423	0.1400
42-1	0.5744	0.151	0.1417	0.1400
39-1	1.0466	0.239	0.1611	0.1600
41-1	0.7997	0.175	0.1622	0.1600
42-2	0.6923	0.151	0.1593	0.1600
41-2	0.9487	0.174	0.1789	0.1800
43-1	0.7051	0.127	0.1774	0.1800
44-1	0.5798	0.086	0.1790	0.1800
43-2	0.9331	0.128	0.1984	0.2000
44-2	0.7855	0.084	0.2031	0.2000

TABLE 10.—METHOD OF COMBINING NAPPE SHAPES FOR WEIR WITH 3:3 DOWNSTREAM SLOPE

TEST	H_s, FEET	P, FEET	ACTUAL h_a/H_s	PLOTTED h_a/H_s
45-1	0.6675	4.221	0.0037	0.0020
45-2	0.5504	4.222	0.0025	0.0020
45-3	0.5283	4.224	0.0025	0.0020
46-1	1.1402	2.484	0.0195	0.0200
47-1	0.9700	2.017	0.0206	0.0200
48-1	0.7208	1.522	0.0205	0.0200
49-1	1.0307	0.884	0.0599	0.0600
50-1	0.7187	0.626	0.0594	0.0600
52-2	0.4586	0.387	0.0602	0.0600
51-1	0.9782	0.468	0.1004	0.1000
52-1	0.8214	0.384	0.1028	0.1000
53-1	0.6648	0.317	0.1005	0.1000
54-1	0.9126	0.273	0.1409	0.1400
58-1	0.5163	0.150	0.1420	0.1400
55-1	1.0331	0.259	0.1579	0.1600
57-1	0.7099	0.179	0.1604	0.1600
58-2	0.6207	0.151	0.1606	0.1600
57-2	0.8959	0.170	0.1807	0.1800
58-3	0.7713	0.151	0.1819	0.1800
60-1	0.4498	0.080	0.1774	0.1800
59-1	0.8227	0.132	0.1990	0.2000
60-2	0.5912	0.079	0.1999	0.2000

TABLE 11.—SUMMARY OF TESTS ON WEIRS WITH 2:1 AND 4:1 DOWNSTREAM SLOPES (BAZIN)

SERIES	P, METERS	H, METERS, STANDARD WEIR	Q, CUBIC METERS PER SECOND	h_s, METERS, EXPERIMENTAL WEIR	A, SQUARE METERS	V, METERS PER SECOND	h_a, METERS	$H_s = h_s + h_a$, METERS	E, METERS	$H_o = H_s - E$, METERS	$C = \frac{Q}{L H_o^{\frac{3}{2}}}$	$\frac{H_o}{P+E}$	$\frac{h_a}{H_s}$	$\frac{E}{H_s}$
							2:1 SLOPE							
17-1	1.137	0.226	0.203	0.205	1.342	0.1513	0.0012	0.2062	0.0020	0.2042	3.988	0.1793	0.0058	0.0097
17-2	1.137	0.331	0.361	0.302	1.439	0.2509	0.0032	0.3052	0.0035	0.3017	3.943	0.2645	0.0148	0.0115
17-3	1.137	0.438	0.551	0.401	1.538	0.3583	0.0065	0.4075	0.0053	0.4022	3.912	0.3521	0.0159	0.0130
29-1	0.351	0.225	0.201	0.203	0.554	0.3628	0.0067	0.2097	0.0040	0.2057	3.902	0.5794	0.0319	0.0191
29-2	0.351	0.337	0.370	0.299	0.650	0.5692	0.0165	0.3155	0.0054	0.3101	3.880	0.8701	0.0523	0.0171
29-3	0.351	0.445	0.564	0.390	0.741	0.7611	0.0295	0.4195	0.0120	0.4075	3.927	1.1226	0.0703	0.0286
							4:1 SLOPE							
18-1	1.133	0.225	0.201	0.208	1.341	0.1499	0.0011	0.2091	0.0003	0.2088	3.816	0.1842	0.0053	0.0014
18-2	1.133	0.328	0.355	0.304	1.437	0.2470	0.0031	0.3071	0.0006	0.3065	3.789	0.2704	0.0101	0.0020
18-3	1.133	0.433	0.542	0.404	1.537	0.3526	0.0063	0.4103	0.0011	0.4092	3.749	0.3608	0.0154	0.0027
30-1	0.348	0.218	0.192	0.202	0.550	0.3491	0.0062	0.2082	0.0002	0.2080	3.664	0.5974	0.0298	0.0010
30-2	0.348	0.330	0.359	0.299	0.647	0.5549	0.0157	0.3147	0.0006	0.3141	3.693	0.9010	0.0499	0.0019
30-3	0.348	0.451	0.577	0.404	0.752	0.7673	0.0300	0.4340	0.0014	0.4326	3.673	1.2381	0.0691	0.0032
			W = 1.0 METER				L = 1.0 METER							

TABLE 12.—COORDINATES OF LOWER NAPPE FOR DIFFERENT VALUES OF $\frac{h_a}{H_s}$ —VERTICAL WEIR

h_a/H_s → / X/H_s ↓	Y/H_s															
	0.002	0.010	0.020	0.030	0.040	0.050	0.060	0.070	0.080	0.090	0.100	0.120	0.140	0.160	0.180	0.200
0.000	0.0000	0.0000	0.0000	0.0000	0.0000	0.0000	0.0000	0.0000	0.0000	0.0000	0.0000	0.0000	0.0000	0.0000	0.0000	0.0000
0.010	0.0150	0.0146	0.0142	0.0138	0.0134	0.0130	0.0126	0.0122	0.0119	0.0115	0.0110	0.0105	0.0100	0.0090	0.0080	0.0070
0.020	0.0280	0.0273	0.0265	0.0258	0.0250	0.0242	0.0235	0.0228	0.0220	0.0210	0.0200	0.0185	0.0180	0.0160	0.0150	0.0133
0.030	0.0395	0.0386	0.0375	0.0362	0.0350	0.0335	0.0320	0.0310	0.0300	0.0285	0.0270	0.0255	0.0240	0.0220	0.0202	0.0187
0.040	0.0490	0.0477	0.0460	0.0450	0.0440	0.0420	0.0400	0.0390	0.0380	0.0360	0.0340	0.0320	0.0300	0.0280	0.0258	0.0240
0.050	0.0575	0.0559	0.0540	0.0525	0.0510	0.0490	0.0470	0.0455	0.0440	0.0419	0.0398	0.0375	0.0355	0.0323	0.0300	0.0280
0.060	0.0650	0.0630	0.0605	0.0588	0.0570	0.0550	0.0530	0.0515	0.0500	0.0473	0.0447	0.0420	0.0400	0.0363	0.0340	0.0315
0.070	0.0710	0.0678	0.0660	0.0642	0.0625	0.0602	0.0580	0.0560	0.0540	0.0520	0.0500	0.0460	0.0435	0.0400	0.0373	0.0343
0.080	0.0765	0.0745	0.0720	0.0695	0.0670	0.0650	0.0630	0.0608	0.0585	0.0562	0.0540	0.0500	0.0470	0.0430	0.0400	0.0370
0.090	0.0820	0.0796	0.0765	0.0742	0.0720	0.0695	0.0670	0.0645	0.0620	0.0597	0.0575	0.0538	0.0500	0.0460	0.0422	0.0390
0.100	0.0860	0.0838	0.0810	0.0785	0.0760	0.0735	0.0710	0.0682	0.0655	0.0628	0.0602	0.0562	0.0520	0.0480	0.0445	0.0407
0.110	0.0900	0.0878	0.0850	0.0820	0.0790	0.0765	0.0740	0.0712	0.0685	0.0658	0.0630	0.0582	0.0543	0.0500	0.0460	0.0420
0.120	0.0940	0.0913	0.0880	0.0852	0.0825	0.0798	0.0770	0.0742	0.0715	0.0685	0.0655	0.0603	0.0560	0.0510	0.0470	0.0434
0.130	0.0975	0.0948	0.0915	0.0882	0.0850	0.0822	0.0795	0.0765	0.0735	0.0703	0.0670	0.0620	0.0568	0.0518	0.0480	0.0440
0.140	0.1000	0.0973	0.0940	0.0910	0.0880	0.0850	0.0820	0.0788	0.0755	0.0721	0.0686	0.0638	0.0580	0.0530	0.0482	0.0442
0.150	0.1025	0.0996	0.0960	0.0930	0.0900	0.0868	0.0835	0.0802	0.0770	0.0735	0.0700	0.0642	0.0586	0.0540	0.0484	0.0446
0.160	0.1045	0.1016	0.0980	0.0950	0.0920	0.0882	0.0845	0.0812	0.0780	0.0748	0.0716	0.0658	0.0595	0.0543	0.0490	0.0450
0.170	0.1065	0.1034	0.0995	0.0965	0.0935	0.0898	0.0860	0.0828	0.0795	0.0757	0.0720	0.0660	0.0598	0.0542	0.0490	0.0448
0.180	0.1080	0.1049	0.1010	0.0978	0.0945	0.0908	0.0870	0.0835	0.0800	0.0765	0.0730	0.0668	0.0600	0.0541	0.0488	0.0440
0.190	0.1095	0.1062	0.1020	0.0988	0.0955	0.0915	0.0875	0.0840	0.0805	0.0772	0.0739	0.0670	0.0600	0.0540	0.0482	0.0438
0.200	0.1105	0.1072	0.1030	0.0998	0.0965	0.0922	0.0880	0.0848	0.0815	0.0778	0.0740	0.0670	0.0599	0.0540	0.0480	0.0436
0.210	0.1115	0.1082	0.1040	0.1005	0.0970	0.0925	0.0880	0.0850	0.0820	0.0781	0.0742	0.0663	0.0598	0.0538	0.0478	0.0425
0.220	0.1120	0.1084	0.1040	0.1008	0.0975	0.0930	0.0885	0.0852	0.0820	0.0781	0.0742	0.0661	0.0590	0.0530	0.0467	0.0417
0.230	0.1120	0.1087	0.1045	0.1012	0.0980	0.0932	0.0885	0.0852	0.0820	0.0781	0.0741	0.0660	0.0580	0.0520	0.0460	0.0403
0.240	0.1120	0.1089	0.1050	0.1015	0.0980	0.0930	0.0880	0.0848	0.0815	0.0778	0.0740	0.0650	0.0577	0.0510	0.0450	0.0390
0.250	0.1120	0.1089	0.1050	0.1012	0.0975	0.0928	0.0880	0.0845	0.0810	0.0767	0.0725	0.0640	0.0566	0.0500	0.0440	0.0380
0.260	0.1120	0.1087	0.1045	0.1010	0.0975	0.0925	0.0875	0.0838	0.0800	0.0760	0.0720	0.0635	0.0560	0.0487	0.0424	0.0365
0.270	0.1120	0.1084	0.1040	0.1005	0.0970	0.0920	0.0870	0.0832	0.0795	0.0752	0.0710	0.0620	0.0545	0.0478	0.0416	0.0355
0.280	0.1115	0.1082	0.1040	0.1000	0.0960	0.0910	0.0860	0.0820	0.0780	0.0740	0.0700	0.0610	0.0535	0.0460	0.0400	0.0340
0.290	0.1110	0.1077	0.1035	0.0995	0.0955	0.0905	0.0855	0.0815	0.0775	0.0729	0.0683	0.0598	0.0520	0.0447	0.0380	0.0320
0.300	0.1105	0.1067	0.1020	0.0980	0.0940	0.0892	0.0845	0.0802	0.0760	0.0716	0.0673	0.0580	0.0503	0.0433	0.0364	0.0300
0.310	0.1100	0.1062	0.1015	0.0972	0.0930	0.0880	0.0830	0.0790	0.0750	0.0705	0.0660	0.0570	0.0490	0.0418	0.0350	0.0283
0.320	0.1090	0.1052	0.1005	0.0962	0.0920	0.0870	0.0820	0.0778	0.0735	0.0688	0.0642	0.0555	0.0477	0.0400	0.0330	0.0270
0.330	0.1080	0.1042	0.0995	0.0948	0.0900	0.0850	0.0800	0.0760	0.0720	0.0671	0.0623	0.0538	0.0458	0.0380	0.0310	0.0250
0.340	0.1070	0.1030	0.0980	0.0932	0.0885	0.0835	0.0785	0.0742	0.0700	0.0652	0.0604	0.0520	0.0440	0.0360	0.0290	0.0230
0.350	0.1060	0.1018	0.0965	0.0918	0.0870	0.0820	0.0770	0.0728	0.0685	0.0636	0.0586	0.0500	0.0420	0.0340	0.0270	0.0207
0.360	0.1040	0.1000	0.0950	0.0902	0.0855	0.0802	0.0750	0.0710	0.0670	0.0620	0.0570	0.0480	0.0397	0.0320	0.0245	0.0180
0.370	0.1025	0.0973	0.0930	0.0882	0.0835	0.0785	0.0735	0.0692	0.0650	0.0599	0.0548	0.0458	0.0373	0.0297	0.0220	0.0160
0.380	0.1010	0.0966	0.0910	0.0862	0.0815	0.0762	0.0710	0.0668	0.0625	0.0574	0.0524	0.0437	0.0353	0.0274	0.0200	0.0140
0.390	0.0990	0.0946	0.0890	0.0842	0.0795	0.0742	0.0690	0.0645	0.0600	0.0550	0.0500	0.0410	0.0328	0.0245	0.0177	0.0105

TABLE 12.—COORDINATES OF LOWER NAPPE FOR DIFFERENT VALUES OF $\frac{h_a}{H_s}$—VERTICAL WEIR—Continued

	Y/H_s															
X/H_s \ h_a/H_s	0.002	0.010	0.020	0.030	0.040	0.050	0.060	0.070	0.080	0.090	0.100	0.120	0.140	0.160	0.180	0.200
0.400	0.0970	0.0926	0.0870	0.0820	0.0770	0.0720	0.0670	0.0625	0.0580	0.0530	0.0480	0.0386	0.0303	0.0220	0.0146	0.0080
0.410	0.0945	0.0901	0.0845	0.0798	0.0750	0.0695	0.0640	0.0600	0.0560	0.0509	0.0458	0.0360	0.0280	0.0197	0.0120	0.0057
0.420	0.0920	0.0876	0.0820	0.0772	0.0725	0.0672	0.0620	0.0575	0.0530	0.0480	0.0430	0.0340	0.0250	0.0164	0.0090	0.0025
0.430	0.0900	0.0856	0.0800	0.0750	0.0700	0.0648	0.0595	0.0550	0.0505	0.0452	0.0400	0.0310	0.0220	0.0140	0.0060	0.0000
0.440	0.0870	0.0828	0.0775	0.0727	0.0680	0.0622	0.0565	0.0522	0.0480	0.0425	0.0370	0.0280	0.0195	0.0110	0.0030	-0.0034
0.450	0.0845	0.0801	0.0745	0.0697	0.0650	0.0595	0.0540	0.0495	0.0450	0.0395	0.0340	0.0250	0.0163	0.0080	0.0000	-0.0060
0.460	0.0820	0.0773	0.0715	0.0667	0.0620	0.0568	0.0515	0.0468	0.0420	0.0367	0.0315	0.0220	0.0138	0.0042	-0.0038	-0.0093
0.470	0.0790	0.0746	0.0690	0.0640	0.0590	0.0535	0.0480	0.0435	0.0390	0.0335	0.0280	0.0183	0.0100	0.0010	-0.0064	-0.0120
0.480	0.0760	0.0716	0.0660	0.0610	0.0560	0.0508	0.0455	0.0408	0.0360	0.0306	0.0253	0.0155	0.0060	-0.0020	-0.0100	-0.0160
0.490	0.0735	0.0691	0.0635	0.0585	0.0535	0.0478	0.0420	0.0372	0.0325	0.0272	0.0220	0.0120	0.0022	-0.0060	-0.0140	-0.0196
0.500	0.070	0.066	0.060	0.055	0.050	0.044	0.039	0.034	0.030	0.024	0.018	0.008	-0.001	-0.010	-0.018	-0.023
0.520	0.064	0.060	0.054	0.048	0.043	0.038	0.032	0.027	0.022	0.017	0.012	0.001	-0.008	-0.018	-0.025	-0.030
0.540	0.056	0.052	0.046	0.041	0.036	0.030	0.025	0.020	0.015	0.010	0.004	-0.005	-0.017	-0.026	-0.034	-0.038
0.560	0.048	0.044	0.039	0.034	0.028	0.022	0.017	0.012	0.007	0.002	-0.004	-0.015	-0.025	-0.035	-0.042	-0.046
0.580	0.040	0.036	0.031	0.026	0.020	0.014	0.009	0.003	-0.002	-0.007	-0.013	-0.024	-0.034	-0.044	-0.050	-0.055
0.600	0.032	0.028	0.022	0.017	0.012	0.006	0.000	-0.005	-0.010	-0.016	-0.022	-0.032	-0.043	-0.052	-0.059	-0.064
0.620	0.024	0.019	0.013	0.008	0.002	-0.003	-0.009	-0.014	-0.020	-0.025	-0.031	-0.042	-0.052	-0.062	-0.068	-0.072
0.640	0.014	0.010	0.004	-0.001	-0.007	-0.012	-0.018	-0.023	-0.028	-0.034	-0.040	-0.051	-0.062	-0.071	-0.078	-0.082
0.660	0.004	0.000	-0.006	-0.012	-0.018	-0.023	-0.028	-0.033	-0.038	-0.044	-0.050	-0.060	-0.071	-0.081	-0.088	-0.091
0.680	-0.006	-0.011	-0.017	-0.022	-0.028	-0.033	-0.038	-0.043	-0.048	-0.054	-0.061	-0.070	-0.081	-0.091	-0.098	-0.101
0.700	-0.016	-0.021	-0.028	-0.033	-0.038	-0.044	-0.049	-0.054	-0.059	-0.065	-0.071	-0.081	-0.091	-0.102	-0.108	-0.111
0.720	-0.027	-0.032	-0.038	-0.044	-0.049	-0.054	-0.060	-0.065	-0.070	-0.076	-0.082	-0.092	-0.102	-0.112	-0.118	-0.122
0.740	-0.038	-0.043	-0.049	-0.054	-0.060	-0.066	-0.072	-0.076	-0.081	-0.087	-0.093	-0.103	-0.114	-0.124	-0.130	-0.132
0.760	-0.050	-0.055	-0.061	-0.066	-0.072	-0.078	-0.083	-0.088	-0.092	-0.098	-0.105	-0.115	-0.125	-0.135	-0.141	-0.143
0.780	-0.062	-0.066	-0.072	-0.078	-0.083	-0.089	-0.095	-0.100	-0.104	-0.110	-0.116	-0.127	-0.137	-0.146	-0.152	-0.154
0.800	-0.074	-0.078	-0.084	-0.090	-0.095	-0.102	-0.108	-0.112	-0.117	-0.122	-0.128	-0.139	-0.150	-0.159	-0.164	-0.166
0.820	-0.086	-0.091	-0.097	-0.102	-0.108	-0.114	-0.120	-0.125	-0.130	-0.136	-0.142	-0.152	-0.162	-0.171	-0.177	-0.178
0.840	-0.098	-0.103	-0.110	-0.116	-0.121	-0.127	-0.133	-0.138	-0.142	-0.148	-0.154	-0.164	-0.175	-0.184	-0.189	-0.189
0.860	-0.112	-0.116	-0.122	-0.128	-0.134	-0.140	-0.146	-0.151	-0.156	-0.162	-0.168	-0.178	-0.188	-0.197	-0.202	-0.202
0.880	-0.125	-0.130	-0.136	-0.142	-0.148	-0.154	-0.159	-0.164	-0.169	-0.175	-0.181	-0.192	-0.202	-0.210	-0.215	-0.215
0.900	-0.138	-0.143	-0.150	-0.156	-0.162	-0.168	-0.173	-0.178	-0.183	-0.189	-0.195	-0.206	-0.216	-0.224	-0.228	-0.228
0.920	-0.152	-0.157	-0.164	-0.170	-0.176	-0.182	-0.188	-0.192	-0.197	-0.203	-0.210	-0.220	-0.230	-0.238	-0.242	-0.241
0.940	-0.167	-0.172	-0.179	-0.184	-0.190	-0.196	-0.202	-0.207	-0.212	-0.218	-0.224	-0.234	-0.244	-0.253	-0.255	-0.254
0.960	-0.182	-0.187	-0.193	-0.199	-0.205	-0.210	-0.216	-0.221	-0.226	-0.232	-0.238	-0.249	-0.258	-0.268	-0.270	-0.268
0.980	-0.198	-0.202	-0.208	-0.214	-0.220	-0.226	-0.231	-0.236	-0.242	-0.248	-0.254	-0.264	-0.274	-0.283	-0.284	-0.283
1.00	-0.214	-0.218	-0.224	-0.230	-0.236	-0.242	-0.247	-0.252	-0.258	-0.264	-0.270	-0.279	-0.290	-0.300	-0.299	-0.298
1.05	-0.256	-0.260	-0.266	-0.272	-0.278	-0.283	-0.288	-0.293	-0.298	-0.304	-0.310	-0.320	-0.330	-0.339	-0.339	-0.337
1.10	-0.300	-0.304	-0.310	-0.315	-0.320	-0.325	-0.330	-0.335	-0.340	-0.346	-0.352	-0.362	-0.372	-0.382	-0.379	-0.377
1.15	-0.345	-0.349	-0.354	-0.360	-0.365	-0.370	-0.375	-0.380	-0.384	-0.390	-0.396	-0.406	-0.417	-0.426	-0.426	-0.417
1.20	-0.393	-0.397	-0.402	-0.407	-0.412	-0.417	-0.422	-0.427	-0.432	-0.438	-0.443	-0.452	-0.463	-0.471	-0.466	-0.460

TABLE 12.—COORDINATES OF LOWER NAPPE FOR DIFFERENT VALUES OF $\frac{h_a}{H_s}$—VERTICAL WEIR—Continued

h_a/H_s → / X/H_s ↓	Y/H_s: 0.002	0.010	0.020	0.030	0.040	0.050	0.060	0.070	0.080	0.090	0.100	0.120	0.140	0.160	0.180	0.200
1.25	-0.443	-0.447	-0.452	-0.457	-0.462	-0.467	-0.472	-0.476	-0.481	-0.486	-0.492	-0.501	-0.513	-0.520	-0.514	-0.504
1.30	-0.495	-0.499	-0.504	-0.508	-0.513	-0.518	-0.522	-0.526	-0.531	-0.537	-0.543	-0.553	-0.563	-0.568	-0.561	-0.551
1.35	-0.550	-0.554	-0.558	-0.562	-0.567	-0.572	-0.576	-0.580	-0.585	-0.591	-0.596	-0.606	-0.616	-0.619	-0.611	-0.600
1.40	-0.606	-0.610	-0.614	-0.618	-0.623	-0.628	-0.632	-0.636	-0.641	-0.646	-0.650	-0.660	-0.670	-0.672	-0.662	-0.650
1.45	-0.664	-0.668	-0.672	-0.677	-0.682	-0.686	-0.690	-0.694	-0.699	-0.703	-0.708	-0.726	-0.726	-0.726	-0.714	-0.703
1.50	-0.724	-0.728	-0.733	-0.737	-0.741	-0.746	-0.750	-0.754	-0.758	-0.763	-0.769	-0.784	-0.784	-0.784	-0.769	-0.758
1.55	-0.785	-0.789	-0.795	-0.799	-0.803	-0.807	-0.811	-0.815	-0.819	-0.824	-0.830	-0.843	-0.843	-0.842	-0.827	-0.817
1.60	-0.850	-0.854	-0.860	-0.864	-0.867	-0.870	-0.874	-0.878	-0.883	-0.889	-0.895	-0.904	-0.904	-0.904	-0.886	-0.874
1.65	-0.917	-0.921	-0.926	-0.930	-0.934	-0.938	-0.941	-0.946	-0.950	-0.955	-0.961	-0.970	-0.968	-0.964	-0.946	-0.933
1.70	-0.987	-0.991	-0.995	-0.998	-1.002	-1.006	-1.010	-1.014	-1.019	-1.023	-1.027	-1.037	-1.034	-1.026	-1.008	-0.996
1.75	-1.058	-1.062	-1.066	-1.070	-1.074	-1.078	-1.082	-1.086	-1.090	-1.093	-1.096	-1.104	-1.102	-1.090	-1.074	-1.060
1.80	-1.132	-1.136	-1.140	-1.144	-1.147	-1.152	-1.156	-1.160	-1.164	-1.167	-1.169	-1.178	-1.174	-1.158	-1.143	-1.127
1.85	-1.207	-1.211	-1.216	-1.220	-1.224	-1.228	-1.232	-1.236	-1.241	-1.243	-1.246	-1.252	-1.246	-1.226	-1.214	-1.196
1.90	-1.287	-1.290	-1.293	-1.297	-1.301	-1.306	-1.310	-1.315	-1.320	-1.322	-1.325	-1.329	-1.320	-1.300	-1.286	-1.266
1.95	-1.368	-1.371	-1.375	-1.378	-1.382	-1.387	-1.392	-1.396	-1.401	-1.403	-1.405	-1.408	-1.398	-1.374	-1.361	-1.337
2.00	-1.451	-1.455	-1.460	-1.464	-1.467	-1.472	-1.476	-1.480	-1.485	-1.486	-1.488	-1.490	-1.480	-1.451	-1.439	-1.411
2.05	-1.536	-1.540	-1.544	-1.584	-1.551	-1.556	-1.560	-1.564	-1.568	-1.570	-1.572	-1.574	-1.562	-1.530	-1.518	-1.486
2.10	-1.621	-1.625	-1.630	-1.634	-1.638	-1.642	-1.645	-1.649	-1.653	-1.657	-1.662	-1.660	-1.648	-1.614	-1.600	-1.566
2.15	-1.708	-1.712	-1.716	-1.721	-1.726	-1.730	-1.734	-1.738	-1.743	-1.747	-1.750	-1.746	-1.732	-1.699	-1.682	-1.646
2.20	-1.798	-1.802	-1.807	-1.812	-1.816	-1.820	-1.825	-1.830	-1.834	-1.736	-1.838	-1.834	-1.820	-1.785	-1.766	-1.728
2.25	-1.890	-1.895	-1.901	-1.906	-1.910	-1.914	-1.918	-1.922	-1.927	-1.926	-1.926	-1.920	-1.906	-1.873	-1.854	-1.810
2.30	-1.986	-1.990	-1.996	-2.001	-2.005	-2.008	-2.012	-2.016	-2.020	-2.019	-2.018	-2.012	-1.994	-1.962	-1.942	-1.896
2.35	-2.081	-2.086	-2.092	-2.097	-2.102	-2.105	-2.108	-2.112	-2.116	-2.115	-2.115	-2.106	-2.088	-2.054	-2.032	-1.984
2.40	-2.179	-2.183	-2.188	-2.193	-2.198	-2.202	-2.206	-2.209	-2.212	-2.212	-2.212	-2.200	-2.180	-2.147	-2.124	-2.074
2.45	-2.280	-2.284	-2.288	-2.294	-2.299	-2.302	-2.306	-2.310	-2.313	-2.312	-2.312	-2.296	-2.276	-2.240	-2.218	-2.165
2.50	-2.384	-2.388	-2.394	-2.400	-2.405	-2.408	-2.410	-2.412	-2.414	-2.414	-2.414	-2.394	-2.371	-2.334	-2.313	-2.257
2.55	-2.490	-2.495	-2.501	-2.508	-2.514	-2.514	-2.514	-2.515	-2.516	-2.516	-2.516	-2.492	-2.468	-2.430	-2.408	-2.350
2.60	-2.602	-2.606	-2.611	-2.617	-2.622	-2.622	-2.621	-2.620	-2.620	-2.614	-2.608	-2.593	-2.568	-2.525	-2.503	-2.444
2.65	-2.712	-2.717	-2.723	-2.728	-2.733	-2.731	-2.728	-2.728	-2.727	-2.626	-2.724	-2.695	-2.668	-2.624	-2.601	-2.540
2.70	-2.824	-2.829	-2.836	-2.840	-2.844	-2.840	-2.836	-2.836	-2.835	-2.832	-2.828	-2.800	-2.770	-2.720	-2.698	-2.637

758318°—48——6

TABLE 13.—COORDINATES OF LOWER NAPPE FOR DIFFERENT VALUES OF $\frac{h_a}{H_s}$ —1:3 WEIR

	Y/H_s															
X/H_s \ h_a/H_s	0.002	0.010	0.020	0.030	0.040	0.050	0.060	0.070	0.080	0.090	0.100	0.120	0.140	0.160	0.180	0.200
0.000	0.000	0.000	0.000	0.000	0.000	0.000	0.000	0.000	0.000	0.000	0.000	0.000	0.000	0.000	0.000	0.000
0.010	0.016	0.016	0.015	0.014	0.013	0.012	0.011	0.011	0.010	0.010	0.010	0.009	0.008	0.008	0.007	0.006
0.020	0.026	0.025	0.025	0.025	0.024	0.023	0.022	0.022	0.021	0.020	0.019	0.017	0.016	0.015	0.013	0.010
0.030	0.036	0.034	0.033	0.032	0.031	0.031	0.030	0.029	0.028	0.027	0.026	0.024	0.023	0.021	0.018	0.016
0.040	0.042	0.042	0.040	0.039	0.038	0.038	0.037	0.036	0.035	0.034	0.033	0.030	0.029	0.026	0.023	0.018
0.050	0.048	0.048	0.046	0.045	0.044	0.043	0.042	0.041	0.040	0.039	0.038	0.036	0.034	0.031	0.026	0.021
0.060	0.054	0.052	0.051	0.050	0.049	0.048	0.047	0.046	0.045	0.044	0.043	0.040	0.038	0.034	0.030	0.024
0.070	0.058	0.057	0.055	0.054	0.053	0.052	0.051	0.051	0.050	0.049	0.047	0.044	0.041	0.038	0.033	0.027
0.080	0.062	0.061	0.059	0.058	0.057	0.056	0.055	0.054	0.053	0.052	0.050	0.047	0.044	0.040	0.036	0.028
0.090	0.066	0.065	0.063	0.063	0.062	0.060	0.058	0.057	0.056	0.055	0.053	0.050	0.047	0.042	0.038	0.030
0.100	0.069	0.067	0.066	0.065	0.064	0.063	0.061	0.060	0.058	0.057	0.056	0.052	0.049	0.044	0.039	0.032
0.110	0.072	0.070	0.068	0.067	0.066	0.065	0.064	0.063	0.061	0.060	0.058	0.054	0.050	0.046	0.041	0.032
0.120	0.074	0.072	0.070	0.069	0.068	0.067	0.066	0.064	0.062	0.061	0.059	0.056	0.052	0.047	0.042	0.034
0.130	0.076	0.074	0.072	0.071	0.070	0.069	0.068	0.066	0.064	0.063	0.061	0.057	0.053	0.048	0.043	0.034
0.140	0.078	0.076	0.074	0.073	0.072	0.071	0.069	0.068	0.066	0.064	0.062	0.058	0.054	0.048	0.044	0.034
0.150	0.080	0.078	0.076	0.075	0.073	0.072	0.070	0.069	0.067	0.065	0.063	0.059	0.055	0.049	0.044	0.034
0.160	0.082	0.079	0.077	0.076	0.074	0.073	0.072	0.070	0.068	0.066	0.064	0.060	0.056	0.050	0.044	0.033
0.170	0.082	0.080	0.078	0.077	0.075	0.074	0.072	0.071	0.069	0.067	0.064	0.060	0.056	0.050	0.044	0.033
0.180	0.083	0.081	0.079	0.078	0.076	0.075	0.073	0.071	0.069	0.067	0.065	0.060	0.056	0.050	0.044	0.032
0.190	0.084	0.082	0.079	0.078	0.076	0.075	0.074	0.072	0.070	0.068	0.065	0.060	0.056	0.050	0.044	0.031
0.200	0.084	0.083	0.079	0.078	0.076	0.075	0.074	0.072	0.070	0.068	0.065	0.060	0.056	0.050	0.044	0.030
0.210	0.085	0.083	0.080	0.079	0.077	0.076	0.074	0.072	0.070	0.068	0.065	0.060	0.056	0.050	0.043	0.029
0.220	0.085	0.083	0.080	0.079	0.077	0.076	0.074	0.072	0.070	0.068	0.065	0.060	0.055	0.049	0.042	0.028
0.230	0.085	0.082	0.080	0.079	0.077	0.076	0.074	0.072	0.069	0.067	0.064	0.059	0.054	0.048	0.041	0.027
0.240	0.084	0.082	0.080	0.078	0.076	0.075	0.073	0.071	0.068	0.066	0.064	0.058	0.054	0.048	0.040	0.025
0.250	0.084	0.082	0.080	0.078	0.076	0.075	0.073	0.071	0.068	0.066	0.063	0.058	0.053	0.047	0.039	0.024
0.260	0.084	0.082	0.079	0.078	0.076	0.074	0.072	0.070	0.067	0.065	0.062	0.057	0.052	0.046	0.038	0.022
0.270	0.084	0.081	0.078	0.076	0.074	0.073	0.071	0.069	0.067	0.065	0.062	0.056	0.051	0.044	0.036	0.020
0.280	0.083	0.080	0.078	0.076	0.074	0.072	0.070	0.068	0.065	0.063	0.061	0.056	0.050	0.043	0.034	0.018
0.290	0.083	0.079	0.076	0.075	0.073	0.071	0.069	0.067	0.064	0.062	0.059	0.054	0.048	0.042	0.033	0.016
0.300	0.082	0.078	0.076	0.074	0.072	0.070	0.068	0.066	0.063	0.061	0.058	0.052	0.047	0.040	0.031	0.014
0.310	0.080	0.077	0.075	0.073	0.071	0.069	0.066	0.064	0.062	0.060	0.057	0.051	0.046	0.038	0.029	0.012
0.320	0.079	0.076	0.073	0.071	0.069	0.067	0.065	0.063	0.060	0.058	0.055	0.049	0.044	0.036	0.027	0.009
0.330	0.078	0.074	0.072	0.070	0.068	0.066	0.064	0.061	0.058	0.056	0.053	0.047	0.042	0.034	0.026	0.006
0.340	0.076	0.073	0.070	0.068	0.066	0.064	0.062	0.059	0.056	0.054	0.051	0.045	0.040	0.033	0.023	0.004
0.350	0.074	0.071	0.069	0.067	0.065	0.063	0.060	0.057	0.054	0.052	0.049	0.043	0.038	0.030	0.021	0.001
0.360	0.073	0.070	0.067	0.065	0.063	0.061	0.058	0.055	0.052	0.050	0.047	0.041	0.036	0.028	0.018	-0.001
0.370	0.071	0.068	0.065	0.063	0.061	0.059	0.056	0.053	0.050	0.048	0.045	0.039	0.034	0.026	0.016	-0.004
0.380	0.070	0.066	0.063	0.061	0.059	0.057	0.054	0.051	0.048	0.045	0.042	0.036	0.032	0.023	0.014	-0.007
0.390	0.068	0.064	0.061	0.059	0.057	0.055	0.052	0.049	0.046	0.043	0.040	0.034	0.029	0.021	0.011	-0.010

TABLE 13.—COORDINATES OF LOWER NAPPE FOR DIFFERENT VALUES OF $\frac{h_a}{H_s}$—1:3 WEIR—Continued

h_a/H_s \ X/H_s	Y/H_s															
	0.002	0.010	0.020	0.030	0.040	0.050	0.060	0.070	0.080	0.090	0.100	0.120	0.140	0.160	0.180	0.200
0.400	0.065	0.062	0.059	0.057	0.055	0.052	0.049	0.046	0.043	0.040	0.037	0.031	0.026	0.018	0.008	-0.014
0.410	0.063	0.060	0.056	0.055	0.053	0.050	0.047	0.044	0.041	0.038	0.034	0.028	0.024	0.015	0.006	-0.016
0.420	0.060	0.058	0.054	0.052	0.050	0.047	0.044	0.041	0.038	0.035	0.031	0.026	0.020	0.012	0.003	-0.020
0.430	0.058	0.055	0.052	0.050	0.048	0.045	0.042	0.039	0.035	0.032	0.028	0.022	0.018	0.010	0.000	-0.023
0.440	0.056	0.052	0.049	0.047	0.045	0.042	0.039	0.036	0.032	0.029	0.025	0.019	0.014	0.006	-0.003	-0.026
0.450	0.053	0.050	0.046	0.044	0.042	0.039	0.036	0.033	0.029	0.026	0.022	0.016	0.011	0.003	-0.006	-0.030
0.460	0.050	0.047	0.043	0.041	0.039	0.036	0.033	0.030	0.026	0.023	0.019	0.012	0.008	0.000	-0.010	-0.033
0.470	0.047	0.044	0.040	0.038	0.036	0.033	0.030	0.027	0.023	0.020	0.016	0.009	0.005	-0.004	-0.014	-0.037
0.480	0.044	0.041	0.037	0.035	0.033	0.030	0.027	0.023	0.019	0.016	0.012	0.006	0.001	-0.008	-0.017	-0.040
0.490	0.041	0.038	0.034	0.032	0.030	0.027	0.023	0.020	0.016	0.012	0.008	0.001	-0.003	-0.011	-0.020	-0.044
0.500	0.038	0.035	0.031	0.029	0.026	0.023	0.020	0.016	0.012	0.009	0.005	-0.002	-0.006	-0.014	-0.024	-0.048
0.520	0.031	0.028	0.024	0.022	0.019	0.016	0.013	0.009	0.005	0.001	-0.003	-0.009	-0.014	-0.022	-0.032	-0.056
0.540	0.024	0.021	0.017	0.015	0.012	0.009	0.005	0.001	-0.003	-0.007	-0.011	-0.018	-0.022	-0.030	-0.039	-0.063
0.560	0.016	0.014	0.009	0.007	0.004	0.001	-0.003	-0.008	-0.012	-0.016	-0.020	-0.026	-0.031	-0.038	-0.048	-0.072
0.580	0.008	0.005	0.001	0.002	-0.004	-0.008	-0.012	-0.017	-0.021	-0.026	-0.030	-0.036	-0.040	-0.047	-0.058	-0.080
0.600	-0.001	-0.003	-0.008	-0.011	-0.013	-0.017	-0.021	-0.025	-0.029	-0.034	-0.039	-0.045	-0.050	-0.056	-0.066	-0.089
0.620	-0.009	-0.012	-0.016	-0.019	-0.022	-0.026	-0.030	-0.035	-0.039	-0.044	-0.048	-0.055	-0.059	-0.066	-0.076	-0.098
0.640	-0.018	-0.021	-0.026	-0.029	-0.032	-0.036	-0.039	-0.044	-0.048	-0.054	-0.059	-0.065	-0.069	-0.076	-0.086	-0.107
0.660	-0.028	-0.031	-0.035	-0.038	-0.041	-0.045	-0.049	-0.054	-0.059	-0.064	-0.068	-0.075	-0.080	-0.086	-0.096	-0.117
0.680	-0.038	-0.041	-0.046	-0.049	-0.052	-0.056	-0.060	-0.065	-0.069	-0.074	-0.079	-0.085	-0.090	-0.097	-0.107	-0.127
0.700	-0.048	-0.052	-0.056	-0.059	-0.062	-0.067	-0.071	-0.076	-0.080	-0.085	-0.090	-0.097	-0.101	-0.108	-0.117	-0.138
0.720	-0.059	-0.064	-0.067	-0.071	-0.074	-0.078	-0.082	-0.087	-0.091	-0.097	-0.102	-0.108	-0.112	-0.119	-0.128	-0.148
0.740	-0.071	-0.075	-0.079	-0.082	-0.085	-0.090	-0.094	-0.098	-0.102	-0.108	-0.114	-0.119	-0.123	-0.131	-0.140	-0.159
0.760	-0.083	-0.086	-0.090	-0.093	-0.096	-0.101	-0.105	-0.110	-0.114	-0.120	-0.126	-0.131	-0.135	-0.142	-0.151	-0.170
0.780	-0.094	-0.098	-0.102	-0.106	-0.109	-0.113	-0.117	-0.122	-0.126	-0.132	-0.138	-0.143	-0.147	-0.154	-0.162	-0.181
0.800	-0.106	-0.111	-0.115	-0.119	-0.122	-0.126	-0.130	-0.135	-0.139	-0.145	-0.151	-0.156	-0.159	-0.166	-0.174	-0.193
0.820	-0.119	-0.124	-0.128	-0.131	-0.134	-0.138	-0.142	-0.147	-0.152	-0.158	-0.163	-0.168	-0.172	-0.178	-0.187	-0.204
0.840	-0.132	-0.137	-0.142	-0.145	-0.148	-0.152	-0.156	-0.160	-0.164	-0.170	-0.176	-0.180	-0.184	-0.191	-0.199	-0.216
0.860	-0.145	-0.151	-0.156	-0.159	-0.162	-0.166	-0.170	-0.174	-0.178	-0.184	-0.189	-0.193	-0.197	-0.204	-0.211	-0.228
0.880	-0.159	-0.164	-0.170	-0.173	-0.176	-0.180	-0.184	-0.188	-0.192	-0.198	-0.203	-0.207	-0.211	-0.217	-0.224	-0.240
0.900	-0.174	-0.178	-0.184	-0.187	-0.190	-0.194	-0.197	-0.201	-0.205	-0.211	-0.216	-0.220	-0.224	-0.230	-0.237	-0.252
0.920	-0.188	-0.194	-0.198	-0.202	-0.205	-0.209	-0.212	-0.216	-0.219	-0.224	-0.229	-0.234	-0.238	-0.244	-0.251	-0.265
0.940	-0.203	-0.208	-0.213	-0.217	-0.220	-0.224	-0.227	-0.231	-0.234	-0.239	-0.244	-0.248	-0.252	-0.258	-0.264	-0.278
0.960	-0.218	-0.224	-0.228	-0.231	-0.234	-0.238	-0.242	-0.245	-0.248	-0.253	-0.257	-0.262	-0.266	-0.272	-0.278	-0.292
0.980	-0.233	-0.238	-0.244	-0.247	-0.250	-0.253	-0.256	-0.259	-0.262	-0.267	-0.272	-0.276	-0.280	-0.286	-0.292	-0.305
1.000	-0.248	-0.254	-0.259	-0.262	-0.265	-0.269	-0.272	-0.275	-0.278	-0.282	-0.286	-0.291	-0.295	-0.300	-0.306	-0.319
1.050	-0.290	-0.295	-0.300	-0.303	-0.306	-0.309	-0.311	-0.314	-0.316	-0.320	-0.324	-0.329	-0.334	-0.339	-0.344	-0.355
1.100	-0.333	-0.338	-0.343	-0.346	-0.348	-0.351	-0.354	-0.357	-0.359	-0.363	-0.366	-0.370	-0.374	-0.380	-0.383	-0.392
1.150	-0.379	-0.384	-0.389	-0.391	-0.393	-0.396	-0.398	-0.401	-0.403	-0.406	-0.409	-0.414	-0.417	-0.422	-0.425	-0.431
1.200	-0.429	-0.432	-0.436	-0.439	-0.441	-0.443	-0.445	-0.447	-0.449	-0.452	-0.455	-0.459	-0.463	-0.467	-0.468	-0.472

TABLE 13.—COORDINATES OF LOWER NAPPE FOR DIFFERENT VALUES OF $\frac{h_a}{H_s}$—1:3 WEIR—Continued

	Y/Hs															
X/Hs \ ha/Hs	0.002	0.010	0.020	0.030	0.040	0.050	0.060	0.070	0.080	0.090	0.100	0.120	0.140	0.160	0.180	0.200
1.250	-0.479	-0.484	-0.487	-0.489	-0.491	-0.493	-0.494	-0.496	-0.498	-0.501	-0.503	-0.506	-0.510	-0.514	-0.514	-0.516
1.300	-0.532	-0.536	-0.539	-0.541	-0.543	-0.545	-0.546	-0.548	-0.550	-0.551	-0.552	-0.555	-0.560	-0.562	-0.562	-0.562
1.350	-0.587	-0.591	-0.593	-0.595	-0.597	-0.599	-0.600	-0.602	-0.603	-0.604	-0.604	-0.608	-0.611	-0.613	-0.611	-0.608
1.400	-0.645	-0.647	-0.649	-0.651	-0.652	-0.653	-0.654	-0.656	-0.657	-0.658	-0.658	-0.660	-0.665	-0.665	-0.661	-0.657
1.450	-0.705	-0.707	-0.709	-0.710	-0.710	-0.711	-0.712	-0.713	-0.714	-0.715	-0.715	-0.717	-0.718	-0.717	-0.714	-0.708
1.500	-0.767	-0.770	-0.772	-0.772	-0.772	-0.771	-0.770	-0.772	-0.773	-0.774	-0.774	-0.776	-0.775	-0.775	-0.768	-0.759
1.550	-0.833	-0.834	-0.836	-0.836	-0.835	-0.835	-0.835	-0.835	-0.834	-0.834	-0.834	-0.837	-0.835	-0.829	-0.823	-0.814
1.600	-0.898	-0.899	-0.901	-0.900	-0.899	-0.898	-0.897	-0.898	-0.898	-0.899	-0.899	-0.898	-0.897	-0.889	-0.881	-0.871
1.650	-0.969	-0.968	-0.968	-0.967	-0.965	-0.965	-0.964	-0.964	-0.963	-0.963	-0.963	-0.962	-0.960	-0.950	-0.941	-0.929
1.700	-1.036	-1.038	-1.036	-1.035	-1.034	-1.033	-1.031	-1.030	-1.029	-1.029	-1.028	-1.026	-1.023	-1.012	-1.020	-0.989
1.750	-1.108	-1.108	-1.106	-1.104	-1.102	-1.102	-1.101	-1.099	-1.097	-1.096	-1.095	-1.091	-1.088	-1.076	-1.065	-1.051
1.800	-1.182	-1.181	-1.178	-1.177	-1.175	-1.174	-1.172	-1.170	-1.168	-1.166	-1.163	-1.159	-1.155	-1.142	-1.131	-1.116
1.850	-1.260	-1.256	-1.253	-1.251	-1.249	-1.247	-1.245	-1.243	-1.240	-1.237	-1.234	-1.229	-1.224	-1.212	-1.199	-1.184
1.900	-1.338	-1.332	-1.328	-1.326	-1.323	-1.321	-1.319	-1.316	-1.313	-1.310	-1.306	-1.299	-1.294	-1.283	-1.270	-1.254
1.950	-1.418	-1.412	-1.408	-1.405	-1.402	-1.399	-1.396	-1.392	-1.388	-1.385	-1.381	-1.373	-1.367	-1.357	-1.343	-1.325
2.000	-1.499	-1.492	-1.487	-1.484	-1.481	-1.478	-1.474	-1.470	-1.465	-1.461	-1.457	-1.449	-1.442	-1.432	-1.419	-1.401
2.050	-1.579	-1.572	-1.565	-1.562	-1.558	-1.555	-1.551	-1.547	-1.543	-1.540	-1.536	-1.528	-1.520	-1.509	-1.496	-1.478
2.100	-1.662	-1.654	-1.647	-1.642	-1.637	-1.634	-1.631	-1.627	-1.622	-1.619	-1.615	-1.606	-1.598	-1.588	-1.576	-1.558
2.150	-1.748	-1.739	-1.731	-1.727	-1.722	-1.719	-1.715	-1.711	-1.706	-1.703	-1.699	-1.691	-1.682	-1.672	-1.657	-1.640
2.200	-1.838	-1.828	-1.819	-1.815	-1.810	-1.807	-1.803	-1.798	-1.793	-1.790	-1.786	-1.778	-1.769	-1.758	-1.742	-1.723
2.250	-1.930	-1.920	-1.910	-1.906	-1.901	-1.897	-1.893	-1.888	-1.883	-1.880	-1.876	-1.868	-1.859	-1.845	-1.829	-1.811
2.300	-2.026	-2.017	-2.005	-2.000	-1.995	-1.991	-1.987	-1.982	-1.977	-1.973	-1.969	-1.961	-1.952	-1.938	-1.921	-1.901
2.350	-2.123	-2.110	-2.101	-2.096	-2.090	-2.086	-2.081	-2.076	-2.071	-2.067	-2.063	-2.054	-2.046	-2.033	-2.012	-1.991
2.400	-2.220	-2.209	-2.198	-2.193	-2.188	-2.183	-2.178	-2.174	-2.169	-2.164	-2.159	-2.150	-2.141	-2.128	-2.105	-2.082
2.450	-2.322	-2.310	-2.301	-2.296	-2.290	-2.285	-2.280	-2.275	-2.270	-2.266	-2.261	-2.251	-2.240	-2.223	-2.201	-2.175
2.500	-2.426	-2.415	-2.403	-2.398	-2.392	-2.387	-2.381	-2.376	-2.371	-2.366	-2.361	-2.351	-2.339	-2.322	-2.298	-2.272
2.550	-2.532	-2.519	-2.508	-2.503	-2.497	-2.492	-2.486	-2.481	-2.475	-2.470	-2.465	-2.454	-2.441	-2.421	-2.396	-2.368
2.600	-2.635	-2.624	-2.613	-2.608	-2.602	-2.597	-2.591	-2.585	-2.579	-2.574	-2.568	-2.556	-2.542	-2.520	-2.496	-2.468
2.650	-2.742	-2.730	-2.718	-2.713	-2.708	-2.703	-2.697	-2.691	-2.684	-2.678	-2.672	-2.660	-2.644	-2.620	-2.597	-2.566
2.700	-2.850	-2.838	-2.828	-2.823	-2.817	-2.810	-2.803	-2.797	-2.791	-2.784	-2.777	-2.765	-2.749	-2.723	-2.698	-2.666
2.750	-2.959	-2.947	-2.937	-2.931	-2.925	-2.919	-2.912	-2.906	-2.899	-2.891	-2.883	-2.871	-2.855	-2.827	-2.801	-2.768
2.800	-3.069	-3.057	-3.047	-3.041	-3.035	-3.029	-3.022	-3.015	-3.008	-2.999	-2.990	-2.977	-2.961	-2.931	-2.906	-2.872

TABLE 14.—COORDINATES OF LOWER NAPPE FOR DIFFERENT VALUES OF $\frac{h_a}{H_s}$ —2:3 WEIR

h_a/H_s \ X/H_s	Y/H_s 0.002	0.010	0.020	0.030	0.040	0.050	0.060	0.070	0.080	0.090	0.100	0.120	0.140	0.160	0.180
0.000	0.000	0.000	0.000	0.000	0.000	0.000	0.000	0.000	0.000	0.000	0.000	0.000	0.000	0.000	0.000
0.010	0.009	0.009	0.008	0.008	0.007	0.007	0.006	0.006	0.006	0.006	0.005	0.005	0.004	0.004	0.003
0.020	0.016	0.015	0.014	0.014	0.014	0.014	0.013	0.013	0.012	0.012	0.011	0.010	0.009	0.008	0.007
0.030	0.023	0.022	0.021	0.021	0.020	0.020	0.019	0.019	0.018	0.018	0.017	0.015	0.014	0.012	0.011
0.040	0.029	0.028	0.027	0.027	0.026	0.025	0.024	0.024	0.023	0.023	0.022	0.020	0.018	0.016	0.014
0.050	0.034	0.033	0.032	0.032	0.031	0.030	0.029	0.029	0.028	0.027	0.026	0.024	0.022	0.020	0.017
0.060	0.039	0.038	0.037	0.036	0.035	0.035	0.034	0.033	0.032	0.031	0.030	0.027	0.025	0.023	0.020
0.070	0.043	0.042	0.041	0.040	0.039	0.038	0.037	0.036	0.035	0.035	0.034	0.031	0.029	0.026	0.023
0.080	0.047	0.046	0.045	0.044	0.043	0.042	0.041	0.040	0.039	0.038	0.037	0.034	0.032	0.029	0.026
0.090	0.050	0.049	0.048	0.047	0.046	0.045	0.044	0.043	0.042	0.041	0.039	0.037	0.034	0.032	0.028
0.100	0.053	0.052	0.050	0.050	0.049	0.048	0.046	0.045	0.044	0.043	0.042	0.039	0.037	0.034	0.030
0.110	0.055	0.054	0.053	0.052	0.051	0.050	0.048	0.047	0.046	0.045	0.044	0.041	0.039	0.036	0.032
0.120	0.057	0.056	0.054	0.054	0.053	0.052	0.050	0.049	0.048	0.047	0.045	0.043	0.040	0.037	0.034
0.130	0.059	0.058	0.056	0.055	0.054	0.053	0.052	0.051	0.049	0.048	0.047	0.045	0.042	0.039	0.035
0.140	0.060	0.059	0.058	0.057	0.056	0.055	0.053	0.052	0.051	0.050	0.048	0.046	0.043	0.040	0.036
0.150	0.061	0.060	0.059	0.058	0.057	0.056	0.054	0.053	0.052	0.051	0.049	0.047	0.044	0.041	0.037
0.160	0.062	0.061	0.060	0.059	0.057	0.056	0.055	0.054	0.053	0.052	0.050	0.047	0.044	0.041	0.038
0.170	0.063	0.062	0.060	0.059	0.058	0.057	0.056	0.055	0.053	0.052	0.050	0.048	0.045	0.042	0.038
0.180	0.063	0.062	0.061	0.060	0.059	0.058	0.056	0.055	0.053	0.052	0.050	0.048	0.045	0.042	0.038
0.190	0.064	0.063	0.062	0.061	0.059	0.058	0.056	0.055	0.054	0.052	0.050	0.048	0.045	0.042	0.038
0.200	0.064	0.063	0.062	0.061	0.059	0.058	0.056	0.055	0.053	0.052	0.050	0.048	0.044	0.041	0.038
0.210	0.064	0.063	0.062	0.061	0.059	0.058	0.056	0.055	0.053	0.052	0.050	0.047	0.044	0.041	0.037
0.220	0.063	0.062	0.061	0.060	0.058	0.057	0.056	0.054	0.052	0.051	0.049	0.046	0.044	0.040	0.038
0.230	0.063	0.062	0.061	0.060	0.058	0.056	0.054	0.053	0.051	0.050	0.048	0.046	0.043	0.039	0.038
0.240	0.062	0.061	0.060	0.059	0.057	0.056	0.054	0.052	0.050	0.049	0.047	0.045	0.041	0.038	0.035
0.250	0.061	0.060	0.059	0.058	0.056	0.054	0.052	0.051	0.049	0.048	0.046	0.044	0.040	0.037	0.034
0.260	0.060	0.059	0.058	0.056	0.054	0.053	0.051	0.050	0.048	0.047	0.045	0.043	0.039	0.036	0.032
0.270	0.059	0.058	0.057	0.055	0.053	0.052	0.050	0.048	0.046	0.045	0.043	0.041	0.037	0.034	0.030
0.280	0.058	0.057	0.056	0.054	0.052	0.050	0.048	0.047	0.045	0.044	0.042	0.039	0.036	0.032	0.029
0.290	0.056	0.055	0.054	0.052	0.050	0.049	0.047	0.046	0.044	0.042	0.040	0.037	0.034	0.030	0.027
0.300	0.055	0.054	0.052	0.050	0.048	0.047	0.045	0.044	0.042	0.040	0.038	0.035	0.032	0.028	0.024
0.310	0.053	0.052	0.050	0.049	0.047	0.046	0.044	0.042	0.040	0.038	0.036	0.033	0.029	0.026	0.023
0.320	0.051	0.050	0.048	0.047	0.045	0.044	0.042	0.040	0.038	0.036	0.034	0.031	0.027	0.024	0.020
0.330	0.049	0.048	0.046	0.044	0.042	0.041	0.039	0.038	0.036	0.034	0.032	0.029	0.025	0.022	0.018
0.340	0.046	0.045	0.044	0.042	0.040	0.039	0.037	0.036	0.034	0.032	0.030	0.027	0.023	0.020	0.016
0.350	0.044	0.043	0.042	0.040	0.038	0.037	0.035	0.034	0.032	0.030	0.028	0.025	0.021	0.017	0.013
0.360	0.042	0.041	0.040	0.038	0.036	0.035	0.033	0.031	0.029	0.028	0.026	0.022	0.018	0.015	0.011
0.370	0.040	0.039	0.038	0.036	0.034	0.032	0.030	0.029	0.027	0.025	0.023	0.020	0.016	0.012	0.008
0.380	0.037	0.036	0.035	0.033	0.031	0.030	0.028	0.026	0.024	0.023	0.021	0.017	0.013	0.009	0.006
0.390	0.035	0.034	0.033	0.031	0.028	0.027	0.025	0.024	0.022	0.020	0.018	0.014	0.010	0.006	0.002

TABLE 14.—COORDINATES OF LOWER NAPPE FOR DIFFERENT VALUES OF $\frac{h_a}{H_s}$—2:3 WEIR—Continued

X/H_s \ h_a/H_s	Y/H_s														
	0.002	0.010	0.020	0.030	0.040	0.050	0.060	0.070	0.080	0.090	0.100	0.120	0.140	0.160	0.180
0.400	0.033	0.032	0.030	0.028	0.026	0.025	0.023	0.021	0.019	0.017	0.015	0.012	0.007	0.004	0.000
0.410	0.030	0.029	0.028	0.026	0.023	0.022	0.020	0.018	0.016	0.014	0.012	0.009	0.004	0.000	-0.003
0.420	0.027	0.026	0.025	0.023	0.020	0.019	0.017	0.015	0.013	0.011	0.009	0.006	0.002	-0.002	-0.006
0.430	0.024	0.023	0.022	0.020	0.017	0.016	0.014	0.012	0.010	0.009	0.007	0.003	-0.002	-0.006	-0.010
0.440	0.021	0.020	0.019	0.017	0.014	0.013	0.011	0.009	0.007	0.005	0.003	-0.001	-0.005	-0.009	-0.014
0.450	0.018	0.017	0.016	0.014	0.011	0.010	0.008	0.006	0.004	0.002	0.000	-0.004	-0.008	-0.013	-0.017
0.460	0.015	0.014	0.013	0.011	0.008	0.006	0.004	0.002	0.000	-0.002	-0.004	-0.008	-0.012	-0.016	-0.020
0.470	0.012	0.011	0.010	0.007	0.004	0.003	0.001	-0.001	-0.003	-0.005	-0.007	-0.011	-0.015	-0.020	-0.024
0.480	0.008	0.007	0.006	0.004	0.001	-0.001	-0.002	-0.005	-0.007	-0.009	-0.011	-0.015	-0.019	-0.024	-0.028
0.490	0.005	0.004	0.002	0.000	-0.002	-0.004	-0.005	-0.008	-0.010	-0.012	-0.014	-0.018	-0.021	-0.028	-0.032
0.500	0.001	0.000	-0.001	-0.004	-0.006	-0.008	-0.009	-0.012	-0.014	-0.016	-0.018	-0.022	-0.026	-0.032	-0.036
0.520	-0.006	-0.008	-0.009	-0.012	-0.014	-0.016	-0.017	-0.019	-0.021	-0.024	-0.026	-0.030	-0.034	-0.040	-0.043
0.540	-0.014	-0.016	-0.017	-0.020	-0.022	-0.023	-0.024	-0.027	-0.030	-0.032	-0.034	-0.038	-0.043	-0.048	-0.052
0.560	-0.023	-0.024	-0.025	-0.028	-0.031	-0.033	-0.034	-0.036	-0.038	-0.041	-0.043	-0.047	-0.052	-0.056	-0.060
0.580	-0.031	-0.033	-0.034	-0.037	-0.040	-0.042	-0.043	-0.045	-0.046	-0.049	-0.052	-0.056	-0.061	-0.066	-0.068
0.600	-0.041	-0.042	-0.043	-0.046	-0.049	-0.051	-0.052	-0.054	-0.056	-0.059	-0.062	-0.066	-0.070	-0.074	-0.078
0.620	-0.050	-0.052	-0.053	-0.056	-0.059	-0.061	-0.062	-0.064	-0.066	-0.069	-0.071	-0.075	-0.080	-0.084	-0.087
0.640	-0.061	-0.062	-0.063	-0.066	-0.068	-0.070	-0.072	-0.074	-0.076	-0.079	-0.081	-0.085	-0.089	-0.094	-0.097
0.660	-0.071	-0.073	-0.074	-0.077	-0.079	-0.081	-0.083	-0.085	-0.087	-0.089	-0.091	-0.096	-0.100	-0.104	-0.106
0.680	-0.082	-0.084	-0.085	-0.087	-0.089	-0.092	-0.094	-0.096	-0.098	-0.100	-0.102	-0.106	-0.110	-0.114	-0.117
0.700	-0.094	-0.095	-0.096	-0.098	-0.100	-0.103	-0.105	-0.107	-0.109	-0.112	-0.114	-0.117	-0.120	-0.124	-0.127
0.720	-0.105	-0.106	-0.107	-0.110	-0.112	-0.114	-0.116	-0.119	-0.121	-0.123	-0.125	-0.129	-0.132	-0.135	-0.138
0.740	-0.116	-0.118	-0.119	-0.122	-0.124	-0.126	-0.128	-0.130	-0.132	-0.135	-0.137	-0.140	-0.143	-0.146	-0.149
0.760	-0.128	-0.130	-0.131	-0.134	-0.136	-0.138	-0.140	-0.142	-0.144	-0.146	-0.148	-0.152	-0.155	-0.158	-0.161
0.780	-0.141	-0.143	-0.144	-0.146	-0.148	-0.150	-0.152	-0.154	-0.156	-0.158	-0.160	-0.164	-0.166	-0.170	-0.173
0.800	-0.153	-0.155	-0.156	-0.159	-0.161	-0.163	-0.165	-0.167	-0.169	-0.171	-0.173	-0.176	-0.179	-0.182	-0.184
0.820	-0.167	-0.168	-0.169	-0.172	-0.174	-0.176	-0.178	-0.180	-0.182	-0.184	-0.186	-0.189	-0.192	-0.194	-0.197
0.840	-0.180	-0.182	-0.183	-0.186	-0.188	-0.190	-0.192	-0.194	-0.196	-0.198	-0.199	-0.202	-0.204	-0.208	-0.210
0.860	-0.194	-0.195	-0.196	-0.199	-0.201	-0.203	-0.205	-0.207	-0.209	-0.211	-0.213	-0.216	-0.218	-0.221	-0.223
0.880	-0.208	-0.210	-0.211	-0.213	-0.215	-0.217	-0.219	-0.221	-0.223	-0.225	-0.227	-0.229	-0.232	-0.234	-0.237
0.900	-0.222	-0.224	-0.225	-0.228	-0.230	-0.232	-0.233	-0.235	-0.237	-0.239	-0.241	-0.243	-0.246	-0.248	-0.251
0.920	-0.236	-0.238	-0.239	-0.242	-0.244	-0.246	-0.247	-0.249	-0.251	-0.253	-0.255	-0.257	-0.260	-0.262	-0.265
0.940	-0.252	-0.253	-0.254	-0.256	-0.258	-0.260	-0.262	-0.264	-0.266	-0.268	-0.269	-0.272	-0.275	-0.277	-0.280
0.960	-0.266	-0.268	-0.269	-0.272	-0.274	-0.276	-0.277	-0.279	-0.280	-0.282	-0.284	-0.287	-0.289	-0.292	-0.294
0.980	-0.282	-0.283	-0.284	-0.287	-0.289	-0.291	-0.292	-0.294	-0.296	-0.298	-0.299	-0.302	-0.305	-0.307	-0.309
1.000	-0.297	-0.299	-0.300	-0.302	-0.304	-0.306	-0.307	-0.309	-0.311	-0.313	-0.314	-0.318	-0.320	-0.322	-0.325
1.050	-0.339	-0.340	-0.341	-0.343	-0.344	-0.346	-0.347	-0.349	-0.350	-0.352	-0.353	-0.356	-0.359	-0.361	-0.364
1.100	-0.384	-0.385	-0.386	-0.387	-0.387	-0.388	-0.389	-0.391	-0.392	-0.394	-0.395	-0.398	-0.401	-0.402	-0.404
1.150	-0.431	-0.432	-0.433	-0.434	-0.434	-0.435	-0.435	-0.436	-0.437	-0.439	-0.440	-0.442	-0.443	-0.444	-0.447
1.200	-0.480	-0.481	-0.481	-0.482	-0.482	-0.482	-0.482	-0.483	-0.483	-0.484	-0.484	-0.486	-0.487	-0.489	-0.491

TABLE 14.—COORDINATES OF LOWER NAPPE FOR DIFFERENT VALUES OF $\frac{h_a}{H_s}$—2:3 WEIR—Continued

h_a/H_s \ X/H_s	Y/H_s 0.002	0.010	0.020	0.030	0.040	0.050	0.060	0.070	0.080	0.090	0.100	0.120	0.140	0.160	0.180
1.250	-0.529	-0.530	-0.530	-0.531	-0.531	-0.532	-0.532	-0.533	-0.533	-0.534	-0.534	-0.535	-0.535	-0.536	-0.537
1.300	-0.583	-0.583	-0.583	-0.583	-0.583	-0.583	-0.583	-0.583	-0.583	-0.583	-0.583	-0.584	-0.584	-0.583	-0.583
1.350	-0.637	-0.637	-0.636	-0.636	-0.636	-0.636	-0.635	-0.635	-0.634	-0.634	-0.634	-0.633	-0.633	-0.632	-0.632
1.400	-0.694	-0.693	-0.692	-0.692	-0.691	-0.691	-0.690	-0.690	-0.689	-0.689	-0.688	-0.687	-0.686	-0.685	-0.683
1.450	-0.752	-0.752	-0.751	-0.751	-0.750	-0.750	-0.750	-0.749	-0.747	-0.746	-0.745	-0.743	-0.741	-0.739	-0.735
1.500	-0.814	-0.814	-0.813	-0.812	-0.811	-0.810	-0.808	-0.808	-0.808	-0.807	-0.805	-0.800	-0.797	-0.794	-0.790
1.550	-0.877	-0.877	-0.876	-0.875	-0.874	-0.873	-0.872	-0.871	-0.869	-0.867	-0.865	-0.860	-0.855	-0.852	-0.846
1.600	-0.941	-0.941	-0.940	-0.939	-0.938	-0.937	-0.935	-0.933	-0.931	-0.929	-0.927	-0.921	-0.916	-0.910	-0.904
1.650	-1.008	-1.007	-1.005	-1.004	-1.003	-1.002	-1.000	-0.998	-0.996	-0.994	-0.991	-0.985	-0.979	-0.970	-0.963
1.700	-1.076	-1.075	-1.073	-1.071	-1.069	-1.068	-1.066	-1.064	-1.062	-1.060	-1.057	-1.049	-1.042	-1.033	-1.023
1.750	-1.148	-1.146	-1.143	-1.141	-1.138	-1.137	-1.136	-1.133	-1.130	-1.127	-1.124	-1.115	-1.108	-1.097	-1.086
1.800	-1.218	-1.216	-1.213	-1.210	-1.207	-1.206	-1.205	-1.203	-1.200	-1.197	-1.193	-1.184	-1.175	-1.163	-1.151
1.850	-1.291	-1.288	-1.284	-1.283	-1.281	-1.279	-1.277	-1.274	-1.271	-1.268	-1.264	-1.253	-1.245	-1.232	-1.216
1.900	-1.367	-1.364	-1.360	-1.358	-1.356	-1.355	-1.353	-1.350	-1.346	-1.342	-1.338	-1.327	-1.317	-1.303	-1.283
1.950	-1.445	-1.442	-1.439	-1.437	-1.434	-1.432	-1.429	-1.426	-1.423	-1.419	-1.415	-1.401	-1.391	-1.375	-1.354
2.000	-1.525	-1.522	-1.518	-1.515	-1.511	-1.509	-1.506	-1.503	-1.500	-1.496	-1.491	-1.476	-1.465	-1.450	-1.426
2.050	-1.608	-1.604	-1.600	-1.596	-1.591	-1.589	-1.586	-1.582	-1.578	-1.574	-1.569	-1.553	-1.541	-1.524	-1.502
2.100	-1.693	-1.688	-1.682	-1.677	-1.672	-1.669	-1.666	-1.662	-1.657	-1.652	-1.647	-1.633	-1.619	-1.600	-1.578
2.150	-1.780	-1.773	-1.766	-1.761	-1.755	-1.752	-1.748	-1.743	-1.738	-1.733	-1.727	-1.712	-1.698	-1.679	-1.656
2.200	-1.869	-1.861	-1.853	-1.847	-1.841	-1.837	-1.833	-1.828	-1.822	-1.816	-1.809	-1.793	-1.778	-1.759	-1.736
2.250	-1.959	-1.951	-1.942	-1.936	-1.929	-1.925	-1.921	-1.915	-1.908	-1.902	-1.896	-1.878	-1.861	-1.843	-1.819
2.300	-2.052	-2.043	-2.034	-2.027	-2.019	-2.016	-2.012	-2.005	-1.998	-1.991	-1.984	-1.966	-1.948	-1.928	-1.904
2.350	-2.146	-2.138	-2.130	-2.122	-2.114	-2.110	-2.105	-2.097	-2.089	-2.082	-2.074	-2.055	-2.036	-2.016	-1.992
2.400	-2.242	-2.234	-2.225	-2.217	-2.209	-2.204	-2.199	-2.191	-2.183	-2.176	-2.169	-2.147	-2.128	-2.107	-2.081
2.450	-2.343	-2.334	-2.325	-2.317	-2.308	-2.303	-2.298	-2.289	-2.280	-2.272	-2.264	-2.243	-2.222	-2.201	-2.173
2.500	-2.447	-2.437	-2.427	-2.418	-2.409	-2.404	-2.399	-2.389	-2.379	-2.371	-2.362	-2.339	-2.318	-2.297	-2.269
2.550	-2.554	-2.543	-2.531	-2.523	-2.514	-2.508	-2.501	-2.491	-2.481	-2.472	-2.462	-2.437	-2.415	-2.393	-2.366

TABLE 15.—COORDINATES OF LOWER NAPPE FOR DIFFERENT VALUES OF $\frac{h_a}{H_s}$—3:3 WEIR

	Y/H_s														
h_a/H_s / X/H_s	0.002	0.010	0.020	0.030	0.040	0.050	0.060	0.070	0.080	0.090	0.100	0.120	0.140	0.160	0.180
0.000	0.000	0.000	0.000	0.000	0.000	0.000	0.000	0.000	0.000	0.000	0.000	0.000	0.000	0.000	0.000
0.010	0.004	0.004	0.004	0.004	0.004	0.004	0.004	0.004	0.004	0.004	0.003	0.003	0.003	0.003	0.003
0.020	0.008	0.008	0.008	0.008	0.008	0.008	0.007	0.007	0.007	0.007	0.007	0.007	0.006	0.006	0.005
0.030	0.013	0.013	0.012	0.012	0.012	0.012	0.011	0.011	0.011	0.011	0.011	0.011	0.010	0.009	0.008
0.040	0.016	0.016	0.015	0.015	0.015	0.015	0.015	0.015	0.015	0.015	0.014	0.013	0.012	0.012	0.011
0.050	0.020	0.019	0.018	0.018	0.018	0.018	0.018	0.018	0.018	0.018	0.017	0.017	0.016	0.015	0.014
0.060	0.023	0.023	0.022	0.022	0.022	0.022	0.021	0.021	0.021	0.020	0.020	0.020	0.020	0.019	0.018
0.070	0.026	0.026	0.025	0.025	0.025	0.025	0.024	0.024	0.024	0.023	0.023	0.023	0.022	0.020	0.019
0.080	0.029	0.029	0.028	0.028	0.028	0.027	0.027	0.027	0.027	0.026	0.026	0.025	0.024	0.022	0.021
0.090	0.032	0.032	0.031	0.031	0.030	0.030	0.029	0.029	0.029	0.028	0.028	0.027	0.026	0.024	0.023
0.100	0.035	0.035	0.034	0.034	0.033	0.033	0.032	0.032	0.031	0.031	0.030	0.029	0.028	0.026	0.025
0.110	0.037	0.037	0.036	0.036	0.035	0.035	0.034	0.034	0.033	0.033	0.032	0.031	0.030	0.028	0.026
0.120	0.039	0.039	0.038	0.038	0.037	0.037	0.036	0.036	0.035	0.035	0.034	0.033	0.032	0.029	0.028
0.130	0.040	0.040	0.039	0.039	0.038	0.038	0.037	0.037	0.036	0.035	0.034	0.033	0.032	0.030	0.028
0.140	0.041	0.041	0.040	0.040	0.039	0.039	0.038	0.038	0.037	0.037	0.036	0.035	0.034	0.031	0.029
0.150	0.042	0.042	0.041	0.041	0.040	0.039	0.038	0.038	0.037	0.037	0.036	0.035	0.034	0.032	0.029
0.160	0.043	0.043	0.042	0.042	0.041	0.040	0.039	0.039	0.038	0.038	0.037	0.036	0.035	0.032	0.030
0.170	0.044	0.043	0.042	0.042	0.041	0.041	0.040	0.040	0.039	0.039	0.038	0.037	0.035	0.032	0.030
0.180	0.044	0.043	0.042	0.042	0.041	0.041	0.040	0.040	0.039	0.039	0.038	0.037	0.036	0.032	0.030
0.190	0.044	0.043	0.042	0.042	0.041	0.041	0.040	0.040	0.039	0.039	0.038	0.037	0.036	0.032	0.029
0.200	0.044	0.043	0.042	0.042	0.041	0.041	0.040	0.040	0.039	0.039	0.038	0.037	0.035	0.032	0.029
0.210	0.044	0.043	0.042	0.042	0.041	0.041	0.040	0.040	0.039	0.038	0.037	0.036	0.035	0.031	0.028
0.220	0.043	0.043	0.042	0.042	0.041	0.040	0.039	0.039	0.038	0.037	0.036	0.035	0.034	0.030	0.027
0.230	0.042	0.042	0.041	0.041	0.040	0.039	0.038	0.038	0.037	0.037	0.036	0.035	0.033	0.029	0.026
0.240	0.042	0.041	0.040	0.040	0.039	0.039	0.038	0.037	0.036	0.035	0.034	0.033	0.032	0.028	0.026
0.250	0.041	0.040	0.039	0.039	0.038	0.037	0.036	0.036	0.035	0.035	0.034	0.032	0.030	0.027	0.024
0.260	0.040	0.039	0.038	0.038	0.037	0.036	0.035	0.035	0.034	0.033	0.032	0.031	0.029	0.025	0.023
0.270	0.038	0.037	0.036	0.036	0.035	0.035	0.034	0.033	0.032	0.031	0.030	0.029	0.027	0.024	0.021
0.280	0.037	0.037	0.036	0.035	0.034	0.033	0.032	0.031	0.030	0.029	0.028	0.027	0.025	0.022	0.020
0.290	0.036	0.035	0.034	0.033	0.032	0.031	0.030	0.030	0.029	0.028	0.027	0.026	0.024	0.020	0.018
0.300	0.034	0.033	0.032	0.032	0.031	0.030	0.029	0.028	0.027	0.026	0.025	0.024	0.022	0.018	0.016
0.310	0.032	0.031	0.030	0.030	0.029	0.028	0.027	0.026	0.025	0.024	0.023	0.022	0.020	0.016	0.013
0.320	0.030	0.029	0.028	0.028	0.027	0.026	0.025	0.024	0.023	0.022	0.021	0.019	0.017	0.014	0.011
0.330	0.028	0.027	0.026	0.025	0.024	0.023	0.022	0.021	0.020	0.019	0.018	0.017	0.015	0.012	0.008
0.340	0.025	0.025	0.024	0.023	0.022	0.021	0.020	0.019	0.018	0.017	0.016	0.015	0.013	0.010	0.006

TABLE 15.—COORDINATES OF LOWER NAPPE FOR DIFFERENT VALUES OF $\frac{h_a}{H_s}$—3:3 WEIR—Continued

h_a/H_s \ X/H_s	Y/H_s														
	0.002	0.010	0.020	0.030	0.040	0.050	0.060	0.070	0.080	0.090	0.100	0.120	0.140	0.160	0.180
0.350	0.022	0.022	0.021	0.021	0.020	0.019	0.018	0.017	0.016	0.015	0.014	0.012	0.010	0.007	0.004
0.360	0.020	0.019	0.018	0.018	0.017	0.017	0.016	0.015	0.014	0.013	0.011	0.010	0.008	0.005	0.002
0.370	0.018	0.017	0.016	0.016	0.015	0.014	0.013	0.012	0.011	0.010	0.008	0.007	0.005	0.003	-0.001
0.380	0.015	0.015	0.014	0.013	0.012	0.011	0.010	0.009	0.008	0.007	0.006	0.004	0.002	0.000	-0.004
0.390	0.012	0.011	0.010	0.010	0.009	0.008	0.007	0.006	0.005	0.004	0.003	0.001	-0.001	-0.003	-0.006
0.400	0.009	0.009	0.008	0.007	0.006	0.006	0.005	0.004	0.003	0.002	0.000	-0.002	-0.004	-0.006	-0.009
0.410	0.006	0.005	0.004	0.004	0.003	0.003	0.002	0.001	-0.001	-0.002	-0.003	-0.005	-0.006	-0.008	-0.012
0.420	0.003	0.002	0.001	0.001	0.000	-0.001	-0.001	-0.003	-0.004	-0.005	-0.006	-0.008	-0.010	-0.012	-0.016
0.430	0.000	-0.001	-0.002	-0.003	-0.003	-0.004	-0.004	-0.006	-0.007	-0.008	-0.009	-0.011	-0.013	-0.015	-0.019
0.440	-0.003	-0.004	-0.004	-0.005	-0.006	-0.007	-0.008	-0.010	-0.011	-0.012	-0.013	-0.015	-0.016	-0.018	-0.022
0.450	-0.007	-0.008	-0.008	-0.009	-0.010	-0.011	-0.011	-0.013	-0.014	-0.015	-0.016	-0.018	-0.019	-0.022	-0.025
0.460	-0.010	-0.011	-0.012	-0.013	-0.014	-0.015	-0.015	-0.017	-0.018	-0.019	-0.020	-0.022	-0.023	-0.025	-0.028
0.470	-0.014	-0.015	-0.015	-0.016	-0.017	-0.018	-0.018	-0.020	-0.021	-0.023	-0.024	-0.025	-0.026	-0.028	-0.032
0.480	-0.018	-0.019	-0.019	-0.020	-0.021	-0.022	-0.022	-0.024	-0.025	-0.027	-0.028	-0.029	-0.030	-0.032	-0.035
0.490	-0.022	-0.023	-0.023	-0.024	-0.025	-0.026	-0.026	-0.028	-0.029	-0.030	-0.031	-0.033	-0.034	-0.036	-0.039
0.500	-0.026	-0.027	-0.027	-0.028	-0.029	-0.030	-0.030	-0.032	-0.033	-0.034	-0.035	-0.037	-0.038	-0.040	-0.042
0.520	-0.034	-0.035	-0.036	-0.037	-0.037	-0.038	-0.038	-0.040	-0.041	-0.042	-0.043	-0.045	-0.046	-0.048	-0.050
0.540	-0.043	-0.044	-0.044	-0.045	-0.046	-0.047	-0.047	-0.049	-0.050	-0.051	-0.052	-0.053	-0.054	-0.056	-0.058
0.560	-0.052	-0.053	-0.053	-0.054	-0.055	-0.056	-0.056	-0.057	-0.058	-0.059	-0.060	-0.062	-0.063	-0.065	-0.066
0.580	-0.062	-0.063	-0.063	-0.064	-0.065	-0.066	-0.066	-0.067	-0.068	-0.069	-0.069	-0.071	-0.072	-0.074	-0.077
0.600	-0.072	-0.073	-0.073	-0.074	-0.075	-0.076	-0.076	-0.077	-0.077	-0.078	-0.078	-0.080	-0.081	-C.084	-0.085
0.620	-0.082	-0.083	-0.083	-0.084	-0.085	-0.086	-0.086	-0.087	-0.087	-0.088	-0.088	-0.090	-0.091	-0.093	-C.095
0.640	-0.093	-0.094	-0.094	-0.095	-0.095	-0.096	-0.096	-0.097	-0.098	-0.099	-0.099	-0.100	-0.101	-0.103	-0.105
0.660	-0.104	-0.105	-0.105	-0.106	-0.106	-0.106	-0.106	-0.107	-0.108	-0.109	-0.109	-0.110	-0.111	-0.113	-0.115
0.680	-0.115	-0.116	-0.116	-0.117	-0.117	-0.118	-0.118	-0.119	-0.119	-0.120	-0.120	-0.121	-0.122	-0.124	-0.126
0.700	-0.126	-0.127	-0.127	-0.128	-0.128	-0.129	-0.129	-0.130	-0.131	-0.132	-0.132	-0.133	-0.133	-0.135	-0.137
0.720	-0.138	-0.139	-0.139	-0.140	-0.140	-0.141	-0.141	-0.142	-0.142	-0.143	-0.143	-0.144	-0.144	-0.147	-0.149
0.740	-0.150	-0.151	-0.151	-0.152	-0.152	-0.153	-0.153	-0.154	-0.154	-0.155	-0.155	-0.156	-0.156	-0.158	-0.160
0.760	-0.162	-0.163	-0.163	-0.164	-0.165	-0.166	-0.166	-0.167	-0.167	-0.167	-0.167	-0.168	-0.168	-0.170	-0.172
0.780	-0.175	-0.176	-0.176	-0.177	-0.178	-0.179	-0.179	-0.179	-0.179	-0.179	-0.179	-0.180	-0.181	-0.182	-0.183
0.800	-0.188	-0.189	-0.189	-0.190	-0.190	-0.191	-0.191	-0.192	-0.192	-0.192	-0.192	-0.193	-0.194	-0.195	-0.196
0.820	-0.201	-0.202	-0.202	-0.203	-0.203	-0.204	-0.204	-0.204	-0.204	-0.204	-0.204	-0.206	-0.207	-0.208	-0.209
0.840	-0.214	-0.215	-0.215	-0.216	-0.217	-0.218	-0.218	-0.218	-0.218	-0.218	-0.218	-0.218	-0.218	-0.221	-0.222
0.860	-0.228	-0.229	-0.229	-0.230	-0.231	-0.232	-0.232	-0.232	-0.232	-0.232	-0.232	-0.232	-0.232	-0.234	-0.237
C 880	-0.243	-0.244	-0.244	-0.245	-0.245	-0.245	-0.245	-0.245	-0.245	-0.245	-0.245	-0.245	-0.245	-0.248	-0.249

TABLE 15.—COORDINATES OF LOWER NAPPE FOR DIFFERENT VALUES OF $\frac{h_a}{H_s}$—3:3 WEIR—Continued

	Y/H_s														
X/H_s \ h_a/H_s	0.002	0.010	0.020	0.030	0.040	0.050	0.060	0.070	0.080	0.090	0.100	0.120	0.140	0.160	0.180
0.900	-0.257	-0.258	-0.258	-0.259	-0.259	-0.259	-0.259	-0.260	-0.260	-0.260	-0.260	-0.261	-0.262	-0.262	-0.264
0.920	-0.273	-0.273	-0.273	-0.274	-0.274	-0.274	-0.274	-0.274	-0.274	-0.274	-0.274	-0.275	-0.276	-0.276	-0.278
0.940	-0.288	-0.289	-0.289	-0.289	-0.289	-0.289	-0.289	-0.289	-0.289	-0.289	-0.289	-0.290	-0.291	-0.291	-0.293
0.960	-0.304	-0.305	-0.305	-0.305	-0.305	-0.305	-0.305	-0.306	-0.306	-0.306	-0.306	-0.306	-0.306	-0.307	-0.307
0.980	-0.319	-0.319	-0.319	-0.319	-0.319	-0.319	-0.319	-0.320	-0.320	-0.320	-0.320	-0.320	-0.320	-0.320	-0.321
1.000	-0.336	-0.336	-0.336	-0.336	-0.336	-0.336	-0.336	-0.337	-0.337	-0.337	-0.337	-0.337	-0.337	-0.337	-0.337
1.050	-0.378	-0.378	-0.378	-0.378	-0.378	-0.378	-0.378	-0.378	-0.378	-0.378	-0.378	-0.378	-0.378	-0.378	-0.378
1.100	-0.423	-0.423	-0.422	-0.422	-0.422	-0.422	-0.422	-0.422	-0.422	-0.422	-0.421	-0.420	-0.419	-0.419	-0.418
1.150	-0.469	-0.468	-0.467	-0.466	-0.465	-0.464	-0.463	-0.463	-0.463	-0.463	-0.462	-0.462	-0.462	-0.461	-0.460
1.200	-0.518	-0.516	-0.514	-0.514	-0.513	-0.512	-0.511	-0.510	-0.509	-0.508	-0.506	-0.506	-0.506	-0.506	-0.503
1.250	-0.569	-0.567	-0.564	-0.563	-0.562	-0.561	-0.560	-0.559	-0.557	-0.556	-0.554	-0.554	-0.554	-0.554	-0.550
1.300	-0.622	-0.620	-0.617	-0.616	-0.614	-0.613	-0.611	-0.610	-0.608	-0.607	-0.605	-0.604	-0.603	-0.601	-0.597
1.350	-0.677	-0.675	-0.672	-0.671	-0.669	-0.667	-0.665	-0.664	-0.662	-0.660	-0.658	-0.657	-0.655	-0.651	-0.647
1.400	-0.733	-0.731	-0.728	-0.726	-0.724	-0.722	-0.720	-0.719	-0.717	-0.715	-0.713	-0.711	-0.708	-0.703	-0.698
1.450	-0.791	-0.788	-0.784	-0.782	-0.780	-0.778	-0.776	-0.775	-0.773	-0.771	-0.769	-0.767	-0.764	-0.757	-0.751
1.500	-0.849	-0.846	-0.842	-0.841	-0.839	-0.837	-0.835	-0.833	-0.831	-0.829	-0.826	-0.823	-0.819	-0.811	-0.806
1.550	-0.909	-0.907	-0.904	-0.903	-0.901	-0.899	-0.897	-0.895	-0.892	-0.889	-0.886	-0.882	-0.877	-0.868	-0.861
1.600	-0.972	-0.970	-0.967	-0.965	-0.963	-0.961	-0.959	-0.957	-0.954	-0.952	-0.949	-0.943	-0.937	-0.927	-0.919
1.650	-1.039	-1.036	-1.032	-1.030	-1.027	-1.025	-1.022	-1.020	-1.018	-1.016	-1.013	-1.006	-0.999	-0.988	-0.979
1.700	-1.106	-1.103	-1.100	-1.098	-1.095	-1.093	-1.090	-1.088	-1.085	-1.082	-1.079	-1.071	-1.063	-1.050	-1.039
1.750	-1.176	-1.173	-1.170	-1.168	-1.165	-1.162	-1.159	-1.156	-1.153	-1.150	-1.147	-1.139	-1.130	-1.113	-1.101
1.800	-1.248	-1.245	-1.241	-1.238	-1.235	-1.232	-1.229	-1.226	-1.223	-1.220	-1.216	-1.206	-1.196	-1.177	-1.163
1.850	-1.320	-1.318	-1.315	-1.312	-1.308	-1.305	-1.301	-1.298	-1.294	-1.291	-1.287	-1.276	-1.265	-1.245	-1.229
1.900	-1.395	-1.393	-1.390	-1.387	1.383	-1.379	-1.375	-1.372	-1.368	-1.365	-1.361	-1.349	-1.336	-1.313	-1.294
1.950	-1.474	-1.470	-1.466	-1.462	-1.458	-1.454	-1.450	-1.446	-1.442	-1.438	-1.434	-1.422	-1.409	-1.383	-1.363
2.000	-1.552	-1.549	-1.545	-1.541	-1.537	-1.533	-1.528	-1.523	-1.518	-1.513	-1.508	-1.495	-1.482	-1.454	-1.443
2.050	-1.635	-1.631	-1.627	-1.622	-1.617	-1.612	-1.607	-1.601	-1.595	-1.589	-1.583	-1.570	-1.557	-1.530	-1.506
2.100	-1.718	-1.714	-1.710	-1.705	-1.700	-1.695	-1.689	-1.683	-1.676	-1.670	-1.663	-1.648	-1.633	-1.603	-1.579
2.150	-1.801	-1.798	-1.794	-1.789	-1.783	-1.778	-1.772	-1.766	-1.759	-1.753	-1.746	-1.729	-1.712	-1.680	-1.654
2.200	-1.889	-1.885	-1.880	-1.874	-1.868	-1.862	-1.855	-1.849	-1.842	-1.835	-1.828	-1.810	-1.791	-1.754	-1.729
2.250	-1.980	-1.975	-1.969	-1.962	-1.955	-1.948	-1.941	-1.935	-1.928	-1.921	-1.914	-1.893	-1.872	-1.834	-1.808
2.300	-2.071	-2.066	-2.061	-2.053	-2.045	-2.037	-2.029	-2.022	-2.015	-2.008	-2.001	-1.979	-1.957	-1.916	-1.889
2.350	-2.167	-2.161	-2.155	-2.147	-2.138	-2.130	-2.121	-2.113	-2.105	-2.097	-2.088	-2.067	-2.046	-2.003	-1.974
2.400	-2.262	-2.256	-2.250	-2.241	-2.232	-2.223	-2.214	-2.205	-2.196	-2.187	-2.178	-2.157	-2.135	-2.092	-2.060
2.450	-2.359	-2.353	-2.347	-2.337	-2.327	-2.317	-2.307	-2.297	-2.289	-2.280	-2.271	-2.249	-2.227	-2.183	-2.150
2.500	-2.460	-2.454	-2.448	-2.437	-2.426	-2.415	-2.404	-2.394	-2.384	-2.374	-2.364	-2.342	-2.320	-2.276	-2.244

TABLE 16.—COORDINATES OF LOWER NAPPE FOR DIFFERENT VALUES OF $\frac{h_a}{H_s}$ — 2:1 WEIR (BAZIN)

X/H_s \ h_a/H_s	0.002	0.010	0.020	0.030	0.040	0.050	0.060	0.070
	Y/H_s							
0.000	0.000	0.000	0.000	0.000	0.000	0.000	0.000	0.000
0.010	0.004	0.004	0.003	0.003	0.003	0.002	0.002	0.002
0.020	0.006	0.006	0.005	0.005	0.005	0.004	0.004	0.004
0.030	0.009	0.009	0.008	0.008	0.007	0.007	0.006	0.006
0.040	0.011	0.011	0.010	0.010	0.009	0.009	0.008	0.008
0.050	0.012	0.012	0.011	0.011	0.010	0.010	0.009	0.009
0.060	0.014	0.013	0.013	0.012	0.012	0.011	0.011	0.010
0.070	0.016	0.016	0.015	0.014	0.014	0.013	0.013	0.012
0.080	0.016	0.016	0.015	0.014	0.014	0.013	0.013	0.012
0.090	0.016	0.016	0.015	0.014	0.014	0.013	0.013	0.012
0.100	0.016	0.016	0.015	0.014	0.014	0.013	0.013	0.012
0.110	0.016	0.016	0.015	0.014	0.014	0.013	0.013	0.012
0.120	0.016	0.016	0.015	0.014	0.013	0.012	0.012	0.011
0.130	0.016	0.016	0.015	0.014	0.013	0.012	0.012	0.011
0.140	0.015	0.015	0.014	0.013	0.012	0.011	0.011	0.010
0.150	0.014	0.014	0.013	0.013	0.012	0.011	0.011	0.010
0.160	0.014	0.014	0.013	0.012	0.011	0.010	0.010	0.009
0.170	0.013	0.013	0.012	0.011	0.010	0.009	0.009	0.008
0.180	0.012	0.012	0.011	0.010	0.009	0.008	0.007	0.006
0.190	0.011	0.011	0.010	0.009	0.008	0.007	0.006	0.005
0.200	0.010	0.010	0.009	0.008	0.007	0.006	0.005	0.004
0.210	0.008	0.008	0.007	0.006	0.005	0.004	0.003	0.002
0.220	0.006	0.006	0.005	0.004	0.003	0.002	0.001	0.000
0.230	0.004	0.004	0.003	0.002	0.001	0.000	-0.001	-0.002
0.240	0.003	0.003	0.002	0.001	0.000	-0.001	-0.002	-0.003
0.250	0.001	0.001	0.000	-0.001	-0.001	-0.002	-0.003	-0.004
0.260	0.000	0.000	-0.002	-0.004	-0.005	-0.006	-0.007	-0.008
0.270	-0.003	-0.004	-0.005	-0.006	-0.007	-0.008	-0.009	-0.010
0.280	-0.005	-0.006	-0.007	-0.008	-0.009	-0.010	-0.011	-0.012
0.290	-0.008	-0.008	-0.009	-0.010	-0.011	-0.012	-0.013	-0.014
0.300	-0.010	-0.011	-0.012	-0.013	-0.014	-0.015	-0.016	-0.017
0.310	-0.012	-0.013	-0.014	-0.015	-0.016	-0.017	-0.018	-0.019
0.320	-0.015	-0.016	-0.017	-0.018	-0.019	-0.020	-0.021	-0.022
0.330	-0.018	-0.018	-0.019	-0.020	-0.021	-0.022	-0.023	-0.024
0.340	-0.020	-0.021	-0.022	-0.023	-0.025	-0.026	-0.027	-0.028
0.350	-0.024	-0.025	-0.026	-0.027	-0.028	-0.029	-0.030	-0.031
0.360	-0.026	-0.027	-0.029	-0.030	-0.031	-0.032	-0.033	-0.034
0.370	-0.030	-0.031	-0.033	-0.034	-0.035	-0.036	-0.037	-0.038
0.380	-0.033	-0.034	-0.036	-0.037	-0.038	-0.039	-0.040	-0.041
0.390	-0.036	-0.037	-0.039	-0.040	-0.041	-0.042	-0.043	-0.044
0.400	-0.040	-0.041	-0.043	-0.044	-0.045	-0.046	-0.047	-0.048
0.410	-0.044	-0.045	-0.047	-0.048	-0.049	-0.050	-0.051	-0.052
0.420	-0.047	-0.048	-0.050	-0.051	-0.052	-0.054	-0.055	-0.056
0.430	-0.051	-0.052	-0.054	-0.055	-0.056	-0.058	-0.059	-0.060
0.440	-0.054	-0.055	-0.057	-0.059	-0.060	-0.062	-0.063	-0.064
0.450	-0.058	-0.059	-0.061	-0.062	-0.063	-0.065	-0.066	-0.068
0.460	-0.061	-0.062	-0.064	-0.066	-0.067	-0.069	-0.071	-0.072
0.470	-0.067	-0.068	-0.070	-0.071	-0.072	-0.073	-0.075	-0.076
0.480	-0.071	-0.072	-0.074	-0.075	-0.076	-0.078	-0.080	-0.081
0.490	-0.076	-0.077	-0.079	-0.080	-0.081	-0.083	-0.085	-0.086

X/H_s \ h_a/H_s	0.002	0.010	0.020	0.030	0.040	0.050	0.060	0.070
	Y/H_s							
0.500	-0.080	-0.081	-0.083	-0.084	-0.086	-0.088	-0.090	-0.091
0.520	-0.090	-0.091	-0.093	-0.094	-0.095	-0.097	-0.099	-0.100
0.540	-0.100	-0.101	-0.103	-0.104	-0.105	-0.107	-0.109	-0.110
0.560	-0.110	-0.111	-0.113	-0.114	-0.115	-0.117	-0.119	-0.120
0.580	-0.120	-0.121	-0.123	-0.124	-0.125	-0.127	-0.129	-0.130
0.600	-0.130	-0.131	-0.133	-0.134	-0.135	-0.137	-0.139	-0.140
0.620	-0.141	-0.142	-0.144	-0.145	-0.146	-0.148	-0.150	-0.151
0.640	-0.153	-0.154	-0.156	-0.157	-0.158	-0.159	-0.161	-0.162
0.660	-0.164	-0.165	-0.167	-0.168	-0.169	-0.170	-0.172	-0.173
0.680	-0.176	-0.177	-0.179	-0.180	-0.181	-0.182	-0.183	-0.184
0.700	-0.188	-0.189	-0.191	-0.192	-0.193	-0.195	-0.196	-0.197
0.720	-0.201	-0.202	-0.203	-0.204	-0.205	-0.207	-0.208	-0.209
0.740	-0.214	-0.215	-0.216	-0.217	-0.218	-0.219	-0.220	-0.221
0.760	-0.227	-0.228	-0.229	-0.230	-0.231	-0.232	-0.233	-0.234
0.780	-0.240	-0.241	-0.242	-0.243	-0.244	-0.245	-0.246	-0.247
0.800	-0.254	-0.254	-0.255	-0.256	-0.257	-0.258	-0.259	-0.260
0.820	-0.268	-0.268	-0.269	-0.270	-0.271	-0.272	-0.273	-0.273
0.840	-0.282	-0.282	-0.283	-0.284	-0.285	-0.286	-0.287	-0.287
0.860	-0.296	-0.296	-0.296	-0.297	-0.298	-0.299	-0.300	-0.301
0.880	-0.310	-0.311	-0.312	-0.313	-0.314	-0.314	-0.315	-0.315
0.900	-0.324	-0.324	-0.325	-0.326	-0.327	-0.328	-0.329	-0.330
0.920	-0.340	-0.341	-0.342	-0.343	-0.343	-0.344	-0.344	-0.344
0.940	-0.356	-0.357	-0.357	-0.358	-0.358	-0.359	-0.359	-0.360
0.960	-0.373	-0.373	-0.374	-0.374	-0.375	-0.375	-0.376	-0.376
0.980	-0.390	-0.390	-0.391	-0.391	-0.391	-0.392	-0.392	-0.392
1.000	-0.406	-0.406	-0.406	-0.406	-0.407	-0.407	-0.407	-0.407
1.050	-0.450	-0.450	-0.450	-0.451	-0.451	-0.451	-0.452	-0.452
1.100	-0.493	-0.493	-0.494	-0.495	-0.496	-0.497	-0.498	-0.498
1.150	-0.540	-0.540	-0.541	-0.542	-0.543	-0.544	-0.545	-0.546
1.200	-0.586	-0.587	-0.589	-0.590	-0.592	-0.593	-0.595	-0.596
1.250	-0.636	-0.637	-0.639	-0.641	-0.643	-0.645	-0.647	-0.648
1.300	-0.690	-0.691	-0.693	-0.695	-0.697	-0.699	-0.701	-0.702
1.350	-0.742	-0.744	-0.746	-0.748	-0.750	-0.752	-0.754	-0.756
1.400	-0.798	-0.800	-0.802	-0.804	-0.806	-0.808	-0.810	-0.812
1.450	-0.856	-0.858	-0.860	-0.863	-0.865	-0.869	-0.871	-0.873
1.500	-0.914	-0.916	-0.919	-0.922	-0.925	-0.928	-0.931	-0.934
1.550	-0.976	-0.978	-0.981	-0.983	-0.985	-0.988	-0.990	-0.993
1.600	-1.044	-1.046	-1.048	-1.050	-1.051	-1.052	-1.054	-1.055
1.650	-1.108	-1.109	-1.111	-1.113	-1.115	-1.117	-1.119	-1.120
1.700	-1.174	-1.175	-1.177	-1.178	-1.180	-1.181	-1.183	-1.184
1.750	-1.242	-1.243	-1.245	-1.246	-1.248	-1.249	-1.251	-1.252
1.800	-1.312	-1.313	-1.314	-1.316	-1.317	-1.318	-1.319	-1.320
1.850	-1.381	-1.382	-1.383	-1.383	-1.384	-1.385	-1.386	-1.387
1.900	-1.450	-1.451	-1.452	-1.453	-1.454	-1.455	-1.456	-1.457
1.950	-1.518	-1.518	-1.519	-1.520	-1.520	-1.521	-1.522	-1.522
2.000	-1.587	-1.587	-1.588	-1.588	-1.589	-1.589	-1.590	-1.590

TABLE 17.—COORDINATES OF LOWER NAPPE FOR DIFFERENT VALUES OF $\frac{h_a}{H_s}$—4:1 WEIR (BAZIN)

Y/H_s

X/H_s \ h_a/H_s	0.002	0.010	0.020	0.030	0.040	0.050	0.060	0.070
0.000	0.000	0.000	0.000	0.000	0.000	0.000	0.000	0.000
0.010	0.002	0.002	0.002	0.002	0.002	0.002	0.002	0.002
0.020	0.003	0.003	0.003	0.003	0.003	0.003	0.003	0.003
0.030	0.004	0.004	0.003	0.003	0.003	0.002	0.002	0.002
0.040	0.004	0.004	0.003	0.003	0.003	0.002	0.002	0.002
0.050	0.004	0.004	0.004	0.003	0.003	0.002	0.002	0.002
0.060	0.004	0.004	0.003	0.003	0.002	0.002	0.001	0.001
0.070	0.003	0.003	0.002	0.002	0.002	0.002	0.001	0.001
0.080	0.003	0.003	0.002	0.002	0.001	0.001	0.000	0.000
0.090	0.002	0.002	0.001	0.001	0.000	0.000	-0.001	-0.001
0.100	0.002	0.001	0.001	0.000	0.000	-0.001	-0.002	-0.003
0.110	0.001	0.000	0.000	-0.001	-0.002	-0.003	-0.003	-0.004
0.120	0.000	-0.001	-0.001	-0.002	-0.003	-0.004	-0.004	-0.005
0.130	-0.002	-0.003	-0.003	-0.004	-0.005	-0.006	-0.006	-0.007
0.140	-0.003	-0.004	-0.005	-0.006	-0.006	-0.007	-0.008	-0.009
0.150	-0.005	-0.006	-0.007	-0.008	-0.009	-0.010	-0.011	-0.012
0.160	-0.007	-0.008	-0.009	-0.010	-0.011	-0.012	-0.013	-0.014
0.170	-0.009	-0.010	-0.011	-0.012	-0.013	-0.014	-0.015	-0.016
0.180	-0.011	-0.012	-0.013	-0.014	-0.015	-0.016	-0.017	-0.018
0.190	-0.013	-0.014	-0.015	-0.016	-0.018	-0.019	-0.020	-0.021
0.200	-0.015	-0.016	-0.018	-0.019	-0.020	-0.021	-0.023	-0.024
0.210	-0.018	-0.019	-0.021	-0.022	-0.023	-0.024	-0.026	-0.027
0.220	-0.020	-0.021	-0.023	-0.024	-0.026	-0.027	-0.029	-0.030
0.230	-0.024	-0.025	-0.027	-0.028	-0.029	-0.030	-0.032	-0.033
0.240	-0.026	-0.027	-0.029	-0.030	-0.032	-0.033	-0.035	-0.036
0.250	-0.029	-0.031	-0.032	-0.034	-0.035	-0.037	-0.038	-0.040
0.260	-0.032	-0.034	-0.035	-0.037	-0.038	-0.040	-0.042	-0.043
0.270	-0.036	-0.037	-0.039	-0.040	-0.042	-0.043	-0.045	-0.046
0.280	-0.039	-0.041	-0.042	-0.044	-0.045	-0.047	-0.048	-0.050
0.290	-0.042	-0.044	-0.045	-0.047	-0.049	-0.051	-0.052	-0.054
0.300	-0.045	-0.047	-0.048	-0.050	-0.052	-0.054	-0.055	-0.057
0.310	-0.048	-0.050	-0.052	-0.054	-0.055	-0.057	-0.059	-0.061
0.320	-0.052	-0.054	-0.055	-0.057	-0.059	-0.061	-0.062	-0.064
0.330	-0.056	-0.058	-0.059	-0.061	-0.063	-0.065	-0.066	-0.068
0.340	-0.059	-0.061	-0.063	-0.065	-0.066	-0.068	-0.070	-0.072
0.350	-0.062	-0.064	-0.066	-0.068	-0.070	-0.072	-0.074	-0.076
0.360	-0.066	-0.068	-0.070	-0.072	-0.074	-0.076	-0.078	-0.080
0.370	-0.069	-0.071	-0.073	-0.075	-0.078	-0.080	-0.082	-0.084
0.380	-0.073	-0.075	-0.077	-0.079	-0.082	-0.084	-0.086	-0.088
0.390	-0.077	-0.079	-0.081	-0.083	-0.086	-0.088	-0.090	-0.092
0.400	-0.080	-0.082	-0.085	-0.087	-0.089	-0.091	-0.094	-0.096
0.410	-0.084	-0.086	-0.088	-0.090	-0.093	-0.095	-0.097	-0.099
0.420	-0.089	-0.091	-0.093	-0.095	-0.097	-0.099	-0.101	-0.103
0.430	-0.093	-0.095	-0.097	-0.099	-0.102	-0.104	-0.106	-0.108
0.440	-0.097	-0.099	-0.101	-0.103	-0.105	-0.107	-0.109	-0.111
0.450	-0.102	-0.104	-0.106	-0.108	-0.110	-0.112	-0.114	-0.116
0.460	-0.107	-0.109	-0.111	-0.113	-0.114	-0.116	-0.118	-0.120
0.470	-0.112	-0.114	-0.116	-0.118	-0.120	-0.122	-0.124	-0.126
0.480	-0.117	-0.119	-0.121	-0.123	-0.124	-0.126	-0.128	-0.130
0.490	-0.121	-0.123	-0.125	-0.127	-0.129	-0.131	-0.133	-0.135

X/H_s \ h_a/H_s	0.002	0.010	0.020	0.030	0.040	0.050	0.060	0.070
0.500	-0.126	-0.128	-0.130	-0.132	-0.134	-0.136	-0.138	-0.140
0.520	-0.137	-0.139	-0.141	-0.143	-0.145	-0.147	-0.149	-0.151
0.540	-0.148	-0.150	-0.152	-0.154	-0.155	-0.157	-0.159	-0.161
0.560	-0.158	-0.160	-0.162	-0.164	-0.166	-0.168	-0.170	-0.172
0.580	-0.170	-0.172	-0.174	-0.176	-0.178	-0.180	-0.182	-0.184
0.600	-0.181	-0.183	-0.185	-0.187	-0.189	-0.192	-0.194	-0.196
0.620	-0.193	-0.195	-0.197	-0.199	-0.202	-0.204	-0.206	-0.208
0.640	-0.206	-0.208	-0.210	-0.212	-0.214	-0.216	-0.218	-0.220
0.660	-0.218	-0.220	-0.222	-0.224	-0.227	-0.229	-0.231	-0.233
0.680	-0.230	-0.232	-0.235	-0.237	-0.239	-0.241	-0.244	-0.246
0.700	-0.244	-0.246	-0.248	-0.250	-0.252	-0.254	-0.256	-0.258
0.720	-0.256	-0.258	-0.261	-0.263	-0.265	-0.267	-0.270	-0.272
0.740	-0.270	-0.272	-0.275	-0.277	-0.279	-0.281	-0.284	-0.286
0.760	-0.282	-0.285	-0.287	-0.290	-0.292	-0.295	-0.297	-0.300
0.780	-0.296	-0.299	-0.301	-0.304	-0.306	-0.309	-0.311	-0.314
0.800	-0.310	-0.313	-0.315	-0.318	-0.320	-0.323	-0.325	-0.328
0.820	-0.324	-0.327	-0.330	-0.333	-0.335	-0.338	-0.341	-0.344
0.840	-0.338	-0.341	-0.344	-0.347	-0.349	-0.352	-0.355	-0.358
0.860	-0.352	-0.355	-0.358	-0.361	-0.365	-0.368	-0.371	-0.374
0.880	-0.368	-0.371	-0.374	-0.377	-0.380	-0.383	-0.386	-0.389
0.900	-0.384	-0.387	-0.390	-0.393	-0.395	-0.398	-0.401	-0.404
0.920	-0.400	-0.403	-0.406	-0.409	-0.411	-0.414	-0.417	-0.420
0.940	-0.416	-0.419	-0.421	-0.424	-0.427	-0.430	-0.432	-0.435
0.960	-0.434	-0.436	-0.439	-0.441	-0.444	-0.446	-0.449	-0.451
0.980	-0.452	-0.454	-0.456	-0.458	-0.460	-0.462	-0.464	-0.466
1.000	-0.470	-0.472	-0.474	-0.476	-0.477	-0.479	-0.481	-0.483
1.050	-0.514	-0.516	-0.517	-0.519	-0.521	-0.523	-0.524	-0.526
1.100	-0.561	-0.563	-0.564	-0.566	-0.567	-0.569	-0.570	-0.572
1.150	-0.610	-0.611	-0.613	-0.614	-0.616	-0.617	-0.619	-0.620
1.200	-0.661	-0.662	-0.664	-0.665	-0.666	-0.667	-0.669	-0.670
1.250	-0.714	-0.715	-0.716	-0.717	-0.719	-0.720	-0.721	-0.722
1.300	-0.768	-0.769	-0.770	-0.771	-0.773	-0.774	-0.775	-0.776
1.350	-0.822	-0.823	-0.824	-0.825	-0.827	-0.828	-0.829	-0.830
1.400	-0.878	-0.879	-0.880	-0.881	-0.883	-0.884	-0.885	-0.886
1.450	-0.937	-0.938	-0.940	-0.941	-0.942	-0.943	-0.945	-0.946
1.500	-0.998	-0.999	-1.000	-1.001	-1.003	-1.004	-1.005	-1.006
1.550	-1.063	-1.064	-1.066	-1.067	-1.068	-1.069	-1.071	-1.072
1.600	-1.122	-1.124	-1.126	-1.128	-1.130	-1.132	-1.134	-1.136
1.650	-1.186	-1.188	-1.190	-1.192	-1.194	-1.196	-1.198	-1.200
1.700	-1.250	-1.252	-1.254	-1.256	-1.258	-1.260	-1.262	-1.264
1.750	-1.335	-1.337	-1.339	-1.341	-1.344	-1.346	-1.348	-1.350
1.800	-1.400	-1.402	-1.403	-1.405	-1.407	-1.409	-1.410	-1.412
1.850	-1.466	-1.468	-1.469	-1.471	-1.472	-1.474	-1.476	-1.477
1.900	-1.530	-1.532	-1.533	-1.535	-1.537	-1.539	-1.540	-1.542
1.950	-1.593	-1.595	-1.597	-1.599	-1.600	-1.602	-1.604	-1.606
2.000	-1.656	-1.658	-1.660	-1.662	-1.664	-1.666	-1.668	-1.670

TABLE 18.—COORDINATES OF UPPER NAPPE FOR DIFFERENT VALUES OF $\frac{h_a}{H_s}$—VERTICAL WEIR

h_a/H_s \ X/H_s	Y/H_s 0.002	0.020	0.040	0.060	0.080	0.100	0.120	0.140	0.160	0.180	0.200
-4.000	0.990										
-3.900	0.990										
-3.800	0.990										
-3.700	0.990	0.974	0.958								
-3.600	0.990	0.974	0.958								
-3.500	0.990	0.974	0.958	0.934	0.911						
-3.400	0.990	0.974	0.957	0.934	0.910						
-3.300	0.990	0.972	0.955	0.932	0.910						
-3.200	0.990	0.972	0.954	0.932	0.910	0.878					
-3.100	0.989	0.971	0.953	0.932	0.910	0.877					
-3.000	0.988	0.970	0.952	0.931	0.910	0.876	0.844	0.812			
-2.900	0.988	0.969	0.950	0.930	0.910	0.875	0.844	0.812			
-2.800	0.987	0.968	0.950	0.930	0.909	0.874	0.843	0.811			
-2.700	0.986	0.968	0.949	0.929	0.909	0.873	0.842	0.811			
-2.600	0.985	0.966	0.948	0.928	0.908	0.872	0.841	0.810			
-2.500	0.984	0.966	0.947	0.928	0.908	0.872	0.841	0.810	0.782		
-2.400	0.983	0.965	0.947	0.927	0.907	0.871	0.840	0.809	0.781		
-2.300	0.982	0.964	0.946	0.926	0.906	0.871	0.840	0.809	0.780		
-2.200	0.981	0.963	0.945	0.925	0.905	0.870	0.839	0.808	0.779	0.760	0.743
-2.100	0.980	0.962	0.944	0.924	0.904	0.870	0.839	0.808	0.778	0.760	0.742
-2.000	0.979	0.961	0.943	0.923	0.903	0.869	0.838	0.807	0.777	0.758	0.741
-1.900	0.978	0.960	0.942	0.922	0.903	0.869	0.838	0.807	0.776	0.758	0.740
-1.800	0.977	0.959	0.941	0.922	0.902	0.868	0.837	0.806	0.776	0.757	0.739
-1.700	0.975	0.958	0.940	0.920	0.901	0.868	0.837	0.806	0.775	0.756	0.738
-1.600	0.974	0.956	0.939	0.920	0.901	0.867	0.836	0.805	0.774	0.755	0.737
-1.500	0.972	0.955	0.938	0.919	0.900	0.866	0.835	0.804	0.773	0.754	0.736
-1.400	0.970	0.954	0.937	0.918	0.899	0.865	0.834	0.803	0.771	0.753	0.735
-1.300	0.967	0.952	0.936	0.917	0.898	0.864	0.833	0.802	0.770	0.752	0.734
-1.200	0.964	0.949	0.934	0.916	0.897	0.863	0.832	0.801	0.769	0.751	0.733
-1.100	0.961	0.946	0.931	0.914	0.894	0.861	0.831	0.800	0.768	0.750	0.732
-1.000	0.958	0.944	0.929	0.911	0.892	0.859	0.829	0.799	0.767	0.749	0.731
-0.900	0.952	0.938	0.924	0.907	0.890	0.856	0.827	0.798	0.765	0.747	0.730
-0.800	0.947	0.934	0.920	0.902	0.885	0.850	0.822	0.795	0.763	0.745	0.727
-0.700	0.940	0.926	0.913	0.896	0.880	0.846	0.820	0.793	0.761	0.742	0.724
-0.600	0.930	0.918	0.907	0.890	0.873	0.840	0.815	0.790	0.759	0.740	0.721
-0.500	0.921	0.910	0.898	0.882	0.865	0.832	0.808	0.783	0.755	0.736	0.718
-0.400	0.911	0.899	0.887	0.872	0.856	0.823	0.800	0.777	0.750	0.731	0.713
-0.300	0.899	0.886	0.873	0.858	0.844	0.812	0.791	0.770	0.744	0.726	0.707
-0.200	0.883	0.871	0.859	0.844	0.830	0.800	0.780	0.760	0.735	0.718	0.700
-0.100	0.866	0.853	0.840	0.826	0.812	0.784	0.766	0.748	0.724	0.708	0.692
0.000	0.845	0.832	0.819	0.804	0.790	0.764	0.748	0.732	0.710	0.696	0.682
0.100	0.820	0.806	0.793	0.780	0.767	0.740	0.726	0.713	0.693	0.680	0.667
0.200	0.790	0.778	0.765	0.752	0.738	0.717	0.703	0.690	0.671	0.660	0.650
0.300	0.755	0.742	0.730	0.718	0.706	0.686	0.673	0.660	0.644	0.635	0.627
0.400	0.714	0.702	0.690	0.680	0.669	0.650	0.637	0.625	0.610	0.603	0.595
0.500	0.670	0.658	0.645	0.634	0.624	0.608	0.596	0.583	0.570	0.564	0.558
0.600	0.619	0.606	0.594	0.584	0.575	0.558	0.546	0.533	0.523	0.518	0.512
0.700	0.560	0.548	0.536	0.528	0.519	0.500	0.490	0.480	0.470	0.465	0.460
0.800	0.494	0.482	0.470	0.462	0.453	0.440	0.429	0.418	0.410	0.404	0.400
0.900	0.423	0.412	0.400	0.390	0.380	0.368	0.359	0.349	0.340	0.335	0.330
1.000	0.344	0.332	0.320	0.310	0.300	0.290	0.280	0.270	0.263	0.258	0.253
1.100	0.252	0.241	0.230	0.222	0.213	0.200	0.194	0.188	0.180	0.175	0.170
1.200	0.153	0.144	0.134	0.127	0.120	0.108	0.102	0.095	0.088	0.083	0.078
1.300	0.048	0.039	0.030	0.024	0.018	0.005	0.000	-0.005	-0.012	-0.016	-0.021
1.400	-0.067	-0.074	-0.080	-0.086	-0.091	-0.104	-0.108	-0.112	-0.120	-0.125	-0.130
1.500	-0.190	-0.195	-0.200	-0.205	-0.210	-0.220	-0.225	-0.230	-0.240	-0.244	-0.245
1.600	-0.317	-0.322	-0.328	-0.332	-0.336	-0.349	-0.352	-0.355	-0.362	-0.366	-0.370
1.700	-0.450	-0.456	-0.461	-0.466	-0.470	-0.481	-0.484	-0.488	-0.496	-0.498	-0.501
1.800	-0.597	-0.601	-0.605	-0.608	-0.612	-0.622	-0.626	-0.630	-0.636	-0.638	-0.641
1.900	-0.750	-0.754	-0.758	-0.761	-0.764	-0.770	-0.774	-0.779	-0.783	-0.786	-0.790
2.000	-0.905	-0.908	-0.911	-0.916	-0.920	-0.925	-0.928	-0.930	-0.934	-0.936	-0.937
2.100	-1.080	-1.082	-1.085	-1.086	-1.088	-1.090	-1.092	-1.095	-1.092	-1.092	-1.095
2.200	-1.255	-1.264	-1.273	-1.272	-1.270	-1.271	-1.268	-1.265	-1.264	-1.262	-1.260
2.300	-1.450	-1.458	-1.465	-1.464	-1.462	-1.460	-1.452	-1.445	-1.442	-1.438	-1.433
2.400	-1.652	-1.661	-1.670	-1.666	-1.662	-1.658	-1.649	-1.640	-1.630	-1.625	-1.620
2.500	-1.865	-1.872	-1.880	-1.876	-1.872	-1.860	-1.850	-1.840	-1.826	-1.818	-1.810
2.600	-2.090	-2.090	-2.090	-2.086	-2.082	-2.068	-2.057	-2.046	-2.023	-2.016	-2.008
2.700	-2.322	-2.317	-2.312	-2.304	-2.296	-2.278	-2.264	-2.250	-2.223	-2.214	-2.207
2.800	-2.554	-2.546	-2.538	-2.526	-2.515	-2.492	-2.476	-2.460	-2.434	-2.422	-2.410
2.900	-2.790	-2.778	-2.767	-2.754	-2.740	-2.719	-2.701	-2.680	-2.655	-2.644	-2.632
3.000	-3.032	-3.021	-3.010	-2.995	-2.980	-2.958	-2.939	-2.910	-2.892	-2.881	-2.870
3.100	-3.285	-3.272	-3.260	-3.245	-3.230	-3.208	-3.192	-3.160	-3.145	-3.132	-3.120
3.200	-3.540	-3.528	-3.515	-3.502	-3.490	-3.462	-3.447	-3.418	-3.405	-3.394	-3.385
3.300	-3.803	-3.792	-3.780	-3.766	-3.752	-3.725	-3.714	-3.690	-3.676	-3.664	-3.654
3.400	-4.074	-4.062	-4.050	-4.040	-4.030	-4.008	-3.994	-3.972	-3.955	-3.946	-3.940

TABLE 19.—COORDINATES OF UPPER NAPPE FOR DIFFERENT VALUES OF $\frac{h_a}{H_s}$—1:3 WEIR

	Y/H_s													
X/H_s \ h_a/H_s	0.002	0.020	0.030	0.040	0.050	0.060	0.070	0.080	0.090	0.100	0.120	0.140	0.160	0.180
-4.000	0.987	0.973	0.962	0.950	0.940	0.929	0.919	0.908	0.897	0.885	0.862	0.838	0.814	0.790
-3.900	0.987	0.973	0.962	0.950	0.940	0.929	0.919	0.908	0.897	0.885	0.862	0.838	0.813	0.790
-3.800	0.987	0.973	0.962	0.950	0.940	0.929	0.919	0.908	0.897	0.885	0.862	0.837	0.812	0.790
-3.700	0.986	0.972	0.961	0.950	0.940	0.929	0.918	0.907	0.896	0.885	0.862	0.837	0.811	0.790
-3.600	0.986	0.972	0.961	0.950	0.939	0.928	0.917	0.906	0.895	0.884	0.862	0.836	0.810	0.790
-3.500	0.986	0.972	0.961	0.950	0.939	0.928	0.917	0.905	0.895	0.884	0.862	0.836	0.810	0.790
-3.400	0.986	0.972	0.961	0.950	0.939	0.928	0.917	0.905	0.894	0.883	0.861	0.836	0.810	0.789
-3.300	0.986	0.971	0.961	0.950	0.939	0.928	0.917	0.905	0.894	0.883	0.861	0.835	0.809	0.789
-3.200	0.986	0.971	0.960	0.949	0.938	0.927	0.916	0.905	0.894	0.883	0.861	0.835	0.808	0.788
-3.100	0.986	0.971	0.960	0.948	0.938	0.927	0.916	0.905	0.894	0.883	0.860	0.834	0.808	0.788
-3.000	0.986	0.970	0.959	0.947	0.937	0.926	0.915	0.904	0.893	0.882	0.860	0.834	0.807	0.787
-2.900	0.986	0.969	0.958	0.946	0.936	0.925	0.914	0.903	0.892	0.881	0.859	0.833	0.806	0.785
-2.800	0.986	0.969	0.958	0.946	0.936	0.925	0.914	0.903	0.892	0.881	0.859	0.832	0.805	0.782
-2.700	0.986	0.969	0.958	0.946	0.936	0.925	0.914	0.903	0.892	0.881	0.859	0.832	0.804	0.781
-2.600	0.986	0.969	0.958	0.946	0.936	0.925	0.914	0.903	0.892	0.881	0.858	0.831	0.804	0.781
-2.500	0.986	0.968	0.957	0.946	0.936	0.925	0.914	0.903	0.892	0.881	0.858	0.831	0.803	0.780
-2.400	0.985	0.968	0.957	0.945	0.935	0.924	0.913	0.902	0.891	0.880	0.857	0.830	0.803	0.780
-2.300	0.984	0.967	0.956	0.944	0.934	0.923	0.913	0.902	0.891	0.879	0.856	0.829	0.802	0.779
-2.200	0.983	0.966	0.955	0.943	0.933	0.923	0.913	0.902	0.890	0.878	0.854	0.828	0.801	0.778
-2.100	0.982	0.965	0.954	0.942	0.932	0.922	0.912	0.902	0.890	0.878	0.853	0.827	0.801	0.776
-2.000	0.980	0.963	0.953	0.942	0.932	0.922	0.912	0.902	0.890	0.877	0.852	0.826	0.800	0.774
-1.900	0.979	0.962	0.952	0.942	0.932	0.922	0.912	0.902	0.890	0.877	0.852	0.826	0.800	0.772
-1.800	0.977	0.960	0.951	0.941	0.932	0.922	0.912	0.902	0.890	0.877	0.851	0.826	0.800	0.770
-1.700	0.973	0.959	0.950	0.940	0.931	0.921	0.911	0.901	0.889	0.876	0.851	0.826	0.800	0.768
-1.600	0.970	0.957	0.948	0.939	0.930	0.920	0.911	0.901	0.889	0.876	0.850	0.825	0.800	0.766
-1.500	0.968	0.954	0.946	0.938	0.929	0.919	0.910	0.900	0.888	0.875	0.850	0.825	0.799	0.762
-1.400	0.963	0.952	0.945	0.937	0.928	0.919	0.910	0.900	0.888	0.875	0.849	0.824	0.798	0.760
-1.300	0.960	0.949	0.942	0.935	0.926	0.917	0.908	0.899	0.887	0.874	0.848	0.823	0.797	0.758
-1.200	0.957	0.944	0.938	0.932	0.924	0.915	0.906	0.897	0.885	0.872	0.847	0.822	0.796	0.754
-1.100	0.952	0.940	0.935	0.930	0.921	0.912	0.903	0.894	0.882	0.870	0.846	0.820	0.794	0.750
-1.000	0.949	0.937	0.932	0.926	0.918	0.909	0.900	0.891	0.880	0.868	0.845	0.819	0.792	0.746
-0.900	0.943	0.931	0.926	0.920	0.912	0.904	0.896	0.887	0.876	0.865	0.842	0.817	0.791	0.742
-0.800	0.938	0.927	0.921	0.914	0.906	0.898	0.890	0.882	0.872	0.861	0.840	0.815	0.789	0.738
-0.700	0.931	0.920	0.914	0.908	0.901	0.893	0.885	0.877	0.867	0.857	0.836	0.811	0.785	0.732
-0.600	0.923	0.911	0.906	0.900	0.893	0.885	0.877	0.869	0.860	0.850	0.830	0.805	0.780	0.729
-0.500	0.913	0.902	0.897	0.891	0.884	0.876	0.868	0.860	0.851	0.842	0.824	0.800	0.775	0.722
-0.400	0.900	0.891	0.886	0.880	0.873	0.865	0.858	0.850	0.842	0.833	0.815	0.792	0.769	0.715
-0.300	0.887	0.878	0.873	0.867	0.860	0.853	0.846	0.839	0.830	0.821	0.803	0.781	0.759	0.707
-0.200	0.870	0.861	0.856	0.850	0.844	0.837	0.830	0.823	0.815	0.807	0.790	0.770	0.749	0.698
-0.100	0.852	0.842	0.838	0.833	0.827	0.820	0.814	0.807	0.799	0.791	0.774	0.755	0.735	0.687
0.000	0.830	0.820	0.816	0.812	0.806	0.800	0.794	0.787	0.779	0.771	0.755	0.737	0.718	0.672
0.100	0.803	0.795	0.791	0.786	0.780	0.774	0.768	0.762	0.755	0.748	0.734	0.716	0.697	0.656
0.200	0.773	0.765	0.761	0.756	0.751	0.745	0.739	0.733	0.727	0.720	0.706	0.688	0.670	0.633
0.300	0.737	0.728	0.724	0.719	0.714	0.709	0.704	0.699	0.693	0.687	0.674	0.656	0.638	0.606
0.400	0.696	0.687	0.683	0.679	0.675	0.670	0.665	0.660	0.654	0.648	0.635	0.617	0.599	0.572
0.500	0.649	0.641	0.638	0.634	0.629	0.624	0.619	0.614	0.608	0.602	0.589	0.573	0.556	0.532
0.600	0.596	0.587	0.584	0.580	0.575	0.570	0.565	0.560	0.555	0.549	0.537	0.521	0.505	0.486
0.700	0.536	0.527	0.524	0.520	0.516	0.511	0.506	0.501	0.496	0.490	0.479	0.463	0.447	0.432
0.800	0.469	0.460	0.457	0.454	0.449	0.444	0.439	0.434	0.429	0.423	0.411	0.398	0.385	0.371
0.900	0.396	0.388	0.384	0.379	0.375	0.370	0.366	0.361	0.356	0.351	0.341	0.328	0.315	0.304
1.000	0.316	0.308	0.304	0.300	0.295	0.290	0.285	0.279	0.275	0.271	0.262	0.249	0.236	0.228
1.100	0.229	0.219	0.216	0.213	0.208	0.202	0.197	0.191	0.186	0.181	0.171	0.161	0.151	0.149
1.200	0.134	0.125	0.121	0.116	0.111	0.106	0.101	0.095	0.090	0.085	0.075	0.068	0.060	0.060
1.300	0.030	0.022	0.018	0.013	0.008	0.002	-0.004	-0.009	-0.015	-0.020	-0.030	-0.033	-0036	-0.036
1.400	-0.082	-0.090	-0.095	-0.099	-0.105	-0.110	-0.115	-0.120	-0.126	-0.131	-0.141	-0.141	-0.141	-0.139
1.500	-0.203	-0.210	-0.215	-0.219	-0.224	-0.229	-0.234	-0.239	-0.244	-0.249	-0.258	-0.257	-0.256	-0.251
1.600	-0.332	-0.338	-0.342	-0.346	-0.351	-0.356	-0.361	-0.365	-0.369	-0.373	-0.380	-0.378	-0.376	-0.367
1.700	-0.468	-0.473	-0.477	-0.480	-0.485	-0.489	-0.494	-0.498	-0.501	-0.504	-0.510	-0.507	-0.503	-0.492
1.800	-0.612	-0.618	-0.620	-0.621	-0.626	-0.630	-0.634	-0.638	-0.640	-0.642	-0.646	-0.640	-0.634	-0.628
1.900	-0.766	-0.768	-0.769	-0.769	-0.773	-0.777	-0.781	-0.785	-0.786	-0.787	-0.789	-0.783	-0.776	-0.768
2.000	-0.927	-0.927	-0.927	-0.927	-0.931	-0.934	-0.937	-0.940	-0.937	-0.934	-0.927	-0.926	-0.925	-0.920
2.100	-1.091	-1.088	-1.090	-1.092	-1.095	-1.097	-1.100	-1.102	-1.102	-1.102	-1.102	-1.094	-1.086	-1.075
2.200	-1.266	-1.265	-1.266	-1.267	-1.269	-1.271	-1.273	-1.275	-1.274	-1.273	-1.270	-1.262	-1.253	-1.243
2.300	-1.453	-1.453	-1.452	-1.450	-1.452	-1.454	-1.456	-1.457	-1.453	-1.449	-1.440	-1.437	-1.433	-1.418
2.400	-1.648	-1.647	-1.645	-1.642	-1.642	-1.641	-1.640	-1.639	-1.637	-1.635	-1.630	-1.625	-1.619	-1.601
2.500	-1.855	-1.852	-1.848	-1.843	-1.842	-1.841	-1.840	-1.838	-1.836	-1.833	-1.827	-1.819	-1.810	-1.793
2.600	-2.072	-2.066	-2.063	-2.060	-2.058	-2.055	-2.053	-2.050	-2.046	-2.042	-2.034	-1.824	-2.014	-1.996
2.700	-2.292	-2.288	-2.283	-2.278	-2.276	-2.273	-2.271	-2.268	-2.263	-2.258	-2.248	-2.235	-2.221	-2.201
2.800	-2.515	-2.513	-2.509	-2.505	-2.501	-2.497	-2.493	-2.488	-2.482	-2.475	-2.461	-2.446	-2.431	-2.409
2.900	-2.747	-2.741	-2.738	-2.735	-2.730	-2.725	-2.720	-2.715	-2.707	-2.699	-2.682	-2.664	-2.646	-2.620

TABLE 20.—COORDINATES OF UPPER NAPPE FOR DIFFERENT VALUES OF $\frac{h_a}{H_s}$—2:3 WEIR

	Y/H_s													
h_a/H_s \ X/H_s	0.002	0.020	0.030	0.040	0.050	0.060	0.070	0.080	0.090	0.100	0.120	0.140	0.160	0.180
-4.000	0.981	0.969	0.958	0.947	0.936	0.925	0.912	0.899	0.886	0.873	0.853	0.832	0.805	0.778
-3.900	0.980	0.969	0.958	0.947	0.936	0.924	0.912	0.899	0.886	0.873	0.853	0.832	0.805	0.778
-3.800	0.980	0.969	0.958	0.947	0.936	0.924	0.912	0.899	0.886	0.873	0.852	0.831	0.804	0.776
-3.700	0.980	0.969	0.958	0.947	0.936	0.924	0.912	0.899	0.886	0.873	0.852	0.831	0.803	0.775
-3.600	0.979	0.968	0.957	0.946	0.935	0.924	0.912	0.899	0.886	0.873	0.852	0.830	0.802	0.773
-3.500	0.979	0.968	0.957	0.446	0.935	0.924	0.912	0.899	0.886	0.873	0.852	0.830	0.801	0.772
-3.400	0.979	0.968	0.957	0.946	0.935	0.924	0.912	0.899	0.886	0.873	0.851	0.829	0.800	0.771
-3.300	0.978	0.966	0.956	0.945	0.935	0.924	0.912	0.899	0.886	0.873	0.851	0.828	0.799	0.770
-3.200	0.978	0.965	0.955	0.945	0.935	0.924	0.912	0.899	0.886	0.873	0.851	0.828	0.799	0.770
-3.100	0.977	0.964	0.954	0.944	0.934	0.923	0.911	0.898	0.886	0.873	0.851	0.828	0.799	0.770
-3.000	0.977	0.963	0.953	0.943	0.933	0.923	0.911	0.898	0.886	0.873	0.850	0.827	0.798	0.769
-2.900	0.977	0.963	0.953	0.943	0.933	0.923	0.911	0.898	0.886	0.873	0.850	0.826	0.797	0.768
-2.800	0.977	0.963	0.953	0.943	0.933	0.922	0.910	0.898	0.886	0.873	0.850	0.826	0.797	0.767
-2.700	0.977	0.963	0.953	0.943	0.933	0.922	0.910	0.897	0.885	0.872	0.849	0.825	0.796	0.766
-2.600	0.976	0.962	0.952	0.942	0.932	0.922	0.910	0.897	0.885	0.872	0.848	0.824	0.795	0.766
-2.500	0.976	0.961	0.952	0.942	0.932	0.222	0.910	0.897	0.884	0.871	0.847	0.823	0.794	0.764
-2.400	0.976	0.961	0.952	0.942	0.932	0.922	0.910	0.897	0.884	0.871	0.847	0.822	0.792	0.762
-2.300	0.974	0.960	0.951	0.941	0.932	0.922	0.910	0.897	0.884	0.871	0.846	0.820	0.791	0.761
-2.200	0.974	0.960	0.951	0.941	0.931	0.921	0.909	0.896	0.883	0.870	0.845	0.820	0.790	0.760
-2.100	0.973	0.960	0.951	0.941	0.931	0.921	0.909	0.896	0.883	0.870	0.845	0.819	0.790	0.760
-2.000	0.972	0.959	0.950	0.940	0.930	0.920	0.908	0.895	0.883	0.870	0.845	0.819	0.789	0.759
-1.900	0.970	0.957	0.948	0.939	0.930	0.920	0.908	0.895	0.883	0.870	0.844	0.817	0.788	0.758
-1.800	0.970	0.954	0.946	0.937	0.929	0.920	0.908	0.895	0.883	0.870	0.843	0.816	0.787	0.757
-1.700	0.968	0.952	0.944	0.936	0.928	0.920	0.908	0.895	0.883	0.870	0.843	0.816	0.786	0.756
-1.600	0.964	0.950	0.943	0.935	0.928	0.920	0.908	0.895	0.882	0.869	0.842	0.815	0.785	0.754
-1.500	0.960	0.946	0.940	0.933	0.927	0.920	0.907	0.894	0.881	0.868	0.841	0.814	0.783	0.752
-1.400	0.958	0.943	0.937	0.931	0.925	0.919	0.906	0.893	0.880	0.867	0.841	0.814	0.783	0.751
-1.300	0.953	0.940	0.935	0.929	0.924	0.918	0.905	0.892	0.879	0.866	0.840	0.814	0.782	0.749
-1.200	0.949	0.938	0.933	0.927	0.922	0.916	0.903	0.890	0.877	0.864	0.839	0.814	0.781	0.747
-1.100	0.942	0.933	0.928	0.923	0.918	0.913	0.901	0.888	0.876	0.863	0.839	0.814	0.780	0.745
-1.000	0.937	0.928	0.923	0.918	0.913	0.907	0.896	0.884	0.872	0.860	0.837	0.813	0.777	0.741
-0.900	0.930	0.921	0.917	0.912	0.908	0.903	0.892	0.881	0.870	0.858	0.834	0.810	0.775	0.739
-0.800	0.921	0.913	0.909	0.905	0.901	0.897	0.886	0.875	0.864	0.853	0.831	0.808	0.771	0.734
-0.700	0.913	0.905	0.902	0.898	0.894	0.890	0.880	0.870	0.860	0.849	0.826	0.803	0.766	0.729
-0.600	0.903	0.896	0.892	0.888	0.884	0.880	0.871	0.861	0.852	0.842	0.820	0.798	0.761	0.723
-0.500	0.892	0.883	0.880	0.876	0.873	0.869	0.860	0.851	0.842	0.833	0.812	0.790	0.754	0.718
-0.400	0.879	0.870	0.867	0.864	0.861	0.858	0.850	0.842	0.833	0.825	0.803	0.780	0.744	0.708
-0.300	0.862	0.857	0.854	0.850	0.846	0.842	0.835	0.827	0.820	0.812	0.790	0.768	0.734	0.699
-0.200	0.845	0.839	0.836	0.832	0.829	0.825	0.819	0.812	0.806	0.799	0.777	0.754	0.722	0.689
-0.100	0.825	0.819	0.816	0.812	0.809	0.805	0.799	0.793	0.787	0.780	0.760	0.739	0.708	0.677
0.000	0.802	0.796	0.793	0.789	0.786	0.782	0.777	0.772	0.767	0.761	0.741	0.720	0.692	0.663
0.100	0.775	0.769	0.766	0.762	0.759	0.755	0.751	0.746	0.741	0.736	0.717	0.698	0.672	0.646
0.200	0.743	0.738	0.735	0.731	0.727	0.723	0.719	0.714	0.709	0.704	0.689	0.673	0.649	0.625
0.300	0.708	0.700	0.697	0.693	0.690	0.686	0.682	0.677	0.673	0.668	0.655	0.641	0.620	0.598
0.400	0.666	0.660	0.656	0.652	0.648	0.644	0.641	0.637	0.633	0.629	0.617	0.604	0.586	0.568
0.500	0.620	0.612	0.609	0.605	0.601	0.597	0.594	0.591	0.588	0.585	0.573	0.561	0.546	0.531
0.600	0.568	0.561	0.558	0.554	0.550	0.546	0.543	0.540	0.537	0.534	0.524	0.513	0.500	0.486
0.700	0.509	0.502	0.499	0.495	0.492	0.488	0.486	0.483	0.481	0.478	0.468	0.458	0.445	0.432
0.800	0.444	0.439	0.436	0.432	0.428	0.424	0.422	0.419	0.417	0.414	0.405	0.396	0.384	0.371
0.900	0.371	0.368	0.364	0.360	0.356	0.351	0.349	0.346	0.344	0.341	0.333	0.325	0.313	0.301
1.000	0.290	0.288	0.285	0.281	0.277	0.273	0.270	0.267	0.264	0.261	0.255	0.248	0.236	0.224
1.100	0.202	0.198	0.195	0.192	0.189	0.185	0.183	0.181	0.179	0.177	0.170	0.163	0.152	0.140
1.200	0.108	0.102	0.099	0.096	0.093	0.090	0.088	0.086	0.084	0.081	0.076	0.070	0.060	0.050
1.300	0.003	0.000	-0.003	-0.006	-0.009	-0.012	-0.015	-0.017	-0.019	-0.021	-0.026	-0.031	-0.040	-0.049
1.400	-0.108	-0.111	-0.114	-0.117	-0.120	-0.123	-0.125	-0.126	-0.128	-0.129	-0.133	-0.137	-0.145	-0.153
1.500	-0.227	-0.230	-0.233	-0.235	-0.237	-0.239	-0.241	-0.242	-0.244	-0.245	-0.250	-0.254	-0.260	-0.265
1.600	-0.353	-0.356	-0.359	-0.361	-0.363	-0.365	-0.367	-0.368	-0.370	-0.371	-0.373	-0.375	-0.379	-0.382
1.700	-0.488	-0.491	-0.492	-0.493	-0.494	-0.495	-0.497	-0.499	-0.501	-0.502	-0.503	-0.503	-0.506	-0.508
1.800	-0.628	-0.630	-0.631	-0.631	-0.632	-0.632	-0.634	-0.636	-0.638	-0.640	-0.641	-0.641	-0.642	-0.642
1.900	-0.779	-0.781	-0.782	-0.782	-0.782	-0.782	-0.783	-0.784	-0.785	-0.786	-0.786	-0.786	-0.787	-0.787
2.000	-0.935	-0.936	-0.937	-0.937	-0.937	-0.937	-0.939	-0.940	-0.941	-0.942	-0.941	-0.939	-0.937	-0.935
2.100	-1.100	-1.099	-1.100	-1.100	-1.100	-1.100	-1.100	-1.101	-1.102	-1.102	-1.099	-1.095	-1.093	-1.091
2.200	-1.273	-1.273	-1.273	-1.273	-1.273	-1.273	-1.273	-1.273	-1.273	-1.273	-1.271	-1.268	-1.264	-1.260
2.300	-1.450	-1.450	-1.450	-1.450	-1.450	-1.450	-1.450	-1.449	-1.449	-1.448	-1.446	-1.444	-1.439	-1.433
2.400	-1.642	-1.642	-1.642	-1.641	-1.640	-1.640	-1.640	-1.639	-1.639	-1.638	-1.634	-1.629	-1.619	-1.609
2.500	-1.844	-1.843	-1.843	-1.843	-1.842	-1.842	-1.840	-1.838	-1.836	-1.834	-1.826	-1.819	-1.806	-1.793
2.600	-2.056	-2.053	-2.053	-2.052	-2.051	-2.050	-2.049	-2.047	-2.045	-2.043	-2.031	-2.018	-2.002	-1.985
2.700	-2.274	-2.269	-2.267	-2.265	-2.263	-2.261	-2.261	-2.260	-2.260	-2.259	-2.242	-2.224	-2.204	-2.183
2.800	-2.498	-2.495	-2.492	-2.489	-2.486	-2.482	-2.480	-2.477	-2.475	-2.472	-2.455	-2.438	-2.416	-2.394
2.900	-2.728	-2.723	-2.719	-2.715	-2.711	-2.706	-2.703	-2.700	-2.697	-2.693	-2.677	-2.661	-2.637	-2.613

TABLE 21.—COORDINATES OF UPPER NAPPE FOR DIFFERENT VALUES OF $\frac{h_a}{H_s}$—3:3 WEIR

	Y/H_s													
h_a/H_s \ X/H_s	0.002	0.020	0.030	0.040	0.050	0.060	0.070	0.080	0.090	0.100	0.120	0.140	0.160	0.180
-4.000	0.980	0.963	0.958	0.949	0.942	0.934	0.919	0.904	0.889	0.874	0.849	0.824	0.796	0.768
-3.900	0.980	0.963	0.956	0.948	0.941	0.933	0.918	0.903	0.888	0.873	0.849	0.824	0.796	0.767
-3.800	0.979	0.963	0.956	0.948	0.941	0.933	0.918	0.903	0.888	0.872	0.848	0.823	0.795	0.766
-3.700	0.979	0.963	0.955	0.947	0.939	0.931	0.917	0.902	0.887	0.872	0.848	0.823	0.795	0.766
-3.600	0.979	0.963	0.955	0.947	0.939	0.931	0.917	0.902	0.887	0.872	0.848	0.823	0.794	0.764
-3.500	0.979	0.963	0.955	0.947	0.939	0.931	0.916	0.901	0.886	0.871	0.847	0.822	0.793	0.763
-3.400	0.978	0.963	0.955	0.947	0.939	0.930	0.916	0.901	0.886	0.871	0.846	0.821	0.792	0.763
-3.300	0.978	0.963	0.955	0.947	0.939	0.930	0.916	0.901	0.886	0.871	0.846	0.820	0.792	0.763
-3.200	0.976	0.963	0.955	0.947	0.939	0.930	0.916	0.901	0.886	0.871	0.845	0.819	0.791	0.763
-3.100	0.975	0.963	0.955	0.947	0.939	0.930	0.916	0.901	0.886	0.871	0.844	0.817	0.790	0.762
-3.000	0.974	0.964	0.956	0.947	0.939	0.930	0.915	0.900	0.885	0.870	0.843	0.816	0.789	0.762
-2.900	0.972	0.963	0.955	0.946	0.938	0.929	0.915	0.900	0.885	0.870	0.842	0.814	0.788	0.761
-2.800	0.971	0.963	0.955	0.946	0.937	0.928	0.914	0.899	0.885	0.870	0.842	0.813	0.787	0.761
-2.700	0.970	0.963	0.955	0.946	0.937	0.928	0.914	0.899	0.884	0.869	0.841	0.812	0.786	0.760
-2.600	0.968	0.963	0.954	0.945	0.936	0.927	0.913	0.898	0.884	0.869	0.841	0.812	0.786	0.760
-2.500	0.966	0.963	0.954	0.944	0.935	0.925	0.911	0.897	0.883	0.868	0.839	0.810	0.785	0.760
-2.400	0.964	0.962	0.953	0.944	0.935	0.925	0.911	0.897	0.883	0.868	0.839	0.810	0.785	0.760
-2.300	0.963	0.960	0.951	0.942	0.933	0.924	0.910	0.896	0.882	0.868	0.839	0.810	0.785	0.759
-2.200	0.962	0.960	0.951	0.942	0.933	0.923	0.909	0.895	0.881	0.867	0.838	0.809	0.784	0.759
-2.100	0.960	0.958	0.949	0.940	0.931	0.922	0.908	0.894	0.880	0.865	0.837	0.808	0.783	0.758
-2.000	0.958	0.956	0.948	0.939	0.930	0.921	0.907	0.893	0.879	0.864	0.836	0.808	0.783	0.758
-1.900	0.956	0.953	0.945	0.937	0.929	0.920	0.906	0.892	0.878	0.863	0.835	0.807	0.783	0.758
-1.800	0.954	0.951	0.943	0.935	0.927	0.919	0.905	0.891	0.877	0.862	0.834	0.806	0.782	0.758
-1.700	0.951	0.948	0.941	0.933	0.926	0.918	0.904	0.890	0.876	0.862	0.833	0.803	0.781	0.758
-1.600	0.948	0.945	0.938	0.930	0.923	0.915	0.902	0.888	0.875	0.861	0.832	0.803	0.781	0.758
-1.500	0.945	0.941	0.934	0.927	0.920	0.913	0.900	0.887	0.874	0.861	0.832	0.803	0.780	0.757
-1.400	0.941	0.938	0.932	0.925	0.918	0.911	0.899	0.886	0.874	0.861	0.832	0.803	0.779	0.755
-1.300	0.938	0.933	0.928	0.922	0.916	0.910	0.898	0.885	0.873	0.860	0.832	0.803	0.779	0.755
-1.200	0.932	0.929	0.924	0.918	0.912	0.906	0.895	0.883	0.871	0.859	0.831	0.802	0.779	0.755
-1.100	0.926	0.923	0.918	0.913	0.908	0.903	0.892	0.880	0.869	0.857	0.830	0.802	0.778	0.753
-1.000	0.920	0.917	0.913	0.908	0.904	0.899	0.888	0.877	0.866	0.854	0.828	0.801	0.777	0.752
-0.900	0.913	0.909	0.905	0.901	0.897	0.893	0.883	0.872	0.861	0.850	0.825	0.800	0.775	0.750
-0.800	0.906	0.902	0.899	0.895	0.892	0.888	0.878	0.868	0.858	0.848	0.824	0.800	0.775	0.750
-0.700	0.898	0.893	0.890	0.886	0.883	0.879	0.870	0.861	0.852	0.843	0.821	0.798	0.773	0.748
-0.600	0.887	0.884	0.881	0.877	0.874	0.870	0.863	0.855	0.847	0.839	0.817	0.794	0.770	0.745
-0.500	0.876	0.872	0.869	0.866	0.863	0.860	0.853	0.846	0.839	0.831	0.811	0.790	0.765	0.740
-0.400	0.862	0.858	0.856	0.853	0.850	0.847	0.841	0.834	0.828	0.821	0.802	0.783	0.760	0.736
-0.300	0.845	0.842	0.839	0.836	0.833	0.830	0.825	0.820	0.815	0.810	0.792	0.774	0.752	0.730
-0.200	0.825	0.822	0.820	0.817	0.814	0.811	0.807	0.803	0.799	0.795	0.778	0.761	0.741	0.721
-0.100	0.802	0.799	0.797	0.795	0.793	0.790	0.787	0.783	0.779	0.775	0.760	0.745	0.727	0.708
0.000	0.776	0.771	0.770	0.768	0.767	0.765	0.762	0.759	0.756	0.752	0.739	0.726	0.710	0.693
0.100	0.748	0.743	0.742	0.741	0.740	0.739	0.737	0.734	0.731	0.728	0.715	0.701	0.688	0.674
0.200	0.716	0.711	0.711	0.710	0.709	0.708	0.706	0.703	0.700	0.697	0.685	0.673	0.662	0.650
0.300	0.679	0.675	0.674	0.673	0.672	0.670	0.668	0.665	0.663	0.660	0.650	0.640	0.630	0.620
0.400	0.638	0.635	0.634	0.633	0.632	0.630	0.628	0.625	0.623	0.620	0.611	0.601	0.592	0.583
0.500	0.593	0.589	0.588	0.586	0.585	0.583	0.581	0.579	0.577	0.574	0.566	0.558	0.550	0.542
0.600	0.541	0.538	0.537	0.535	0.533	0.531	0.529	0.526	0.524	0.521	0.515	0.508	0.500	0.491
0.700	0.481	0.478	0.477	0.475	0.474	0.472	0.470	0.467	0.465	0.462	0.456	0.450	0.445	0.439
0.800	0.417	0.413	0.413	0.412	0.411	0.410	0.407	0.404	0.401	0.398	0.393	0.388	0.383	0.378
0.900	0.346	0.342	0.341	0.340	0.339	0.338	0.336	0.334	0.332	0.329	0.325	0.321	0.317	0.312
1.000	0.268	0.265	0.264	0.262	0.261	0.259	0.258	0.256	0.255	0.253	0.249	0.244	0.242	0.239
1.100	0.182	0.178	0.177	0.176	0.175	0.173	0.172	0.170	0.169	0.167	0.163	0.159	0.159	0.159
1.200	0.086	0.082	0.082	0.081	0.080	0.079	0.078	0.077	0.076	0.075	0.072	0.068	0.070	0.072
1.300	-0.016	-0.019	-0.020	-0.020	-0.021	-0.021	-0.022	-0.023	-0.024	-0.025	-0.028	-0.030	-0.026	-0.021
1.400	-0.127	-0.129	-0.130	-0.131	-0.132	-0.132	-0.133	-0.133	-0.133	-0.133	-0.135	-0.136	-0.131	-0.125
1.500	-0.246	-0.246	-0.247	-0.247	-0.247	-0.247	-0.247	-0.247	-0.247	-0.247	-0.248	-0.249	-0.243	-0.236
1.600	-0.372	-0.372	-0.372	-0.371	-0.371	-0.370	-0.371	-0.371	-0.372	-0.372	-0.370	-0.367	-0.363	-0.359
1.700	-0.500	-0.500	-0.500	-0.500	-0.500	-0.499	-0.499	-0.499	-0.499	-0.499	-0.496	-0.493	-0.491	-0.488
1.800	-0.639	-0.639	-0.639	-0.639	-0.639	-0.639	-0.639	-0.639	-0.639	-0.639	-0.634	-0.629	-0.625	-0.620
1.900	-0.782	-0.781	-0.781	-0.780	-0.780	-0.779	-0.780	-0.780	-0.780	-0.780	-0.776	-0.771	-0.766	-0.761
2.000	-0.935	-0.932	-0.932	-0.932	-0.932	-0.931	-0.931	-0.931	-0.931	-0.931	-0.925	-0.919	-0.913	-0.906
2.100	-1.101	-1.097	-1.097	-1.096	-1.095	-1.094	-1.094	-1.094	-1.094	-1.093	-1.086	-1.079	-1.071	-1.062
2.200	-1.278	-1.274	-1.272	-1.269	-1.266	-1.263	-1.263	-1.263	-1.263	-1.263	-1.254	-1.245	-1.036	-1.227
2.300	-1.465	-1.459	-1.456	-1.453	-1.450	-1.447	-1.445	-1.443	-1.441	-1.439	-1.431	-1.422	-1.410	-1.397
2.400	-1.652	-1.648	-1.646	-1.643	-1.641	-1.638	-1.636	-1.634	-1.631	-1.629	-1.619	-1.609	-1.591	-1.573
2.500	-1.851	-1.843	-1.841	-1.839	-1.837	-1.835	-1.832	-1.829	-1.826	-1.823	-1.811	-1.798	-1.779	-1.760
2.600	-2.061	-2.053	-2.050	-2.047	-2.044	-2.041	-2.037	-2.032	-2.027	-2.022	-2.008	-1.993	-1.969	-1.945
2.700	-2.275	-2.261	-2.259	-2.256	-2.254	-2.251	-2.247	-2.242	-2.237	-2.232	-2.216	-2.200	-2.171	-2.141
2.800	-2.494	-2.479	-2.477	-2.474	-2.472	-2.469	-2.465	-2.460	-2.455	-2.450	-2.433	-2.415	-2.382	-2.349
2.900	-2.721	-2.703	-2.701	-2.698	-2.695	-2.692	-2.687	-2.681	-2.675	-2.669	-2.650	-2.631	-2.597	-2.563

TABLE 22.—COORDINATES OF UPPER NAPPE FOR DIFFERENT VALUES OF $\frac{h_a}{H_s}$—2:1 WEIR (BAZIN)

X/H_s \ h_a/H_s	Y/H_s 0.002	0.02	0.04	0.06	0.07	X/H_s \ h_a/H_s	0.002	0.02	0.04	0.06	0.07
-3.500	0.969	0.961	0.950	0.941	0.937	-0.500	0.831	0.828	0.824	0.821	0.819
-3.400	0.968	0.959	0.950	0.940	0.935	-0.400	0.816	0.813	0.809	0.805	0.803
-3.300	0.967	0.957	0.948	0.938	0.933	-0.300	0.798	0.795	0.791	0.787	0.785
-3.200	0.966	0.956	0.947	0.937	0.932	-0.200	0.778	0.775	0.771	0.768	0.766
-3.100	0.965	0.955	0.946	0.936	0.931	-0.100	0.755	0.751	0.748	0.744	0.742
-3.000	0.963	0.954	0.944	0.935	0.930	0.000	0.728	0.724	0.721	0.717	0.715
-2.900	0.961	0.952	0.943	0.934	0.929	0.100	0.696	0.693	0.690	0.687	0.685
-2.800	0.959	0.950	0.941	0.932	0.928	0.200	0.662	0.659	0.655	0.652	0.650
-2.700	0.957	0.948	0.939	0.930	0.926	0.300	0.624	0.620	0.616	0.612	0.610
-2.600	0.955	0.946	0.937	0.928	0.924	0.400	0.580	0.577	0.574	0.570	0.569
-2.500	0.952	0.943	0.935	0.926	0.922	0.500	0.531	0.528	0.525	0.522	0.520
-2.400	0.950	0.942	0.933	0.925	0.921	0.600	0.474	0.470	0.467	0.463	0.461
-2.300	0.948	0.940	0.931	0.923	0.919	0.700	0.411	0.408	0.405	0.402	0.400
-2.200	0.944	0.936	0.929	0.921	0.917	0.800	0.342	0.339	0.335	0.332	0.330
-2.100	0.941	0.934	0.926	0.919	0.915	0.900	0.267	0.263	0.260	0.256	0.254
-2.000	0.938	0.931	0.923	0.916	0.912	1.000	0.185	0.181	0.176	0.172	0.170
-1.900	0.935	0.928	0.920	0.913	0.909	1.100	0.095	0.091	0.086	0.082	0.080
-1.800	0.930	0.923	0.916	0.909	0.905	1.200	0.000	-0.004	-0.009	-0.013	-0.015
-1.700	0.927	0.920	0.912	0.905	0.901	1.300	-0.105	-0.108	-0.112	-0.115	-0.117
-1.600	0.923	0.916	0.909	0.902	0.898	1.400	-0.214	-0.217	-0.220	-0.223	-0.225
-1.500	0.919	0.912	0.905	0.898	0.894	1.500	-0.334	-0.337	-0.340	-0.343	-0.344
-1.400	0.913	0.906	0.900	0.893	0.890	1.600	-0.460	-0.463	-0.466	-0.469	-0.470
-1.300	0.908	0.902	0.895	0.889	0.886	1.700	-0.591	-0.594	-0.596	-0.599	-0.600
-1.200	0.902	0.896	0.889	0.883	0.880	1.800	-0.730	-0.733	-0.736	-0.739	-0.740
-1.100	0.895	0.889	0.884	0.878	0.875	1.900	-0.875	-0.876	-0.878	-0.879	-0.880
-1.000	0.889	0.884	0.878	0.873	0.870	2.000	-1.026	-1.028	-1.029	-1.031	-1.032
-.900	0.880	0.875	0.870	0.865	0.862	2.100	-1.190	-1.190	-1.190	-1.190	-1.190
-.800	0.870	0.865	0.860	0.855	0.852	2.200	-1.363	-1.362	-1.361	-1.360	-1.360
-.700	0.860	0.855	0.851	0.846	0.844	2.300	-1.542	-1.540	-1.538	-1.536	-1.535
-.600	0.845	0.843	0.838	0.834	0.832	2.400	-1.730	-1.726	-1.723	-1.719	-1.717

758318°—48——7

TABLE 23.—COORDINATES OF UPPER NAPPE FOR DIFFERENT VALUES OF $\frac{h_a}{H_s}$ —4:1 WEIR (BAZIN)

Y/H_s											
X/H_s \ h_a/H_s	0.002	0.02	0.04	0.06	0.07	X/H_s \ h_a/H_s	0.002	0.02	0.04	0.06	0.07
-3.500	0.934	0.931	0.928	0.925	0.923	-0.500	0.766	0.762	0.758	0.754	0.752
-3.400	0.933	0.930	0.927	0.924	0.922	-0.400	0.749	0.746	0.742	0.739	0.737
-3.300	0.931	0.928	0.925	0.922	0.921	-0.300	0.730	0.726	0.723	0.719	0.717
-3.200	0.929	0.926	0.923	0.920	0.919	-0.200	0.708	0.705	0.702	0.699	0.697
-3.100	0.927	0.924	0.921	0.918	0.917	-0.100	0.685	0.681	0.677	0.673	0.671
-3.000	0.926	0.923	0.920	0.917	0.915	0.000	0.658	0.654	0.651	0.647	0.645
-2.900	0.923	0.920	0.917	0.914	0.912	0.100	0.627	0.623	0.619	0.615	0.613
-2.800	0.921	0.918	0.915	0.912	0.910	0.200	0.592	0.588	0.584	0.580	0.578
-2.700	0.918	0.915	0.912	0.909	0.907	0.300	0.551	0.547	0.544	0.540	0.538
-2.600	0.914	0.911	0.909	0.906	0.905	0.400	0.503	0.499	0.495	0.491	0.489
-2.500	0.912	0.909	0.906	0.903	0.902	0.500	0.451	0.447	0.442	0.438	0.436
-2.400	0.908	0.905	0.903	0.900	0.899	0.600	0.393	0.388	0.384	0.379	0.377
-2.300	0.904	0.902	0.899	0.897	0.896	0.700	0.330	0.326	0.321	0.317	0.315
-2.200	0.901	0.898	0.896	0.893	0.892	0.800	0.259	0.254	0.249	0.244	0.242
-2.100	0.898	0.895	0.892	0.889	0.888	0.900	0.178	0.173	0.168	0.163	0.161
-2.000	0.894	0.891	0.888	0.885	0.884	1.000	0.092	0.087	0.082	0.077	0.074
-1.900	0.890	0.887	0.884	0.881	0.880	1.100	-0.002	-0.007	-0.012	-0.017	-0.020
-1.800	0.886	0.883	0.880	0.877	0.875	1.200	-0.103	-0.008	-0.013	-0.018	-0.121
-1.700	0.881	0.878	0.875	0.872	0.870	1.300	-0.212	-0.217	-0.223	-0.228	-0.231
-1.600	0.876	0.873	0.870	0.867	0.865	1.400	-0.327	-0.332	-0.338	-0.343	-0.346
-1.500	0.871	0.868	0.865	0.862	0.860	1.500	-0.448	-0.452	-0.457	-0.461	-0.463
-1.400	0.864	0.861	0.858	0.855	0.853	1.600	-0.572	-0.576	-0.581	-0.585	-0.587
-1.300	0.857	0.854	0.851	0.848	0.846	1.700	-0.705	-0.709	-0.714	-0.718	-0.720
-1.200	0.848	0.845	0.842	0.839	0.837	1.800	-0.846	-0.850	-0.853	-0.857	-0.859
-1.100	0.840	0.837	0.833	0.830	0.828	1.900	-1.000	-1.003	-1.006	-1.009	-1.011
-1.000	0.830	0.827	0.823	0.820	0.818	2.000	-1.161	-1.164	-1.166	-1.169	-1.170
-0.900	0.819	0.815	0.812	0.808	0.806	2.100	-1.328	-1.331	-1.334	-1.337	-1.338
-0.800	0.807	0.804	0.800	0.797	0.795	2.200	-1.507	-1.509	-1.511	-1.513	-1.514
-0.700	0.793	0.789	0.786	0.782	0.780	2.300	-1.692	-1.694	-1.695	-1.697	-1.698
-0.600	0.780	0.776	0.772	0.768	0.766	2.400	-1.885	-1.886	-1.887	-1.888	-1.888

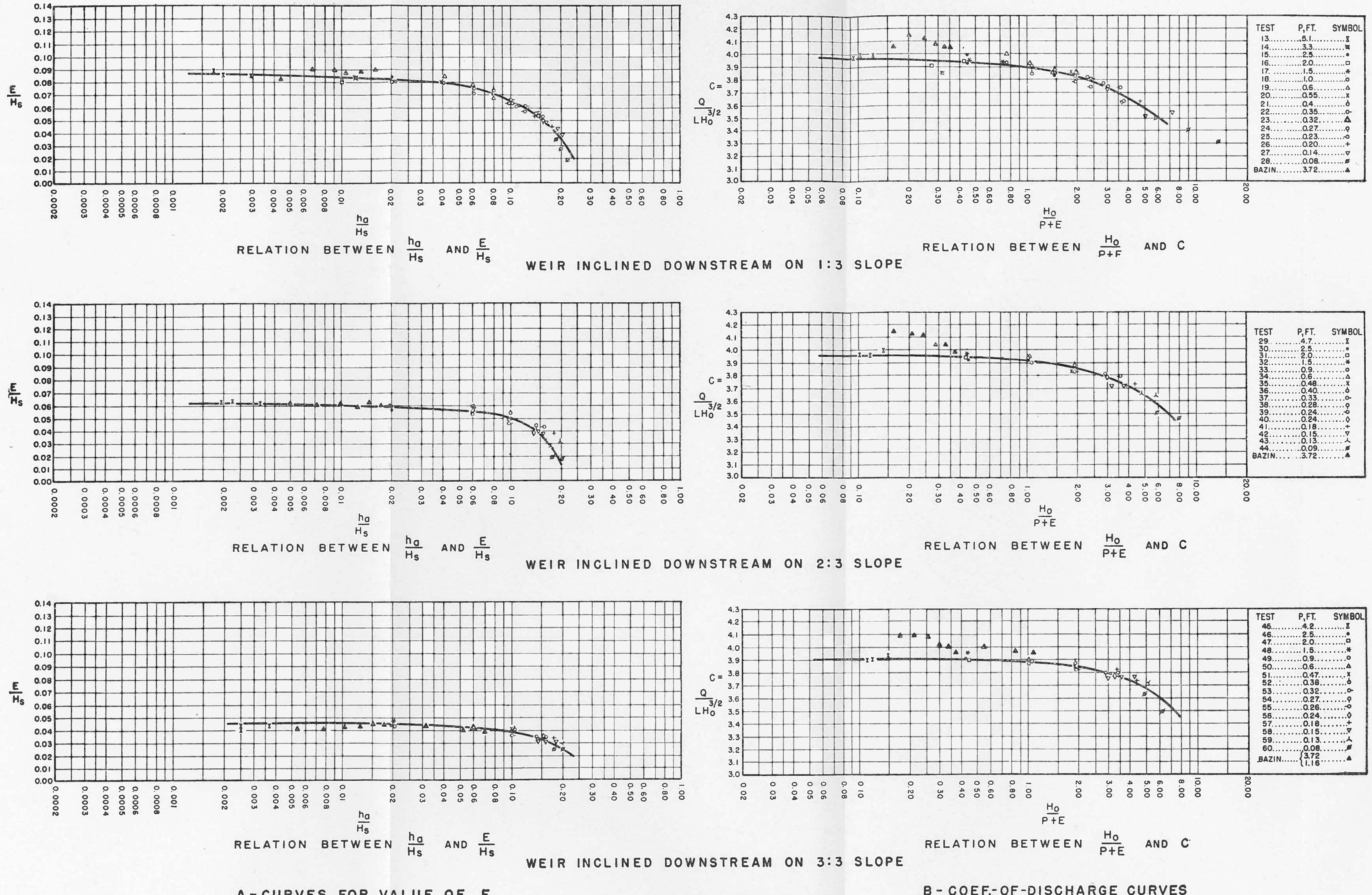

FIGURE 21.—VALUES OF *E* AND *C* FOR SLOPING WEIRS.

Figure 22–A shows a comparison of curves for the 1:3, 2:3, and 3:3 weirs, together with similar curves for the vertical weir and Bazin's 2:1 and 4:1 downstream-sloping weirs. The curves are spaced quite uniformly except at the right end, where instability of flow is approached.

28. Discharge Coefficients.—The actual discharge coefficients for the 1:3, 2:3, and 3:3 sloping weirs are shown plotted against $\frac{H_o}{P+E}$ in figure 21–B. Bazin's coefficients, indicated by black triangles, are higher than those obtained in the more recent experiments. This is also true for the vertical weir, as shown in figure 15–B. Bazin's discharge measurements are consistently 2.5 percent higher for all weirs studied in this series of experiments.

For comparative purposes the above three curves have been combined with similar curves for the vertical and Bazin's 2:1 and 4:1 sloping weirs in figure 22–B. It is interesting to note that the order of the four test curves at the right end is the reverse of that at the left. The vertical-weir curve indicates the highest discharge coefficients for large approach depths, while the curve for the 3:3 sloping weir shows the highest coefficients for the smaller approach depths. In no case is the variation in coefficients for the four weirs appreciable. The points for Bazin's 2:1 and 4:1 sloping weirs are insufficient to establish very reliable curves.

29. Reduction of Pressure on Upstream Face of 1:3, 2:3, and 3:3 Sloping Weirs.—The drop in pressure on the upstream face of the sloping weirs was observed by means of piezometers, as in the case of the vertical weir. The drop in pressure, which is considered as $H_s - h_p$, is plotted with respect to d, the distance of any piezometer from the sharp crest of the weir. These two variables are expressed in terms of unit head and are shown plotted in figures 23, 24, and 25 for the 1:3, 2:3, and 3:3 sloping weirs, respectively.

The method of computing the magnitude of the pressure reduction was explained in section 20. The magnitude of the pressure reduction on the upstream face of the 1:3, 2:3, and 3:3 sloping weirs is shown plotted with respect to $\frac{h_a}{H_s}$ in figure 26–A. The curve for the vertical weir has also been included on this figure for comparative purposes. The term $ft.^2$ is the pressure-reduction area, as illustrated in figure 18, or the volume of the pressure reduction when unit length of dam is considered. The actual pressure reduction in pounds is obtained by multiplying this volume by 62.5, the unit weight of water. The comparison indicates that the reduction of pressure increases as the weir is sloped downstream.

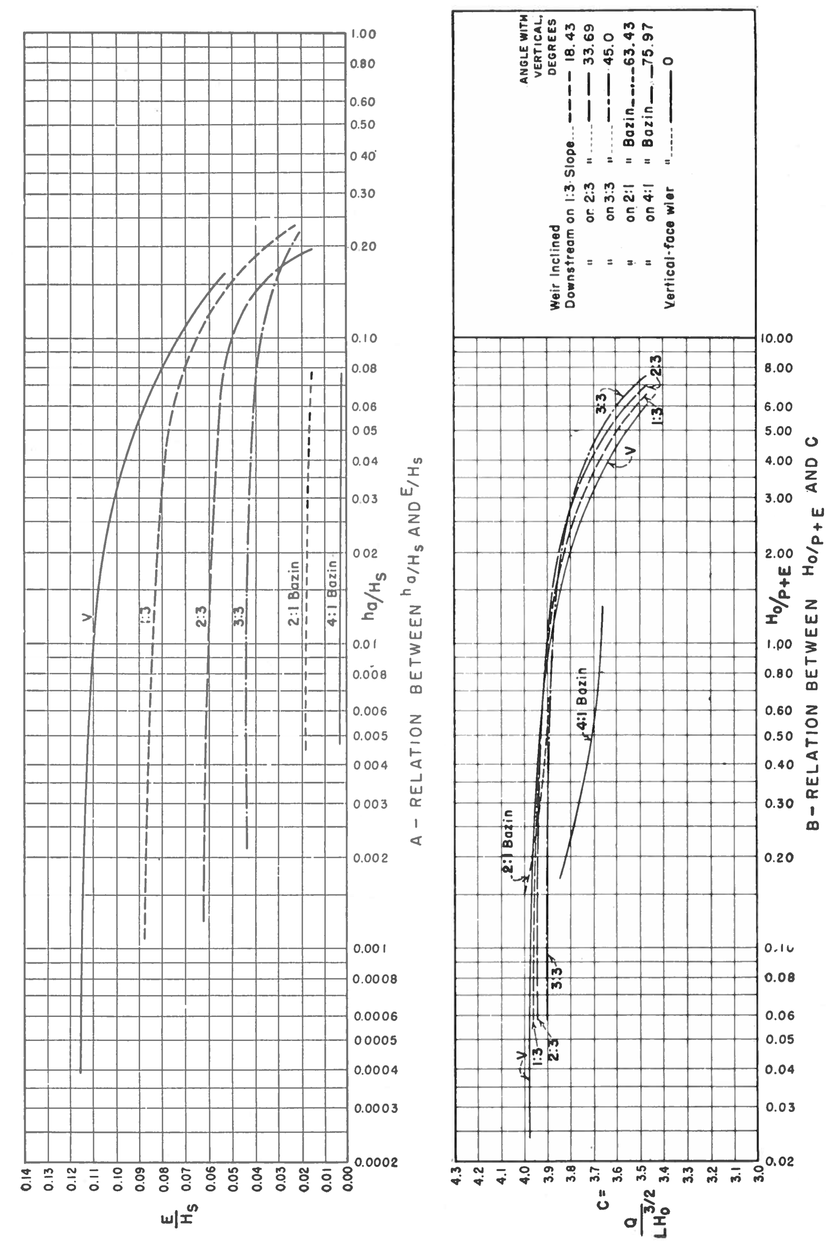

FIGURE 22.—COMPARISON OF *E* AND *C* FOR VERTICAL AND SLOPING WEIRS.

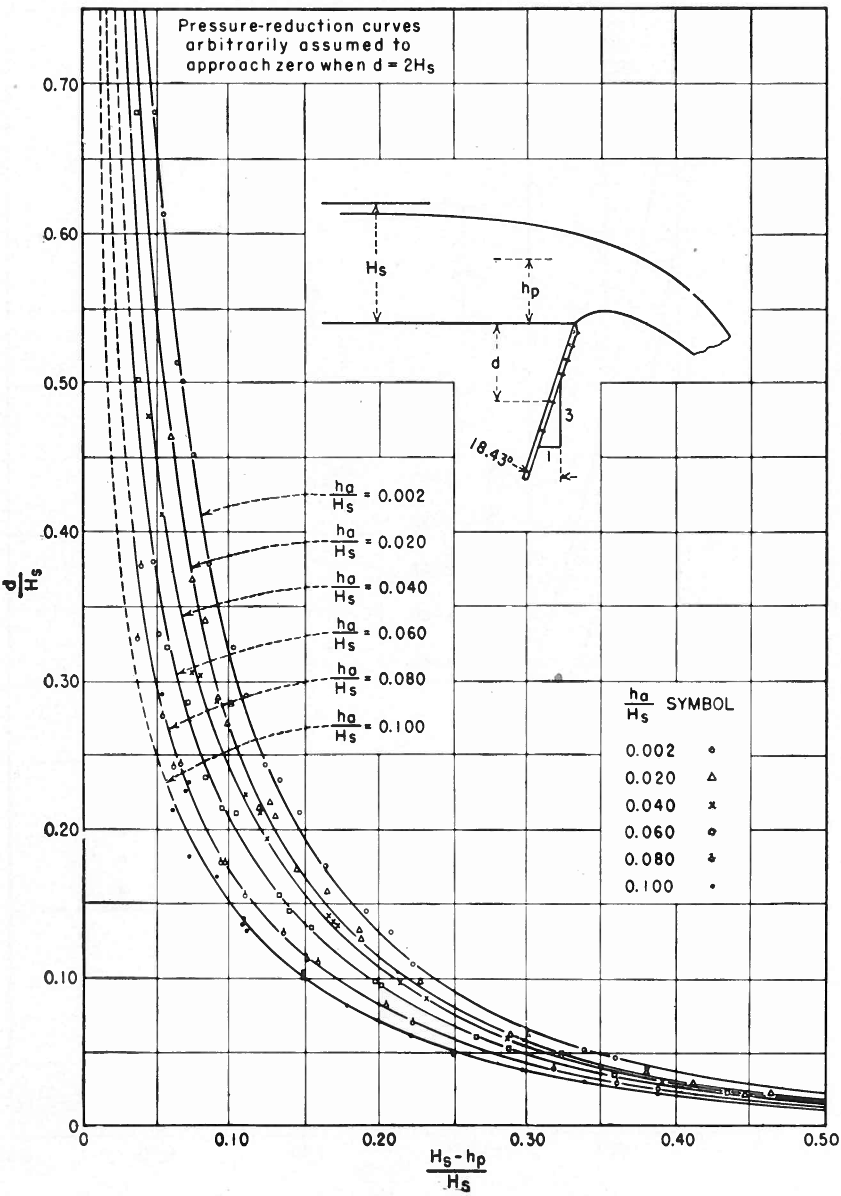

FIGURE 23.—REDUCTION OF PRESSURE ON UPSTREAM FACE OF 1:3 SLOPING WEIR.

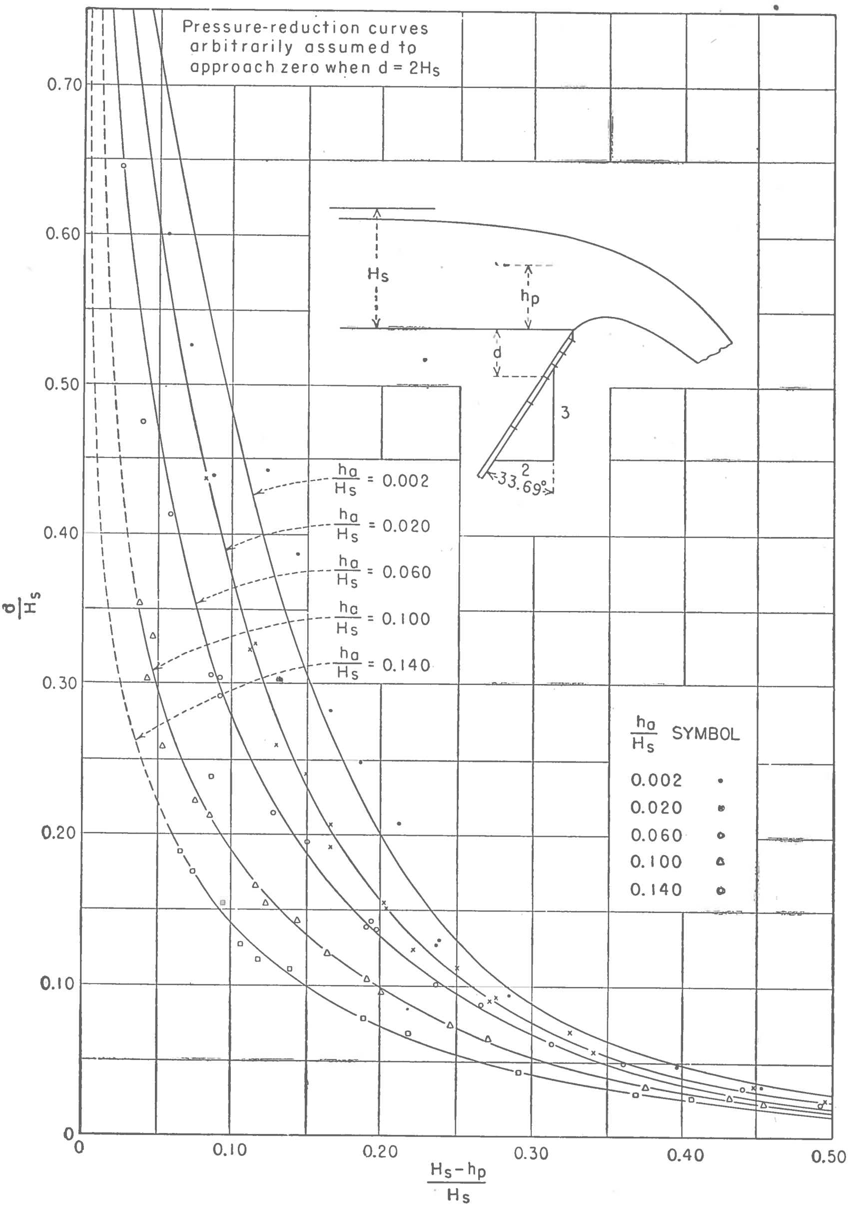

FIGURE 24.—REDUCTION OF PRESSURE ON UPSTREAM FACE OF 2:3 SLOPING WEIR.

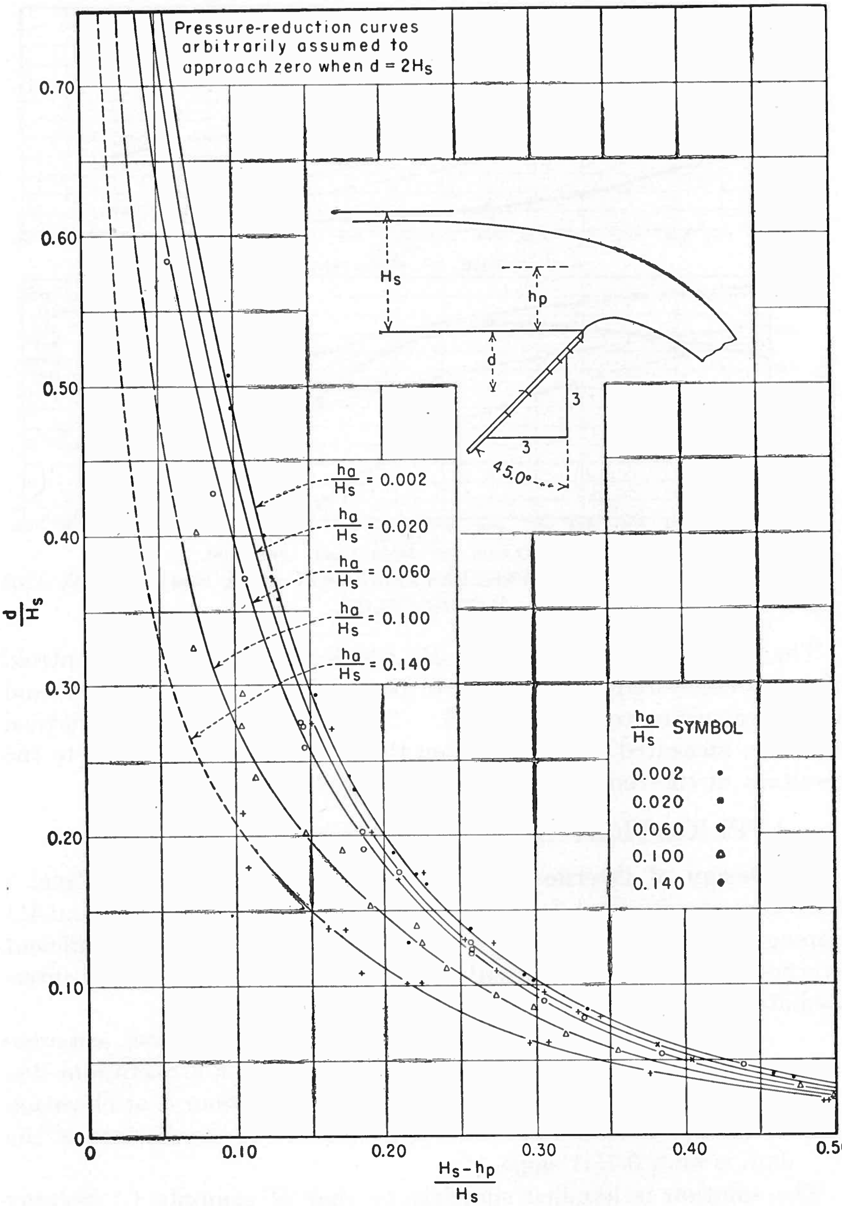

FIGURE 25.—REDUCTION OF PRESSURE ON UPSTREAM FACE OF 3:3 SLOPING WEIR.

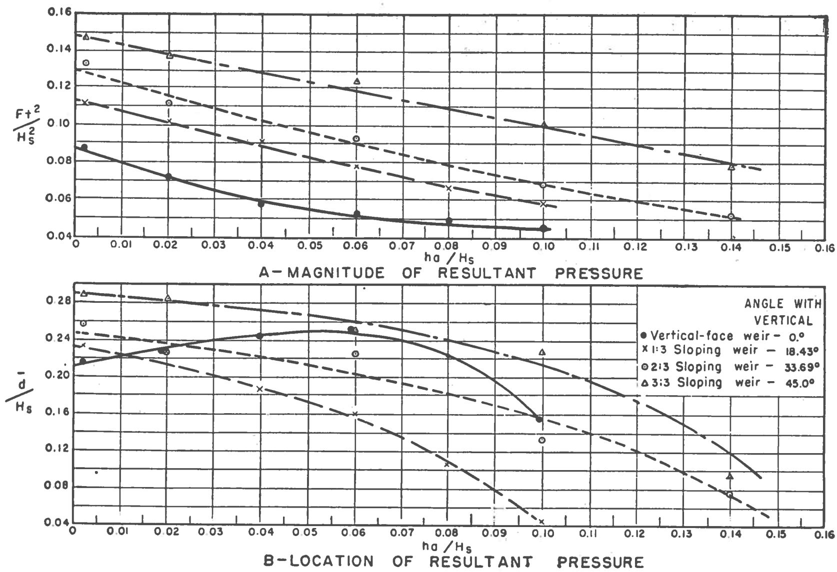

FIGURE 26.—RESULTANT OF PRESSURE-REDUCTION AREA FOR VERTICAL AND SLOPING WEIRS.

The position of the resultant, R_2, which acts through the centroid of the pressure-reduction area, can be obtained for the 1:3, 2:3, and 3:3 sloping weirs from figure 26–B. The term $\bar{d}$ represents the vertical distance, measured downward from the sharp crest of the weir to the resultant at the centroid of the pressure-reduction area.

APPLICATION OF EXPERIMENTAL RESULTS

30. Design of Overflow Section With Sloping Upstream Face.—With the experimental data for the vertical, 1:3, 2:3, 3:3, 2:1, and 4:1 sloping weirs, it is possible to design an economical and efficient overflow section for a dam with any one of these slopes or any intermediate downstream slope.

Example 4.—Design the overflow section of a low, concrete gravity dam, with crest at elevation 180.0, for a maximum discharge of 200,000 second-feet. The approach floor is at elevation 155.0; the crest is 1,200 feet long; and the upstream face of the dam is on a 0.75:1 slope.

The solution is handled similarly to that of example 1. Solving equation 12 for

$$H_o = \sqrt[2/3]{\frac{Q}{CL}},$$

and assuming $C=3.80$,

$$H_o = \sqrt[2/3]{\frac{200{,}000}{3.80\times 1{,}200}} = \sqrt[2/3]{43.86} = 12.44 \text{ feet (approximately)}$$

and

$$\frac{H_o}{P+E}=\frac{12.44}{25}=0.498.$$

From figure 22–B, a more accurate value of $C=3.91$ is obtained for a slope of 0.75:1, or 36.87 degrees from the vertical.

Repeating this operation with the new value of C,

$$H_o=\sqrt[2/3]{\frac{200{,}000}{3.91\times 1{,}200}}=\sqrt[2/3]{42.63}=12.20 \text{ feet,}$$

and

$$\frac{H_o}{P+E}=\frac{12.20}{25}=0.488.$$

From figure 22–B, the coefficient of discharge remains 3.91 for the above value of $\frac{H_o}{P+E}$.

The next step is to find the values of h_a and H_s.

$q=\frac{Q}{L}=\frac{200{,}000}{1{,}200}=166.67$ second-feet per foot of crest; then

$$V_a=\frac{q}{P+E+H_o} \tag{14}$$

or

$$V_a=\frac{166.67}{25+12.20}=4.48 \text{ feet per second,}$$

and $h_a=0.312$ feet (approximate velocity head of approach).

The process can be repeated to obtain a more accurate value of h_a.

$$V_a=\frac{q}{P+E+H_o-\mathrm{h}_a} \tag{15}$$

or

$$V_a=\frac{166.67}{25+12.20-0.312}=4.52 \text{ feet per second,}$$

and

$h_a=0.318$ feet (true velocity of approach).

To determine H_s, reference is made to figure 27, which was constructed for the purpose of eliminating a portion of the cut-and-try process. These curves were not used in the solution of example 1 but will be utilized in the present problem.

$$\frac{h_a}{H_o}=\frac{0.318}{12.20}=0.0261.$$

Entering figure 27 with the above value, $\frac{H_s}{H_o}=1.057$ for an angle of 36.87 degrees with the vertical.

Then

$$H_s=1.057\times 12.20—12.88 \text{ feet,}$$

and

$$\frac{h_a}{H_s}=\frac{0.318}{12.88}=0.0247.$$

With these values and tables 14 and 15, the coordinates for the overflow section can be determined. It is necessary in this case to interpolate between values in the two tables, since the upstream slope of 36.87 degrees for the overflow section lies between the 2:3 and 3:3 slopes. The coordinates have been tabulated in table 24 and are shown plotted in figure 28–A.

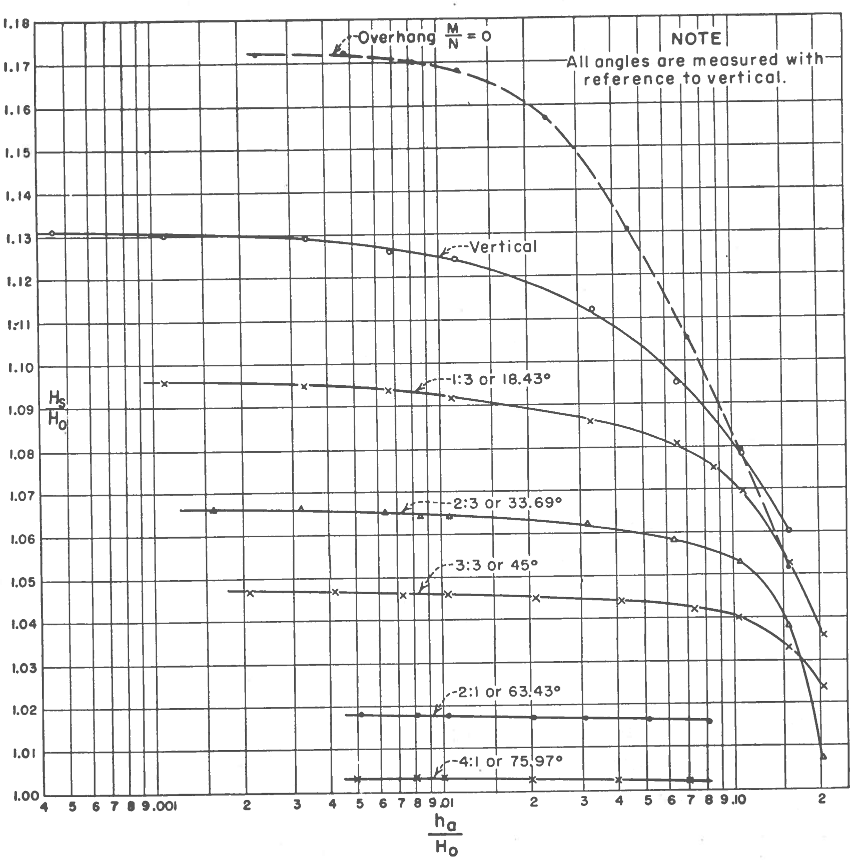

FIGURE 27.—RELATION OF $\frac{h_a}{H_0}$ TO $\frac{H_s}{H_0}$.

TABLE 24.—COORDINATES FOR OVERFLOW SECTION—EXAMPLE 4

$\frac{X}{H_s}$	$\frac{Y}{H_s}$ 33.69° Weir	45° Weir	36.87° Weir	X, feet	Y, 36.87° Weir	Y, elevation, feet
1	2	3	4	5	6	7
0.000	0.000	0.000	0.000	0.00	0.00	179.28
0.050	0.032	0.018	0.028	0.64	0.36	179.64
0.100	0.050	0.034	0.046	1.29	0.59	179.87
0.150	0.059	0.041	0.054	1.93	0.70	179.98
0.180	0.061	0.042	0.056	2.32	0.72	180.00
0.200	0.062	0.042	0.056	2.58	0.72	180.00
0.220	0.061	0.042	0.056	2.83	0.72	180.00
0.250	0.059	0.039	0.053	3.22	0.68	179.96
0.300	0.051	0.032	0.046	3.86	0.59	179.87
0.350	0.041	0.021	0.035	4.51	0.45	179.73
0.400	0.029	0.008	0.023	5.15	0.30	179.58
0.450	0.015	−0.008	0.009	5.80	0.12	179.40
0.500	−0.002	−0.027	−0.009	6.44	−0.12	179.16
0.600	−0.044	−0.073	−0.052	7.73	−0.67	178.61
0.700	−0.097	−0.127	−0.105	9.02	−1.35	177.93
0.800	−0.157	−0.189	−0.166	10.30	−2.14	177.14
0.900	−0.226	−0.258	−0.235	11.59	−3.03	176.25
1.000	−0.310	−0.336	−0.311	12.88	−4.00	175.28
1.200	−0.481	−0.514	−0.490	15.46	−6.31	172.97
1.400	−0.692	−0.727	−0.702	18.03	−9.04	170.24
1.600	−0.940	−0.966	−0.947	20.61	−12.20	167.08
1.800	−1.212	−1.240	−1.220	23.18	−15.71	163.57
2.000	−1.517	−1.543	−1.524	25.76	−19.63	159.65
2.200	−1.850	−1.877	−1.858	28.34	−23.93	155.35
2.400	−2.222	−2.246	−2.229	30.91	−28.71	150.57

Should the upper-surface coordinates be desired, these can be obtained in the same manner from tables 20 and 21.

31. Design of Overflow Section with Shallow Approach Channel.—In the design of spillways for earth dams, the approach channel is usually made shallow so as to minimize the cost of the required excavation. This type of spillway is quite common, and the design of the overflow section has been difficult because of the many unknown factors involved. With the foregoing information, however, safe designs may be performed with considerable increase in efficiency of the spillways.

Example 5.—Figure 29 shows a plan and section of an earth-dam spillway with a net crest width of 77.0 feet, crest elevation at 460.0, approach channel at elevation 455.0, and maximum reservoir surface at elevation 500.0. Investigate the design, using the results of the recent weir experiments.

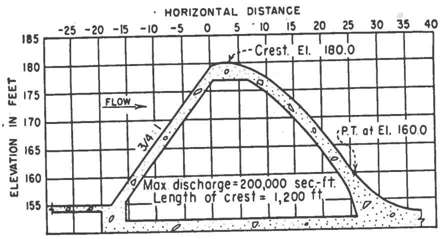

A - RESULTS OF EXAMPLE 4

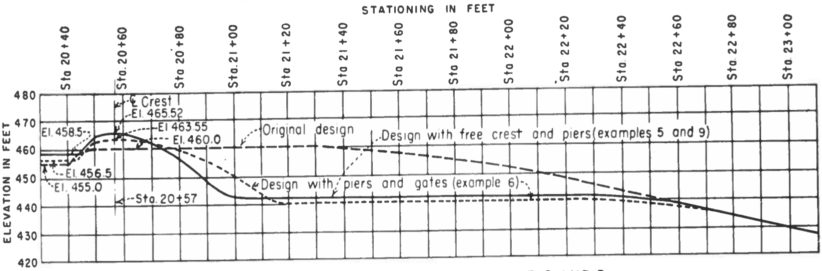

B - RESULTS OF EXAMPLES 5, 6, AND 9

FIGURE 28.—RESULTS OF EXAMPLES 4, 5, 6, AND 9—WEIRS SLOPING DOWNSTREAM.

In the original model tests the coefficient of discharge in the equation $Q=CLH^{3/2}$ was a constant of 2.85 for all heads. Substituting values in the equation for the maximum discharge, $Q=2.85\times77\times40^{3/2}=$ 55,520 second-feet.

Application of the more recent data indicates that a saving may be obtained in either one of two ways: by raising the crest; or by maintaining the crest at the same elevation and reducing the width of the spillway. In either case, the dimensions of the gates can be reduced.

In this example the crest will be raised; and a free overflow section, with piers but without gates, with a net width of 77.0 feet, will be assumed. The new crest elevation can be obtained by solving for the head, H_0.

Assuming $C=3.60$ for the new overflow section, with a 45° (or 3:3) slope on the upstream face, and solving equation 12 for $H_0^{3/?}$,

$$H_0^{3/2}=\frac{Q}{CL}=\frac{55{,}520}{3.60\times77.0}=200.29,$$

and

$$H_o=34.23 \text{ feet (approximately)}.$$

For stable flow conditions in which undulating wave action is absent, $\frac{H_0}{P+E}$ should not exceed the value of 5.0, see figure 22–B. Undulating waves in the approach channel will produce an unsteady flow in the spillway. The result will not be serious, but the design is not sound from a hydraulic standpoint.

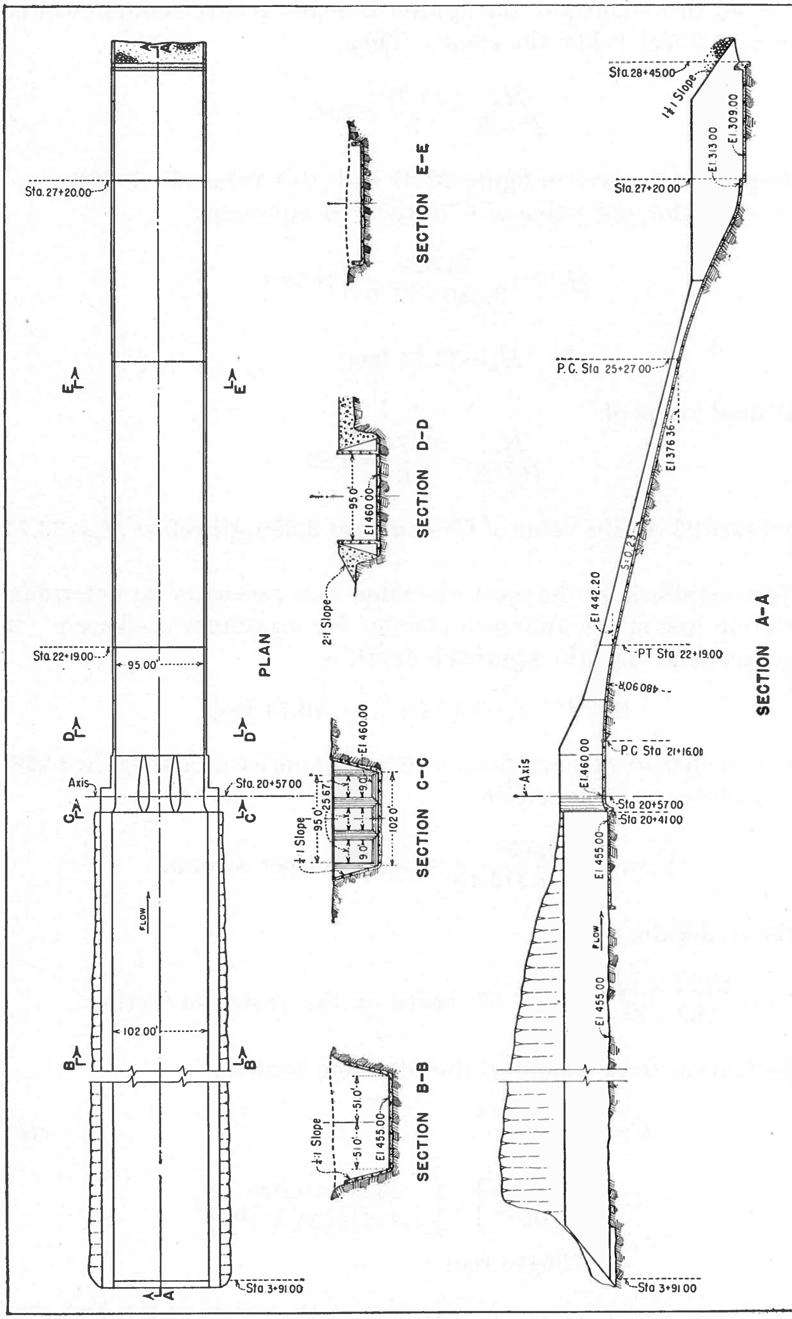

FIGURE 29.—SPILLWAY FOR EXAMPLES 5, 6, AND 9.

To avoid this condition, the approach depth in this example will be chosen at 7.0 feet below the crest. Then

$$\frac{H_o}{P+E}=\frac{34.23}{7}=4.89$$

Entering the 3:3 curve in figure 22–B with this value, $C=3.680$. Substituting the new value of C in the first equation,

$$H_o^{3/2}=\frac{55,520}{3.680\times 77.0}=195.93$$

and

$$H_o=33.74 \text{ feet.}$$

The final value of

$$\frac{H_o}{P+E}=\frac{33.74}{7.0}=4.82$$

From figure 22–B, the value of C remains at 3,680; therefore $H_o=33.74$ feet.

Before establishing the crest elevation it is necessary to determine the friction loss in the approach channel for maximum discharge. It will be assumed that the approach depth is

$$h_o+P+E=33.74+7.0=40.74 \text{ feet.}$$

and the coefficient of roughness, n, for the approach channel is 0.020. Then the velocity of approach,

$$V_a=\frac{55,520}{40.74\times 112.18}=13.27 \text{ feet per second,}$$

and the hydraulic radius,

$$r=\frac{40.74\times 112.18}{102\times 84.00}=24.57, \text{ based on the upstream section.}$$

Substituting these values in the Manning formula,

$$V=\frac{1.486r^{2/3}s^{1/2}}{n}, \qquad (16)$$

$$s=\left[\frac{V_a n}{1.486r^{2/3}}\right]^2=\left[\frac{13.27\times 0.020}{1.486\times (24.57)^{2/3}}\right]^2,$$

$$=0.000446 \text{ foot}$$

loss per linear foot of channel. Neglecting the entrance loss and considering the channel 1,650 feet long, the total friction loss

$$sl=0.000446\times 1,650=0.736 \text{ foot.}$$

A more accurate value of sl can be obtained by repeating the last process using average values of V_a and r. For the sake of clarity in outlining the over-all method of approach, the final value of sl will be taken as 0.736 foot. This will establish the crest at $500.0-33.74=465.52$ feet elevation, and the approach floor at a level 7.0 feet lower, or elevation 458.5 as shown in figure 28–B. This results in a saving of 3.5 feet of excavation in an approach channel 1,650 feet in length.

The next step is the design of the overflow shape.

With $H_o=33.74$ feet and $V_a=13.27$ feet per second, $h_a=2.74$ feet, and

$$\frac{h_a}{H_o}=\frac{2.74}{33.74}=0.0812.$$

Entering the 3:3 curve in figure 27 with the above value of $\frac{h_a}{H_o}$,

$$\frac{H_s}{H_o}=1.042.$$

Then

$$H_s=1.042\times 33.74=35.16 \text{ feet.}$$

and

$$\frac{h_a}{H_s}=\frac{2.74}{35.16}=0.0779.$$

With these values of H_s and $\frac{h_a}{H_s}$, the coordinates for the shape of the overflow section are obtained from table 15. These are listed in table 25 and are shown plotted in figure 28–B by the heavy full line. The coefficient of discharge was increased from 2.85 to 3.68 by rounding the overflow section and placing the approach floor at a level 7 feet, instead of 5 feet, below the crest. The method for obtaining the position of the downstream floor will be explained in chapter VIII, example 9.

In cases such as this, where piers are present, the overflow section is designed to fit the shape of nappe produced by a strip of water one foot in width flowing midway between piers. This portion of the overflow section will usually be unaffected by pier disturbances. Velocities near the piers will naturally differ from those midway between piers; consequently the sheet of water adjacent to the piers will not necessarily fit the overflow shape as designed. Provision for this discrepancy in shape can be made by providing blunt downstream noses on the piers, which will produce a rent in the sheet of water, allowing air to enter beneath the lower nappe when required.

It happens that the spillway chosen for this problem has three slide gates at the crest for controlling the flow. In the above problem the overflow section was considered as a free crest with piers, and the coordinates in table 25 apply for this condition.

TABLE 25.—FREE OVERFLOW SECTION WITH SHALLOW APPROACH CHANNEL—EXAMPLE 5

$\frac{X}{H_s}$ 1	$\frac{Y}{H_s}$ 2	X, feet 3	Y, feet 4	X, station, feet 5	Y, elevation, feet 6
0. 000	0. 000	0. 00	0. 00	20+50. 67	464. 15
0. 030	0. 011	1. 05	0. 39	51. 72	464. 54
0. 060	0. 021	2. 11	0. 74	52. 78	464. 89
0. 090	0. 029	3. 16	1. 02	53. 83	465. 17
0. 120	0. 035	4. 22	1. 23	54. 89	465. 38
0. 150	0. 037	5. 27	1. 30	55. 94	465. 45
0. 170	0. 039	5. 98	1. 37	56. 65	465. 52
0. 180	0. 039	6. 33	1. 37	20+57. 00	465. 52
0. 190	0. 039	6. 68	1. 37	57. 35	465. 52
0. 200	0. 039	7. 03	1. 37	57. 70	465. 52
0. 250	0. 035	8. 79	1. 23	59. 46	465. 38
0. 300	0. 027	10. 55	0. 95	61. 22	465. 10
0. 350	0. 016	12. 31	0. 56	62. 98	464. 71
0. 400	0. 003	14. 06	0. 11	64. 73	464. 26
0. 450	−0. 014	15. 82	−0. 49	66. 49	463. 66
0. 500	−0. 033	17. 58	−1. 16	68. 25	462. 99
0. 540	−0. 050	18. 99	−1. 76	69. 66	462. 39
0. 600	−0. 077	21. 10	−2. 71	71. 77	461. 44
0. 700	−0. 131	24. 61	−4. 61	75. 28	459. 54
0. 800	−0. 192	28. 13	−6. 75	78. 80	457. 40
0. 900	−0. 260	31. 64	−9. 14	82. 31	455. 01
1. 000	−0. 337	35. 16	−11. 85	85. 83	452. 30
1. 200	−0. 509	42. 19	−17. 90	92. 86	446. 25
1. 400	−0. 717	49. 22	−25. 21	20+99. 89	438. 94

The jet produced by a partial gate opening may skip over the above profile, depending on the type of gate and the conditions of operation. Although the head may be the same for a full gate opening as for a partial opening, the lower surfaces of the jets need not correspond, even though no contraction exists at the lower surface in either case. The explanation is as follows: The streamlines are horizontal and parallel as they leave the gate for the small gate openings; whereas, for full gate opening the streamlines are neither horizontal nor parallel as they flow over the section, but have components in a downward direction. It has therefore been customary to design the upstream portion of an overflow section with gates, as in example 5, and the downstream portion to fit the lower side of the jet issuing from a small gate opening, as illustrated in the following section.

32. Design of Overflow Section With Shallow Approach Channel and Gates on Crest.—The important portion of an overflow section, so far as efficiency is concerned, is that upstream from the crest. By flattening the downstream portion, the coefficient will not be decreased seriously, provided that the flattening is not severe or that submerged flow does not exist downstream.

Example 6.—Redesign the overflow section in example 5 to accommodate three vertical slide gates on the high point of the crest, with pier widths of 9.0 feet, as shown in figure 29. The maximum reservoir surface remains at elevation 500.0; the maximum discharge is 55,520 second-feet; and the net length of crest is 77.0 feet.

Assuming $C=3.35$, which is about 10 percent less than in example 5,

$$H_o^{3/2}=\frac{55{,}520}{3.35\times 77.0}=215.24,$$

and

$$H_o=35.92 \text{ feet.}$$

With the approach floor 7.0 feet below the overflow crest, the approach depth will be 35.92+7.0=42.92 feet.

Then the velocity of approach

$$V_a=\frac{55{,}520}{42.92\times 112.73}=11.47 \text{ feet per second.}$$

and the hydraulic radius,

$$r=\frac{42.92\times 112.75}{102+(2\times 44.24)}=25.40.$$

Assuming $n=0.020$, as in the former example,

$$sl=l\left[\frac{V_a n}{1.486 r^{2/3}}\right]^2$$

or

$$sl=1{,}650\left[\frac{11.47\times 0.020}{1.486\times (25.40)^{2/3}}\right]=0.527 \text{ feet.}$$

The crest will then be at

$$500.00-35.92-0.53=463.55 \text{ feet, elevation,}$$

and the approach floor at a level about 7.0 feet lower, or elevation 456.5.

The design of the upstream portion of the overflow section is similar to that in the preceding example.

With $H_0=35.92$ feet and $V_a=11.47$ feet per second, $h_a=2.04$ feet, and

$$\frac{h_a}{H_o}=\frac{2.04}{35.92}=0.0568.$$

From the 3:3 curve in figure 27, for the above value of $\frac{h_a}{H_o}, \frac{H_s}{H_0}=1.044.$

Then

$$H_s=1.044\times 35.92=37.50 \text{ feet.}$$

and

$$\frac{h_a}{H_s}=\frac{2.04}{37.50}=0.0544.$$

Entering table 15 with the above value of H_s and $\frac{h_a}{H_s}$, the coordinates for the overflow section upstream from the crest are obtained. These are tabulated in the upper portion of table 26.

TABLE 26.—OVERFLOW SECTION WITH SHALLOW APPROACH CHANNEL, GATES ON CREST—EXAMPLE 6

	$\frac{X}{H_s}$	$\frac{Y}{H_s}$	X, feet	Y, feet	X, station, feet	Y, elevation, feet
	1	2	3	4	5	6
	0.000	0.000	0.00	0.00	20+49.88	462.01
	0.030	0.011	1.12	0.45	51.00	462.46
	0.060	0.022	2.25	0.82	52.13	462.83
	0.090	0.030	3.38	1.12	53.26	463.13
	0.120	0.037	4.50	1.39	54.38	463.40
	0.150	0.039	5.62	1.46	55.50	463.47
	0.180	0.041	6.75	1.54	56.63	463.55
Crest	0.190	0.041	7.12	1.54	20+57.00	463.55
	Trajectory Computations					
	Crest		0.00	0.00	20+57.00	463.55
			3.00	−0.07	60.00	463.48
			6.00	−0.26	63.00	463.29
			9.00	−0.59	66.00	462.96
			12.00	−1.04	69.00	462.51
			15.00	−1.63	72.00	461.92
			18.00	−2.35	75.00	461.20
			21.00	−3.20	78.00	460.35
			25.00	−4.53	82.00	459.02
			30.00	−6.52	87.00	457.03
			35.00	−8.88	92.00	454.67
			40.00	−11.60	20+97.00	451.95
			45.00	−14.68	21+02.00	448.87
			50.00	−18.12	07.00	445.43
			55.00	−21.93	12.00	441.62
			60.00	−26.10	17.00	437.45
			65.00	−30.63	22.00	432.92
			70.00	−35.52	27.00	428.03
			75.00	−40.78	32.00	422.77
			80.00	−46.40	21+37.00	417.15

The downstream surface will be designed to fit the shape of the theoretical trajectory of the jet issuing from a 1-foot gate opening at maximum head. Two factors of safety are involved in this assumption: first, the theoretical trajectory should be flatter than the actual, due to air resistance in the latter; and second, it is improbable that the spillway will ever be operated at full head with a 1-foot gate opening.

The streamlines will issue from the gates horizontally under a maximum head of $500.00-463.55-0.50=35.95$ feet.
This head will develop a velocity of

$$V=C_v\sqrt{2_gH_o} \tag{17}$$

or $V=0.98\times48.09=47.13$ feet per second.

The issuing jet may be treated in the same manner as a projectile; hence, the following equations are applicable when the initial velocity is in a horizontal direction,

$$X=Vt \tag{18}$$

and

$$Y=\frac{1}{2}\,gt^2. \tag{19}$$

Substituting the value of t from the first equation into the second,

$$Y=\frac{1}{2}g\left[\frac{X}{V}\right]^2=16.1\left[\frac{X}{47.13}\right]^2=0.00725X^2. \tag{20}$$

The origin of these coordinates will be taken at the crest of the overflow section, or, specifically, at station 20+57.00 and elevation 463.55.

By assuming values of X and solving for Y, the lower portion of table 26 was obtained. The values from table 26 are shown plotted in figure 28–B by a dotted line. The overflow section is flatter for flows at small gate openings and maximum head than for the free crest, but not nearly so flat as in the original design.

The saving that can be effected by use of the more efficient overflow shapes depends on various factors such as topography, type of material to be moved, and general profile of spillway. The purpose in presenting the above examples was not to criticize but to illustrate the use of the information contained in this bulletin.

CHAPTER V—WEIRS WITH UPSTREAM OVERHANG AND WEIRS WITH UPSTREAM OFFSETS AND RISERS

ANALYSIS OF EXPERIMENTAL RESULTS

33. Weir Shapes Tested.—Two different types of weirs were studied in this test series: (1) the upstream overhang weir, type C; and (2) the upstream offset weir with risers, type D, see figure 6. These weirs resemble each other in shape, but the results are widely different. The same terminology is used as heretofore, with the addition of the symbols *M*, the height of the riser, and *N*, the offset dimension, see figures 6 and 30. The offset angle was 45 degrees throughout the series. The resulting overflow sections obtained from the above two types of weirs are indicated in figure 1–F. In both cases the offsetting of the upstream face is primarily an economy for saving concrete or masonry.

34. Analysis of Nappe-Shape Results, Type C Weir.—Three type C weirs were tested, each with a different overhang dimension as listed in figure 6, tests 150–1 to 177–1. The variable *N*, see figure 30, must also appear in the similitude relations for the type C weir. A summary of all tests made on the type C weir is shown in table 27, ex-

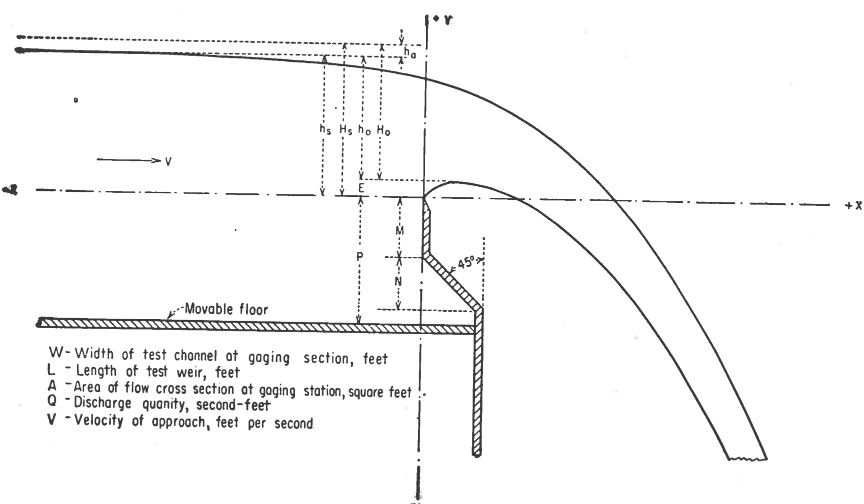

FIGURE 30.—PRINCIPAL ELEMENTS OF THE OFFSET OVERFALL CREST.

TABLE 27.—SUMMARY OF TESTS ON WEIRS WITH 45° UPSTREAM OVERHANG

1 TEST	2 P, FEET	3 Q, SECOND-FEET	4 W, FEET	5 h_s, FEET	6 A, SQUARE FEET	7 V, FEET PER SECOND	8 h_a, FEET	9 E, FEET	10 H_o, FEET	11 $H_o^{\frac{3}{2}}$	12 L, FEET
					$\frac{M}{N}=0$						
150-1	4.939	7.58	2.069	1.129	12.555	0.604	0.0057	0.157	0.978	0.967	2.006
150-2	4.939	5.87		0.960	12.205	0.481	0.0036	0.135	0.829	0.755	
150-3	4.939	4.21		0.767	11.806	0.357	0.0020	0.120	0.649	0.523	
151-1	1.463	8.21		1.143	5.392	1.523	0.0361	0.148	1.031	1.047	
152-1	1.315	6.65		0.992	4.773	1.393	0.0302	0.132	0.890	0.840	
153-1	1.002	4.54		0.761	3.648	1.245	0.0241	0.098	0.687	0.569	
154-1	0.738	7.02		0.972	3.538	1.984	0.0612	0.109	0.924	0.888	
155-1	0.649	5.98		0.878	3.159	1.893	0.0557	0.096	0.838	0.767	
156-1	0.462	6.58		0.884	2.785	2.363	0.0868	0.077	0.894	0.845	
157-1	0.354	4.42		0.677	2.133	2.072	0.0667	0.060	0.684	0.566	
158-1	0.332	6.905		0.874	2.495	2.768	0.1191	0.070	0.923	0.887	
159-1	0.277	5.405		0.744	2.112	2.559	0.1018	0.057	0.789	0.701	
160-1	4.780	5.97	2.069	0.956	11.868	0.503	0.0039	0.138	0.822	0.745	2.006
160-2	4.780	4.09		0.748	11.437	0.358	0.0020	0.112	0.638	0.510	
161-1	1.309	6.61		0.984	4.744	1.393	0.0302	0.129	0.885	0.833	
162-1	1.002	4.45		0.751	3.627	1.227	0.0234	0.099	0.675	0.555	
163-1	0.737	7.06		0.977	3.546	1.991	0.0617	0.107	0.932	0.900	
164-1	0.643	5.92		0.869	3.128	1.893	0.0557	0.093	0.832	0.759	
165-1	0.465	6.82		0.907	2.839	2.402	0.0897	0.078	0.919	0.881	
166-1	0.351	4.31		0.666	2.104	2.048	0.0652	0.057	0.674	0.553	
167-1	0.325	6.97		0.881	2.495	2.794	0.1214	0.062	0.940	0.911	
168-1	0.279	5.37		0.742	2.112	2.543	0.1005	0.052	0.791	0.704	
169-1	0.230	6.77		0.834	2.201	3.076	0.1471	0.049	0.932	0.900	
170-1	0.167	4.46		0.638	1.666	2.677	0.1114	0.036	0.713	0.602	
171-1	5.136	7.66	2.069	1.136	12.977	0.590	0.0054	0.160	0.981	0.972	2.006
171-2	5.136	4.91		0.847	12.379	0.397	0.0025	0.130	0.720	0.611	
172-1	1.460	8.03		1.116	5.330	1.507	0.0353	0.145	1.006	1.009	
173-1	1.314	6.78		0.992	4.771	1.421	0.0314	0.125	0.898	0.851	
174-1	0.736	7.09		0.966	3.521	2.014	0.0630	0.093	0.936	0.906	
175-1	0.647	5.80		0.846	3.089	1.878	0.0548	0.083	0.818	0.740	
176-1	0.508	7.63		0.972	3.062	2.492	0.0966	0.082	0.987	0.981	
177-1	0.462	6.75		0.898	2.814	2.399	0.0894	0.077	0.910	0.868	

TABLE 27.—SUMMARY OF TESTS ON WEIRS WITH 45° UPSTREAM OVERHANG—Con.

1 TEST	13 $LH_o^{\frac{3}{2}}$	14 C	15 $P+E$, FEET	16 $\frac{H_o}{P+E}$	17 H_s, FEET	18 $\frac{h_a}{H_s}$	19 $\frac{E}{H_s}$	20 N, FEET	21 M, FEET	22 $\frac{N}{H_s}$	23 NAPPE PROFILES
					$\frac{M}{N}=0$						
150-1	1.940	3.907	5.096	0.192	1.135	0.0050	0.138	0.153	0	0.135	*
150-2	1.515	3.875	5.074	0.163	0.964	0.0037	0.140			0.159	*
150-3	1.049	4.013	5.059	0.128	0.769	0.0026	0.156			0.199	*
151-1	2.100	3.910	1.611	0.640	1.179	0.0306	0.126			0.130	*
152-1	1.685	3.947	1.447	0.615	1.022	0.0295	0.129			0.150	*
153-1	1.141	3.979	1.100	0.625	0.785	0.0307	0.125			0.195	*
154-1	1.781	3.942	0.847	1.091	1.033	0.0592	0.106			0.148	*
155-1	1.539	3.886	0.745	1.125	0.934	0.0596	0.103			0.164	*
156-1	1.695	3.882	0.539	1.659	0.971	0.0894	0.079			0.158	*
157-1	1.135	3.894	0.414	1.652	0.744	0.0897	0.081			0.206	*
158-1	1.779	3.881	0.402	2.296	0.993	0.1199	0.070			0.154	*
159-1	1.406	3.844	0.334	2.362	0.846	0.1203	0.067			0.181	*
160-1	1.494	3.996	4.918	0.167	0.960	0.0041	0.144	0.076	0	0.079	*
160-2	1.023	3.998	4.892	0.130	0.750	0.0027	0.149			0.101	*
161-1	1.671	3.956	1.438	0.615	1.014	0.0298	0.127			0.075	*
162-1	1.113	3.998	1.101	0.613	0.774	0.0302	0.128			0.098	*
163-1	1.805	3.911	0.844	1.104	1.039	0.0594	0.103			0.073	*
164-1	1.523	3.887	0.736	1.130	0.925	0.0602	0.101			0.082	*
165-1	1.767	3.860	0.543	1.692	0.997	0.0900	0.078			0.076	*
166-1	1.109	3.886	0.408	1.652	0.731	0.0892	0.078			0.104	*
167-1	1.827	3.815	0.387	2.429	1.002	0.1212	0.062			0.076	*
168-1	1.412	3.803	0.331	2.390	0.843	0.1192	0.062			0.090	*
169-1	1.805	3.751	0.279	3.341	0.981	0.1499	0.050			0.077	*
170-1	1.208	3.692	0.203	3.512	0.749	0.1487	0.048			0.101	*
171-1	1.950	3.928	5.296	0.185	1.141	0.0047	0.140	0.305	0	0.267	*
171-2	1.226	4.005	5.266	0.137	0.850	0.0029	0.153			0.359	*
172-1	2.024	3.967	1.605	0.626	1.151	0.0307	0.126			0.265	*
173-1	1.707	3.972	1.439	0.624	1.023	0.0307	0.122			0.298	*
174-1	1.817	3.902	0.829	1.129	1.029	0.0612	0.090			0.296	*
175-1	1.484	3.908	0.730	1.014	0.901	0.0648	0.092			0.339	*
176-1	1.968	3.877	0.590	1.673	1.069	0.0904	0.077			0.285	*
177-1	1.741	3.877	0.539	1.688	0.987	0.0906	0.078			0.309	*

* RUNS IN WHICH NAPPE PROFILES WERE MEASURED.

pressed as $\frac{M}{N}=0$. Nappe shapes were measured for all runs shown on this table.

The X and Y coordinates for each run were plotted to a large scale and smooth curves drawn through the points. Coordinate points were then read from the curves and divided by their respective heads, H_s. This removed irregularities inherent in the original coordinate points. The latter coordinates, expressed in terms of unit head, were then plotted and grouped according to their respective values of $\frac{h_a}{H_s}$ and $\frac{N}{H_s}$, as shown in table 28. In other words, if $\frac{h_a}{H_s}$ were held constant at 0.002, a set of nappe profiles, in terms of unit head, could be plotted for values of $\frac{N}{H_s}$ ranging from 0.080 to 0.360. Likewise, for a constant value of $\frac{h_a}{H_s}=0.03$, a second set of profiles could be plotted for values of $\frac{N}{H_s}$ ranging from 0.080 to 0.300. A third, fourth, fifth, and sixth set could also be plotted for values of $\frac{h_a}{H_s}$ of 0.06, 0.09, 0.12, and 0.15, respectively. These six sets of curves would then represent the entire range of conditions covered in the tests for $\frac{M}{N}=0$.

The variation in the nappe profiles due to changes in the value of $\frac{N}{H_s}$ was found to be small. For this reason an average line was drawn through each of the six sets, one for each value of $\frac{h_a}{H_s}$; namely, 0.002, 0.03, 0.06, 0.09, 0.12, and 0.15. The coordinates for the resulting six curves were tabulated for the lower nappe surface in table 29. The intermediate values of $\frac{h_a}{H_s}$ in the table were obtained by interpolation from the six curves. The values in this table differ considerably from those of table 12 for the vertical-face weir.

The $\frac{X}{H_s}$ and $\frac{Y}{H_s}$ coordinates for the upper nappe surface were obtained in the same manner as those for the lower surface. These are tabulated for various values of $\frac{h_a}{H_s}$ in table 30.

35. Analysis of Nappe-Shape Results, Type D Weir.—The type D weir shown in figures 6 and 30, involved still another variable, namely, the height of the riser, M. Naturally, the number of tests required and the amount of work involved to prepare the data from this weir were fourfold. This is evidenced from table 31, which contains a complete summary of tests made on the type D weir. The asterisks

TABLE 28.—METHOD OF COMBINING NAPPE SHAPES FOR WEIRS WITH 45° OVERHANG

$\frac{M}{N} = 0$, $M = 0$

TEST	H_s, FEET	$\frac{h_a}{H_s}$	N, FEET	ACTUAL $\frac{N}{H_s}$	PLOTTED $\frac{N}{H_s}$
		$\frac{h_a}{H_s} = 0.002$			
160-1	0.960	0.0041	0.076	0.079	0.080
160-2	0.750	0.0027	0.076	0.101	0.100
150-1	1.135	0.0050	0.153	0.135	0.140
150-2	0.964	0.0037	0.153	0.159	0.160
150-3	0.769	0.0026	0.153	0.199	0.200
171-1	1.141	0.0047	0.305	0.267	0.270
171-2	0.850	0.0029	0.305	0.359	0.360
		$\frac{h_a}{H_s} = 0.03$			
161-1	1.014	0.0298	0.076	0.075	0.080
162-1	0.774	0.0302	0.076	0.098	0.100
151-1	1.179	0.0306	0.153	0.130	0.130
152-1	1.022	0.0295	0.153	0.150	0.150
153-1	0.785	0.0307	0.153	0.195	0.200
172-1	1.151	0.0307	0.305	0.265	0.260
173-1	1.023	0.0307	0.305	0.298	0.300
		$\frac{h_a}{H_s} = 0.06$			
163-1	1.039	0.0594	0.076	0.073	0.070
164-1	0.925	0.0602	0.076	0.082	0.080
154-1	1.033	0.0592	0.153	0.148	0.150
155-1	0.934	0.0596	0.153	0.164	0.160
174-1	1.029	0.0612	0.305	0.296	0.300
175-1	0.901	0.0648	0.305	0.339	0.340
		$\frac{h_a}{H_s} = 0.09$			
165-1	0.997	0.0900	0.076	0.076	0.080
166-1	0.731	0.0892	0.076	0.104	0.100
156-1	0.971	0.0894	0.153	0.158	0.160
157-1	0.744	0.0894	0.153	0.206	0.200
176-1	1.069	0.0904	0.305	0.285	0.290
177-1	0.987	0.0906	0.305	0.309	0.310
		$\frac{h_a}{H_s} = 0.12$			
167-1	1.002	0.1212	0.076	0.076	0.080
168-1	0.843	0.1192	0.076	0.090	0.090
158-1	0.993	0.1199	0.153	0.154	0.150
159-1	0.846	0.1203	0.153	0.181	0.180
		$\frac{h_a}{H_s} = 0.15$			
169-1	0.981	0.1499	0.076	0.077	0.080
170-1	0.749	0.1487	0.076	0.101	0.100

TABLE 29.—COORDINATES OF LOWER NAPPE FOR DIFFERENT VALUES OF $\frac{h_a}{H_s}$—OVERHANG WEIRS

h_a/H_s \ X/H_s	Y/H_s 0.002	0.010	0.020	0.030	0.040	0.050	0.060	0.070	0.080	0.090	0.100	0.120	0.140
0.000	0.0000	0.0000	0.0000	0.0000	0.0000	0.0000	0.0000	0.0000	0.0000	0.0000	0.0000	0.0000	0.0000
0.010	0.0470	0.0423	0.0376	0.0330	0.0300	0.0270	0.0240	0.0213	0.0186	0.0160	0.0146	0.0117	0.0092
0.020	0.0640	0.0593	0.0546	0.0500	0.0460	0.0420	0.0380	0.0350	0.0320	0.0290	0.0261	0.0202	0.0161
0.030	0.0756	0.0707	0.0658	0.0608	0.0572	0.0536	0.0500	0.0459	0.0418	0.0378	0.0346	0.0282	0.0229
0.040	0.0840	0.0793	0.0746	0.0700	0.0657	0.0614	0.0572	0.0530	0.0488	0.0445	0.0415	0.0353	0.0284
0.050	0.0920	0.0873	0.0826	0.0780	0.0733	0.0686	0.0640	0.0595	0.0550	0.0505	0.0472	0.0405	0.0335
0.060	0.0985	0.0938	0.0891	0.0845	0.0797	0.0749	0.0700	0.0653	0.0606	0.0560	0.0527	0.0460	0.0373
0.070	0.1045	0.0997	0.0949	0.0900	0.0847	0.0794	0.0740	0.0694	0.0648	0.0602	0.0564	0.0493	0.0404
0.080	0.1100	0.1047	0.0994	0.0942	0.0891	0.0840	0.0790	0.0740	0.0690	0.0640	0.0600	0.0520	0.0428
0.090	0.1150	0.1093	0.1036	0.0980	0.0930	0.0880	0.0830	0.0777	0.0724	0.0670	0.0628	0.0545	0.0448
0.100	0.1192	0.1135	0.1078	0.1020	0.0967	0.0914	0.0860	0.0807	0.0754	0.0700	0.0657	0.0570	0.0471
0.110	0.1225	0.1167	0.1109	0.1052	0.0998	0.0944	0.0890	0.0833	0.0776	0.0720	0.0675	0.0584	0.0488
0.120	0.1260	0.1200	0.1140	0.1080	0.1026	0.0972	0.0918	0.0859	0.0800	0.0742	0.0695	0.0600	0.0503
0.130	0.1288	0.1227	0.1166	0.1105	0.1049	0.0993	0.0938	0.0879	0.0820	0.0760	0.0712	0.0617	0.0514
0.140	0.1313	0.1252	0.1191	0.1130	0.1072	0.1014	0.0955	0.0895	0.0835	0.0775	0.0723	0.0620	0.0523
0.150	0.1335	0.1274	0.1213	0.1153	0.1090	0.1027	0.0963	0.0903	0.0843	0.0784	0.0733	0.0630	0.0530
0.160	0.1350	0.1290	0.1230	0.1170	0.1106	0.1042	0.0977	0.0915	0.0853	0.0790	0.0739	0.0637	0.0534
0.170	0.1368	0.1306	0.1244	0.1183	0.1116	0.1049	0.0983	0.0921	0.0859	0.0798	0.0745	0.0640	0.0535
0.180	0.1382	0.1321	0.1260	0.1200	0.1130	0.1060	0.0990	0.0926	0.0863	0.0800	0.0747	0.0640	0.0533
0.190	0.1400	0.1335	0.1270	0.1204	0.1135	0.1066	0.0997	0.0931	0.0865	0.0800	0.0746	0.0638	0.0532
0.200	0.1405	0.1343	0.1281	0.1218	0.1145	0.1072	0.0998	0.0932	0.0866	0.0800	0.0743	0.0630	0.0528
0.210	0.1415	0.1350	0.1285	0.1220	0.1146	0.1072	0.0997	0.0930	0.0863	0.0797	0.0740	0.0623	0.0518
0.220	0.1420	0.1353	0.1286	0.1220	0.1143	0.1066	0.0990	0.0925	0.0860	0.0795	0.0737	0.0620	0.0513
0.230	0.1420	0.1353	0.1286	0.1219	0.1141	0.1063	0.0985	0.0918	0.0851	0.0785	0.0727	0.0610	0.0505
0.240	0.1418	0.1351	0.1284	0.1218	0.1138	0.1058	0.0977	0.0912	0.0846	0.0780	0.0720	0.0600	0.0493
0.250	0.1418	0.1351	0.1284	0.1216	0.1132	0.1048	0.0965	0.0900	0.0835	0.0770	0.0710	0.0590	0.0480
0.260	0.1417	0.1346	0.1275	0.1204	0.1122	0.1040	0.0958	0.0892	0.0826	0.0760	0.0699	0.0578	0.0467
0.270	0.1416	0.1344	0.1272	0.1200	0.1115	0.1030	0.0945	0.0878	0.0811	0.0745	0.0686	0.0567	0.0452
0.280	0.1410	0.1337	0.1264	0.1190	0.1106	0.1022	0.0938	0.0871	0.0804	0.0736	0.0677	0.0558	0.0439
0.290	0.1402	0.1327	0.1252	0.1178	0.1092	0.1006	0.0920	0.0853	0.0786	0.0720	0.0660	0.0540	0.0419
0.300	0.1396	0.1317	0.1238	0.1160	0.1077	0.0994	0.0910	0.0840	0.0770	0.0700	0.0640	0.0520	0.0400
0.310	0.1380	0.1302	0.1224	0.1147	0.1063	0.0979	0.0895	0.0824	0.0753	0.0683	0.0625	0.0510	0.0382
0.320	0.1375	0.1293	0.1211	0.1130	0.1047	0.0964	0.0880	0.0810	0.0740	0.0670	0.0612	0.0495	0.0362
0.330	0.1360	0.1277	0.1194	0.1110	0.1027	0.0944	0.0860	0.0791	0.0722	0.0653	0.0592	0.0470	0.0339
0.340	0.1342	0.1259	0.1176	0.1093	0.1009	0.0925	0.0840	0.0772	0.0704	0.0635	0.0572	0.0445	0.0315

TABLE 29.—COORDINATES OF LOWER NAPPE FOR DIFFERENT VALUES OF $\frac{h_a}{H_s}$—OVERHANG WEIRS—Continued

h_a/H_s \ X/H_s	Y/H_s												
	0.002	0.010	0.020	0.030	0.040	0.050	0.060	0.070	0.080	0.090	0.100	0.120	0.140
0.350	0.1325	0.1242	0.1159	0.1075	0.0990	0.0905	0.0820	0.0752	0.0684	0.0615	0.0551	0.0422	0.0289
0.360	0.1307	0.1225	0.1143	0.1060	0.0973	0.0886	0.0800	0.0731	0.0662	0.0593	0.0529	0.0400	0.0267
0.370	0.1290	0.1207	0.1124	0.1040	0.0953	0.0866	0.0780	0.0708	0.0636	0.0565	0.0502	0.0377	0.0244
0.380	0.1270	0.1185	0.1100	0.1015	0.0929	0.0843	0.0757	0.0685	0.0613	0.0540	0.0477	0.0350	0.0217
0.390	0.1246	0.1161	0.1076	0.0990	0.0903	0.0816	0.0730	0.0660	0.0590	0.0520	0.0453	0.0320	0.0188
0.400	0.1225	0.1137	0.1049	0.0962	0.0876	0.0790	0.0703	0.0633	0.0563	0.0493	0.0424	0.0296	0.0163
0.410	0.1202	0.1115	0.1028	0.0940	0.0853	0.0766	0.0680	0.0608	0.0536	0.0464	0.0396	0.0260	0.0127
0.420	0.1180	0.1093	0.1006	0.0918	0.0829	0.0740	0.0650	0.0579	0.0508	0.0438	0.0369	0.0232	0.0101
0.430	0.1150	0.1062	0.0974	0.0886	0.0798	0.0710	0.0622	0.0550	0.0478	0.0405	0.0337	0.0200	0.0067
0.440	0.1120	0.1033	0.0946	0.0860	0.0770	0.0680	0.0590	0.0520	0.0450	0.0380	0.0310	0.0170	0.0042
0.450	0.1097	0.1006	0.0915	0.0823	0.0735	0.0647	0.0560	0.0488	0.0416	0.0345	0.0276	0.0138	0.0008
0.460	0.1060	0.0973	0.0886	0.0800	0.0710	0.0620	0.0530	0.0458	0.0386	0.0315	0.0243	0.0100	-0.0023
0.470	0.1034	0.0943	0.0852	0.0762	0.0674	0.0586	0.0497	0.0425	0.0353	0.0280	0.0208	0.0063	-0.0059
0.480	0.1000	0.0910	0.0820	0.0730	0.0640	0.0550	0.0460	0.0387	0.0314	0.0240	0.0172	0.0035	-0.0092
0.490	0.0960	0.0872	0.0784	0.0696	0.0605	0.0514	0.0423	0.0350	0.0277	0.0205	0.0137	0.0000	-0.0120
0.500	0.093	0.084	0.075	0.066	0.057	0.048	0.039	0.032	0.024	0.017	0.010	-0.004	-0.016
0.520	0.085	0.076	0.067	0.058	0.049	0.040	0.032	0.025	0.018	0.010	0.003	-0.012	-0.024
0.540	0.077	0.068	0.059	0.051	0.042	0.033	0.023	0.016	0.009	0.001	-0.006	-0.020	-0.032
0.560	0.068	0.059	0.050	0.042	0.033	0.024	0.015	0.008	0.000	-0.008	-0.015	-0.028	-0.037
0.580	0.059	0.050	0.041	0.033	0.024	0.015	0.006	-0.002	-0.010	-0.017	-0.024	-0.037	-0.049
0.600	0.049	0.041	0.033	0.024	0.015	0.006	-0.003	-0.011	-0.019	-0.026	-0.033	-0.046	-0.058
0.620	0.039	0.031	0.023	0.014	0.005	-0.004	-0.013	-0.021	-0.029	-0.036	-0.043	-0.056	-0.068
0.640	0.029	0.021	0.012	0.003	-0.006	-0.015	-0.023	-0.031	-0.039	-0.047	-0.053	-0.066	-0.077
0.660	0.018	0.009	0.000	-0.008	-0.017	-0.026	-0.034	-0.042	-0.050	-0.058	-0.064	-0.076	-0.087
0.680	0.006	-0.002	-0.010	-0.018	-0.027	-0.036	-0.045	-0.053	-0.061	-0.068	-0.074	-0.087	-0.098
0.700	-0.005	-0.013	-0.022	-0.030	-0.039	-0.048	-0.056	-0.064	-0.072	-0.080	-0.086	-0.098	-0.109
0.720	-0.017	-0.025	-0.033	-0.042	-0.051	-0.060	-0.068	-0.076	-0.084	-0.092	-0.098	-0.110	-0.119
0.740	-0.029	-0.037	-0.045	-0.054	-0.063	-0.072	-0.080	-0.088	-0.096	-0.103	-0.109	-0.121	-0.131
0.760	-0.042	-0.050	-0.058	-0.066	-0.075	-0.084	-0.092	-0.100	-0.108	-0.116	-0.122	-0.133	-0.142
0.780	-0.054	-0.062	-0.070	-0.079	-0.088	-0.097	-0.105	-0.113	-0.121	-0.128	-0.134	-0.145	-0.154
0.800	-0.066	-0.075	-0.084	-0.092	-0.101	-0.110	-0.119	-0.126	-0.133	-0.141	-0.146	-0.157	-0.166
0.820	-0.080	-0.089	-0.098	-0.106	-0.115	-0.124	-0.132	-0.139	-0.146	-0.152	-0.158	-0.170	-0.179
0.840	-0.093	-0.102	-0.111	-0.120	-0.129	-0.138	-0.146	-0.153	-0.160	-0.168	-0.173	-0.184	-0.192
0.860	-0.107	-0.116	-0.125	-0.135	-0.143	-0.151	-0.160	-0.167	-0.174	-0.182	-0.187	-0.196	-0.205
0.880	-0.121	-0.130	-0.139	-0.148	-0.157	-0.166	-0.175	-0.182	-0.189	-0.196	-0.200	-0.211	-0.219

TABLE 29.—COORDINATES OF LOWER NAPPE FOR DIFFERENT VALUES OF $\frac{h_a}{H_s}$—OVERHANG WEIRS—Continued

	Y/H_s												
X/H_s \ h_a/H_s	0.002	0.010	0.020	0.030	0.040	0.050	0.060	0.070	0.080	0.090	0.100	0.120	0.140
0.900	-0.136	-0.145	-0.154	-0.163	-0.172	-0.181	-0.190	-0.197	-0.204	-0.210	-0.215	-0.224	-0.232
0.920	-0.152	-0.161	-0.170	-0.178	-0.187	-0.196	-0.204	-0.211	-0.218	-0.226	-0.230	-0.239	-0.246
0.940	-0.167	-0.176	-0.185	-0.194	-0.203	-0.212	-0.220	-0.227	-0.234	-0.241	-0.245	-0.254	-0.261
0.960	-0.182	-0.191	-0.200	-0.209	-0.218	-0.227	-0.236	-0.243	-0.250	-0.256	-0.260	-0.269	-0.276
0.980	-0.199	-0.207	-0.215	-0.224	-0.233	-0.242	-0.251	-0.258	-0.265	-0.272	-0.276	-0.284	-0.291
1.000	-0.215	-0.224	-0.233	-0.242	-0.250	-0.258	-0.266	-0.274	-0.282	-0.290	-0.293	-0.300	-0.307
1.050	-0.260	-0.268	-0.276	-0.284	-0.292	-0.300	-0.308	-0.316	-0.324	-0.332	-0.335	-0.342	-0.346
1.100	-0.305	-0.313	-0.321	-0.328	-0.336	-0.344	-0.352	-0.360	-0.368	-0.375	-0.378	-0.383	-0.386
1.150	-0.352	-0.360	-0.368	-0.375	-0.382	-0.389	-0.396	-0.404	-0.412	-0.419	-0.421	-0.426	-0.429
1.200	-0.403	-0.410	-0.417	-0.423	-0.430	-0.437	-0.443	-0.450	-0.457	-0.465	-0.467	-0.471	-0.473
1.250	-0.456	-0.463	-0.470	-0.476	-0.481	-0.486	-0.492	-0.499	-0.506	-0.512	-0.514	-0.518	-0.518
1.300	-0.512	-0.518	-0.524	-0.530	-0.535	-0.540	-0.544	-0.549	-0.554	-0.560	-0.562	-0.565	-0.564
1.350	-0.569	-0.574	-0.579	-0.585	-0.589	-0.593	-0.598	-0.603	-0.608	-0.612	-0.613	-0.616	-0.613
1.400	-0.630	-0.634	-0.638	-0.642	-0.646	-0.650	-0.653	-0.657	-0.661	-0.664	-0.665	-0.668	-0.664
1.450	-0.692	-0.695	-0.698	-0.702	-0.705	-0.708	-0.710	-0.713	-0.716	-0.719	-0.719	-0.720	-0.717
1.500	-0.756	-0.758	-0.760	-0.762	-0.764	-0.766	-0.769	-0.771	-0.773	-0.776	-0.776	-0.776	-0.771
1.550	-0.823	-0.824	-0.825	-0.827	-0.828	-0.829	-0.830	-0.832	-0.834	-0.835	-0.835	-0.834	-0.828
1.600	-0.892	-0.892	-0.893	-0.894	-0.894	-0.895	-0.896	-0.896	-0.896	-0.896	-0.895	-0.894	-0.888
1.650	-0.960	-0.960	-0.961	-0.962	-0.962	-0.962	-0.962	-0.961	-0.961	-0.961	-0.959	-0.954	-0.947
1.700	-1.032	-1.032	-1.033	-1.033	-1.033	-1.032	-1.031	-1.029	-1.027	-1.026	-1.023	-1.018	-1.010
1.750	-1.108	-1.108	-1.108	-1.108	-1.106	-1.104	-1.102	-1.099	-1.096	-1.093	-1.089	-1.081	-1.074
1.800	-1.183	-1.183	-1.182	-1.181	-1.179	-1.177	-1.174	-1.171	-1.168	-1.164	-1.159	-1.150	-1.142
1.850	-1.260	-1.259	-1.258	-1.256	-1.253	-1.250	-1.248	-1.244	-1.240	-1.236	-1.231	-1.220	-1.211
1.900	-1.340	-1.338	-1.336	-1.333	-1.330	-1.327	-1.324	-1.320	-1.316	-1.313	-1.306	-1.293	-1.282
1.950	-1.424	-1.420	-1.416	-1.413	-1.410	-1.407	-1.403	-1.398	-1.393	-1.389	-1.382	-1.368	-1.356
2.000	-1.509	-1.505	-1.501	-1.496	-1.492	-1.488	-1.483	-1.478	-1.473	-1.468	-1.461	-1.446	-1.431
2.050	-1.595	-1.591	-1.587	-1.582	-1.576	-1.570	-1.564	-1.559	-1.554	-1.548	-1.540	-1.524	-1.507
2.100	-1.683	-1.679	-1.675	-1.670	-1.663	-1.656	-1.648	-1.642	-1.636	-1.630	-1.622	-1.605	-1.585
2.150	-1.772	-1.767	-1.762	-1.758	-1.751	-1.744	-1.736	-1.729	-1.722	-1.716	-1.707	-1.688	-1.665
2.200	-1.865	-1.859	-1.853	-1.848	-1.840	-1.832	-1.824	-1.817	-1.810	-1.802	-1.792	-1.772	-1.746
2.250	-1.959	-1.953	-1.948	-1.940	-1.931	-1.922	-1.914	-1.906	-1.898	-1.890	-1.879	-1.858	-1.828

TABLE 30.—COORDINATES OF UPPER NAPPE FOR DIFFERENT VALUES OF $\frac{h_a}{H_s}$— OVERHANG WEIRS

	Y/H_s							
X/H_s \ h_a/H_s	0.002	0.02	0.04	0.06	0.08	0.10	0.12	0.14
-3.500	0.995	0.972						
-3.400	0.994	0.972						
-3.300	0.994	0.972						
-3.200	0.994	0.972	0.949	0.925				
-3.100	0.994	0.972	0.948	0.924	0.908	0.886	0.858	0.831
-3.000	0.994	0.972	0.948	0.923	0.907	0.885	0.858	0.831
-2.900	0.994	0.971	0.947	0.922	0.906	0.884	0.857	0.831
-2.800	0.994	0.971	0.946	0.921	0.905	0.884	0.857	0.830
-2.700	0.993	0.970	0.945	0.921	0.904	0.882	0.856	0.830
-2.600	0.993	0.970	0.945	0.920	0.902	0.881	0.856	0.830
-2.500	0.993	0.969	0.945	0.920	0.901	0.880	0.855	0.830
-2.400	0.993	0.969	0.944	0.919	0.900	0.879	0.855	0.829
-2.300	0.993	0.969	0.944	0.919	0.900	0.878	0.854	0.829
-2.200	0.992	0.968	0.943	0.918	0.899	0.877	0.853	0.829
-2.100	0.992	0.968	0.943	0.918	0.898	0.876	0.853	0.829
-2.000	0.992	0.968	0.943	0.917	0.897	0.875	0.852	0.828
-1.900	0.992	0.967	0.942	0.916	0.896	0.875	0.852	0.828
-1.800	0.991	0.967	0.942	0.915	0.894	0.873	0.851	0.828
-1.700	0.991	0.966	0.942	0.914	0.893	0.872	0.851	0.827
-1.600	0.990	0.966	0.942	0.913	0.892	0.871	0.850	0.827
-1.500	0.988	0.965	0.939	0.912	0.891	0.870	0.850	0.826
-1.400	0.987	0.964	0.939	0.912	0.890	0.869	0.849	0.826
-1.300	0.982	0.961	0.938	0.911	0.889	0.868	0.848	0.825
-1.200	0.979	0.960	0.937	0.910	0.889	0.867	0.845	0.823
-1.100	0.975	0.956	0.934	0.909	0.887	0.865	0.842	0.819
-1.000	0.970	0.951	0.931	0.908	0.885	0.861	0.838	0.815
-0.900	0.966	0.947	0.927	0.905	0.880	0.856	0.833	0.810
-0.800	0.960	0.941	0.922	0.901	0.877	0.853	0.830	0.807
-0.700	0.953	0.934	0.915	0.896	0.872	0.848	0.825	0.802
-0.600	0.947	0.928	0.908	0.888	0.866	0.843	0.818	0.793
-0.500	0.938	0.918	0.899	0.880	0.859	0.836	0.811	0.786
-0.400	0.928	0.908	0.889	0.871	0.850	0.828	0.803	0.778
-0.300	0.914	0.895	0.878	0.861	0.840	0.818	0.793	0.768
-0.200	0.898	0.879	0.862	0.846	0.827	0.806	0.782	0.758
-0.100	0.882	0.863	0.845	0.829	0.811	0.791	0.768	0.745
0.000	0.860	0.842	0.825	0.809	0.792	0.772	0.751	0.730
0.100	0.832	0.815	0.799	0.784	0.769	0.752	0.733	0.714
0.200	0.803	0.786	0.870	0.754	0.739	0.724	0.708	0.692
0.300	0.767	0.751	0.736	0.721	0.707	0.693	0.678	0.663
0.400	0.724	0.709	0.695	0.680	0.667	0.654	0.643	0.632
0.500	0.676	0.661	0.647	0.635	0.622	0.611	0.601	0.591
0.600	0.622	0.607	0.594	0.582	0.570	0.559	0.550	0.541
0.700	0.562	0.547	0.534	0.522	0.511	0.501	0.492	0.483
0.800	0.496	0.481	0.469	0.458	0.446	0.436	0.429	0.422
0.900	0.422	0.407	0.394	0.383	0.373	0.365	0.358	0.351
1.000	0.338	0.327	0.315	0.302	0.294	0.287	0.280	0.273
1.100	0.248	0.237	0.226	0.215	0.208	0.202	0.197	0.192
1.200	0.149	0.138	0.129	0.120	0.114	0.108	0.103	0.098
1.300	0.038	0.030	0.022	0.015	0.012	0.008	0.003	-0.002
1.400	-0.078	-0.087	-0.094	-0.097	-0.102	-0.105	-0.106	-0.007
1.500	-0.208	-0.215	-0.220	-0.222	-0.222	-0.222	-0.222	-0.222
1.600	-0.347	-0.353	-0.355	-0.352	-0.352	-0.351	-0.350	-0.349
1.700	-0.500	-0.501	-0.499	-0.492	-0.492	-0.490	-0.485	-0.480
1.800	-0.650	-0.652	-0.652	-0.650	-0.645	-0.638	-0.630	-0.622
1.900	-0.810	-0.812	-0.812	-0.811	-0.804	-0.793	-0.780	-0.767
2.000	-0.983	-0.982	-0.980	-0.975	-0.960	-0.946	-0.935	-0.924
2.100	-1.160	-1.157	-1.152	-1.147	-1.130	-1.115	-1.100	-0.985
2.200	-1.350	-1.141	-1.333	-1.325	-1.308	-1.292	-1.277	-1.262
2.300	-1.544	-1.535	-1.523	-1.508	-1.495	-1.479	-1.460	-1.441
2.400	-1.750	-1.737	-1.723	-1.707	-1.688	-1.669	-1.650	-1.631
2.500	-1.960	-1.947	-1.932	-1.915	-1.892	-1.870	-1.850	-1.830
2.600	-2.170	-2.157	-2.141	-2.122	-2.101	-2.079	-2.055	-2.031

TABLE 31.—SUMMARY OF TESTS ON 45° OFFSET WEIRS WITH RISERS

1 TEST	2 P, FEET	3 Q, SECOND FEET	4 W, FEET	5 h_s, FEET	6 A, SQUARE FEET	7 V, FEET PER SECOND	8 h_a, FEET	9 E, FEET	10 H_o, FEET	11 $H_o^{\frac{3}{2}}$	12 L, FEET
						$\frac{M}{N} = 0.25$					
94-1	4.487	7.48	2.069	1.089	11.537	0.648	0.0066	0.147	0.9486	0.9239	2.006
94-2	4.484	4.00		0.717	10.761	0.372	0.0021	0.086	0.6331	0.5037	
94-3	4.484	3.26		0.637	10.595	0.308	0.0015	0.080	0.5585	0.4174	
95-1	1.900	6.66		0.974	5.946	1.120	0.0195	0.080	0.9135	0.8731	
95-2	1.900	3.34		0.637	5.249	0.636	0.0063	0.075	0.5683	0.4285	
96-1	0.983	3.32		0.619	3.315	1.002	0.0156	0.064	0.5706	0.4310	
96-2	0.984	4.09		0.702	3.488	1.173	0.0214	0.070	0.6534	0.5282	
96-3	0.984	6.95		0.967	4.037	1.722	0.0461	0.063	0.9501	0.9261	
97-1	0.758	5.31		0.802	3.228	1.645	0.0421	0.074	0.7701	0.6758	
97-2	0.757	7.14		0.966	3.565	2.003	0.0625	0.083	0.9455	0.9194	
97-3	0.894	7.15		0.967	3.850	1.857	0.0536	0.085	0.9356	0.9050	
98-1	0.894	3.57		0.637	3.168	1.127	0.0198	0.064	0.5928	0.4564	
99-1	0.400	3.56		0.597	2.063	1.726	0.0463	0.037	0.6063	0.4721	
99-2	0.401	4.95		0.730	2.340	2.115	0.0696	0.053	0.7466	0.6451	
99-3	0.401	5.29		0.760	2.402	2.202	0.0753	0.059	0.7763	0.6841	
100-1	0.552	4.50		0.706	2.603	1.729	0.0465	0.062	0.6905	0.5738	
						$\frac{M}{N} = 0.5$					
70-1	4.865	6.50	2.069	0.981	12.095	0.537	0.0045	0.114	0.871	0.814	2.006
70-2	4.865	4.05		0.714	11.543	0.351	0.0019	0.084	0.632	0.502	
71-1	1.512	6.37		0.939	5.071	1.256	0.0245	0.105	0.858	0.795	
71-2	1.512	6.59		0.964	5.123	1.286	0.0257	0.107	0.883	0.829	
71-3	1.512	8.08		1.094	5.392	1.499	0.0350	0.119	1.010	1.015	
71-4	1.513	8.07		1.094	5.394	1.496	0.0348	0.119	1.010	1.015	
72-1	0.989	5.02		0.788	3.677	1.365	0.0290	0.079	0.738	0.634	
72-2	0.989	5.97		0.877	3.861	1.546	0.0372	0.088	0.826	0.751	
72-3	0.984	4.02		0.685	3.453	1.163	0.0210	0.073	0.633	0.504	
72-4	0.985	4.02		0.704	3.495	1.149	0.0206	0.073	0.652	0.526	
73-1	0.748	6.74		0.927	3.466	1.945	0.0588	0.087	0.899	0.852	
73-2	0.748	6.98		0.946	3.505	1.991	0.0617	0.088	0.920	0.882	
74-1	0.778	8.85		1.093	3.871	2.286	0.0812	0.100	1.074	1.113	
74-2	0.777	2.94		0.554	2.754	1.068	0.0177	0.051	0.521	0.376	
75-1	0.500	6.55		0.873	2.841	2.306	0.0827	0.069	0.887	0.835	
75-2	0.497	7.00		0.909	2.909	2.406	0.0900	0.074	0.925	0.890	
75-3	0.491	8.99		1.051	3.190	2.818	0.1234	0.086	1.088	1.136	
75-4	0.492	4.13		0.658	2.379	1.736	0.0469	0.058	0.647	0.520	
70-3	4.771	8.91		1.209	12.372	0.720	0.0081	0.141	1.076	1.116	
101-1	4.399	5.01	2.069	0.826	10.811	0.463	0.0033	0.103	0.7263	0.619	2.006
101-2	4.399	4.07		0.726	10.604	0.384	0.0023	0.088	0.640	0.512	
101-3	4.399	3.22		0.608	10.359	0.311	0.0015	0.074	0.536	0.392	
102-1	0.990	3.22		0.588	3.265	0.986	0.0151	0.061	0.542	0.399	
102-2	0.990	4.04		0.689	3.474	1.163	0.0210	0.070	0.640	0.512	
103-1	0.897	4.05		0.686	3.275	1.237	0.0238	0.063	0.647	0.520	
103-2	0.897	3.43		0.616	3.130	1.096	0.0187	0.065	0.570	0.430	
103-3	0.897	7.74		1.022	3.970	1.950	0.0591	0.090	0.991	0.987	
104-1	0.684	6.05		0.862	3.199	1.891	0.0556	0.076	0.842	0.773	
104-2	0.684	6.04		0.862	3.199	1.888	0.0554	0.076	0.841	0.771	
104-3	0.684	8.83		1.080	3.650	2.419	0.0909	0.089	1.082	1.126	
104-4	0.684	4.36		0.703	2.870	1.519	0.0359	0.063	0.676	0.556	
105-1	0.555	4.57		0.713	2.623	1.742	0.0472	0.063	0.697	0.582	
105-2	0.555	4.42		0.698	2.592	1.705	0.0452	0.061	0.682	0.563	
105-3	0.552	8.34		1.022	3.257	2.561	0.1020	0.083	1.041	1.062	
105-4	0.552	8.31		1.021	3.255	2.553	0.1013	0.081	1.041	1.062	
106-1	0.509	7.07		0.921	2.959	2.389	0.0887	0.076	0.934	0.903	
106-2	0.511	7.29		0.939	3.000	2.430	0.0918	0.075	0.956	0.936	

TABLE 31.—SUMMARY OF TESTS ON 45° OFFSET WEIRS WITH RISERS—Continued

1 TEST	13 $LH_o^{\frac{3}{2}}$	14 C	15 $P+E$, FEET	16 $\frac{H_o}{P+E}$	17 H_s, FEET	18 $\frac{h_a}{H_s}$	19 $\frac{E}{H_s}$	20 N, FEET	21 M, FEET	22 $\frac{N}{H_s}$	23 NAPPE PROFILES
$\frac{M}{N} = 0.25$											
94-1	1.853	4.037	4.634	0.205	1.096	0.0060	0.134	0.310	0.079	0.283	*
94-2	1.010	3.960	4.570	0.138	0.719	0.0029	0.120			0.431	*
94-3	0.837	3.895	4.564	0.122	0.638	0.0023	0.125			0.486	*
95-1	1.751	3.804	1.980	0.461	0.993	0.0196	0.081			0.312	
95-2	0.860	3.883	1.975	0.288	0.643	0.0098	0.117			0.481	
96-1	0.865	3.838	1.047	0.545	0.635	0.0246	0.101			0.488	
96-2	1.060	3.858	1.054	0.620	0.723	0.0296	0.097			0.429	*
96-3	1.858	3.741	1.047	0.907	1.013	0.0455	0.062			0.306	
97-1	1.356	3.916	0.832	0.926	0.844	0.0499	0.088			0.367	
97-2	1.844	3.872	0.840	1.126	1.028	0.0608	0.081			0.301	
97-3	1.815	3.939	0.979	0.955	1.021	0.0525	0.083			0.304	*
98-1	0.916	3.897	0.958	0.619	0.657	0.0301	0.097			0.472	*
99-1	0.947	3.759	0.437	1.387	0.643	0.0720	0.058			0.482	
99-2	1.294	3.825	0.454	1.644	0.800	0.0870	0.066			0.388	
99-3	1.372	3.856	0.460	1.688	0.835	0.0901	0.071			0.371	*
100-1	1.151	3.910	0.614	1.125	0.752	0.0618	0.082			0.412	*
$\frac{M}{N} = 0.5$											
70-1	1.632	3.983	4.979	0.175	0.986	0.0046	0.116	0.156	0.079	0.158	*
70-2	1.008	4.018	4.949	0.128	0.716	0.0026	0.117			0.218	*
71-1	1.596	3.991	1.617	0.531	0.963	0.0254	0.109			0.162	
71-2	1.664	3.960	1.619	0.545	0.990	0.0260	0.108			0.158	
71-3	2.036	3.969	1.631	0.619	1.129	0.0310	0.105			0.138	
71-4	2.035	3.966	1.632	0.619	1.129	0.0308	0.105			0.138	*
72-1	1.272	3.947	1.068	0.691	0.817	0.0355	0.097			0.191	
72-2	1.507	3.962	1.077	0.767	0.914	0.0407	0.096			0.171	
72-3	1.010	3.975	1.057	0.599	0.706	0.0297	0.103			0.221	
72-4	1.055	3.806	1.058	0.616	0.725	0.0284	0.101			0.215	*
73-1	1.709	3.944	0.835	1.076	0.986	0.0596	0.088			0.158	
73-2	1.769	3.946	0.836	1.100	1.008	0.0612	0.087			0.155	*
74-1	2.233	3.963	0.878	1.223	1.174	0.0691	0.085			0.133	
74-2	0.754	3.899	0.828	0.629	0.572	0.0310	0.089			0.273	
75-1	1.675	3.910	0.569	1.558	0.956	0.0865	0.072			0.163	
75-2	1.785	3.922	0.571	1.620	0.999	0.0901	0.074			0.156	*
75-3	2.278	3.946	0.577	1.886	1.174	0.1051	0.073			0.133	
75-4	1.044	3.956	0.550	1.176	0.705	0.0665	0.082			0.221	
70-3	2.239	3.979	4.912	0.219	1.217	0.0066	0.116			0.128	
101-1	1.242	4.034	4.502	0.161	0.829	0.0040	0.124	0.310	0.155	0.374	
101-2	1.027	3.963	4.487	0.143	0.728	0.0032	0.121			0.426	*
101-3	0.786	4.097	4.473	0.120	0.610	0.0025	0.121			0.508	*
102-1	0.800	4.025	1.051	0.516	0.603	0.0250	0.101			0.514	
102-2	1.027	3.934	1.060	0.604	0.710	0.0296	0.099			0.437	*
103-1	1.043	3.883	0.960	0.674	0.710	0.0335	0.089			0.437	
103-2	0.863	3.975	0.962	0.593	0.635	0.0294	0.102			0.488	*
103-3	1.980	3.909	0.987	1.004	1.081	0.0547	0.083			0.287	
104-1	1.551	3.901	0.760	1.108	0.918	0.0606	0.083			0.338	
104-2	1.547	3.904	0.760	1.107	0.917	0.0604	0.083			0.338	*
104-3	2.259	3.909	0.773	1.400	1.171	0.0776	0.076			0.265	
104-4	1.115	3.910	0.747	0.905	0.739	0.0486	0.085			0.419	
105-1	1.167	3.916	0.618	1.128	0.760	0.0621	0.083			0.408	
105-2	1.129	3.915	0.616	1.107	0.743	0.0608	0.082			0.417	*
105-3	2.130	3.915	0.635	1.639	1.124	0.0907	0.074			0.276	
105-4	2.130	3.901	0.633	1.645	1.122	0.0903	0.072			0.276	*
106-1	1.811	3.904	0.585	1.597	1.010	0.0878	0.075			0.307	
106-2	1.878	3.882	0.586	1.631	1.031	0.0890	0.073			0.301	*

* RUNS IN WHICH NAPPE PROFILES WERE MEASURED.

TABLE 31.—SUMMARY OF TESTS ON 45° OFFSET WEIRS WITH RISERS—Continued

1 TEST	2 P, FEET	3 Q, SECOND-FEET	4 W, FEET	5 h_s, FEET	6 A, SQUARE FEET	7 V, FEET PER SECOND	8 h_a, FEET	9 E, FEET	10 H_o, FEET	11 $H_o^{\frac{3}{2}}$	12 L, FEET
$\frac{M}{N}=1.0$											
76-1	4.928	8.91	2.069	1.206	12.691	0.702	0.0076	0.134	1.080	1.122	2.006
76-2	4.928	6.53		0.968	12.199	0.521	0.0042	0.107	0.865	0.805	
76-3	4.928	3.795		0.722	11.690	0.325	0.0016	0.082	0.642	0.514	
77-1	1.506	9.06		1.177	5.551	1.632	0.0414	0.125	1.093	1.143	
77-2	1.506	6.74		0.977	5.137	1.312	0.0268	0.103	0.901	0.855	
77-3	1.506	7.97		1.087	5.365	1.486	0.0343	0.114	1.007	1.011	
77-4	1.506	3.81		0.677	4.517	0.843	0.0111	0.076	0.612	0.479	
78-1	0.747	9.19		1.119	3.861	2.380	0.0881	0.097	1.110	1.170	
78-2	0.747	6.945		0.950	3.511	1.978	0.0608	0.083	0.928	0.894	
78-3	0.747	6.940		0.947	3.505	1.980	0.0609	0.082	0.926	0.891	
78-4	0.747	3.79		0.684	2.961	1.280	0.0255	0.078	0.632	0.502	
79-1	0.497	9.24		1.073	3.248	2.845	0.1259	0.085	1.114	1.176	
79-2	0.497	7.02		0.917	2.926	2.399	0.0894	0.063	0.943	0.916	
79-3	0.497	7.09		0.922	2.936	2.415	0.0906	0.072	0.941	0.913	
79-4	0.497	3.76		0.625	2.321	1.620	0.0408	0.053	0.613	0.480	
107-1	4.716	5.36	2.069	0.857	11.531	0.465	0.0034	0.097	0.763	0.667	2.006
107-2	4.716	3.57		0.655	11.113	0.321	0.0016	0.078	0.579	0.441	
108-1	0.982	3.52		0.627	3.329	1.057	0.0174	0.061	0.583	0.445	
108-2	0.982	4.00		0.676	3.430	1.166	0.0211	0.069	0.628	0.498	
108-3	0.982	5.37		0.816	3.720	1.444	0.0324	0.081	0.767	0.672	
109-1	0.658	5.36		0.793	3.002	1.785	0.0496	0.074	0.769	0.674	
109-2	0.658	5.55		0.811	3.039	1.826	0.0519	0.073	0.790	0.702	
109-3	0.658	8.96		1.083	3.602	2.488	0.0962	0.090	1.089	1.136	
109-4	0.658	8.87		1.077	3.590	2.471	0.0949	0.090	1.082	1.126	
110-1	4.183	5.42	2.069	0.873	10.461	0.518	0.0042	0.105	0.772	0.678	2.006
110-2	4.183	4.11		0.725	10.155	0.405	0.0026	0.088	0.640	0.512	
111-1	1.012	4.94		0.784	3.716	1.328	0.0275	0.083	0.728	0.621	
111-2	1.012	4.33		0.718	3.579	1.210	0.0228	0.075	0.666	0.544	
111-3	1.012	5.97		0.884	3.923	1.522	0.0360	0.094	0.826	0.751	
111-4	1.012	8.26		1.082	4.332	1.907	0.0565	0.109	1.030	1.045	
112-1	0.656	6.03		0.860	3.137	1.922	0.0573	0.080	0.837	0.766	
112-2	0.656	5.77		0.837	3.089	1.868	0.0543	0.075	0.816	0.737	
112-3	0.657	3.85		0.652	2.708	1.422	0.0314	0.064	0.619	0.487	
112-4	0.657	9.10		1.098	3.631	2.506	0.0976	0.096	1.100	1.154	
113-1	0.446	7.68		0.955	2.899	2.649	0.1091	0.074	0.990	0.985	
113-2	0.449	6.05		0.832	2.650	2.283	0.0810	0.068	0.845	0.777	
113-3	0.451	6.17		0.841	2.673	2.308	0.0828	0.064	0.860	0.798	
114-1	0.294	4.16		0.634	1.920	2.167	0.0730	0.046	0.661	0.537	
115-1	0.343	4.21		0.645	2.044	2.060	0.0660	0.051	0.660	0.536	
115-2	0.343	4.14		0.640	2.034	2.035	0.0644	0.047	0.657	0.533	
115-A	0.336	6.81		0.862	2.479	2.747	0.1173	0.060	0.919	0.881	
115-B	0.273	5.14		0.717	2.048	2.510	0.0979	0.047	0.768	0.673	
115-C	0.249	4.41		0.645	1.850	2.384	0.0884	0.041	0.692	0.576	

TABLE 31.—SUMMARY OF TESTS ON 45° OFFSET WEIRS WITH RISERS—Continued

1 TEST	13 $LH_o^{\frac{3}{2}}$	14 C	15 $P+E$, FEET	16 $\frac{H_o}{P+E}$	17 H_s, FEET	18 $\frac{h_a}{H_s}$	19 $\frac{E}{H_s}$	20 N, FEET	21 M, FEET	22 $\frac{N}{H_s}$	23 NAPPE PROFILES
$\frac{M}{N}$ = 1.0											
76-1	2.251	3 958	5.062	0 213	1 214	0.0063	0.110	0.156	0.155	0.129	
76-2	1.615	3.932	5.035	0.172	0 972	0.0043	0.110			0.160	*
76-3	1.031	3.681	5.010	0.128	0 724	0 0022	0.113			0.216	*
77-1	2.293	3.951	1.631	0 670	1.218	0.0340	0.103			0.128	
77-2	1.715	3.930	1.609	0.560	1.004	0.0267	0.103			0.155	
77-3	2 028	3.930	1.620	0.622	1 121	0.0306	0.102			0.139	*
77-4	0.961	3.965	1.582	0.387	0.688	0.0161	0.110			0.227	
78-1	2.347	3.916	0.844	1 315	1.207	0.0730	0.080			0.129	
78-2	1.793	3.873	0.830	1.118	1.011	0.0602	0.082			0.154	
78-3	1.787	3.884	0.829	1.117	1.008	0.0604	0.081			0.155	*
78-4	1.007	3.764	0.825	0.766	0 709	0.0359	0.110			0.220	
79-1	2.359	3.917	0.582	1.914	1.199	0.1050	0.071			0.130	
79-2	1.837	3.821	0.560	1.684	1.006	0.0888	0.063			0.155	
79-3	1.831	3.872	0.569	1.654	1 013	0.0895	0.071			0.154	*
79-4	0.963	3.904	0.550	1.115	0 666	0 0613	0.079			0.234	
107-1	1 338	4.006	4.813	0.159	0.860	0.0040	0.113	0.310	0.305	0.360	
107-2	0.885	4.034	4.794	0 121	0.657	0.0024	0.119			0.472	*
108-1	0 893	3 942	1.043	0.559	0.644	0.0270	0.095			0.481	
108-2	0 999	4.004	1.051	0.598	0.697	0.0303	0.099			0.445	*
108-3	1.348	3 984	1 063	0.722	0.848	0.0382	0.096			0.366	
109-1	1.352	3.964	0.732	1.051	0.843	0.0588	0.088			0.368	
109-2	1.408	3.942	0.731	1.081	0 863	0.0601	0.085			0.359	*
109-3	2 279	3.932	0.748	1.456	1.179	0.0816	0.076			0.263	
109-4	2.259	3.927	0.748	1.447	1.172	0.0810	0.077			0.265	*
110-1	1.360	3.985	4.288	0.180	0.877	0.0048	0.120	0.076	0.079	0.086	
110-2	1.027	4.002	4.271	0.150	0.728	0.0036	0.121			0.104	*
111-1	1.246	3.965	1.095	0.665	0.811	0.0339	0.102			0.094	
111-2	1.091	3.969	1.087	0.613	0.741	0.0308	0.101			0.103	*
111-3	1.507	3.962	1.106	0.747	0.920	0.0390	0.102			0.083	
111-4	2.096	3.941	1.121	0.919	1.139	0.0496	0.096			0.067	
112-1	1.537	3.923	0.736	1.137	0.917	0.0625	0.087			0.083	
112-2	1.478	3.904	0.731	1.116	0.891	0.0609	0.084			0.085	*
112-3	0.977	3.941	0.721	0.859	0.683	0.0460	0.094			0.111	
112-4	2.315	3.931	0.753	1.461	1.196	0.0816	0.080			0.064	
113-1	1.976	3.887	0.520	1.904	1.064	0.1025	0.070			0.071	
113-2	1.559	3.881	0.517	1.634	0.913	0.0887	0.074			0.083	
113-3	1.601	3.854	0.515	1.670	0.924	0.0896	0.069			0.082	*
114-1	1.077	3.863	0.340	1.944	0.707	0.1032	0.065			0.104	
115-1	1.075	3.916	0.394	1.675	0.711	0.0930	0.072			0.107	
115-2	1.069	3.873	0.390	1.685	0.704	0.0914	0.068			0.108	*
115-A	1.767	3.854	0.396	2.321	0.979	0.1198	0.061			0.078	*
115-B	1.350	3.807	0.320	2.400	0.815	0.1201	0.058			0.093	*
115-C	1.155	3.818	0.290	2.386	0.733	0.1206	0.056			0.104	*

* RUNS IN WHICH NAPPE PROFILES WERE MEASURED.

TABLE 31.—SUMMARY OF TESTS ON 45° OFFSET WEIRS WITH RISERS—Continued

1 TEST	2 P, FEET	3 Q, SECOND-FEET	4 W, FEET	5 h_s, FEET	6 A, SQUARE FEET	7 V, FEET PER SECOND	8 h_a, FEET	9 E, FEET	10 H_o, FEET	11 $H_o^{\frac{3}{2}}$	12 L, FEET
					$\frac{M}{N} = 2.0$						
80-1	4.583	9.00	2.069	1.214	11.994	0.750	0.0087	0.135	1.088	1.135	2.006
80-2	4.583	7.50		1.082	11.721	0.640	0.0064	0.124	0.964	0.947	
80-3	4.584	6.22		0.928	11.404	0.545	0.0046	0.102	0.831	0.758	
80-4	4.585	3.95		0.723	10.982	0.360	0.0020	0.079	0.646	0.519	
81-1	1.493	8.97		1.167	5.503	1.630	0.0413	0.121	1.087	1.133	
81-2	1.493	8.02		1.087	5.338	1.502	0.0351	0.112	1.010	1.015	
81-3	1.493	6.02		0.906	4.964	1.213	0.0229	0.096	0.833	0.760	
81-4	1.493	3.99		0.695	4.527	0.881	0.0120	0.077	0.630	0.500	
82-1	0.996	3.98		0.680	3.468	1.148	0.0205	0.070	0.631	0.501	
82-2	0.996	4.13		0.696	3.501	1.180	0.0216	0.071	0.647	0.520	
82-3	0.996	5.99		0.884	3.890	1.540	0.0369	0.086	0.835	0.763	
82-4	0.995	9.32		1.156	4.450	2.094	0.0682	0.107	1.117	1.181	
83-1	0.729	9.33		1.128	3.842	2.428	0.0916	0.096	1.124	1.192	
83-2	0.729	6.73		0.930	3.432	1.961	0.0598	0.086	0.904	0.860	
83-3	0.729	6.72		0.928	3.428	1.960	0.0597	0.084	0.904	0.860	
83-4	0.734	4.41		0.713	2.994	1.473	0.0338	0.068	0.679	0.560	
84-1	0.644	4.39		0.701	2.783	1.577	0.0387	0.069	0.671	0.550	
84-2	0.644	4.76		0.739	2.861	1.664	0.0430	0.071	0.711	0.600	
84-3	0.644	5.25		0.785	2.957	1.775	0.0490	0.073	0.761	0.664	
84-4	0.642	5.42		0.803	2.990	1.813	0.0511	0.072	0.782	0.692	
84-5	0.642	9.35		1.116	3.637	2.571	0.1028	0.097	1.122	1.189	
85-1	0.499	4.06		0.658	2.394	1.696	0.0447	0.058	0.645	0.518	
85-2	0.499	6.91		0.912	2.919	2.367	0.0871	0.077	0.922	0.885	
85-3	0.499	7.19		0.934	2.965	2.425	0.0914	0.079	0.946	0.920	
85-4	0.502	8.32		1.018	3.147	2.644	0.1087	0.084	1.043	1.065	
85-5	0.502	7.45		0.954	3.012	2.473	0.0950	0.081	0.968	0.952	
85-6	0.499	7.42		0.951	3.000	2.473	0.0950	0.077	0.969	0.954	
116-1	4.370	7.52	2.069	1.081	11.278	0.667	0.0069	0.126	0.962	0.943	2.006
116-2	4.370	5.45		0.871	10.844	0.503	0.0039	0.096	0.779	0.688	
116-3	4.370	3.86		0.691	10.471	0.369	0.0021	0.083	0.610	0.476	
117-1	0.975	3.87		0.665	3.393	1.141	0.0202	0.064	0.621	0.489	
117-2	0.975	3.90		0.670	3.404	1.146	0.0204	0.070	0.620	0.488	
117-3	0.975	5.98		0.880	3.838	1.558	0.0377	0.087	0.831	0.757	
117-4	0.972	7.81		1.036	4.155	1.880	0.0549	0.102	0.989	0.983	
118-1	0.642	5.11		0.775	2.932	1.743	0.0473	0.068	0.754	0.655	
118-2	0.642	5.41		0.801	2.986	1.812	0.0510	0.073	0.779	0.688	
118-3	0.642	7.97		1.016	3.430	2.324	0.0840	0.083	1.017	1.026	
118-4	0.642	3.28		0.586	2.541	1.291	0.0259	0.056	0.556	0.415	
119-1	0.383	5.14		0.743	2.330	2.206	0.0756	0.056	0.763	0.666	
119-2	0.383	4.96		0.728	2.299	2.157	0.0723	0.057	0.743	0.640	
120-1	0.343	4.31		0.660	2.075	2.077	0.0671	0.044	0.683	0.564	
120-2	0.343	4.00		0.625	2.003	1.997	0.0620	0.048	0.639	0.511	
120-3	0.342	6.52		0.843	2.454	2.657	0.1098	0.062	0.891	0.841	
120-A	0.340	6.93		0.874	2.512	2.759	0.1183	0.059	0.932	0.900	
120-B	0.301	5.86		0.780	2.237	2.620	0.1067	0.051	0.836	0.764	

TABLE 31.—SUMMARY OF TESTS ON 45° OFFSET WEIRS WITH RISERS—Continued

1 TEST	13 $LH_o^{\frac{3}{2}}$	14 C	15 $P+E$, FEET	16 $\frac{H_o}{P+E}$	17 H_s, FEET	18 $\frac{h_a}{H_s}$	19 $\frac{E}{H_s}$	20 N, FEET	21 M, FEET	22 $\frac{N}{H_s}$	23 NAPPE PROFILES
$\frac{M}{N} = 2.0$											
80-1	2.277	3.953	4.718	0.231	1.223	0.0071	0.110	0.156	0.305	0.128	
80-2	1.900	3.947	4.707	0.205	1.088	0.0059	0.114			0.143	*
80-3	1.521	4.089	4.686	0.177	0.933	0.0049	0.109			0.167	*
80-4	1.041	3.794	4.664	0.139	0.725	0.0027	0.109			0.215	
81-1	2.273	3.946	1.614	0.673	1.208	0.0342	0.100			0.129	
81-2	2.036	3.939	1.605	0.629	1.122	0.0313	0.100			0.139	*
81-3	1.525	3.948	1.589	0.524	0.929	0.0247	0.103			0.168	
81-4	1.003	3.978	1.570	0.401	0.707	0.0170	0.109			0.221	
82-1	1.005	3.960	1.066	0.592	0.701	0.0292	0.100			0.223	
82-2	1.043	3.960	1.067	0.606	0.718	0.0301	0.099			0.217	*
82-3	1.531	3.912	1.082	0.772	0.921	0.0401	0.093			0.169	
82-4	2.369	3.934	1.102	1.014	1.224	0.0557	0.087			0.127	
83-1	2.391	3.902	0.825	1.362	1.220	0.0751	0.079			0.128	
83-2	1.725	3.901	0.815	1.109	0.990	0.0604	0.087			0.158	
83-3	1.725	3.896	0.813	1.112	0.988	0.0604	0.085			0.158	*
83-4	1.123	3.927	0.802	0.847	0.747	0.0452	0.091			0.209	
84-1	1.103	3.980	0.713	0.941	0.740	0.0523	0.093			0.211	
84-2	1.204	3.953	0.715	0.994	0.782	0.0550	0.091			0.199	
84-3	1.332	3.941	0.717	1.061	0.834	0.0588	0.088			0.187	
84-4	1.388	3.905	0.714	1.095	0.854	0.0598	0.084			0.183	*
84-5	2.385	3.920	0.739	1.518	1.219	0.0843	0.080			0.128	
85-1	1.039	3.908	0.557	1.158	0.703	0.0636	0.083			0.222	
85-2	1.775	3.893	0.576	1.601	0.999	0.0872	0.077			0.156	
85-3	1.846	3.895	0.578	1.637	1.025	0.0892	0.077			0.152	
85-4	2.136	3.895	0.586	1.780	1.127	0.0965	0.075			0.138	
85-5	1.910	3.901	0.583	1.660	1.049	0.0906	0.077			0.149	
85-6	1.914	3.877	0.576	1.682	1.046	0.0908	0.074			0.149	*
116-1	1.893	3.973	4.496	0.214	1.088	0.0063	0.116	0.076	0.155	0.070	
116-2	1.379	3.952	4.466	0.174	0.875	0.0045	0.110			0.087	
116-3	0.956	4.038	4.453	0.137	0.693	0.0030	0.120			0.110	*
117-1	0.982	3.941	1.039	0.598	0.685	0.0295	0.093			0.111	
117-2	0.979	3.984	1.045	0.593	0.690	0.0296	0.101			0.110	*
117-3	1.520	3.934	1.062	0.782	0.918	0.0411	0.095			0.083	
117-4	1.973	3.958	1.074	0.921	1.091	0.0503	0.094			0.070	
118-1	1.313	3.892	0.710	1.062	0.822	0.0576	0.083			0.092	
118-2	1.379	3.923	0.715	1.090	0.852	0.0598	0.086			0.089	*
118-3	2.057	3.875	0.725	1.403	1.100	0.0764	0.067			0.069	
118-4	0.832	3.942	0.698	0.797	0.612	0.0423	0.092			0.124	
119-1	1.337	3.844	0.439	1.738	0.819	0.0923	0.068			0.093	
119-2	1.285	3.860	0.440	1.689	0.800	0.0904	0.071			0.095	*
120-1	1.132	3.807	0.387	1.765	0.727	0.0923	0.061			0.105	
120-2	1.025	3.902	0.391	1.634	0.687	0.0903	0.070			0.111	*
120-3	1.687	3.865	0.404	2.205	0.953	0.1152	0.065			0.080	
120-A	1.805	3.839	0.399	2.336	0.991	0.1194	0.060			0.077	*
120-B	1.533	3.823	0.352	2.375	0.887	0.1203	0.057			0.086	*

* RUNS IN WHICH NAPPE PROFILES WERE MEASURED.

TABLE 31.—SUMMARY OF TESTS ON 45° OFFSET WEIRS WITH RISERS—Continued

1 TEST	2 P, FEET	3 Q, SECOND-FEET	4 W, FEET	5 h_s, FEET	6 A, SQUARE FEET	7 V, FEET PER SECOND	8 h_a, FEET	9 E, FEET	10 H_o, FEET	11 $H_o^{3/2}$	12 L, FEET
$\frac{M}{N} = 3.0$											
121-1	4.234	3.67	2.069	0.665	10.136	0.362	0.0020	0.079	0.588	0.451	2.006
121-2	4.236	6.12		0.941	10.711	0.571	0.0051	0.106	0.840	0.770	
121-3	4.238	7.98		1.121	11.088	0.720	0.0081	0.130	0.999	0.998	
122-1	2.019	5.18		0.826	5.887	0.880	0.0120	0.093	0.745	0.643	
122-2	2.019	7.88		1.089	6.430	1.226	0.0233	0.123	0.989	0.983	
123-1	1.511	7.69		1.059	5.317	1.446	0.0325	0.115	0.977	0.966	
124-1	1.241	6.25		0.916	4.463	1.400	0.0305	0.094	0.853	0.788	
125-1	1.015	4.26		0.706	3.561	1.196	0.0222	0.074	0.654	0.529	
126-1	0.731	6.64		0.917	3.410	1.947	0.0589	0.086	0.890	0.840	
127-1	0.648	5.54		0.811	3.019	1.835	0.0524	0.076	0.787	0.698	
128-1	0.589	4.86		0.745	2.760	1.761	0.0483	0.068	0.725	0.617	
128-2	0.585	8.36		1.030	3.341	2.502	0.0973	0.087	1.040	1.061	
129-1	0.502	7.56		0.955	3.015	2.507	0.0977	0.077	0.976	0.964	
130-1	0.453	6.41		0.860	2.717	2.359	0.0865	0.065	0.882	0.828	
131-1	0.350	4.32		0.663	2.096	2.061	0.0661	0.050	0.679	0.559	
$\frac{M}{N} = 4.0$											
132-1	4.664	7.83	2.069	1.106	11.938	0.656	0.0067	0.125	0.988	0.982	2.006
132-2	4.666	4.15		0.724	11.152	0.372	0.0021	0.085	0.641	0.513	
132-3	4.669	5.96		0.925	11.574	0.515	0.0041	0.106	0.823	0.747	
133-1	1.515	7.67		1.058	5.324	1.441	0.0323	0.116	0.974	0.961	
134-1	1.321	6.25		0.922	4.641	1.347	0.0282	0.098	0.852	0.786	
135-1	1.020	4.29		0.714	3.588	1.196	0.0222	0.077	0.659	0.535	
136-1	0.735	6.60		0.911	3.406	1.938	0.0584	0.086	0.883	0.830	
137-1	0.644	5.44		0.802	2.992	1.818	0.0514	0.077	0.776	0.684	
138-1	0.594	4.84		0.744	2.768	1.749	0.0476	0.070	0.722	0.614	
139-1	0.507	7.35		0.942	2.998	2.452	0.0935	0.079	0.957	0.936	
140-1	0.460	6.38		0.861	2.733	2.334	0.0847	0.073	0.873	0.816	
141-1	0.427	5.72		0.801	2.541	2.251	0.0788	0.067	0.813	0.733	
$\frac{M}{N} = 5.0$											
142-1	4.776	7.89	2.069	1.113	12.184	0.648	0.0066	0.123	0.997	0.996	2.006
142-2	4.776	3.56		0.655	11.237	0.317	0.0016	0.078	0.579	0.441	
142-3	4.776	5.99		0.928	11.802	0.508	0.0040	0.106	0.826	0.751	
143-1	1.514	7.62		1.054	5.313	1.434	0.0320	0.115	0.971	0.957	
144-1	1.321	6.23		0.919	4.634	1.344	0.0281	0.098	0.849	0.782	
145-1	1.015	4.24		0.707	3.563	1.190	0.0220	0.075	0.654	0.529	
146-1	0.732	6.60		0.914	3.406	1.938	0.0584	0.087	0.885	0.833	
147-1	0.644	5.46		0.808	3.004	1.818	0.0514	0.078	0.781	0.690	
148-1	0.596	4.85		0.745	2.775	1.748	0.0475	0.078	0.715	0.605	
149-1	0.516	7.57		0.965	3.064	2.471	0.0949	0.094	0.966	0.949	

TABLE 31.—SUMMARY OF TESTS ON 45° OFFSET WEIRS WITH RISERS—Continued

1 TEST	13 $LH_0^{\frac{3}{2}}$	14 C	15 $P+E$, FEET	16 $\frac{H_0}{P+E}$	17 H_s, FEET	18 $\frac{h_a}{H_s}$	19 $\frac{E}{H_s}$	20 N, FEET	21 M, FEET	22 $\frac{N}{H_s}$	23 NAPPE PROFILES
$\frac{M}{N} = 3.0$											
121-1	0.905	4.055	4.313	0.136	0.667	0.0030	0.118	0.076	0.233	0.114	*
121-2	1.544	3.964	4.342	0.193	0.946	0.0054	0.112			0.080	*
121-3	2.003	3.984	4.368	0.229	1.129	0.0072	0.115			0.067	*
122-1	1.290	4.016	2.112	0.353	0.838	0.0143	0.111			0.091	
122-2	1.973	3.994	2.142	0.462	1.112	0.0209	0.111			0.068	
123-1	1.937	3.970	1.626	0.601	1.092	0.0298	0.105			0.070	*
124-1	1.580	3.956	1.335	0.639	0.947	0.0322	0.099			0.080	*
125-1	1.061	4.015	1.089	0.600	0.728	0.0305	0.102			0.104	*
126-1	1.684	3.943	0.817	1.089	0.976	0.0603	0.088			0.078	*
127-1	1.401	3.954	0.724	1.087	0.863	0.0607	0.088			0.088	*
128-1	1.238	3.926	0.657	1.104	0.793	0.0609	0.086			0.096	*
128-2	2.128	3.929	0.672	1.548	1.127	0.0863	0.077			0.067	
129-1	1.934	3.909	0.579	1.686	1.053	0.0928	0.073			0.072	*
130-1	1.662	3.857	0.518	1.703	0.947	0.0913	0.069			0.080	*
131-1	1.122	3.850	0.400	1.698	0.729	0.0907	0.069			0.104	*
$\frac{M}{N} = 4.0$											
132-1	1.970	3.975	4.789	0.206	1.113	0.0060	0.112	0.076	0.305	0.068	*
132-2	1.029	4.033	4.751	0.135	0.726	0.0029	0.117			0.105	*
132-3	1.498	3.979	4.775	0.172	0.929	0.0044	0.114			0.082	*
133-1	1.928	3.978	1.631	0.597	1.090	0.0296	0.106			0.070	*
134-1	1.577	3.963	1.419	0.600	0.950	0.0297	0.103			0.080	*
135-1	1.073	3.998	1.097	0.601	0.736	0.0302	0.105			0.103	*
136-1	1.665	3.964	0.821	1.076	0.969	0.0603	0.089			0.078	*
137-1	1.372	3.965	0.721	1.076	0.853	0.0603	0.090			0.089	*
138-1	1.232	3.929	0.664	1.087	0.792	0.0601	0.088			0.096	*
139-1	1.878	3.914	0.586	1.633	1.036	0.0903	0.076			0.073	*
140-1	1.637	3.897	0.533	1.638	0.946	0.0895	0.077			0.080	*
141-1	1.470	3.891	0.494	1.646	0.880	0.0895	0.076			0.086	*
$\frac{M}{N} = 5.0$											
142-1	1.998	3.949	4.899	0.204	1.120	0.0059	0.110	0.076	0.392	0.068	*
142-2	0.885	4.023	4.854	0.119	0.657	0.0024	0.119			0.116	*
142-3	1.507	3.975	4.882	0.169	0.932	0.0043	0.114			0.082	*
143-1	1.920	3.969	1.629	0.596	1.086	0.0295	0.106			0.070	*
144-1	1.569	3.971	1.419	0.598	0.947	0.0296	0.103			0.080	*
145-1	1.061	3.996	1.090	0.600	0.729	0.0302	0.103			0.104	*
146-1	1.671	3.950	0.819	1.081	0.972	0.0601	0.090			0.078	*
147-1	1.384	3.945	0.722	1.082	0.859	0.0598	0.091			0.088	*
148-1	1.214	3.995	0.674	1.061	0.793	0.0599	0.098			0.096	*
149-1	1.904	3.976	0.610	1.584	1.060	0.0895	0.089			0.072	*

* RUNS IN WHICH NAPPE PROFILES WERE MEASURED.

indicate complete runs, in which the nappe shapes were measured; the remainder of the runs were made to obtain additional data on the coefficients of discharge. Weirs were constructed and tested with values of $\frac{M}{N}$ equal to 0.25, 0.50, 1.0, 2.0, 3.0, 4.0, and 5.0, see figure 30.

The X and Y coordinates were handled in the same manner as described for the overhang weirs in the preceding section. After changing the coordinates to the $\frac{X}{H_s}$ and $\frac{Y}{H_s}$ form, the runs were grouped according to their respective values of $\frac{h_a}{H_s}$, $\frac{N}{H_s}$, and $\frac{M}{N}$, as shown in table 32. In this case both $\frac{h_a}{H_s}$ and $\frac{M}{N}$ were held constant for a given set of curves, with $\frac{N}{H_s}$ as a variable. In other words, for $\frac{M}{N}=1.0$ and $\frac{h_a}{H_s}=0.002$, a set of curves was obtained which varied with value of $\frac{N}{H_s}$. A second, third, fourth, and fifth set were obtained for $\frac{M}{N}=1.0$ with $\frac{h_a}{H_s}$ equal to 0.03, 0.06, 0.09, and 0.12, respectively. The same procedure was repeated for $\frac{M}{N}$ equal to 2.0, and for $\frac{M}{N}$ equal to 0.25, 0.50, 3.0, 4.0, and 5.0, except that in the latter cases the set for $\frac{h_a}{H_s}$ equal to 0.12 was omitted. Altogether, 30 sets of curves were thus made, which is evident from table 32. As many as three weirs of different dimensions, but having the same value of $\frac{M}{N}$, were tested to obtain data for one set of curves. This was primarily to make certain that the similitude relationships could be correlated on this type of weir.

After the data had been prepared as described above, it was found, as in the case of the overhang weir, that the nappe shapes varied only slightly with the value of $\frac{N}{H_s}$ for the ranges traversed in these tests. It was therefore decided to drop the variable $\frac{N}{H_s}$ and combine the nappe shapes, using only the criteria $\frac{M}{N}$ and $\frac{h_a}{H_s}$. In other words, each of the 30 sets of curves described above was replaced by a single average curve, thus leaving only 30 curves to tabulate instead of 30 sets of curves, a tremendous step in simplification of the process.

TABLE 32.—COMBINING NAPPE SHAPES—WEIRS WITH 45° OFFSET AND RISERS

TEST	H_s, FEET	$\frac{h_a}{H_s}$	M, FEET	N, FEET	ACTUAL $\frac{N}{H_s}$	PLOTTED $\frac{N}{H_s}$
$\frac{M}{N}$ = 0.25						
$\frac{h_a}{H_s}$ = 0.002						
94-1	1.096	0.0060	0.079	0.310	0.283	0.280
94-2	0.719	0.0029	0.079	0.310	0.431	0.280
94-3	0.638	0.0023	0.079	0.310	0.486	0.480
$\frac{h_a}{H_s}$ = 0.03						
96-2	0.723	0.0296	0.079	0.310	0.429	0.430
98-1	0.657	0.0301	0.079	0.310	0.472	0.470
$\frac{h_a}{H_s}$ = 0.06						
97-3	1.021	0.0525	0.079	0.310	0.304	0.300
100-1	0.752	0.0618	0.079	0.310	0.412	0.400
$\frac{h_a}{H_s}$ = 0.09						
99-3	0.835	0.0901	0.079	0.310	0.371	0.370
$\frac{M}{N}$ = 0.50						
$\frac{h_a}{H_s}$ = 0.002						
70-1	0.986	0.0046	0.079	0.156	0.158	0.160
70-2	0.716	0.0026	0.079	0.156	0.218	0.160
101-2	0.728	0.0032	0.155	0.310	0.426	0.160
101-3	0.610	0.0025	0.155	0.310	0.508	0.500
$\frac{h_a}{H_s}$ = 0.03						
71-4	1.129	0.0308	0.079	0.156	0.138	0.140
72-4	0.725	0.0284	0.079	0.156	0.215	0.140
102-2	0.710	0.0296	0.155	0.310	0.437	0.140
103-2	0.635	0.0294	0.155	0.310	0.488	0.490
$\frac{h_a}{H_s}$ = 0.06						
73-2	1.008	0.0612	0.079	0.156	0.155	0.160
104-2	0.917	0.0604	0.155	0.310	0.338	0.160
105-2	0.743	0.0608	0.155	0.310	0.417	0.420
$\frac{h_a}{H_s}$ = 0.09						
75-2	0.999	0.0901	0.079	0.156	0.156	0.160
105-4	1.122	0.0903	0.155	0.310	0.276	0.160
106-2	1.031	0.0890	0.155	0.310	0.301	0.300

TABLE 32.—COMBINING NAPPE SHAPES—WEIRS WITH 45° OFFSET AND RISERS—Continued

TEST	H_s, FEET	$\frac{h_a}{H_s}$	M, FEET	N, FEET	ACTUAL $\frac{N}{H_s}$	PLOTTED $\frac{N}{H_s}$
$\frac{M}{N} = 1.0$						
			$\frac{h_a}{H_s} = 0.002$			
110-2	0.728	0.0036	0.079	0.076	0.104	0.100
76-2	0.972	0.0043	0.155	0.156	0.160	0.100
76-3	0.724	0.0022	0.155	0.156	0.216	0.100
107-2	0.657	0.0024	0.305	0.310	0.472	0.470
			$\frac{h_a}{H_s} = 0.03$			
111-2	0.741	0.0308	0.079	0.076	0.103	0.100
77-3	1.121	0.0306	0.155	0.156	0.139	0.100
108-2	0.697	0.0303	0.305	0.310	0.445	0.450
			$\frac{h_a}{H_s} = 0.06$			
112-2	0.891	0.0609	0.079	0.076	0.085	0.080
78-3	1.008	0.0604	0.155	0.156	0.155	0.080
109-2	0.863	0.0601	0.305	0.310	0.359	0.360
			$\frac{h_a}{H_s} = 0.09$			
113-3	0.924	0.0896	0.079	0.076	0.082	0.080
115-2	0.704	0.0914	0.079	0.076	0.108	0.080
79-3	1.013	0.0895	0.155	0.156	0.154	0.080
109-4	1.172	0.0810	0.305	0.310	0.265	0.270
			$\frac{h_a}{H_s} = 0.12$			
115-A	0.979	0.1198	0.079	0.076	0.078	0.080
115-B	0.815	0.1201	0.079	0.076	0.093	0.080
115-C	0.733	0.1206	0.079	0.076	0.104	0.100
$\frac{M}{N} = 2.0$						
			$\frac{h_a}{H_s} = 0.002$			
116-3	0.693	0.0030	0.155	0.076	0.110	0.110
80-2	1.088	0.0059	0.305	0.156	0.143	0.110
80-3	0.933	0.0049	0.305	0.156	0.167	0.170
			$\frac{h_a}{H_s} = 0.03$			
117-2	0.690	0.0296	0.155	0.076	0.110	0.110
81-2	1.122	0.0313	0.305	0.156	0.139	0.110
82-2	0.718	0.0301	0.305	0.156	0.217	0.220
			$\frac{h_a}{H_s} = 0.06$			
118-2	0.852	0.0598	0.155	0.076	0.089	0.090
83-3	0.988	0.0604	0.305	0.156	0.158	0.090
84-4	0.854	0.0598	0.305	0.156	0.183	0.180
			$\frac{h_a}{H_s} = 0.09$			
119-2	0.800	0.0904	0.155	0.076	0.095	0.090
120-2	0.687	0.0903	0.155	0.076	0.111	0.090
85-6	1.046	0.0908	0.305	0.156	0.149	0.150
			$\frac{h_a}{H_s} = 0.12$			
120-A	0.991	0.1194	0.155	0.076	0.077	0.080
120-B	0.887	0.1203	0.155	0.076	0.086	0.090

TABLE 32.—COMBINING NAPPE SHAPES—WEIRS WITH 45° OFFSET AND RISERS—Continued

TEST	H_S, FEET	$\frac{h_a}{H_S}$	M, FEET	N, FEET	ACTUAL $\frac{N}{H_S}$	PLOTTED $\frac{N}{H_S}$
$\frac{M}{N} = 3.0$						
			$\frac{h_a}{H_S} = 0.002$			
121-3	1.129	0.0072	0.233	0.076	0.067	0.070
121-2	0.946	0.0054	0.233	0.076	0.080	0.070
121-1	0.667	0.0030	0.233	0.076	0.114	0.110
			$\frac{h_a}{H_S} = 0.03$			
123-1	1.092	0.0298	0.233	0.076	0.070	0.070
124-1	0.947	0.0322	0.233	0.076	0.080	0.070
125-1	0.728	0.0305	0.233	0.076	0.104	0.100
			$\frac{h_a}{H_S} = 0.06$			
126-1	0.976	0.0603	0.233	0.076	0.078	0.080
127-1	0.863	0.0607	0.233	0.076	0.088	0.080
128-1	0.793	0.0609	0.233	0.076	0.096	0.100
			$\frac{h_a}{H_S} = 0.09$			
129-1	1.053	0.0928	0.233	0.076	0.072	0.070
130-1	0.947	0.0913	0.233	0.076	0.080	0.070
131-1	0.729	0.0907	0.233	0.076	0.104	0.100
$\frac{M}{N} = 4.0$						
			$\frac{h_a}{H_S} = 0.002$			
132-1	1.113	0.0060	0.305	0.076	0.068	0.070
132-3	0.929	0.0044	0.305	0.076	0.082	0.070
132-2	0.726	0.0029	0.305	0.076	0.105	0.100
			$\frac{h_a}{H_S} = 0.03$			
133-1	1.090	0.0296	0.305	0.076	0.070	0.070
134-1	0.950	0.0297	0.305	0.076	0.080	0.070
135-1	0.736	0.0302	0.305	0.076	0.103	0.100
			$\frac{h_a}{H_S} = 0.06$			
136-1	0.969	0.0603	0.305	0.076	0.078	0.080
137-1	0.853	0.0603	0.305	0.076	0.089	0.080
138-1	0.792	0.0601	0.305	0.076	0.096	0.100
			$\frac{h_a}{H_S} = 0.09$			
139-1	1.036	0.0903	0.305	0.076	0.073	0.070
140-1	0.946	0.0895	0.305	0.076	0.080	0.070
141-1	0.880	0.0895	0.305	0.076	0.086	0.090

TABLE 32.—COMBINING NAPPE SHAPES—WEIRS WITH 45° OFFSET AND RISERS—Continued

$\frac{M}{N} = 5.0$						
TEST	H_s, FEET	$\frac{h_a}{H_s}$	M, FEET	N, FEET	ACTUAL $\frac{N}{H_s}$	PLOTTED $\frac{N}{H_s}$
			$\frac{h_a}{H_s}=0.002$			
142-1	1.120	0.0059	0.392	0.076	0.068	0.070
142-3	0.932	0.0043	0.392	0.076	0.082	0.070
142-2	0.657	0.0024	0 392	0.076	0.116	0.120
			$\frac{h_a}{H_s}=0.003$			
143-1	1.086	0.0295	0.392	0.076	0.070	0.070
144-1	0.947	0.0296	0.392	0.076	0.080	0.070
145-1	0.729	0.0302	0.392	0.076	0.104	0.100
			$\frac{h_a}{H_s}=0.06$			
146-1	0.972	0.0601	0.392	0.076	0.078	0.080
147-1	0.859	0.0598	0.392	0.076	0.088	0.080
148-1	0.793	0.0599	0.392	0.076	0.096	0.100
			$\frac{h_a}{H_s}=0.09$			
149-1	1.060	0.0895	0.392	0.076	0.072	0.070

The new curves were then combined into seven new sets, with the value $\frac{h_a}{H_s}$ as the variable in each. The result was a separate set of nappe-shape profiles, in terms of unit head, for $\frac{M}{N}$=0.25, 0.50, 1.0, 2.0, 3.0, 4.0, and 5.0. A comparison showed that these seven sets of curves were practically coincident with one another except for the set obtained for $\frac{M}{N}$=0.25, which was erratic, due undoubtedly to unstable flow conditions. Thus the remaining six sets of curves were reduced to a single set applicable to all offset weirs with risers falling within the range of these experiments.

It was anticipated during the planning of the test program that the results from the weir for $\frac{M}{N}$ equal to 5.0 would very nearly approach those for the vertical-face weir. This was apparently the case in the region between the weir crest and the high point of the nappe, but did not hold true farther downstream. From the high point of the lower nappe downstream, the profiles from the offset weirs fell con-

TABLE 33.—COORDINATES OF LOWER NAPPE FOR DIFFERENT VALUES OF $\frac{h_a}{H_s}$—OFFSET WEIRS

	Y/Hs												
ha/Hs X/Hs	0.002	0.010	0.020	0.030	0.040	0.050	0.060	0.070	0.080	0.090	0.100	0.120	0.140
0.000	0.000	0.000	0.000	0.000	0.000	0.000	0.000	0.000	0.000	0.000	0.000	0.000	0.000
0.010	0.017	0.016	0.016	0.015	0.014	0.014	0.013	0.012	0.012	0.011	0.010	0.009	0.008
0.020	0.029	0.028	0.027	0.026	0.026	0.025	0.025	0.024	0.022	0.021	0.020	0.017	0.014
0.030	0.041	0.040	0.038	0.037	0.035	0.034	0.033	0.032	0.031	0.030	0.028	0.024	0.020
0.040	0.050	0.049	0.047	0.045	0.043	0.042	0.041	0.040	0.039	0.037	0.035	0.030	0.025
0.050	0.059	0.057	0.055	0.053	0.052	0.050	0.049	0.048	0.046	0.044	0.041	0.035	0.029
0.060	0.066	0.063	0.061	0.059	0.057	0.056	0.055	0.053	0.051	0.049	0.046	0.039	0.032
0.070	0.072	0.069	0.067	0.065	0.063	0.061	0.060	0.058	0.056	0.054	0.050	0.043	0.035
0.080	0.077	0.074	0.072	0.070	0.068	0.066	0.064	0.062	0.060	0.058	0.054	0.046	0.038
0.090	0.082	0.079	0.077	0.075	0.073	0.070	0.068	0.066	0.064	0.061	0.057	0.049	0.041
0.100	0.087	0.085	0.082	0.079	0.077	0.074	0.071	0.069	0.067	0.064	0.060	0.051	0.042
0.110	0.091	0.088	0.085	0.082	0.079	0.076	0.074	0.072	0.069	0.066	0.062	0.053	0.044
0.120	0.095	0.092	0.089	0.086	0.083	0.080	0.076	0.074	0.071	0.069	0.064	0.054	0.044
0.130	0.098	0.095	0.092	0.089	0.086	0.083	0.079	0.076	0.073	0.070	0.065	0.055	0.045
0.140	0.100	0.097	0.094	0.091	0.088	0.085	0.081	0.078	0.075	0.072	0.067	0.056	0.045
0.150	0.102	0.099	0.096	0.093	0.089	0.086	0.083	0.080	0.077	0.073	0.068	0.057	0.046
0.160	0.105	0.102	0.098	0.095	0.092	0.088	0.084	0.080	0.076	0.073	0.068	0.057	0.046
0.170	0.106	0.103	0.099	0.096	0.093	0.089	0.086	0.082	0.078	0.074	0.069	0.058	0.047
0.180	0.108	0.105	0.101	0.097	0.094	0.091	0.087	0.083	0.079	0.074	0.069	0.058	0.047
0.190	0.109	0.106	0.102	0.098	0.095	0.092	0.088	0.084	0.080	0.075	0.069	0.058	0.047
0.200	0.110	0.107	0.103	0.099	0.095	0.091	0.088	0.084	0.080	0.075	0.069	0.058	0.047
0.210	0.111	0.108	0.104	0.100	0.096	0.092	0.088	0.083	0.078	0.074	0.068	0.057	0.046
0.220	0.112	0.109	0.105	0.101	0.096	0.092	0.088	0.083	0.078	0.074	0.068	0.057	0.046
0.230	0.113	0.109	0.105	0.101	0.096	0.092	0.088	0.083	0.078	0.074	0.068	0.056	0.044
0.240	0.113	0.109	0.105	0.100	0.095	0.091	0.087	0.082	0.077	0.073	0.067	0.055	0.043
0.250	0.114	0.110	0.105	0.100	0.095	0.091	0.087	0.082	0.077	0.072	0.066	0.054	0.042
0.260	0.114	0.110	0.105	0.100	0.096	0.091	0.086	0.081	0.076	0.071	0.065	0.053	0.041
0.270	0.114	0.109	0.104	0.099	0.095	0.090	0.085	0.080	0.075	0.070	0.064	0.052	0.040
0.280	0.113	0.109	0.104	0.099	0.094	0.089	0.084	0.079	0.074	0.069	0.063	0.051	0.039
0.290	0.112	0.108	0.103	0.098	0.093	0.088	0.083	0.078	0.073	0.068	0.062	0.049	0.036
0.300	0.112	0.107	0.102	0.097	0.092	0.087	0.082	0.077	0.072	0.066	0.060	0.047	0.034
0.310	0.111	0.106	0.101	0.096	0.091	0.085	0.080	0.075	0.070	0.065	0.059	0.046	0.033
0.320	0.110	0.105	0.100	0.095	0.089	0.083	0.078	0.073	0.068	0.063	0.057	0.044	0.031
0.330	0.109	0.103	0.098	0.093	0.087	0.081	0.076	0.071	0.066	0.061	0.055	0.042	0.029
0.340	0.107	0.102	0.097	0.092	0.086	0.080	0.074	0.069	0.064	0.060	0.053	0.040	0.027

TABLE 33.—COORDINATES OF LOWER NAPPE FOR DIFFERENT VALUES OF $\frac{h_a}{H_s}$—OFFSET WEIRS—Continued

h_a/H_s \ X/H_s	Y/H_s												
	0.002	0.010	0.020	0.030	0.040	0.050	0.060	0.070	0.080	0.090	0.100	0.120	0.140
0.350	0.106	0.100	0.095	0.090	0.084	0.078	0.072	0.067	0.062	0.057	0.051	0.038	0.025
0.360	0.104	0.098	0.093	0.088	0.083	0.077	0.071	0.066	0.061	0.056	0.049	0.036	0.023
0.370	0.103	0.098	0.092	0.086	0.080	0.074	0.068	0.063	0.058	0.053	0.047	0.034	0.021
0.380	0.101	0.096	0.090	0.084	0.078	0.072	0.066	0.061	0.056	0.051	0.044	0.031	0.018
0.390	0.099	0.094	0.088	0.082	0.076	0.070	0.064	0.059	0.054	0.049	0.042	0.029	0.016
0.400	0.096	0.090	0.085	0.080	0.074	0.068	0.062	0.056	0.051	0.046	0.039	0.025	0.011
0.410	0.094	0.089	0.083	0.077	0.071	0.065	0.059	0.054	0.049	0.043	0.037	0.024	0.011
0.420	0.092	0.087	0.081	0.075	0.069	0.063	0.057	0.052	0.047	0.041	0.034	0.021	0.008
0.430	0.088	0.082	0.077	0.072	0.066	0.060	0.054	0.049	0.044	0.038	0.031	0.018	0.005
0.440	0.086	0.080	0.075	0.070	0.063	0.057	0.051	0.046	0.041	0.035	0.028	0.015	0.002
0.450	0.083	0.077	0.072	0.067	0.060	0.054	0.048	0.043	0.038	0.032	0.025	0.012	−0.001
0.460	0.080	0.075	0.070	0.064	0.057	0.051	0.045	0.040	0.035	0.029	0.022	0.009	−0.004
0.470	0.077	0.072	0.065	0.060	0.054	0.048	0.042	0.037	0.032	0.026	0.019	0.006	−0.007
0.480	0.074	0.069	0.063	0.057	0.051	0.045	0.039	0.034	0.028	0.022	0.016	0.003	−0.009
0.490	0.071	0.066	0.060	0.054	0.047	0.041	0.035	0.030	0.025	0.019	0.012	−0.001	−0.014
0.500	0.068	0.063	0.057	0.051	0.045	0.039	0.032	0.026	0.020	0.015	0.008	−0.005	−0.018
0.520	0.060	0.054	0.049	0.044	0.037	0.031	0.025	0.019	0.013	0.007	0.000	−0.012	−0.024
0.540	0.053	0.048	0.043	0.038	0.031	0.024	0.017	0.011	0.005	−0.001	−0.008	−0.020	−0.032
0.560	0.045	0.040	0.034	0.028	0.022	0.016	0.009	0.003	−0.003	−0.009	−0.015	−0.028	−0.041
0.580	0.036	0.031	0.025	0.019	0.013	0.006	0.000	−0.006	−0.012	−0.018	−0.024	−0.037	−0.050
0.600	0.027	0.022	0.016	0.010	0.003	−0.003	−0.009	−0.015	−0.021	−0.027	−0.033	−0.046	−0.059
0.620	0.018	0.013	0.007	0.001	−0.006	−0.012	−0.018	−0.024	−0.030	−0.037	−0.043	−0.056	−0.069
0.640	0.008	0.003	−0.003	−0.009	−0.016	−0.022	−0.028	−0.034	−0.040	−0.047	−0.053	−0.066	−0.079
0.660	−0.002	−0.008	−0.014	−0.019	−0.025	−0.032	−0.039	−0.045	−0.051	−0.058	−0.064	−0.076	−0.088
0.680	−0.012	−0.018	−0.024	−0.030	−0.037	−0.043	−0.049	−0.055	−0.061	−0.068	−0.074	−0.087	−0.100
0.700	−0.023	−0.029	−0.035	−0.041	−0.048	−0.055	−0.061	−0.067	−0.073	−0.079	−0.085	−0.098	−0.111
0.720	−0.034	−0.040	−0.046	−0.053	−0.059	−0.065	−0.072	−0.078	−0.084	−0.090	−0.096	−0.109	−0.122
0.740	−0.045	−0.051	−0.057	−0.064	−0.071	−0.078	−0.084	−0.090	−0.096	−0.102	−0.108	−0.121	−0.134
0.760	−0.057	−0.064	−0.071	−0.078	−0.084	−0.090	−0.096	−0.102	−0.108	−0.114	−0.120	−0.133	−0.146
0.780	−0.069	−0.076	−0.083	−0.089	−0.095	−0.102	−0.108	−0.114	−0.120	−0.126	−0.132	−0.145	−0.158
0.800	−0.082	−0.089	−0.096	−0.102	−0.109	−0.116	−0.122	−0.128	−0.134	−0.140	−0.146	−0.158	−0.170
0.820	−0.094	−0.101	−0.108	−0.115	−0.121	−0.128	−0.134	−0.140	−0.146	−0.153	−0.159	−0.171	−0.193
0.840	−0.107	−0.114	−0.121	−0.128	−0.134	−0.140	−0.147	−0.154	−0.161	−0.167	−0.173	−0.184	−0.195
0.860	−0.121	−0.128	−0.135	−0.141	−0.148	−0.155	−0.161	−0.168	−0.175	−0.181	−0.187	−0.198	−0.209
0.880	−0.135	−0.142	−0.149	−0.155	−0.162	−0.169	−0.175	−0.182	−0.189	−0.195	−0.200	−0.211	−0.222

TABLE 33.—COORDINATES OF LOWER NAPPE FOR DIFFERENT VALUES OF $\frac{h_a}{H_s}$—OFFSET WEIRS—Continued

	Y/H_s												
X/H_s \ h_a/H_s	0.002	0.010	0.020	0.030	0.040	0.050	0.060	0.070	0.080	0.090	0.100	0.120	0.140
0.900	-0.150	-0.156	-0.162	-0.169	-0.176	-0.183	-0.190	-0.197	-0.204	-0.210	-0.215	-0.225	-0.235
0.920	-0.164	-0.171	-0.178	-0.184	-0.191	-0.198	-0.204	-0.211	-0.218	-0.225	-0.230	-0.240	-0.250
0.940	-0.179	-0.186	-0.193	-0.199	-0.206	-0.213	-0.219	-0.226	-0.233	-0.240	-0.245	-0.254	-0.263
0.960	-0.195	-0.201	-0.207	-0.214	-0.221	-0.228	-0.235	-0.242	-0.249	-0.255	-0.260	-0.269	-0.278
0.980	-0.210	-0.217	-0.224	-0.230	-0.237	-0.244	-0.250	-0.257	-0.264	-0.271	-0.275	-0.284	-0.293
1.000	-0.226	-0.233	-0.240	-0.246	-0.253	-0.260	-0.267	-0.273	-0.279	-0.286	-0.291	-0.300	-0.309
1.050	-0.268	-0.274	-0.280	-0.287	-0.294	-0.301	-0.308	-0.315	-0.322	-0.328	-0.332	-0.341	-0.350
1.100	-0.311	-0.318	-0.325	-0.331	-0.338	-0.345	-0.351	-0.358	-0.365	-0.371	-0.375	-0.383	-0.391
1.150	-0.355	-0.362	-0.369	-0.376	-0.383	-0.390	-0.396	-0.402	-0.408	-0.415	-0.419	-0.427	-0.435
1.200	-0.404	-0.411	-0.418	-0.424	-0.430	-0.437	-0.443	-0.449	-0.455	-0.461	-0.465	-0.474	-0.483
1.250	-0.453	-0.460	-0.467	-0.473	-0.480	-0.486	-0.493	-0.498	-0.503	-0.509	-0.513	-0.521	-0.529
1.300	-0.506	-0.513	-0.518	-0.524	-0.531	-0.538	-0.545	-0.550	-0.555	-0.559	-0.563	-0.572	-0.581
1.350	-0.560	-0.566	-0.572	-0.578	-0.585	-0.592	-0.598	-0.602	-0.606	-0.611	-0.615	-0.623	-0.631
1.400	-0.617	-0.623	-0.629	-0.634	-0.640	-0.646	-0.652	-0.657	-0.662	-0.666	-0.669	-0.676	-0.683
1.450	-0.677	-0.682	-0.687	-0.692	-0.698	-0.703	-0.709	-0.713	-0.717	-0.721	-0.724	-0.731	-0.738
1.500	-0.739	-0.743	-0.747	-0.752	-0.757	-0.762	-0.767	-0.771	-0.775	-0.779	-0.782	-0.787	-0.792
1.550	-0.802	-0.806	-0.810	-0.815	-0.819	-0.823	-0.827	-0.831	-0.835	-0.839	-0.840	-0.843	-0.846
1.600	-0.868	-0.871	-0.874	-0.878	-0.882	-0.886	-0.890	-0.893	-0.897	-0.900	-0.900	-0.900	-0.900
1.650	-0.933	-0.936	-0.939	-0.943	-0.948	-0.953	-0.957	-0.859	-0.861	-0.963	-0.962	-0.960	-0.958
1.700	-1.002	-1.004	-1.006	-1.009	-1.013	-1.017	-1.021	-1.023	-1.025	-1.027	-1.025	-1.021	-1.017
1.750	-1.073	-1.075	-1.077	-1.080	-1.083	-1.086	-1.089	-1.090	-1.091	-1.092	-1.090	-1.085	-1.080
1.800	-1.148	-1.150	-1.152	-1.154	-1.156	-1.158	-1.160	-1.160	-1.160	-1.160	-1.157	-1.150	-1.143
1.850	-1.228	-1.229	-1.230	-1.231	-1.231	-1.231	-1.231	-1.231	-1.231	-1.231	-1.228	-1.221	-1.214
1.900	-1.308	-1.308	-1.308	-1.308	-1.308	-1.309	-1.309	-1.307	-1.305	-1.304	-1.300	-1.293	-1.286
1.950	-1.392	-1.392	-1.392	-1.392	-1.390	-1.388	-1.385	-1.383	-1.381	-1.379	-1.375	-1.368	-1.361
2.000	-1.479	-1.477	-1.475	-1.474	-1.470	-1.467	-1.464	-1.461	-1.458	-1.455	-1.452	-1.445	-1.438
2.050	-1.564	-1.563	-1.561	-1.559	-1.556	-1.552	-1.548	-1.544	-1.539	-1.534	-1.531	-1.524	-1.517
2.100	-1.651	-1.649	-1.647	-1.644	-1.639	-1.635	-1.631	-1.626	-1.621	-1.616	-1.612	1.603	-1.594
2.150	-1.739	-1.736	-1.733	-1.730	-1.725	-1.720	-1.715	1.710	-1.705	-1.700	-1.695	-1.686	-1.677
2.200	-1.830	-1.826	-1.822	-1.817	-1.812	-1.807	-1.802	-1.897	-1.791	-1.785	-1.780	-1.770	-1.760

sistently inside of those obtained from the vertical weir. An explanation for this deviation is given in the following section.

The final $\frac{X}{H_s}$ and $\frac{Y}{H_s}$ coordinates of the lower nappe shape for offset weirs with values of $\frac{M}{N}$ ranging from 0.50 to 5.0 are tabulated in table 33. This range includes most of the practical shapes that will occur on this type of overflow section. Sections for which the value of $\frac{M}{N}$ falls between 0.0 and 0.5 are not recommended.

A table of coordinates for the upper nappe surface has not been prepared for the offset weirs. Instead, it is recommended that table 18, for the vertical-face weir, be used. There is little difference between the two, and, because of irregularities of flow on the overhang and offset weirs, greater accuracy in the selection of the upper-nappe-surface coordinates is not warranted.

36. Flow Characteristics of Overhang and Offset-Type Weirs.—It was observed during the experiments on the vertical weir and the three weirs sloping downstream, that the lower nappe surface was very smooth and had a glassy appearance, during runs in which the head was not excessive or the approach channel too shallow. No vortices or disturbances of any consequence were noticed upstream, which, with favorable current-meter measurements, would indicate that approach conditions were satisfactory. As the head became excessive and the channel floor approached the level of the weir crest, critical flow in the channel caused undulating waves; the entire sheet of water springing from the weir fluctuated periodically and the glassy nappe surfaces disappeared. Head-gage readings were no longer accurate, and nappe-profile measurements could not be correlated with previous data. Therefore, the recorded experimental data were confined to the region of stable flow.

The nappe surfaces produced by the overhang and offset weirs, on the other hand, were in some cases smooth but never glassy. In every instance, spiraling *ropes* played back and forth across the weir, making it difficult to measure the lower surface. These disturbances were small and formed only occasionally for the lower heads, but were proportionately larger and greater in number for the greater discharges. They formed at the weir and broke a short distance downstream, spraying the man operating the lower coordinometer.

Flow conditions for the overhang and offset weirs were in another respect the opposite to those encountered on the vertical weir and weirs sloping downstream. Flow for the vertical and sloping weirs was steadier for deep approach conditions than for shallow approach depths; on the contrary, the flow for the overhang and offset weirs, although never comparing in steadiness with that from the vertical weir or weirs sloping downstream, was rougher and more unstable for the deeper approach conditions than with the floor raised in the proximity of the weir crest.

At first it was surmised that the spiraling ropes on the lower nappe surface were caused by the water not following the upstream face of the weir but skipping at the upper corner of the offset. This supposition, however, was soon disproved by measurements of the pressures on the upstream face. Pressures at the upper corner were less than those on the flatter portions of the weir, but the differences were not sufficient to indicate skipping. The results of the pressure measurements on the upstream face of these weirs are discussed in section 39. Two other factors which tend to prove that lowered pressures on the upstream face were not responsible for the disturbance are: first, the same rough flow conditions existed on weirs with both high and low risers; and second, little improvement, if any, was noticeable for the overhang weirs, which were without risers.

Another explanation for the rough flow from the overhang and offset weirs lies in the turbulence created in the approach channel. Long, slim vortices intermittently formed and broke near each end of the weir. These formed in the approach channel, extended up into the sheet of water passing over the weir, and usually broke a short distance downstream from the weir. These vortices, however, appeared to be independent of the ropes on the lower surface of the nappe. Rouse [20] noted the same vortices on a vertical weir, and his explanation is:

> In the case of very abrupt changes in direction in conduits of rectangular cross section, the combined effect of separation and secondary spiral motion may give rise to an intense, intermittent vortex motion in each of the outer corners. While the existence of a free surface is not essential to this phenomenon, similar effects may be observed directly upstream from a sluice gate or weir. The reduction in velocity due to drag along the lower boundary produces a normal reversal of flow in the region of stagnation at the base of the weir. However, the velocity defect is more pronounced at the junction between the floor and either wall, which considerably augments the tendency toward flow reversal at the sides and leads to the formation of a vortex normal to the floor near each corner. As soon as such a vortex is established, the pressure gradient leading to its formation no longer exists, and the secondary motion abruptly ceases. Thereupon, the cycle begins once again. Since low pressures accompany the high tangential velocities, the vortex filament may be ventilated from the downstream side, a tube of air often penetrating the flow well past the plane of the weir.

Mr. Rouse includes two excellent photographs of this phenomenon in his book.

---

[20] Rouse, Hunter, Fluid Mechanics for Hydraulic Engineers, 1st ed., p. 271, McGraw-Hill Book Co. Quotation reprinted by permission.

After the vortices and rough flow on the overhang and offset weirs had been observed, these weirs were replaced with the vertical weir for the purpose of again comparing flow conditions. The glassy nappe surfaces reappeared, ropes were absent, and there were no visible signs of vortices forming in the approach channel, although it was assumed that a certain amount of turbulence must exist at each end of the weir. It is difficult to understand why a small offset or overhang projection on the upstream face of a weir with a large approach depth is sufficient to disrupt the excellent flow conditions encountered on the vertical weir. Evidently the offset or overhang greatly accentuates the occurrence of the phenomenon described by Rouse. This effect would not be as pronounced on a long spillway section as the tests on the overhang and offset weirs indicate, since the side walls are responsible for a good share of the disturbance on the weir.

From consideration of the above statements, one would not expect to obtain duplicate nappe profiles from the vertical and offset weirs, even though the value of M for the latter would be large, because (1) the roughness of the nappe surfaces of the offset weir indicates that some dissipation of energy has occurred before the water leaves the weir, and (2) the resistance of the air to the rough nappe surfaces is greater than it would be to the smoother nappe surfaces produced by the vertical weir.

The conclusion to be drawn from the above discussion is that overflow sections with plain upstream faces are conducive to stable flow conditions, whereas those with offsets and breaks in the upstream face are not, although many of the latter sections are in existence and appear to be giving satisfactory service. One point is definitely certain, spillway sections are not recommended with values of $\frac{M}{N}$ less than 0.5 unless this value is zero. For values greater than zero and less than 0.5, flow conditions are extremely unstable, as was evidenced by plotting some of the nappe profiles or observing the coefficients of discharge for $\frac{M}{N}=0.25$ in figure 31.

37. Relation of E to Velocity of Approach.—To make it possible to convert any head on the weir to the equivalent head on an overflow section, or vice versa, curves have been plotted showing the relation of $\frac{E}{H_s}$ to $\frac{h_a}{H_s}$ for the various values of $\frac{M}{N}$ tested. The actual points are shown plotted in figures 31–A and 32–A. The value of E for the overhang weir, when $\frac{M}{N}=0$, is considerably higher than that for other weirs. The value of E for the weir with $\frac{M}{N}=0.25$ appears to fall

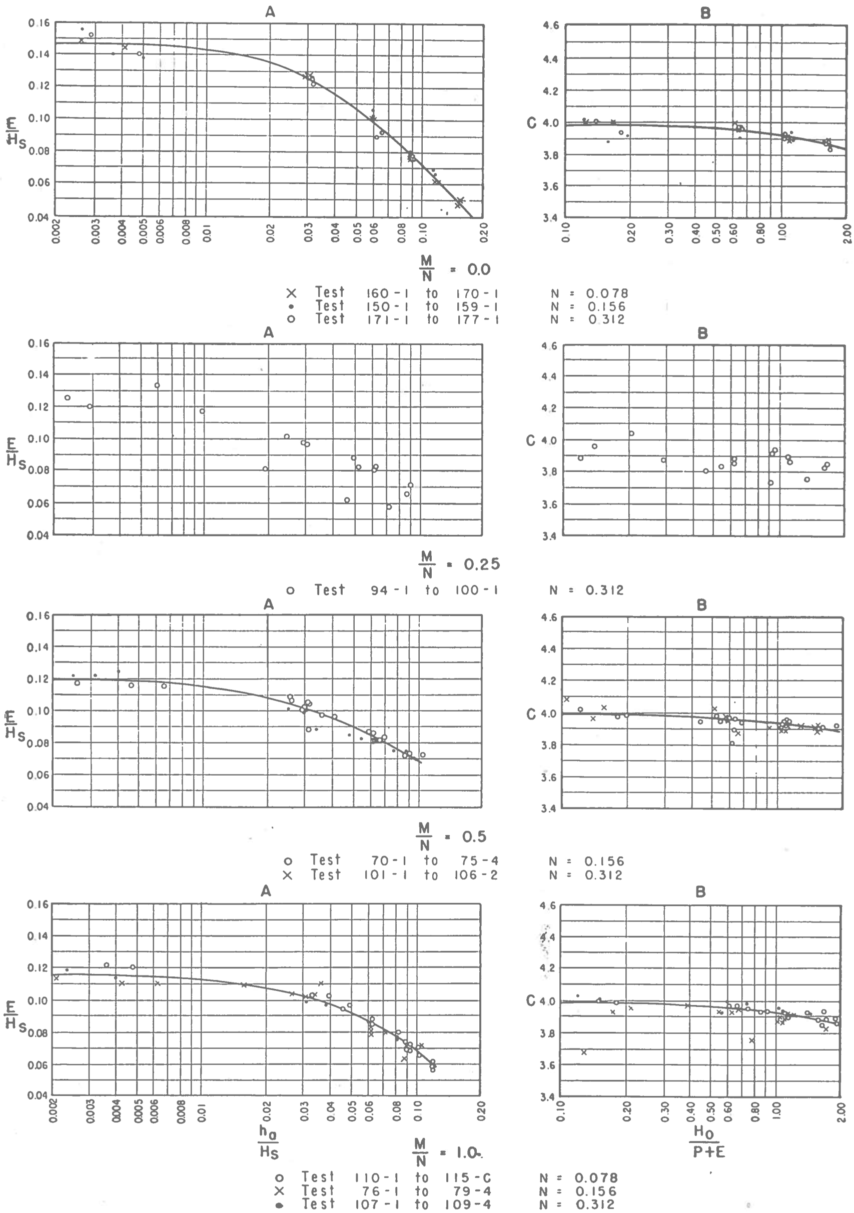

A-CURVES FOR VALUES OF E B-COEFFICIENT-OF-DISCHARGE CURVES

FIGURE 37.—VALUES OF *E* AND *C* FOR OVERHANG AND OFFSET WEIRS.

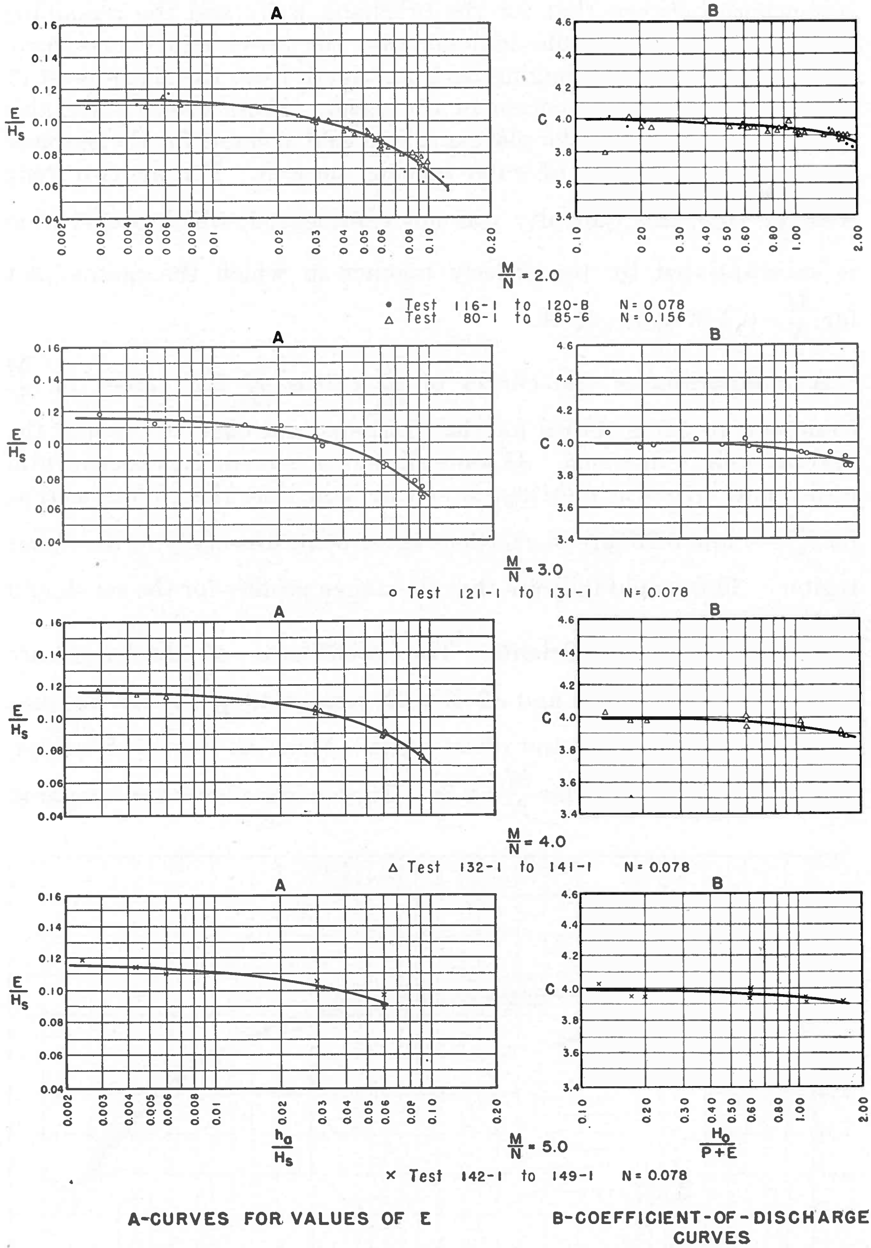

FIGURE 32.—VALUES OF *E* AND *C* FOR OFFSET WEIRS.

somewhere between that for the overhang weirs and the remaining offset weirs, which would indicate that the lower nappe may have been intermittently springing back and forth from the sharp crest of the riser to the upper corner of the offset. From observation, this action did appear to take place and it would account for the extreme instability of the sheet of water leaving the weir. For the two weirs with $\frac{M}{N}=0.5$, this difficulty was not experienced, which observation is substantiated by the orderly manner in which the points plot for $\frac{M}{N}=0.5$ in figure 31–A.

A comparison of the curves of $\frac{E}{H_s}$ versus $\frac{h_a}{H_s}$ for values of $\frac{M}{N}$ from zero to 5.0 is shown for the overhang and offset weirs and the vertical weir in figure 33. If some allowance is made for experimental errors and errors in plotting, it can be said that the curves, except for $\frac{M}{N}=0$ and 0.25, are in excellent agreement, especially in the upper region. This would indicate that the nappe profiles for the set should be the same.

38. Discharge Coefficients.—The coefficients of discharge are plotted in figures 31–B and 32–B with respect to $\frac{H_o}{P+E}$ for all runs made on the overhang and offset weirs. Here, as for the E-values, the points are scattered for $\frac{M}{N}=0.25$. These same curves are compared

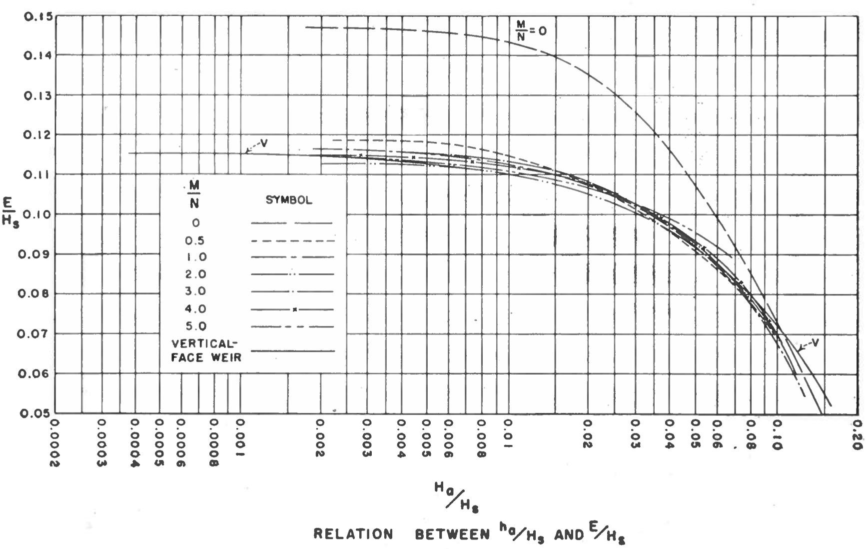

FIGURE 33.—COMPARISON OF *E* FOR VERTICAL, OVERHANG, AND OFFSET WEIRS.

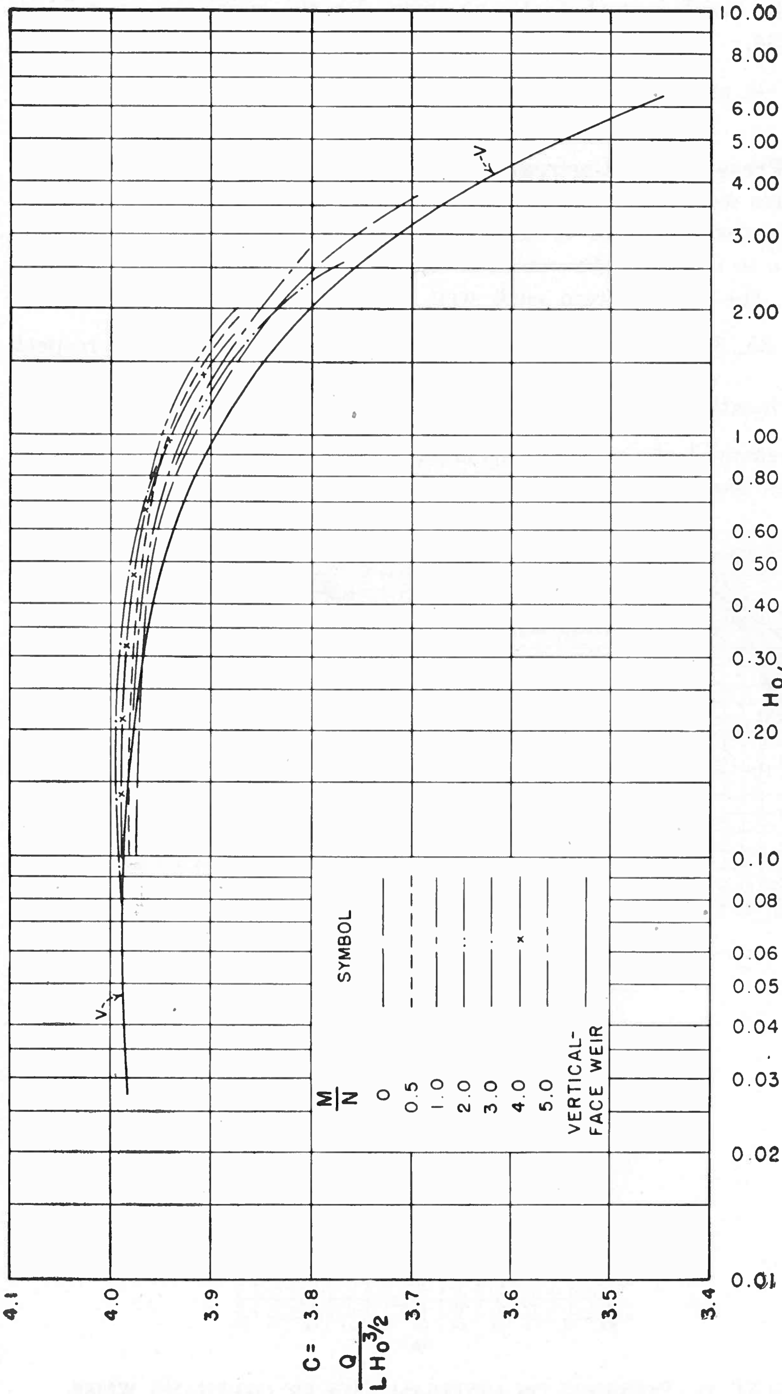

FIGURE 34.—COMPARISON OF C FOR VERTICAL, OVERHANG, AND OFFSET WEIRS.

with the coefficient-of-discharge curve for the vertical-face weir in figure 34. The coefficients for all these weirs, including the weirs for $\frac{M}{N}=0$, are practically the same, especially for the larger approach depths.

39. Pressures on Upstream Face of Overhang and Offset Weirs.—Pressures were measured normal to the upstream face of all overhang and offset weirs. Due to the variation in the weir shapes, it was not possible to combine the results in any satisfactory manner. For this reason, the results from each weir have been plotted separately in figures 35, 36, and 37. Values of $\frac{h_p}{H_s}$ have been plotted with respect to the location of the pressure measurement $\frac{d}{N}$, where h_p is the presure measured above the sharp crest of the weir and d is the distance from the sharp crest to each piezometer on the weir face.

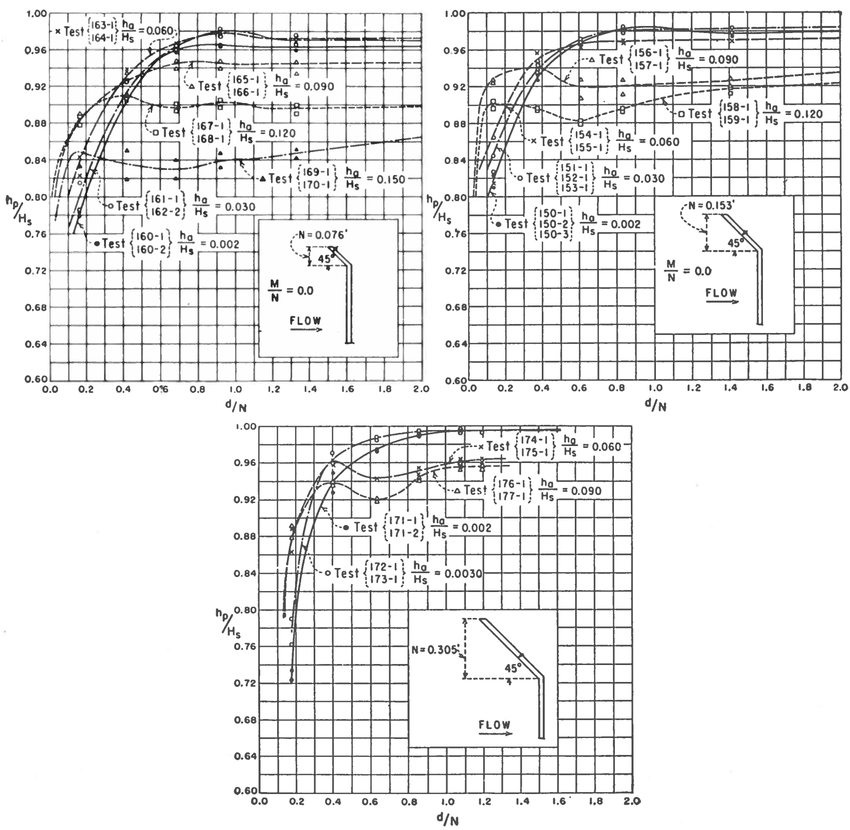

FIGURE 35.—PRESSURES ON UPSTREAM FACE OF OVERHANG WEIRS.

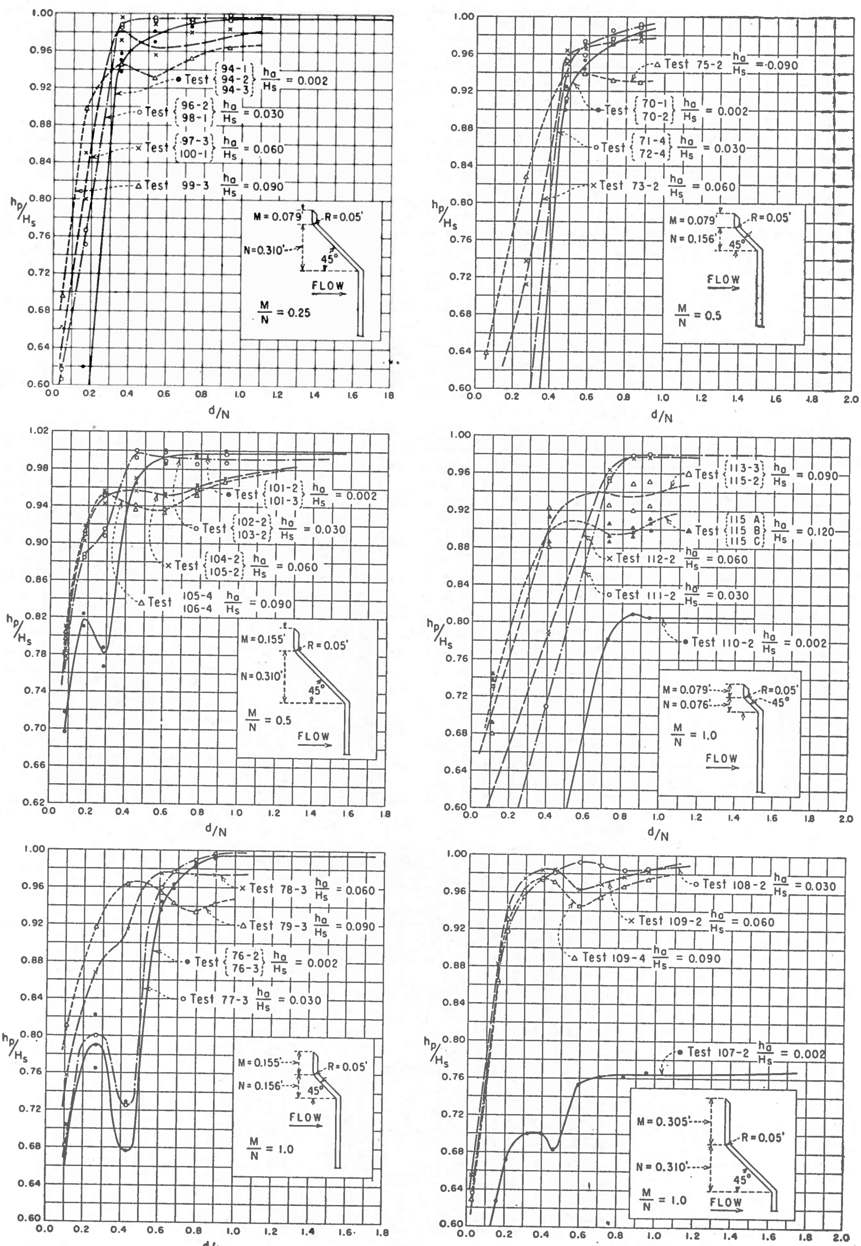

FIGURE 36.—PRESSURES ON UPSTREAM FACE OF OFFSET WEIRS.

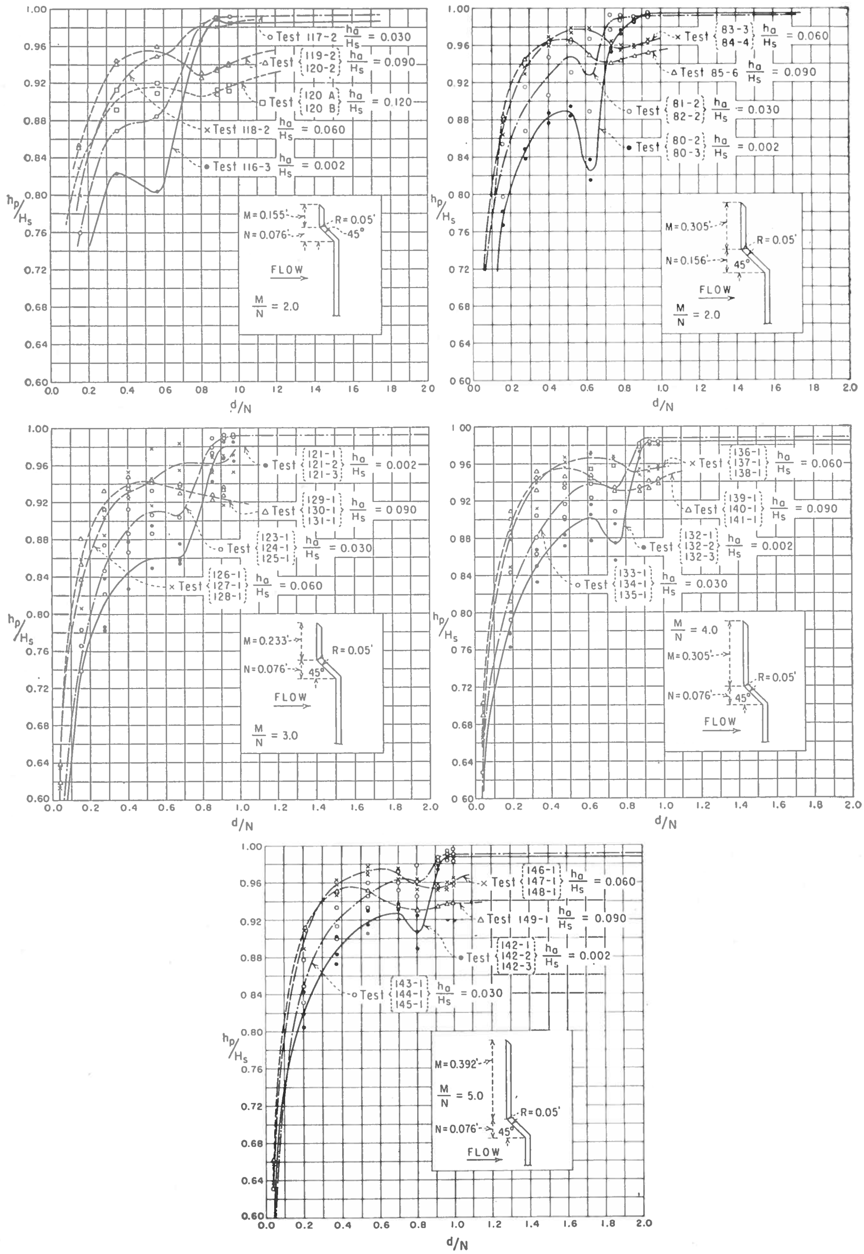

FIGURE 37.—PRESSURES ON UPSTREAM FACE OF OFFSET WEIRS.

Figure 35 shows no unusual pressure conditions on the three overhang weirs. This is also true for the offset weir with $\frac{M}{N}=0.25$, where flow conditions were unstable. The majority of the remaining offset weirs show a reduction of pressure on the face of the riser immediately above the upper corner of the offset, which reduction is most pronounced with the larger approach depths. Evidently there is very little flow up the face of the weir for the higher approach velocities.

Figures 36 and 37 indicate that the radius at the upper corner of the offset was insufficient for most of the weirs tested. It is recommended that this radius be made as long as practicable on prototype designs.

APPLICATION OF EXPERIMENTAL RESULTS

40. Design of Overflow Dam Section With Overhang on Upstream Face.—The procedure for determining the coordinates for a section with an overhang on the upstream face is the same as that used for a weir with vertical upstream face, except for the use of different tables and curves. It is advisable to confine the value of N to the range of these experiments. No difficulties are anticipated, however, even though the upper portion of the range be exceeded moderately. The solution to example 1 is repeated with an overhang on the upstream face of the dam.

> *Example 7.*—Given a maximum water surface elevation of 1,000.0 for a total discharge of 75,000 second-feet, with the average approach floor at elevation 880.0. Determine the crest elevation and coordinates for the shape of an overflow section with a crest length of 250 feet and a 45° overhang on the upstream face, the overhang having a vertical dimension of 7 feet.

In figure 34, the coefficients of discharge for the vertical and overhang weirs nearly coincide. Therefore, C will be assumed as 3.96, which was the final value obtained in example 1. Also, from the same source, $H_o=17.90$ feet and $P+E=102.10$ feet. The high point on the crest remains the same as in the first example, at elevation 982.10, and the velocity head of approach, h_a, remains at 0.097.

Also, $$\frac{h_a}{H_o}=\frac{0.097}{17.90}=0.0054.$$

From the curve for $\frac{M}{N}=0$ in figure 27,

$$\frac{H_s}{H_o}=1.1715 \text{ for the above value of } \frac{h_a}{H_o}.$$

$$H_s=1.172\times 17.90=20.98 \text{ feet.}$$

Then

$$\frac{h_a}{H_s}=\frac{0.097}{20.98}=0.0046,$$

and

$$\frac{N}{H_s}=\frac{7}{20.98}=0.334.$$

It is found by consulting table 28 that this value falls within the range of the experiments on overhang weirs. Table 34 shows the coordinates for the lower nappe surface, obtained by using the above values of H_s and $\frac{h_a}{H_s}$, and table 29, which contains experimental data for dams with an overhang on the upstream face.

TABLE 34.—COORDINATES FOR OVERHANG OVERFLOW SECTION—EXAMPLE 7

$\frac{X}{H_s}$ 1	$\frac{Y}{H_s}$ 2	X, feet 3	Y, feet 4	Y, elevation, feet 5
0. 000	0. 000	0. 00	0. 00	979. 17
0. 050	0. 0905	1. 05	1. 90	981. 07
0. 100	0. 1173	2. 10	2. 46	981. 63
0. 150	0. 1315	3. 15	2. 76	981. 93
0. 200	0. 1385	4. 20	2. 91	982. 08
0. 250	0. 1396	5. 24	2. 93	982. 10
0. 300	0. 1370	6. 29	2. 87	982. 04
0. 350	0. 1298	7. 34	2. 72	981. 89
0. 400	0. 1196	8. 39	2. 51	981. 68
0. 450	0. 1067	9. 44	2. 24	981. 41
0. 500	0. 090	10. 49	1. 89	981. 06
0. 600	0. 046	12. 59	0. 97	980. 14
0. 700	−0. 008	14. 69	−0. 17	979. 00
0. 800	−0. 069	16. 78	−1. 45	977. 72
0. 900	−0. 139	18. 88	−2. 92	976. 25
1. 000	−0. 218	20. 98	−4. 57	974. 60
1. 200	−0. 405	25. 18	−8. 50	970. 67
1. 400	−0. 631	29. 37	−13. 24	965. 93
1. 600	−0. 892	33. 57	−18. 71	960. 46
1. 800	−1. 183	37. 76	−24. 82	954. 35
2. 000	−1. 508	41. 96	−31. 64	947. 53
2. 200	−1. 863	46. 16	−39. 09	940. 08

For comparative purposes, the coordinates from table 34 have been plotted, together with those of example 1 for the vertical-face dam, in figure 38. The resulting shape for the overhang section is shown as a dotted line, while the shape for the vertical-face dam is indicated by a full line. The shapes of the two sections are considerably different, although both sections were subjected to the same head and approach conditions.

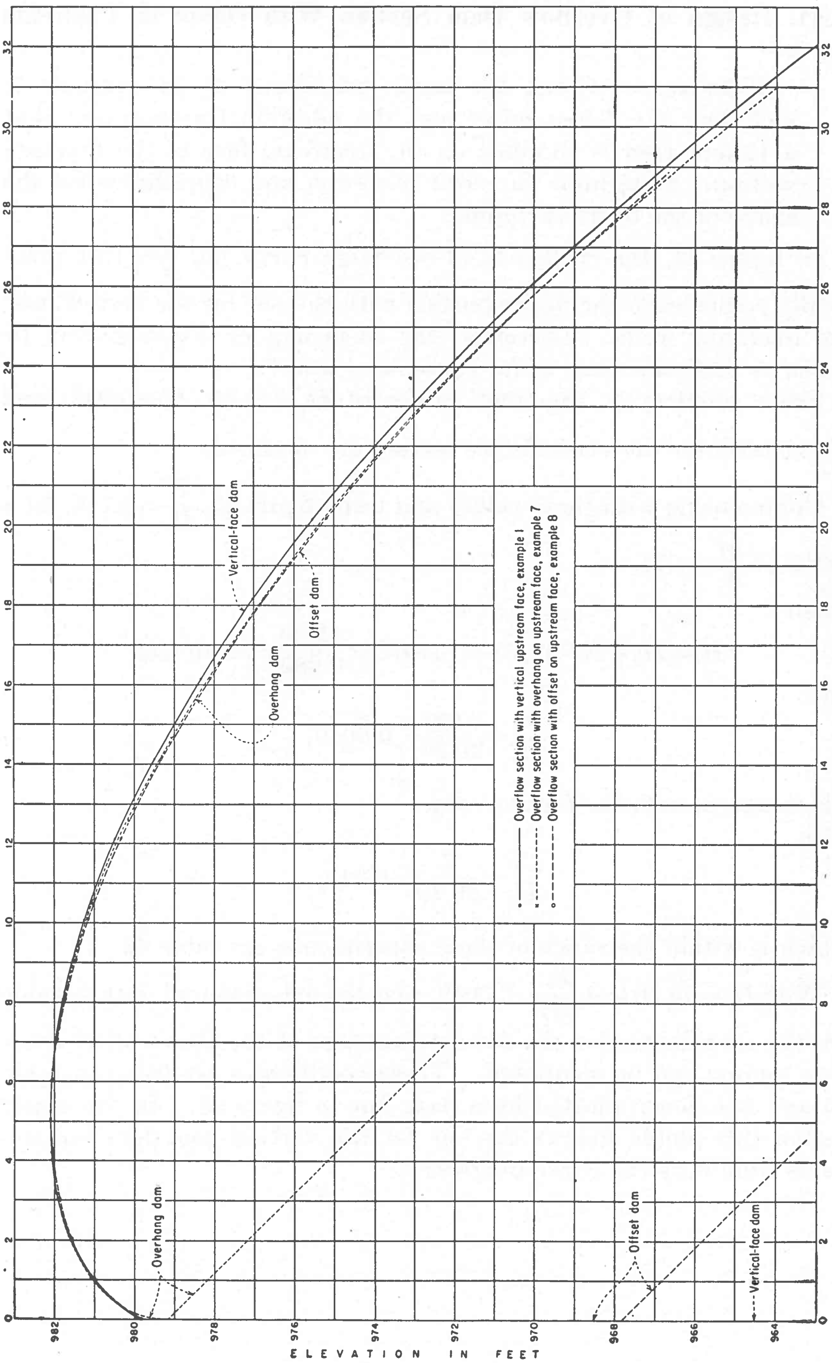

FIGURE 38.—COMPARISON OF RESULTS—EXAMPLES 1, 7, AND 8.

41. Design of Overflow Dam Section With Offset in Upstream Face.—

> *Example 8.*—Given the same conditions as in example 7, including the 7-foot offset and the additional assumption that a 12-foot riser is specified on the upstream face of the overflow section. Determine the crest elevation and coordinates for the shape of the overflow profile.

In figure 34, the coefficient-of-discharge curve for $\frac{M}{N}=1.71$ practically coincides in the upper portion with the one for the vertical and the overhang weirs. Therefore, the coefficient of discharge will be taken as 3.96, the same as for examples 1 and 7.

From problem 1, the final values of $H_s=20.18$, $h_a=0.098$, and $\frac{h_a}{H_s}=0.0049$ for the vertical-face section are obtained.

Commencing with these values and using figure 33, $\frac{E}{H_s}=0.114$, for a value of $\frac{M}{N}=1.71$.

Then

$$H_s=H_o+E=17.90+0.114H_s=\frac{17.90}{0.886}=20.20 \text{ feet},$$

and

$$\frac{h_a}{H_s}=\frac{0.098}{20.20}=0.0049,$$

which agrees with the former value.

Also,

$$\frac{N}{H_s}=\frac{7}{20.20}=0.347,$$

which is within the range of these experiments, see table 32.

With $H_s=20.20$ feet, $\frac{h_a}{H_s}=0.0049$, and the experimental data in table 33, the coordinates for the downstream face of the above offset overflow section can be computed. These coordinates are listed in table 35 and are shown plotted by a dash line in figure 38. In the upper region this profile follows the one for the vertical-face dam but departs from it as the curve progresses.

TABLE 35.—COORDINATES FOR OFFSET OVERFLOW SECTION—EXAMPLE 8

$\frac{X}{H_s}$ 1	$\frac{Y}{H_s}$ 2	X, feet 3	Y, feet 4	Y, elevation feet 5
0. 00	0. 000	0. 00	0. 00	987. 82
0. 05	0. 058	1. 01	1. 17	980. 99
0. 10	0. 086	2. 02	1. 74	981. 56
0. 15	0. 101	3. 03	2. 04	981. 86
0. 20	0. 109	4. 04	2. 20	982. 02
0. 25	0. 113	5. 05	2. 28	982. 10
0. 30	0. 110	6. 06	2. 22	982. 04
0. 35	0. 104	7. 07	2. 10	981. 92
0. 40	0. 094	8. 08	1. 90	981. 72
0. 45	0. 081	9. 09	1. 64	981. 46
0. 50	0. 066	10. 10	1. 33	981. 15
0. 60	0. 025	12. 12	0. 50	980. 32
0. 70	−0. 025	14. 14	−0. 50	979. 32
0. 80	−0. 085	16. 16	−1. 72	978. 10
0. 90	−0. 152	18. 18	−3. 07	976. 75
1. 00	−0. 229	20. 20	−4. 63	975. 19
1. 20	−0. 407	24. 24	−8. 22	971. 60
1. 40	−0. 619	28. 28	−12. 50	967. 32
1. 60	−0. 869	32. 32	−17. 55	962. 27
1. 80	−1. 149	36. 36	−23. 21	956. 61
2. 00	−1. 478	40. 40	−29. 86	949. 96
2. 20	−1. 329	44. 44	−36. 95	942. 87

CHAPTER VI—VERIFICATION OF EXPERIMENTAL DATA

PRESSURES ON DOWNSTREAM FACE OF OVERFLOW SECTIONS AND DISCHARGE COEFFICIENTS

42. Pressures on Overflow Faces.—Although little doubt existed that overflow sections designed from the previously described experimental results would perform as expected, some form of verification was desired. This was accomplished in the laboratory by constructing and testing models of the dam sections of examples 1, 4, 7, and 8. Each model was constructed accurately to scale, of sheet metal, and was provided with a sufficient number of piezometers to permit observing the pressures over the entire extent of the downstream face. Although all models were not constructed to the same scale, all were 1.5 feet wide and each was tested in turn in a flume of the same width. The section with vertical upstream face (example 1) was constructed on a 1:30 scale from the coordinates listed in table 3. When operated at the designed head, H_o, of 17.90 feet, corresponding to a head on the model of 0.597 foot, all piezometric pressures were atmospheric or above, as can be observed from figure 39–A. The manometer glasses, shown in this figure, had the same horizontal spacing as the piezometers in the overflow section; hence, the pressures may be read directly from the photograph. The smaller divisions on the board are 0.01 foot apart, model scale. As the manometer tubes were small, a few drops of aerosol were placed in each glass to relieve surface tension. The pressures as observed with the small manometer tubes were checked using manometer tubes with one-half-inch inside diameter, and the results were found to agree.

A model of the overflow section of example 4, which represents a comparatively low dam, was constructed on a scale of 1:8 from the coordinates of table 24. Pressures on the downstream face of this section for the designed head of 12.2 feet, or a head on the model of 1.525 feet, are shown in figure 39–B. In this case, four piezometers near the crest showed negative pressures. The largest observed was −0.06 foot of water, model, or −0.48 foot of water, prototype, which is a negligible amount. Because of the sloping upstream face, this section did not possess as definite a spring point as the section in the former example, which may account for the fact that the water surfaces in the manometers did not coincide with the outline of the overflow section. In both figures 39–A and 39–B a few of the upstream piezometers showed positive pressures, which indicates that the shape of the models at the spring point did not agree exactly with the experimental results. It is difficult to avoid some irregularity in the pressures on a model, as a very small change in the section near the spring point greatly affects the pressures immediately downstream. Also, it is extremely difficult to construct these sections exactly to scale in all respects and install all piezometers exactly normal to the overflow face.

A model of the overflow section of example 7 was constructed on a scale of 1:30 from the coordinates of table 34. Except for the overhang on the upstream face, conditions of head and discharge were similar to those of example 1. Pressures on the downstream face, for a designed head of 17.90 feet, are shown in figure 40–A.

The extreme upstream piezometer registered a positive pressure of 2.7 feet of water, prototype, while small negative pressures existed immediately downstream. The pressures on this type of section are extremely sensitive to any minute change in shape near the spring point. A slight change could cause the positive as well as the negative pressures to coincide with the profile line. Negative pressures indicate that the sheet of water has a tendency to skip over the surface, while positive pressures are a direct result of impingement of the sheet against the overflow face.

A model of the offset overflow section of example 8 was also constructed on a 1:30 scale, and the coordinates used in this case are listed in table 35. The resulting pressures experienced on the downstream face of this model for a designed head of 17.90 feet are shown in figure 40–B. All pressures are positive for flow at the designed head.

It is felt that the above verification of pressures obtained from the models, which were proportioned from the foregoing experimental data in this bulletin, is altogether satisfactory. The results should be as favorable for the prototype structures.

There are many overflow spillways in existence which operate under negative pressure without detrimental results. In fact, there are few overflow sections in existence that will perform without some negative pressure on the face when operating at their respective designed heads. The above confirmation tests indicate the difficulties involved even when the design is made from reliable experimental data. It is not the intention to create the impression that all overflow spillways should be designed to operate with little or no vacuum beneath the overfalling sheet of water. In fact, there are cases where it is economically advisable to design spillways to operate with subatmospheric pressures as great as half an atmosphere. In

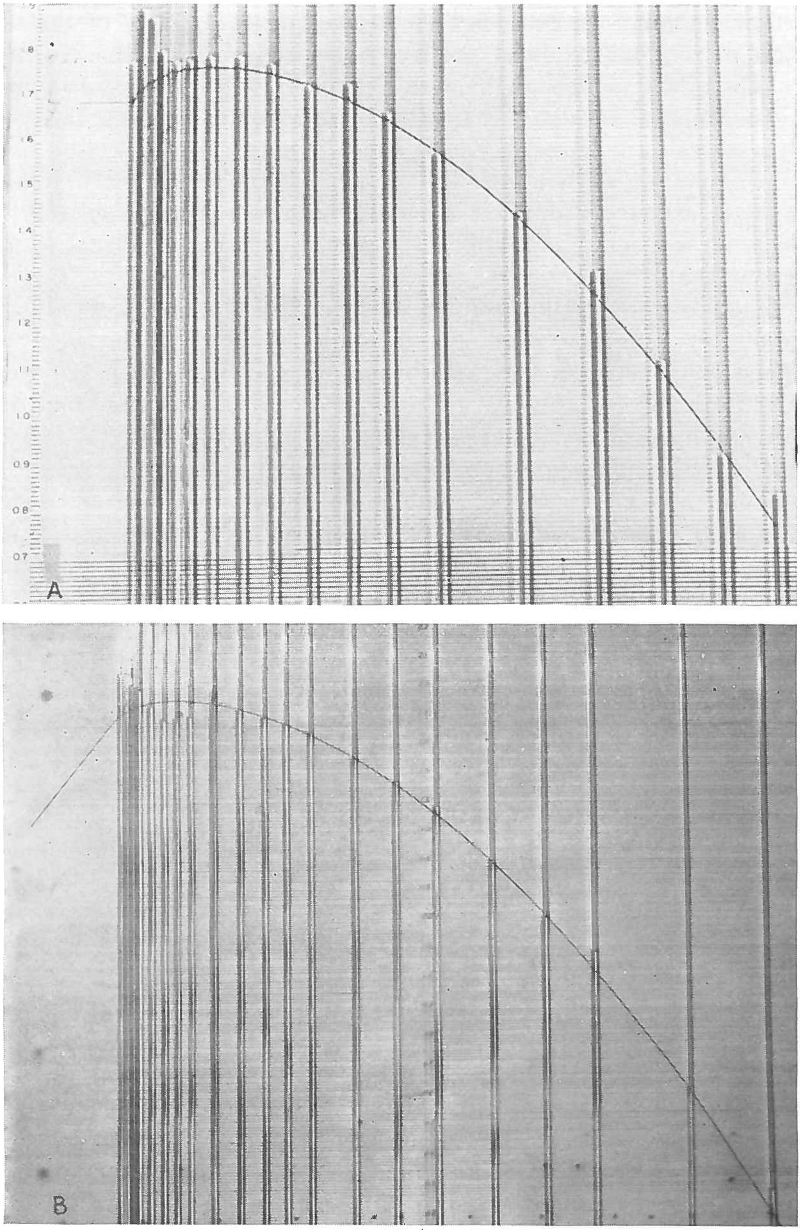

FIGURE 39.—PRESSURES ON SPILLWAY FACE—VERTICAL AND SLOPING UPSTREAM FACE.

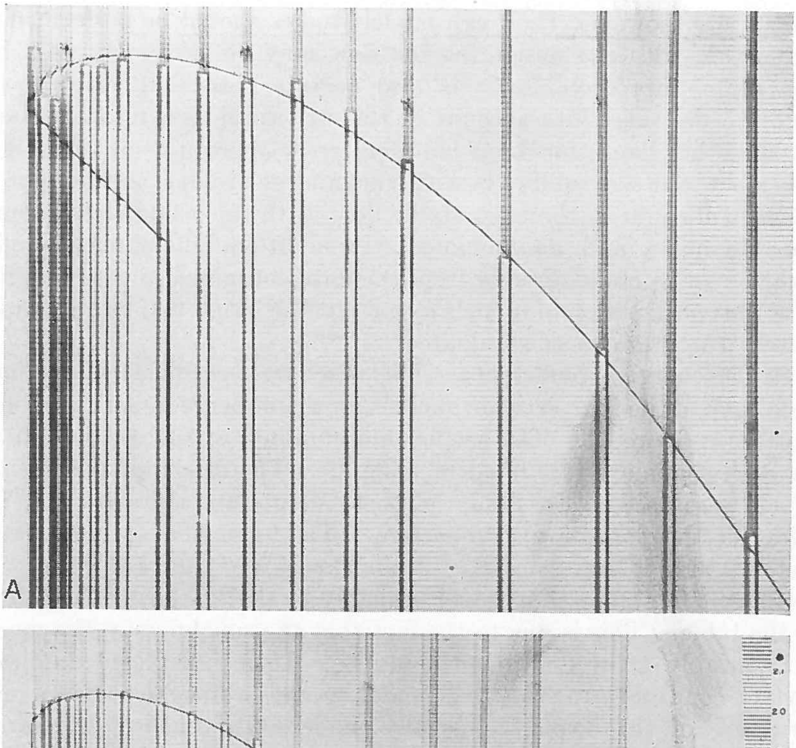

FIGURE 40.—PRESSURES ON SPILLWAY FACE—OVERHANG AND OFFSET SECTIONS.

these cases, however, thorough model studies should be performed in connection with the design, as the flow may be extremely unstable and quite unpredictable; it is also necessary to take these lower negative pressures into account in the structural design of the dam. On the other hand, for dams handling great quantities of water it is advisable to design spillways with vacuumless profiles, as this type of design will result in the most stable flow, with the least splash, objectionable noise, and maintenance. In addition, vacuumless profile designs can be made directly from the data contained in this bulletin; thus the construction of models for all but the larger and more complicated structures can be eliminated.

43. Discharge Coefficients.—The discharge coefficients obtained from each of the four overflow models for a number of heads have been plotted in figure 41. The coefficients obtained at the designed head for each shape are tabulated in table 36. The discharge coefficients which were used in the design of these shapes are also shown in the table for the purpose of comparison. The agreement is quite satisfactory, and it can be stated from experience that the prototype coefficients for these shapes will probably be slightly larger than those in the table. This is due to the fact that the roughness in the model is invariably greater than it should be. It is difficult to duplicate surface conditions to scale in a model, as the prototype surfaces on a structure of this type are usually made quite smooth. Negative pressure under the nappe tends to increase the value of the discharge coefficient.

TABLE 36.—COMPARISON OF DISCHARGE COEFFICIENTS—EXAMPLES 1, 4, 7, AND 8

Example No.	Designed head, H_o, feet	Coefficient of discharge		Type of overflow section
		From model	From design data	
1	17. 90	4. 00	3. 96	Vertical upstream face.
4	12. 20	3. 98	3. 91	3/4:1 slope on upstream face.
7	17. 90	4. 03	3. 96	Overhang on upstream face.
8	17. 90	4. 00	3. 96	Offset on upstream face.

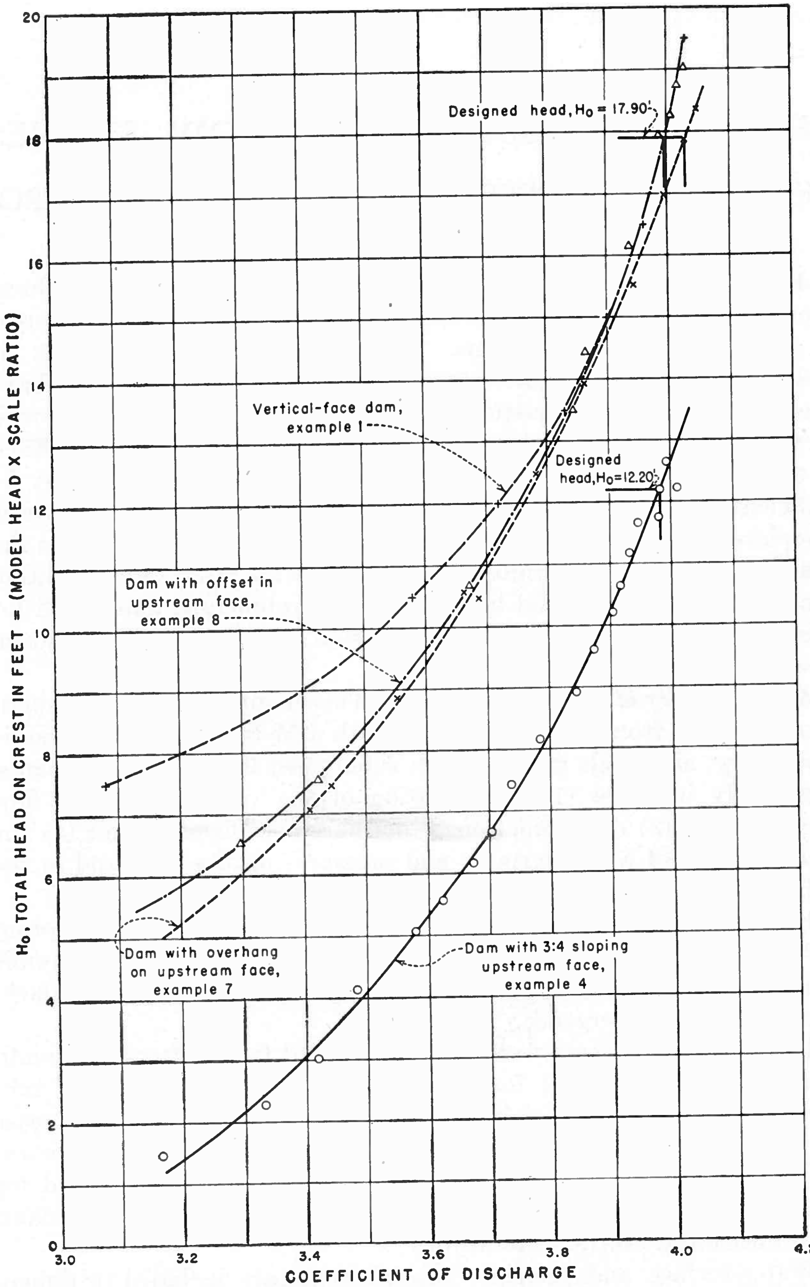

FIGURE 41.—DISCHARGE-COEFFICIENT CURVES FROM MODELS IN EXAMPLES 1, 4, 7, AND 8.

CHAPTER VII—SUBMERGED FLOW STUDIES

DECREASE IN COEFFICIENT OF DISCHARGE PRODUCED BY SUBMERGED FLOW

44. Introduction.—Many attempts by different individuals have been made to piece together experimental data from various sources on flow over submerged dams. As submerged flow, at its best, is unstable, it is not difficult to understand why these attempts have been only partially successful. A listing of the most prominent work on submerged flow over dams is included in the bibliography. Even if this material could be pieced together, its scope would not be sufficient to represent the picture as a whole. A laboratory study was therefore made in an attempt to obtain as complete an account as the available time would permit. The object of the study was to obtain general information to aid in the design of submerged dams, and for this reason the results have been expressed in the most general form, that of dimensionless numbers.

45. Summary of Testing Program.—This chapter is based on experimental results from two small dams which were tested in the hydraulic laboratory, and deals entirely with submerged flow over these dams. The study included (1) investigation of the various types of flow encountered, (2) determination of discharge coefficients, and (3) the measurement of water surfaces and pressures on the dam and in the stilling basin, to aid in stability determinations.

Four distinct types of flow were prevalent on the downstream apron: (1) Flow at supercritical velocities, (2) flow involving the hydraulic jump, (3) flow accompanied by a drowned jump, and (4) flow approaching complete submergence.

Discharge coefficients were first determined for the free-flow condition, then redetermined for the various conditions involving submergence. The difference between the two is termed the "decrease in the coefficient of discharge due to submergence." This factor expressed in percent of the free-flow coefficient has been plotted for practically all combinations of flow which can occur on small dams with horizontal downstream aprons.

Water-surface and pressure measurements are included in dimensionless coordinates for a representative number of flow combinations. These plots are intended to aid the designer in picturing the type of flow to be encountered, and at the same time offer actual values of pressure for stability determinations. Four examples have been included to demonstrate the possible uses of the experimental information obtained in the study.

46. Test Equipment.—The experiments were performed on two different pieces of equipment. The first set of experiments was performed using a sheet-metal overflow dam constructed according to the coordinates for Dam A in figure 42. The dam was installed in a rectangular sheet-metal-lined flume 1.52 feet wide and approximately 24 feet long. Adjustable floors were provided both upstream and downstream from the dam in addition to the main floor of the flume, see figure 43. For all positions, the adjustable floors were sealed tightly against the dam and side walls to prevent flow around these floors. The second set of experiments was performed in another but similar flume 1.95 feet in width and 30 feet long, in which another sheet-metal dam, constructed according to the coordinates for Dam B in figure 42, was installed.

In both cases the movable floors were similarly constructed, the positions of the gages were in similar locations, and the controls were alike in most respects. The upstream head-gage connection, in each case, was located in the movable floor a distance approximately 15 H_o, or 15 times the designed head, upstream from the crest of the dam. This was connected to a transparent pot on the outside of the flume, from which head readings were measured by a hook gage. The tailwater level was obtained from a point gage located a distance 4 H_o downstream from the crest of the dam. Water-surface profiles along the flume were obtained from a point gage which could be moved along a 4-inch channel iron located over the center of the flume. Pressure measurements on the dam and on the downstream floor were obtained on Dam B from piezometers located normal to these surfaces as shown in figure 43. The discharge to the model was measured through the accurately calibrated laboratory Venturi meter system. Regulation of the tailwater on Dam B was accomplished by means of an adjustable hinged gate located at the downstream end of the flume.

47. Test Procedure.—Initial tests were made to obtain the data required to construct curves for the free-discharge condition corresponding to different positions of the upstream floor; the downstream floor was removed completely and free flow allowed to prevail for these tests. The curves are shown in figure 42 for two upstream floor positions for Dam A and one floor position for Dam B. The second curve for Dam B was obtained after changes were made in the approach channel to the dam. After the tests on Dam A, it was learned that the effect on the flow produced by the upstream floor position could be segregated from the effect produced by the downstream conditions. In other words, the entire effect of the upstream floor is

DAM SHAPE COORDINATES IN FEET

DAM A		DAM B	
X	Y	X	Y
0	0	0	0
0.034	0.038	0.052	0.061
0.067	0.057	0.104	0.096
0.101	0.068	0.156	0.117
0.135	0.074	0.208	0.131
0.168	0.075	0.260	0.138
0.202	0.073	0.312	0.140
0.235	0.073	0.364	0.139
0.270	0.064	0.416	0.135
0.303	0.056	0.468	0.128
0.336	0.046	0.520	0.118
0.404	0.021	0.572	0.106
0.471	-0.012	0.624	0.091
0.538	-0.050	0.702	0.065
0.605	-0.094	0.806	0.022
0.673	-0.145	0.910	-0.030
0.807	-0.265	1.014	-0.088
0.942	-0.408	1.118	-0.153
1.076	-0.572	1.222	-0.230
1.211	-0.762	1.300	-0.286
1.345	-0.977	1.560	-0.518
1.480	-1.210	1.820	-0.795
1.614	-1.466	2.080	-1.113
1.749	-1.751	2.340	-1.478

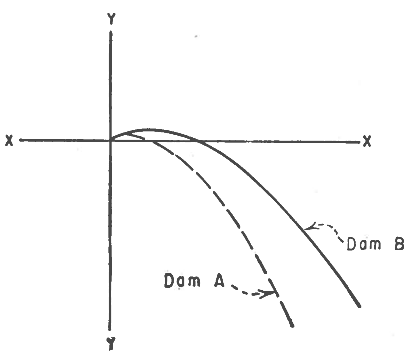

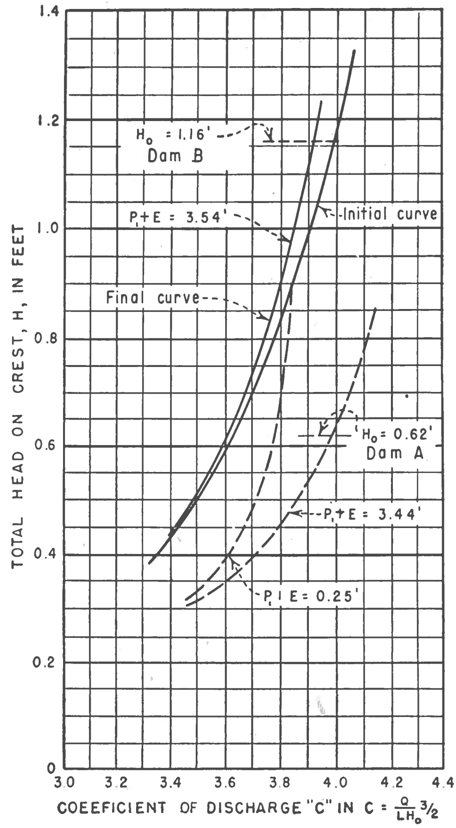

DAM A----
Designed head, H_o = 0.62'
P_1 + E = 3.44' and 0.25'
Length of crest = 1.52'

DAM B——
Designed head, H_o = 1.16'
P_1 + E = 3.54'
Length of crest = 1.95'

FIGURE 42.—DAM COORDINATES AND FREE CREST COEFFICIENT-OF-DISCHARGE CURVES.

accounted for in the free-flow coefficient curves in figure 42. For this reason it was not necessary to employ more than one upstream floor position for Dam B.

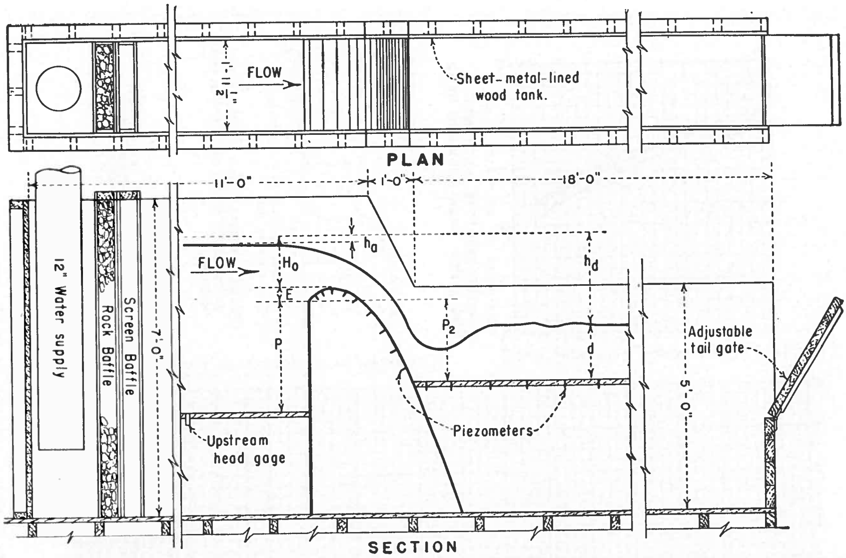

FIGURE 43.—SECTION OF EXPERIMENTAL FLUME FOR SUBMERGED FLOW TESTS.

Upon completion of the free-flow coefficient curves, the upstream floor was set in one of the calibrated positions and the downstream floor was fixed in a position approaching the crest of the dam. A constant head was maintained on the dam while readings of the discharge and depth of flow over the downstream floor were made for various tailwater depths. Flow conditions encountered varied from supercritical velocities to flow at practically complete submergence, the discharge in the latter case approaching zero. The procedure involved from 6 to 8 runs, each made with the same head but with the tailgate in a different position. The same test was repeated while a second head was maintained on the crest of the dam. After this the downstream floor was lowered to a second position and the 12 to 16 runs, outlined above, repeated. This entire routine was repeated for floor positions varying from the crest of the dam to the permanent floor of the flume. In the case of Dam A, the upstream floor was shifted to the second calibrated position and certain runs repeated. The testing on Dam A was limited to supercritical velocities on the downstream floor while that on Dam B included 4 types of flow. The coefficient of discharge was obtained for each run, and the decrease in coefficient of discharge due to submergence and also due to the presence of the downstream floor was obtained for each run by subtracting the coefficient of discharge, as computed above, from the free-flow coefficient of figure 42 for a corresponding flow condition. The experimental points thus obtained have been tabulated and included as table 37.

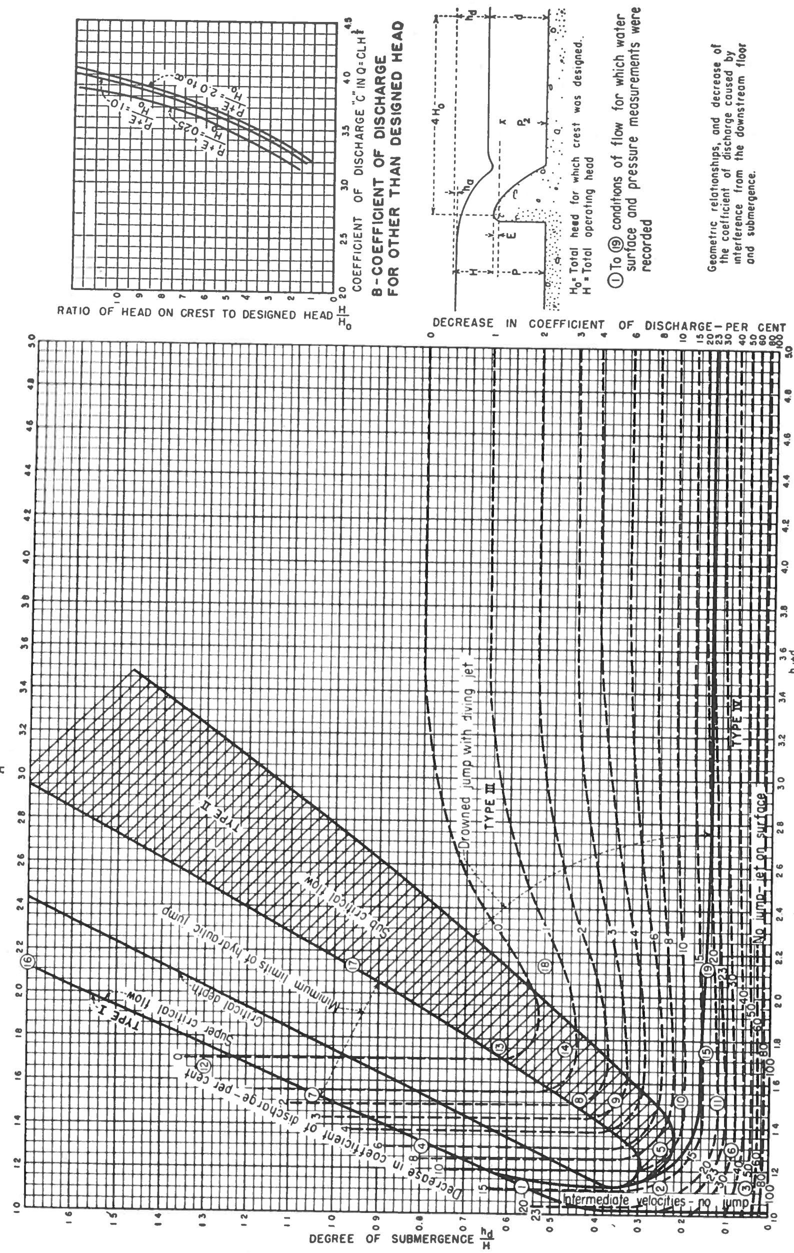

FIGURE 44.—CHARACTERISTICS OF FLOW OVER SUBMERGED DAMS—GENERAL RELATIONSHIPS.

The nomenclature used in the column headings of table 37 is illustrated by the sketch in figure 44. Column 1 indicates the discharge per foot of dam for each run; column 2 shows the total head on the crest of the dam, including velocity head of approach; and column 3 is the coefficient of discharge obtained by substituting these values in the expression $C=\frac{Q}{LH^{3/2}}$. The tabulation in column 4 represents the difference between the free-discharge coefficient and the coefficient obtained with submerged flow, for the same dam operating at identical heads. The positions of the upstream and downstream floors, throughout the test, are recorded in columns 5 and 6, respectively. Columns 7 and 8 involve purely geometrical relationships, namely, the degree of submergence and the position of the downstream floor with respect to the head on the crest. Column 9 indicates the type of flow encountered downstream from the dam for each run, see figure 44–A. The symbol H_o, when encountered, indicates only the total designed head for a given dam, while H represents any total head applied to the same dam.

48. Test Results on Coefficients of Discharge.—The data contained in table 37 were used to plot the dimensionless curves in figure 44–A. For the sake of clarity the points are not shown on the graph. The main coordinates involve the degree of submergence and the position of the downstream floor. The heavy solid lines divide the graph into zones comprising the various types of flow encountered, such as supercritical flow, the hydraulic jump, drowned jump, and flow approaching complete submergence. The dashed lines indicate the decrease in the coefficient of discharge in per cent, based on the coefficient of discharge for free flow at the same head. Beginning at the top of the sheet and reading downward, the flow designated as "type I" was at supercritical velocities, illustrated by plots 4, 7, 12, and 16 of figures 45 and 46. The decrease in the coefficient of discharge in this region is not caused by submergence in the usual sense, but is entirely an effect produced by the downstream apron.

As the tailwater was raised, or the value of $\frac{h_d}{H}$ decreased, a hydraulic jump occurred in which both supercritical and tranquil flow were present. The former is the type I flow and the latter is represented by the zone designated as "type II flow." The curves comprising types I and II should not be confused with the depth versus specific energy curve, commonly associated with hydraulic jump computations, as the latter represents values of depths and energy for one discharge. Many discharges are represented in the curves of figure

TABLE 37.—COMPILATION OF EXPERIMENTAL DATA—SUBMERGED DAM STUDIES

DAM A								
1	2	3	4	5	6	7	8	9
q, DISCHARGE PER FOOT OF WIDTH	H, FEET	C	PER CENT DECREASE IN C	P_1+E, FEET	P_2+E, FEET	$\frac{h_d}{H}$	$\frac{h_d+d}{H}$	TYPE OF FLOW
1.865	0.598	4.034	0	3.44	0.602	1.575	2.006	1
1.865	0.600	4.013	0		0.475	1.330	1.792	
1.826	0.599	3.949	1.28		0.349	1.064	1.583	
1.793	0.599	3.878	3.05		0.270	0.936	1.451	
1.751	0.600	3.767	5.82		0.209	0.809	1.348	
1.692	0.599	3.658	8.55		0.140	0.668	1.234	
1.580	0.599	3.417	14.58		0.037	0.534	1.062	
1.177	0.518	3.157	18.56		0.038	0.506	1.073	
1.200	0.516	3.237	16.49		0.063	0.574	1.122	
1.259	0.520	3.357	13.40		0.085	0.617	1.163	
1.311	0.520	3.497	9.79		0.109	0.660	1.210	
1.347	0.519	3.603	7.22		0.135	0.713	1.260	
1.384	0.521	3.678	5.15		0.160	0.770	1.307	
1.397	0.520	3.724	4.12		0.185	0.833	1.356	
1.416	0.521	3.766	2.84		0.212	0.893	1.407	
1.418	0.520	3.782	2.58		0.237	0.946	1.456	
2.279	0.713	3.785	6.82		0.242	0.787	1.339	
2.308	0.713	3.834	5.60		0.270	0.837	1.379	
2.347	0.713	3.899	3.90		0.305	0.898	1.427	
2.382	0.714	3.949	2.68		0.339	0.952	1.475	
2.398	0.713	3.983	1.95		0.370	1.008	1.519	
1.949	0.710	3.257	19.48		0.058	0.492	1.082	
2.016	0.712	3.356	17.05		0.100	0.570	1.140	
2.138	0.716	3.528	12.91		0.142	0.630	1.198	
2.226	0.714	3.690	9.01		0.192	0.707	1.269	
0.682	0.372	3.006	16.60	0.251	0.024	0.562	1.065	1
0.826	0.382	3.500	3.58		0.138	0.874	1.361	
0.846	0.383	3.573	1.65		0.175	0.987	1.457	
0.846	0.383	3.573	1.65		0.211	1.104	1.551	
0.859	0.384	3.609	0.55		0.254	1.219	1.661	
1.220	0.542	3.059	18.62		0.024	0.515	1.044	
1.338	0.549	3.290	12.50		0.063	0.563	1.115	
1.443	0.562	3.427	9.02		0.102	0.644	1.181	
1.482	0.564	3.498	7.16		0.138	0.725	1.245	
1.547	0.569	3.603	4.51		0.175	0.794	1.308	
1.567	0.571	3.632	3.97		0.211	0.877	1.370	
1.587	0.574	3.650	3.44		0.254	0.958	1.443	
1.593	0.570	3.704	2.12		0.290	1.037	1.509	
1.639	0.579	3.720	1.59		0.322	1.109	1.556	
2.170	0.798	3.045	20.63		0.024	0.476	1.030	
2.308	0.807	3.183	16.97		0.063	0.509	1.078	
2.465	0.821	3.316	13.31		0.102	0.553	1.124	
2.570	0.831	3.394	11.49		0.138	0.617	1.166	
2.380	0.772	3.511	8.36		0.175	0.676	1.227	
2.413	0.774	3.545	7.57		0.211	0.748	1.273	
2.426	0.769	3.599	6.00		0.254	0.809	1.330	
2.498	0.771	3.692	3.66		0.290	0.857	1.376	
2.505	0.769	3.716	2.87		0.322	0.931	1.419	
1.831	0.599	3.96	0.50	3.44	3.44	0.763	6.74	3
1.819	0.596	3.96	0.25			0.753	6.77	
1.792	0.594	3.92	1.02			0.630	6.79	
1.766	0.596	3.85	3.00			0.522	6.77	
1.734	0.596	3.78	4.75			0.379	6.77	
1.694	0.597	3.68	7.25			0.283	6.76	
1.622	0.601	3.49	12.50			0.196	6.72	
1.105	0.591	2.44	38.25			0.115	6.82	
0.327	0.592	0.72	81.30			0.012	6.81	4
2.891	0.812	3.96	3.88			0.668	5.29	3
2.885	0.815	3.93	4.84			0.550	5.22	
2.852	0.813	3.90	5.34			0.430	5.24	
2.792	0.809	3.85	6.32			0.372	5.25	
2.622	0.813	3.59	12.85			0.408	5.24	
2.530	0.807	3.50	14.85			0.401	5.26	
2.369	0.809	3.26	20.65			0.359	5.25	
2.210	0.811	3.03	26.50			0.315	5.24	
2.120	0.813	2.90	29.40			0.289	5.24	
2.053	0.815	2.80	32.20			0.275	5.22	
1.930	0.811	2.65	35.70			0.237	5.24	
1.610	0.808	2.22	46.00			0.158	5.26	
1.040	0.808	1.44	64.90			0.066	5.26	

TABLE 37.—COMPILATION OF EXPERIMENTAL DATA—SUBMERGED DAM STUDIES—Continued

DAM B								
1	2	3	4	5	6	7	8	9
q, DISCHARGE PER FOOT OF WIDTH	H, FEET	C	PER CENT DECREASE IN C	P_1+E, FEET	P_2+E, FEET	$\frac{h_d}{H}$	$\frac{h_d+d}{H}$	TYPE OF FLOW
2.809	0819	3.791	0.052	3.54	3.54	0.729	5.322	3 AND 4
2.789	0820	3.755	1.57			0.555	5.317	
2.748	0.820	3.700	3.93			0.469	5.317	
2.702	0.820	3.638	4.64			0.394	5.317	
2.640	0.819	3.562	6.54			0.314	5.322	
2.496	0.817	3.380	11.33			0.203	5.333	
2.078	0.816	2.819	26.00			0.166	5.338	
1.898	0.815	2.578	32.35			0.137	5.344	
1.718	0.812	2 347	38.30			0.109	5.360	
1.171	0.809	1.609	57 70			0.029	5.376	
4.109	1.042	3.861	2.03			0.640	4.340	
4.032	1.041	3.796	3.65			0.495	4.400	
3.934	1.041	3.704	6.00			0.386	4.400	
3 883	1.051	3.602	8.81			0.221	4 370	
3.703	1.038	3.500	11.21			0.250	4.410	
2.820	1.050	2.620	33.70			0.132	4.370	
2.178	1 034	2.072	47.45			0 089	4.425	
1.790	1.043	1.680	57 40			0.065	4.395	
1.484	1.033	1 414	64.05			0.050	4.425	
1 114	1.037	1.055	73.20			0.049	4.410	
3.356	1.055	3 096	21.62		0.034	0.532	1.032	4
3 254	1.044	3.050	22.62		0.024	0.392	1.023	
3.225	1.047	3 012	23.65		0.024	0.287	1.023	
3.087	1.047	2.882	26.94		0.022	0.165	1.021	
2.262	1.041	2.130	46.02		0.022	0.079	1.021	
1.507	1.039	1 423	63 91		0.022	0.050	1.021	
1 465	0.609	3 089	14.40		0.026	0.555	1.043	1
1 460	0.610	3.065	15.09		0.022	0 385	1 036	4
1.456	0610	3.058	15.29		0.022	0.126	1.036	
1.287	0.609	2 713	24.82		0.022	0 122	1.036	
1.148	0.608	2 421	32.89		0.022	0.108	1 036	
0.832	0.610	1.747	51 60		0.022	0.046	1 036	
3.793	1.049	3.518	10 91		0.190	0.650	1.154	
3.778	1.049	3.517	10.94		0.191	0.564	1.154	
3.765	1 046	3.519	10.82		0 188	0.514	1 180	1
3.770	1 048	3.514	10.99		0.185	0 458	1 176	
3.724	1.048	3 470	12 10		0.185	0.299	1 176	4
3.587	1.048	3.340	15.29		0.186	0.183	1 176	
3 092	1 037	2.928	25.72		0 187	0.108	1 180	
1 189	0610	2.558	29.14		0.186	0.079	1.303	
3.937	1.044	3.690	5.67		0.305	0.773	1.292	1
3.942	1.048	3 674	6.96		0.301	0.748	1.287	
3 932	1.046	3.675	6.91		0.295	0.700	1.282	
3 898	1.043	3.660	7.22		0.293	0.353	1.281	2
3.852	1.043	3.616	8.33		0.305	0.290	1 292	
3.693	1 041	3 477	11.84		0.305	0.216	1.293	
3.233	1.043	3.035	23.08		0.298	0.136	1.286	4
2 943	1.040	2 773	29.65		0.296	0.114	1.285	
1.746	0.617	3 602	0.44		0.302	1.052	1.490	1
1 733	0.617	3.575	1 18		0.293	0.942	1 474	
1.723	0.616	3 562	1.49		0.300	0.502	1.487	2
1.718	0.616	3.551	1 79		0.298	0.393	1.484	
1 700	0.617	3.506	3.09		0.295	0.314	1.478	
1 644	0.616	3.397	6.05		0.294	0.206	1 477	3
1 543	0.616	3.190	11.78		0.294	0.138	1.477	4
1 289	0.621	2.637	27.17		0.296	0.081	1 477	
1.171	0.614	2 433	32.67		0.296	0.065	1.482	
0 991	0.613	2 064	42.87		0.296	0.049	1.482	
1 713	0617	3.549	1 90		0.300	1 055	1 486	1
1 695	0.615	3.518	2.68		0.294	0.311	1.478	2
1.181	0 616	2 442	32.46		0.294	0.065	1.477	4
0 991	0.615	2.058	43.07		0.294	0.046	1.477	
1.713	0.617	3.533	2.34		0.294	0.360	1.476	2
1.721	0.617	3.549	1.90		0.296	0.888	1.480	1
4.006	1.056	3.693	4.32		0.355	0.841	1.336	
3.991	1.054	3.688	4.43		0.345	0.807	1.327	
3.996	1.055	3.685	4.53		0.345	0.774	1.327	
3.980	1.055	3.671	4.89		0.349	0.739	1.331	
3.898	1.050	3 622	6.06		0 352	0.304	1.335	2
3.821	1.054	3.531	8.49		0.346	0.269	1.328	
3.695	1.053	3.408	11.66		0.345	0.222	1.328	
3.472	1.057	3 195	17.24		0.344	0.185	1.325	3
3.277	1.057	3 015	21.91		0.350	0.169	1.331	
2.866	1.052	2.655	31.18		0.346	0.109	1.329	4
2.280	1 049	2 123	44.94		0.346	0.073	1.330	

TABLE 37.—COMPILATION OF EXPERIMENTAL DATA—SUBMERGED DAM STUDIES—Continued.

DAM B— Continued								
1 q, DISCHARGE PER FOOT OF WIDTH	2 H, FEET	3 C	4 PER CENT DECREASE IN C	5 P_1+E, FEET	6 P_2+E, FEET	7 $\frac{h_d}{H}$	8 $\frac{h_d+d}{H}$	9 TYPE OF FLOW
1.736	0.617	3.581	1.02	3.54	0.353	1.154	1.572	1
1.728	0.616	3.572	1.22		0.347	1.028	1.563	
1.731	0.616	3.577	1.08		0.353	0.542	1.573	2
1.715	0.616	3.545	1.96		0.348	0.433	1.564	
1.710	0.616	3.535	2.24		0.346	0.364	1.561	
1.677	0.616	3.466	4.15		0.344	0.269	1.558	3
1.592	0.615	3.305	8.58		0.343	0.171	1.558	
1.320	0.616	2.728	24.55		0.346	0.096	1.561	4
4.027	1.047	3.760	2.59		0.440	0.930	1.420	1
4.063	1.056	3.745	2.98		0.436	0.903	1.413	
4.042	1.056	3.726	3.47		0.429	0.348	1.406	2
3.991	1.055	3.681	4.63		0.429	0.322	1.407	
3.477	1.055	3.207	16.91		0.434	0.194	1.411	3
1.739	0.616	3.593	0.55		0.440	1.331	1.714	1
1.736	0.617	3.581	0.42		0.435	1.246	1.705	
1.736	0.617	3.581	0.42		0.435	0.511	1.705	2
1.713	0.617	3.533	1.75		0.435	0.366	1.705	3
1.053	0.614	2.188	39.12		0.435	0.055	1.708	4
4.063	1.050	3.776	2.15		0.492	0.995	1.469	1
4.088	1.056	3.769	2.36		0.488	0.968	1.462	
4.032	1.056	3.717	3.70		0.483	0.380	1.457	2
3.975	1.055	3.667	5.00		0.482	0.290	1.457	
3.811	1.054	3.522	8.75		0.482	0.216	1.457	3
2.342	1.044	2.195	43.06		0.482	0.065	1.462	4
1.739	0.616	3.593	0.05		0.483	1.429	1.784	1
1.739	0.616	3.593	0.05		0.483	1.242	1.784	
1.739	0.617	3.586	0.28		0.483	0.546	1.784	2
1.736	0.617	3.581	0.42		0.483	0.434	1.784	
1.703	0.617	3.512	2.34		0.483	0.311	1.784	3
1.633	0.616	3.376	6.09		0.483	0.198	1.784	
1.469	0.616	3.036	15.57		0.482	0.122	1.782	4
1.071	0.615	2.223	38.15		0.482	0.049	1.784	
4.093	1.054	3.783	2.50		0.546	1.061	1.518	1
4.083	1.051	3.788	2.34		0.542	0.971	1.516	
4.096	1.054	3.785	2.44		0.540	0.418	1.512	2
3.919	1.055	3.614	6.80		0.541	0.258	1.513	3
3.693	1.055	3.406	12.22		0.540	0.189	1.513	
3.410	1.052	3.160	18.53		0.540	0.159	1.516	
3.087	1.050	2.869	26.01		0.540	0.133	1.514	4
2.188	1.048	2.039	47.38		0.540	0.056	1.515	
1.751	0.617	3.612	0.22		0.546	1.530	1.884	1
1.746	0.617	3.602	0.49		0.541	1.355	1.878	
1.746	0.617	3.602	0.49		0.541	0.666	1.878	2
1.739	0.617	3.585	0.96		0.541	0.497	1.878	
1.713	0.616	3.533	2.40		0.541	0.367	1.878	3
1.697	0.617	3.501	3.28		0.541	0.282	1.878	
1.376	0.617	2.839	21.57		0.541	0.102	1.878	4
1.063	0.615	2.207	39.03		0.541	0.049	1.878	
4.181	1.056	3.854	0.41		0.854	1.400	1.809	1
4.191	1.057	3.859	0.34		0.844	1.302	1.798	
4.183	1.058	3.846	0.69		0.845	0.616	1.799	2
4.037	1.050	3.752	2.92		0.845	0.301	1.805	3
3.911	1.051	2.996	22.54		0.844	0.150	1.803	
3.231	1.054	3.614	6.59		0.845	0.258	1.802	
2.455	1.048	2.288	40.79		0.844	0.084	1.805	4
1.744	0.617	3.594	0.03		0.851	2.068	2.379	1
1.751	0.617	3.594	0.03		0.847	2.013	2.377	
1.751	0.618	3.594	0.05		0.845	1.008	2.377	2
1.728	0.617	3.565	0.83		0.845	0.548	2.377	3
1.708	0.619	3.507	2.53		0.845	0.359	2.376	
1.410	0.640	2.753	24.85		0.845	0.131	2.320	4
0.955	0.620	1.958	45.58		0.845	0.048	2.363	
4.194	1.056	3.867	0.07		1.022	1.581	1.967	1
4.194	1.056	3.867	0.07		1.010	1.507	1.956	
4.152	1.057	3.817	1.39		1.011	0.629	1.956	2
4.114	1.056	3.792	2.27		1.007	0.454	1.953	3
3.993	1.055	3.683	4.81		1.006	0.297	1.954	
3.683	1.051	3.415	13.18		1.006	0.207	1.957	
3.161	1.053	2.924	24.38		1.006	0.147	1.955	3 AND 4
2.517	1.050	2.339	39.46		1.006	0.044	1.958	4
4.290	1.056	3.953	0.25		2.442	1.762	3.312	2
4.275	1.054	3.948	0.10		2.449	1.350	3.324	
4.275	1.054	3.948	0.10		2.433	1.092	3.308	3
4.275	1.057	3.932	0.61		2.432	0.790	3.301	4
4.235	1.057	3.894	1.56		2.432	0.563	3.301	3
4.157	1.057	3.823	3.36		2.432	0.457	3.301	
4.095	1.056	3.770	4.65		2.432	0.377	3.303	
3.365	1.052	3.118	21.06		2.440	0.209	3.319	

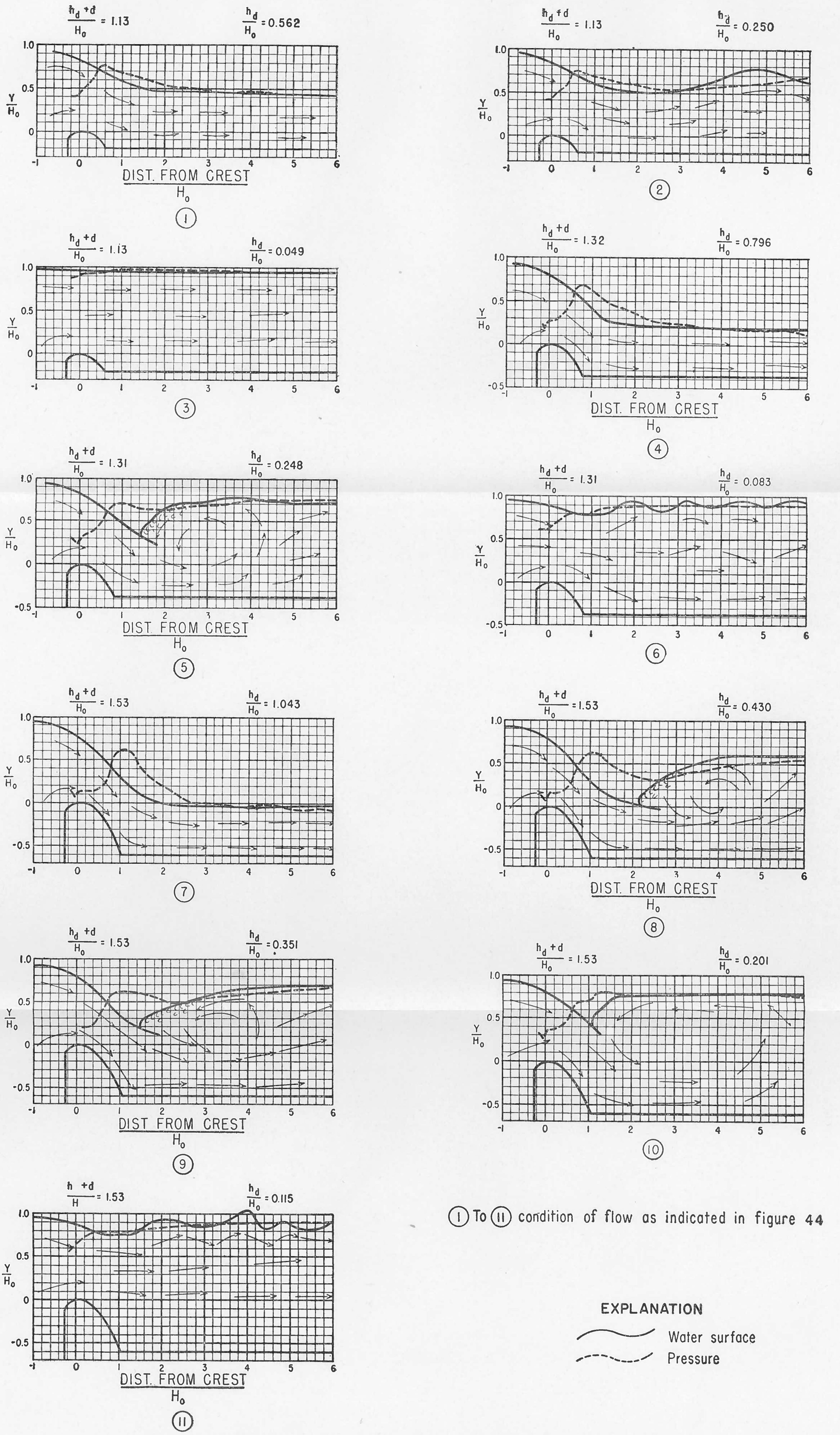

FIGURE 45.—FLOW OVER SUBMERGED DAMS—TYPICAL PRESSURE AND SURFACE PROFILES. 758318°—48 (Faces page 154)

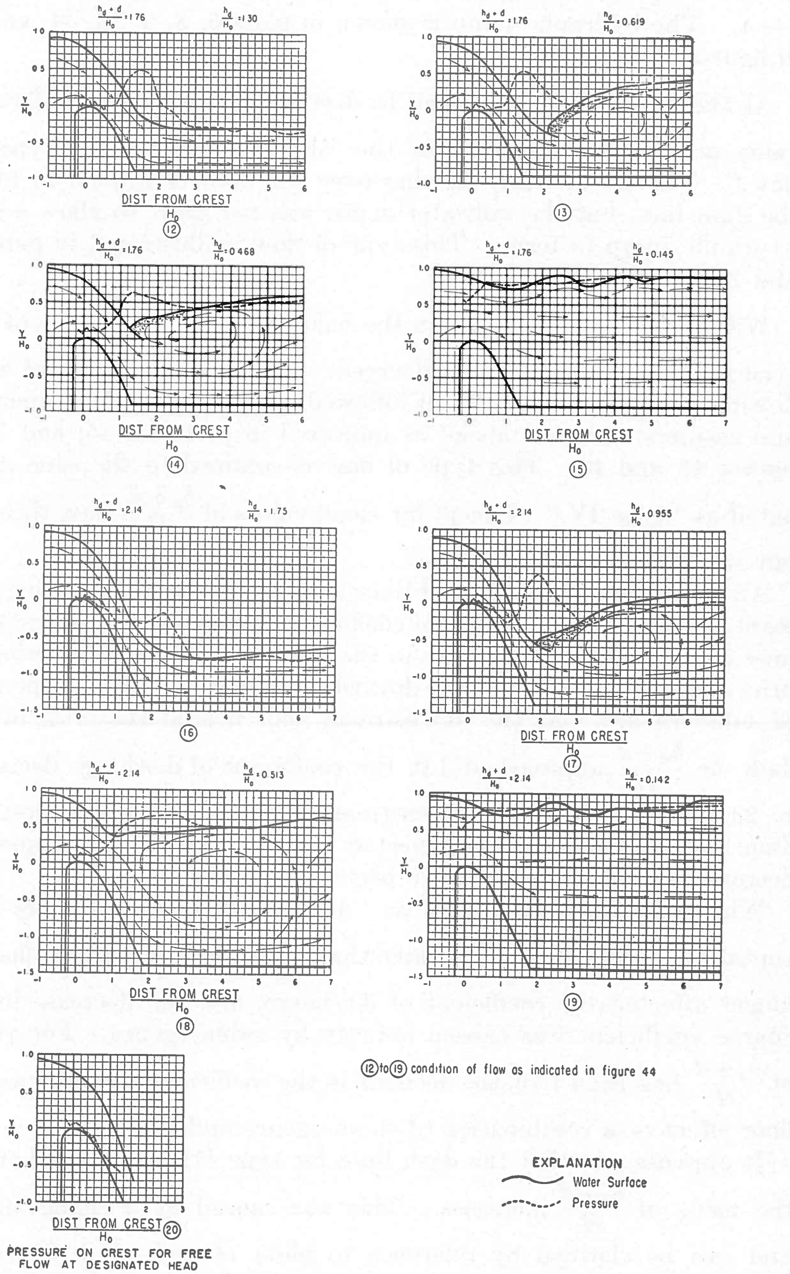

FIGURE 46.—FLOW OVER SUBMERGED DAMS—TYPICAL PRESSURE AND SURFACE PROFILES—Continued.

44–A. The hydraulic jump is shown in plots 5, 8, 9, 13, 14, and 17 of figures 45 and 46.

As the value of $\frac{h_d}{H}$ continued to decrease, a third type of flow became prevalent, designated as the "drowned jump" or "type III flow." The jet of water flowing over the dam continued to follow the dam face, but the tailwater depth was too great to allow a good hydraulic jump to form. This type of flow is illustrated in plots 10 and 18 of figures 45 and 46.

With still further decrease in the value of $\frac{h_d}{H}$, a fourth type of flow occurred, which was truly submerged. In this case, the jet of water flowing over the dam no longer followed down the face, but separated and assumed a course ahead as indicated in plots 11, 15, and 19 of figures 45 and 46. This type of flow is confined to the zone designated as "type IV." Except for small values of $\frac{h_d+d}{H}$, flow throughout zone IV was very unstable.

An inspection of the dashed lines in figure 44–A, representing constant decrease in the discharge coefficient, indicates that where these lines are vertical, the decrease in the coefficient of discharge was due principally to the effect of the downstream floor and was independent of submergence. As the downstream floor neared the crest of the dam, or $\frac{h_d+d}{H}$ approached 1.0, the coefficient of discharge decreased to 23 percent. With the downstream floor level with the crest, the dam was virtually a broad-crested weir for which the theoretical decrease should approximate 23 percent.

Where the lines designated as "decrease in coefficient" are horizontal for values of $\frac{h_d+d}{H}$ greater than 1.70, the downstream floor no longer affected the coefficient of discharge, and the decrease in discharge coefficient was caused entirely by submergence. For values of $\frac{h_d+d}{H}$ less than 1.70, the decrease in the coefficient was produced by floor effect or a combination of submergence and floor effect.

It appears odd that the dash lines for type III flow should rise as the value of $\frac{h_d+d}{H}$ increases. This was caused by a change in flow and can be clarified by reference to plots 14 and 18 in figure 46. Plot 14 is type II flow and plot 18 is type III flow, but the value of $\frac{h_d}{H}$ is practically the same for the two. In the first case, a true hydraulic jump existed and little submergence effect was present. In the second case, the tailwater depth was approximately the same, but the backwater effect was more pronounced. In other words, the point of contact between the jet falling over the dam and the tailwater occurs at $\frac{Y}{H_o}+0.15$ in plot 14 and 0.35 in plot 18. In all cases, the depth of flow on the downstream floor was measured at a point $4H_o$, or four times the designed head, downstream from the crest of the dam.

Free-flow coefficients of discharge have been plotted in figure 44–B against the ratio of the operating head to the designed head on a dam, for different depths of the approach channel. The data for plotting the curves were obtained principally from models tested, over a period of time, in the hydraulic laboratory. A check with similar data from other sources [21] showed excellent agreement. The purpose of the curves in figure 44–B is to aid the designer in determining the reduction or increase in the free-flow coefficient for a given dam operating at other than the designed head.

49. Test Results on Pressures.—In addition to typing the flow and plotting the decrease in the coefficient of discharge for each case, pressures and water-surface profiles were measured along the flume for a few representative types of flow on Dam B. The runs were all made with the dam operating at the designed head, H_o, and the results have been plotted in dimensionless terms with respect to this head, see figures 45 and 46. The axes of coordinates originate at the crest of the dam. The conditions under which the runs were made are indicated by the numbers within the circles in figure 44–A. These runs were made in an effort to provide data on stability determinations for small dams.

50. Application of Results.—The following examples serve to illustrate the use of the foregoing information on submerged dams. Earth-dam spillways are usually flat in longitudinal cross section, since they closely follow the profile of the dam. The gate section and upstream portion of one of these is shown by the dashed line in figure 47 labeled "original design." The coefficient of discharge for this spillway is 2.85. In contrast, the coefficient of discharge for the shape indicated by the solid line labeled "floor positions producing no decrease in discharge coefficient," on the same figure, is 3.68. The latter shape was designed such that the overflow section would fit the shape of the under nappe of the sheet of water flowing over it for the maximum discharge condition, and the downstream floor was lowered sufficiently to produce no decrease in discharge coefficient from that source. This phase of design has been discussed in the preceding pages. The

[21] Lane, E. W., Spillways and Stream-Bed Protection, Davis Handbook of Applied Hydraulics, 1942, p. 341. Voorduin, W. L., Hydraulic Formulas, Davis Handbook of Applied Hydraulics, 1942, p. 23. Cox, Glen Nelson, The Submerged Weir as a Measuring Device, Univ. of Wis., Eng. Exp. Sta. Bull. No. 67.

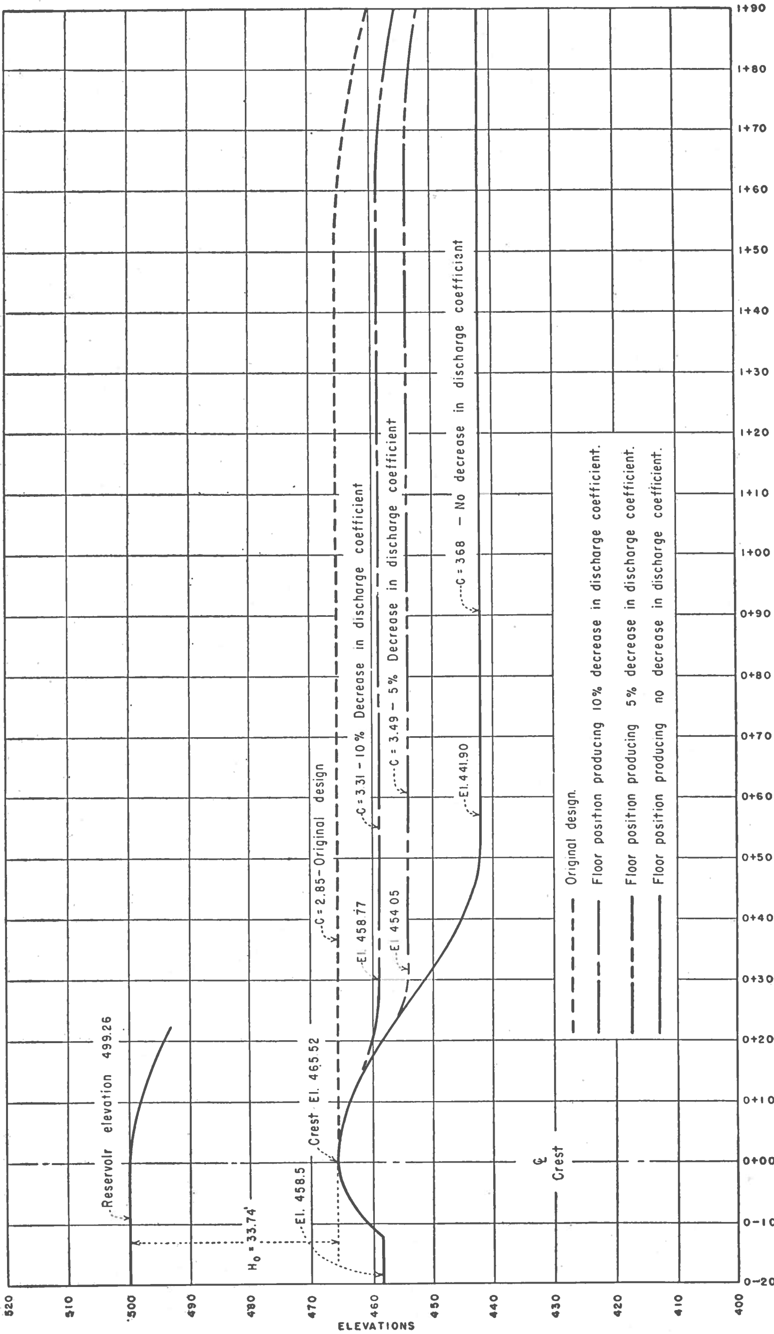

FIGURE 47.—SUBMERGED DAM STUDIES—RESULTS OF EXAMPLE 9.

economy involved in providing a small ogee at the gate section is evident from the above coefficient, and it is now common practice to design earth-dam gate sections in this manner. The following example illustrates the method of determining the position of the floor downstream from the ogee.

> *Example 9.*—Design the downstream portion of the overflow section of the earth-dam spillway in figure 47 for a minimum amount of excavation, allowing no decrease in the free-flow coefficient of discharge for the maximum discharge condition.

The crest of the overflow section is at elevation 465.52 and the total head on the crest is $H_o=33.74$ feet; thus the energy gradient immediately upstream from the crest will be at elevation 499.26 feet. The flow immediately downstream from the overflow section will occur at less than critical depth and will therefore resemble that of type I in figure 44–A. Tailwater is not a consideration in this case.

By following down the line for type I flow, see figure 44–A, to the dashed line labeled "zero percent decrease in the coefficient of discharge," the values of the main coordinates at this point are

$$\frac{h_d}{H_o}=1.24 \text{ and } \frac{h_d+d}{H_o}=1.70$$

$$h_d=1.24\times 33.74=41.84 \text{ feet, and}$$

$$h_d+d=1.70\times 33.74=57.36 \text{ feet.}$$

The position of the floor should therefore be 57.36 feet below the energy gradient for the maximum flow condition, or $499.26-57.36=441.90$ feet in elevation. This floor is indicated by the solid line in figure 47.

The depth of flow on this horizontal floor at a distance $4H_o$, or 120 feet, downstream from the crest is $d=57.36-41.84=15.52$ feet, and graph 12 in figure 46 indicates the type of flow to be expected. The coefficient of discharge for the downstream floor at elevation 441.90 will be 3.68, see figure 47.

The above procedure illustrates the method used in determining the position of the downstream floor for the spillway section of example 5, see figure 9, for no decrease in the coefficient of discharge due to downstream flow conditions. As a matter of interest, the downstream floor positions for decreases of 5 and 10 percent in the coefficient of discharge are also shown in figure 47. The type of flow encountered in the latter two cases will be similar to that shown in graph 4, figure 45. The three floor positions in figure 47 show that the downstream floor can be raised considerably for only a small sacrifice in efficiency. In any case, however, the efficiency of a proposed spillway will necessarily be balanced against certain economic factors. The purpose of the

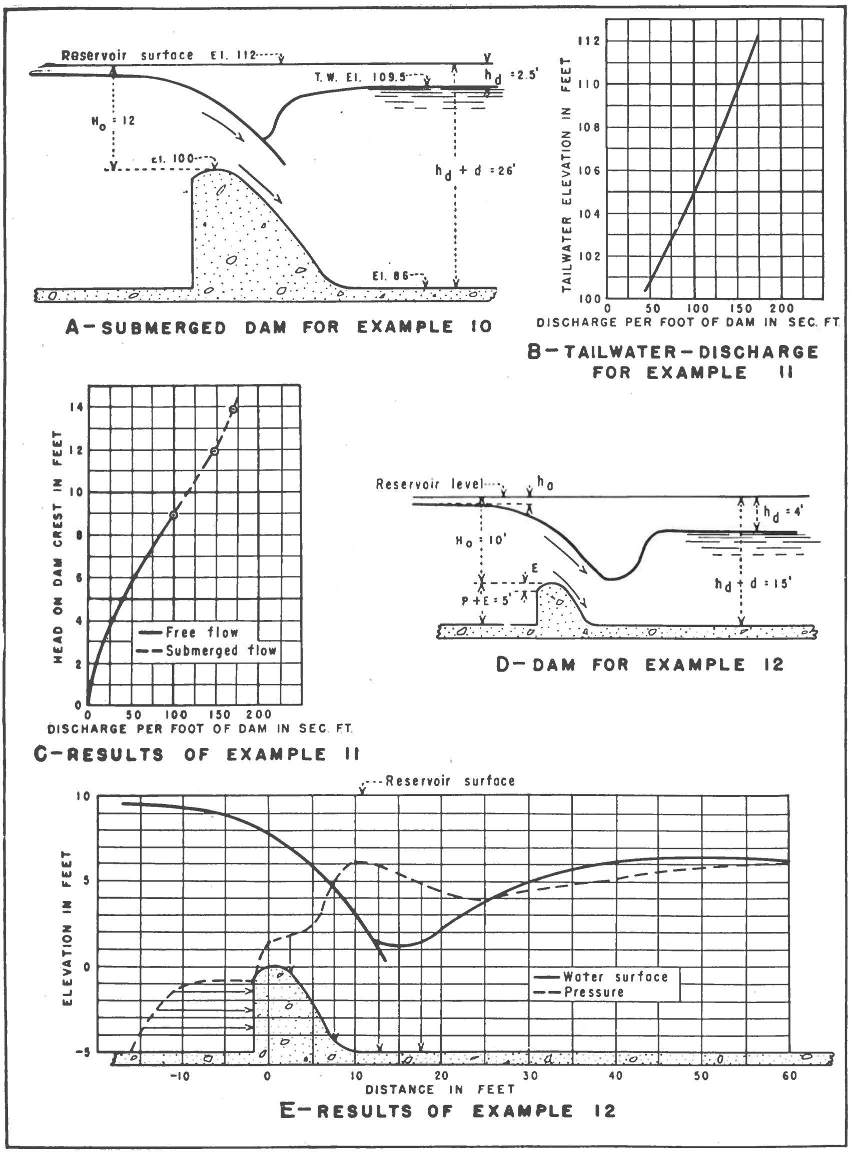

FIGURE 48.—SUBMERGED DAM STUDIES—RESULTS OF EXAMPLES 10, 11, AND 12.

information given in figure 47 is to illustrate the possibility of increasing the efficiencies of earth-dam spillways of this type.

Example 10.—Given the dam shown in figure 48–A, for which the shape and free-flow coefficient of discharge were determined by the method previously described. Compute the discharge per foot of crest length and determine the type of flow which will be encountered for the conditions shown. The free-flow coefficient of discharge is 3.90.

$$\frac{h_d}{H_0}=\frac{2.5}{12}=0.208$$

$$\frac{h_d+d}{H_o}=\frac{26}{12}=2.168$$

Entering figure 44–A with these values, it is found that the point falls within region III. A drowned jump will occur and the coefficient of discharge will be 9 percent less than the free-flow coefficient.

The actual coefficient of discharge for the flow conditions shown will therefore be $C_s=3.90\times 0.91=3.55$.

The discharge per foot of length of dam will be

$$q=CH^{3/2} \tag{21}$$

or

$$q=3.55\times 12^{3/2}=14.75 \text{ second-feet.}$$

These examples serve as an introduction to the use of the curves in figure 44–A. The solution of the following example requires successive approximations.

Example 11.—Given the tailwater curve shown in figure 48–B for the dam in example 10. Compute a headwater curve for the same range of discharges.

One point on the head-discharge curve was determined in example 10. A second point will be chosen for a discharge of 170 second-feet per foot of crest, which will involve greater than the designed head on the crest. This corresponds to a tailwater elevation of 112.0, see figure 48–B.

Assuming $H=13.5$ feet,

$$\frac{h_d}{H}=\frac{1.5}{13.5}=0.111 \text{ and}$$

$$\frac{h_d+d}{H}=\frac{27.5}{13.5}=2.04.$$

From figure 44–A, the decrease in the coefficient of discharge, compared to that for a free crest, is 25 percent; and the flow is indicative of region IV.

The ratio of the estimated head to the designed head is $\frac{13.5}{12}=1.125$.

From graph B in figure 44, the free-flow discharge coefficient for a head of 13.5 feet on the crest and $\frac{P_1+E}{H_0}=\frac{14}{12}=1.165$, is 3.99.

758318°—48——12

The actual coefficient of discharge is therefore $3.99\times0.75=2.99$.

Then

$$H^{3/2}=\frac{q}{C}=\frac{170}{2.99}=56.9, \text{ and } H=14.8 \text{ feet,}$$

which is larger than the assumed value.

Choosing a new value of $H=13.9$, the process is repeated. Other new values are

$$\frac{h_d}{H}=\frac{1.9}{13.9}=0.137,$$

$$\frac{h_d+d}{H}=\frac{27.9}{13.9}=2.007,$$

and

$$\frac{H}{H_o}=\frac{13.9}{12}=1.16.$$

From figure 44–A, $C=18$ percent decrease, and from figure 44–B, C for free crest$=4.00$.

The actual coefficient of discharge for the case at hand is

$$C_s=4.00\times0.82=3.28.$$

Then

$$H^{3/2}=\frac{170}{3.28}=52.0, \text{ and } H=13.93 \text{ feet,}$$

which agrees reasonably well with the assumed value. This locates a second point on the head-discharge curve in figure 48–C.

An attempt now will be made to determine the head at which submergence begins. Choosing a discharge of 100 second-feet, the tailwater is at elevation 105.0, see figure 48–B.

Assuming

$$H=9 \text{ feet,}$$

$$\frac{h_d}{H}=\frac{4}{9}=0.445,$$

$$\frac{h_d+d}{H}=\frac{23}{9}=2.558,$$

and

$$\frac{H}{H_o}=\frac{9}{12}=0.75.$$

From figure 44–A, $C=1.7$ percent decrease, and from figure 44–B, the free-flow coefficient $C=3.77$.

Then

$$C_s=3.77\times0.983=3.706,$$

$$H^{3/2}=\frac{100}{3.706}=27.0, \text{ and } H=9.00 \text{ feet.}$$

This agrees with the assumed head and thus locates a third value very close to the point at which submerged flow begins. The remainder of the curve is completed by substituting free-flow coefficients in the equation $q = CH^{3/2}$. The complete head-discharge curve is shown in figure 48–C.

Example 12.—From the dimensions shown in figure 48–D, determine the approximate water surface and the hydraulic pressures opposing uplift on the dam and apron, for the head and tailwater elevations given. The free-flow coefficient $C=3.80$.

From figure 44–A,

$$\frac{h_d}{H_o} = \frac{4}{10} = 0.40$$

and

$$\frac{h_d + d}{H_o} = \frac{15}{10} = 1.50.$$

The curves also show that a hydraulic jump can be expected downstream from the dam for these conditions, accompanied by a 2.5 percent decrease in the coefficient of discharge. The decrease is produced principally by floor effect and not submergence. Figure 44–A also indicates that flow over the dam will be similar to that shown in graphs 8 and 9 of figure 45. It should again be mentioned that the diagrams in figures 45 and 46 are for flow at the designed head only, at which pressures on the dam for the free-flow condition approach zero.

The water-surface and pressure curves for example 12 can be obtained by averaging the coordinates from graphs 8 and 9, figure 45, and multiplying the values by H_o as outlined in table 38.

TABLE 38.—PRESSURES AND WATER SURFACE PROFILES ON DOWNSTREAM APRON—EXAMPLE 12

$\frac{X}{H_0}$	X, feet	Water surface		Pressure profile	
		$\frac{Y}{H_0}$	Y, feet	$\frac{Y}{H_0}$	Y, feet
−1.0	−10	0.92	9.2		
−0.5	−5	0.89	8.9		
0.0	0	0.79	7.9	0.15	1.5
0.5	5	0.59	5.9	0.24	2.4
1.0	10	0.31	3.1	0.62	6.2
1.5	15	0.13	1.3	0.55	5.5
2.0	20	0.22	2.2	0.44	4.4
2.5	25	0.38	3.8	0.41	4.1
3.0	30	0.49	4.9	0.45	4.5
3.5	35	0.57	5.7	0.49	4.9
4.0	40	0.62	6.2	0.52	5.2
5.0	50	0.64	6.4	0.58	5.8
6.0	60	0.64	6.4	0.62	6.2

The water surface and hydraulic gradient from table 38 have been plotted in figure 48–E. The pressures have been plotted vertically above the points at which they were measured.

The pressures on the upstream face of the dam can be obtained from figure 17. To illustrate the method of procedure, the pressures on the upstream face of the dam in example 12 will be determined.

$$C_s=3.80\times 0.975=3.706,$$

$$q=CH^{3/2}=3.706\times 10^{3/2}=117.2 \text{ second-feet per foot of crest.}$$

$$V_a=\frac{q}{A}=\frac{117.2}{15}=7.81 \text{ feet per second,}$$

and

$$h_a=\frac{V_a^2}{2g}=\frac{(7.81)^2}{2g}=0.948 \text{ feet (velocity head of approach).}$$

$$\frac{h_a}{H_o}=\frac{0.948}{10}=0.0948.$$

Entering figure 27 with this value,

$$\frac{H_s}{H_o}=1.084 \text{ for the vertical-face dam,}$$

and

$$H_s=1.084\times 10=10.84 \text{ feet.}$$

Then

$$\frac{h_a}{H_s}=\frac{0.948}{10.84}=0.0875.$$

Entering figure 15–A with this value of $\frac{h_a}{H_s}$,

$$\frac{E}{H_s}=0.078,$$

and

$$E=0.078\times 10.84=0.85 \text{ feet.}$$

By choosing values of $\frac{d}{H_s}$ and making use of figure 17, the pressures on the upstream face of the dam are obtained. The method is illustrated in table 39, for which the coordinates are referred to the spring point of the overflow section and are shown plotted in figure 48–E. The next step constitutes determining the forces produced by uplift pressures, weight of the concrete in the dam and apron, and other loads; then the dam and apron can be analyzed in sections or as a whole for stability. This example purposely supplies only the downward and horizontally acting hydraulic pressures on the dam and apron.

TABLE 39.—PRESSURES ON UPSTREAM FACE OF DAM—EXAMPLE 12

$\frac{h_a}{H_s}=0.0875$ $H_s=10.84$ feet

d, feet	$\frac{d}{H_s}$	$\frac{H_s-h_p}{H_s}$	h_p, feet	h_p+d, feet
0. 0	0. 000	1. 000	0. 00	0. 00
0. 1	0. 009	0. 400	6. 50	6. 60
0. 2	0. 018	0. 300	7. 59	7. 79
0. 5	0. 046	0. 210	8. 56	9. 06
1. 0	0. 092	0. 120	9. 54	10. 54
2. 0	0. 184	0. 060	10. 19	12. 19
3. 0	0. 277	0. 035	10. 46	13. 46
4. 0	0. 369	0. 024	10. 58	14. 58

CHAPTER VIII—OVERFLOW SECTIONS FOR HOOVER DAM SPILLWAYS

ANALYSIS OF DISCHARGE COEFFICIENTS

51. Scope of Tests.—In the design of the overflow section for the Hoover Dam spillways, reliable information was especially lacking concerning efficient sections with high discharge coefficients. The Hoover Dam spillways were of such unprecedented magnitude that neither efficiency nor safety could be ignored. It was to insure satisfactory design of these structures that the experiments described in this bulletin were instigated. It happened, however, that the experimental field proved much too broad to cover satisfactorily in the few months allotted for study prior to construction of the spillways. Therefore, the next alternative was to design the overflow sections from the best design data available at the time and to construct hydraulic models of these from which the discharge capacity and pressures could be actually observed. This was done, on a more or less cut-and-try basis. The studies described in this chapter were made previous to the development of the experimental data described in the first chapters of this bulletin; so that there is no logical connection between the two as far as order or material is concerned. The following information is therefore a chronological development of the final Hoover Dam spillway overflow section to supplement the material in Bulletin 1 of Part VI, "Model Studies of Spillways."

52. Glory-Hole Spillway, Model C–1.—Two morning-glory-type spillways were proposed, see page 19 of Bulletin 1, Part VI. The model showed that it would be economically impossible, with the pattern of approach channel required by conditions at Hoover Dam, to secure a satisfactory condition of flow over the crest and in the vertical shaft. A concentration of flow occurred along a radial line from the center of the shaft to that part of the crest nearest the canyon wall, where the two approach channels met. As a result of this concentration, water did not flow down the shaft equally distributed around the wall, but rather in a concentrated stream that jumped across the top of the shaft from the side next to the canyon wall, finally dropping down the shaft with an irregular distribution.

As the depth of flow over the spillway increased, the concentrated flow over the crest next to the canyon wall tended to seal the top of the shaft from the side next to the canyon wall, finally dropping down the shaft with an irregular distribution.

As the depth of flow over the spillway increased, the concentrated flow over the crest next to the canyon wall tended to seal the top of the shaft, causing an undesirable suction and pulsation which interfered with the operation of the spillway. Since it was not economically feasible to locate the spillways so as to avoid the concentration of flow, work on the glory-hole type of spillway was discontinued and studies were concentrated on the side-channel type.

53. Side-Channel Spillway With Free Crest, Model C–2.—The first side-channel spillway, with free crest, is described on page 22 of Bulletin 1, Part VI. The model was constructed on a scale of 1:60. A profile of the overflow section, together with coordinates and the coefficient-of-discharge curve, is shown in figure 49. The section was designed for a head of 10.9 feet and a discharge of 100 thousand second-feet. The coefficient of discharge increased uniformly up to a head of 14 feet, at which point a coefficient of 4.07 was reached. The coefficient then dropped, due to submergence of the crest by backwater in the side channel. It appears that, were it not for this submergence, the coefficient would have continued to increase beyond 4.07; this indicates that subatmospheric pressures existed on the overflow section, since the maximum coefficient obtained on the vertical-face weir in the experiments described in chapter III of this bulletin was only 3.95. No measurements were made of pressures on the model.

Utilizing the data from the vertical-face weir experiments of chapter III, the overflow section was redesigned for a discharge of 142.9 second-feet per foot of crest, a head of 10.9 feet, and an approach depth equal to four times the head. The coefficient of discharge obtained in this study was 3.98 for the design head. The resulting shape is indicated by the dotted line in the lower part of figure 49. The profiles obtained by the two methods agree surprisingly well. The difference in coefficients probably indicates that very slight negative pressures did exist on the original section.

54. Side-Channel Spillway With Stoney Gate and Free Crest, Model C–3.—The second side-channel spillway design consisted of a channel with a Stoney gate at the upstream end and a free crest length of 400 feet, as described on page 38 of Bulletin 1, Part VI. The overflow section, see figure 50, was designed for a maximum discharge of 50 thousand second-feet at a head of 10.7 feet, and the model was on a scale of 1:60. The depth of approach to the major portion of the overflow section was 6 feet; this is reflected in the coefficient of discharge, which reached a maximum of 3.82, but reached only 3.67 for the designed head. Large contractions at each end of the overflow section interfered with normal flow over the crest thus reducing the

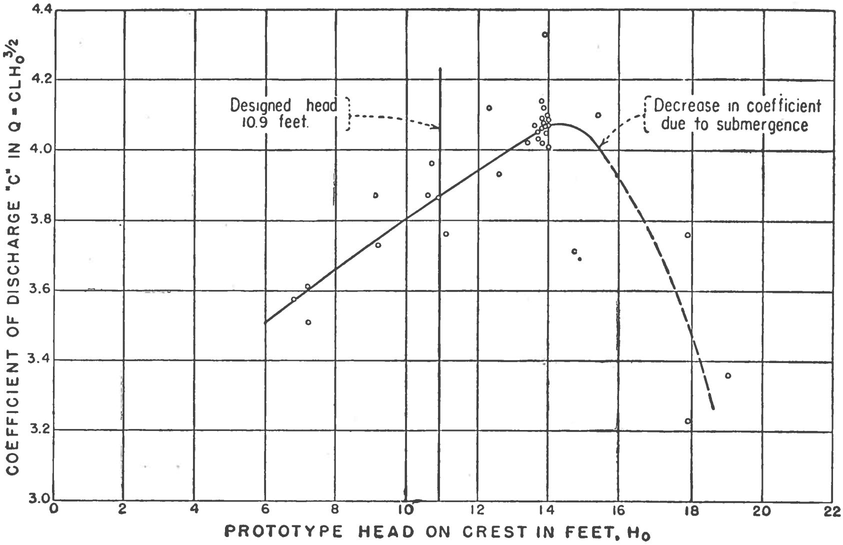

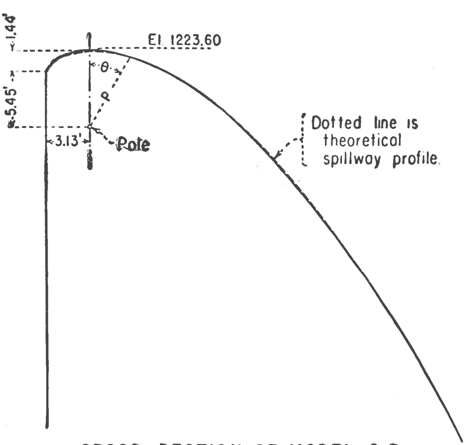

TABLE OF CREST COORDINATES

θ	P, FEET	θ	P, FEET
− 35°	5.14	40°	6.02
− 30°	5.32	50°	6.43
− 25°	5.40	60°	7.03
− 20°	5.43	70°	7.85
− 15°	5.45	80°	9.05
− 10°	5.45	90°	10.73
− 5°	5.45	100°	13.06
0°	5.45	110°	16.93
10°	5.46	120°	23.17
20°	5.56	130°	33.86
30°	5.73	CREST CONTINUES FROM LAST POINT ON ½:1 SLOPE	

CROSS SECTION OF MODEL C-2
FREE CREST WITHOUT GATES OR PIERS
SCALE RATIO 1:60

FIGURE 49.—COEFFICIENT-OF-DISCHARGE CURVES—MODEL C-2.

coefficient of discharge. Wing walls were installed at each end of the overflow section to remedy this condition, and it appears from the coefficient-of-discharge curve, shown as a dash line in figure 50, that these were very effective. The maximum coefficient was raised to 4.02 and the designed-head coefficient to 3.77. The hydraulic characteristics of the Stoney gate have been discussed in Bulletin 1 of Part VI.

55. Side-Channel Spillway With Drum Gates, Models M–1, M–2, and M–3.—At this stage of the design it was decided to increase the discharge capacity to 200 thousand second-feet per spillway for a head of 26.6 feet on the crest and to install four 16 by 100-foot drum gates on the overflow section, as described on page 54 of Bulletin 1, Part VI, thus making a clear crest length of 400 feet. Addition of the drum gates made it necessary to abandon the more efficient overflow shapes, such as were used on models C–2 and C–3. In this series of model tests several crest shapes were studied on each model, of which shapes 3 to 8 are shown in figures 51 to 55, inclusive. A profile of shape 3, model M–1, with coordinate points is shown at the left of figure 51. The coefficient-of-discharge curve, shown at the top of the same figure, for the gates fully down indicates a coefficient of 3.53 for the designed head of 26.6 feet. This is considerably lower than for the two previous shapes, as would be expected. The model was constructed to a 1:20 scale.

Model M–2, described on page 75 of Bulletin 1, Part VI, embodied the same overflow shape as the M–1 model but was constructed on a 1:100 scale, was of opposite hand, and was without piers or gates. No record of a calibration can be found for this model.

Model M–3 was constructed to a scale of 1:20, as described on page 97 of Bulletin 1. This and all subsequent designs described in this chapter were planned for a maximum discharge of 200 thousand second-feet, a maximum head of 26.6 feet on the crest, and four 16 by 100-foot drum gates on the overflow section. Two shapes, namely, 3 and 4, were studied on model M–3, for which calibration curves were available, see figure 51. The M–3 shapes varied from the M–1 profile only in the upstream portion. The coordinates downstream from the point of compound curve were the same in all three cases. Shape 3, model M–3, is indicated by the full line on the right profile in figure 51, and the coefficient curve is plotted as a full line at the top of the same figure. The profiles for model M–1, shape 3, and model M–3, shape 3, are identical except that the crest was established at elevation 1205.7 on the former and elevation 1205.4 on the latter. The coefficient-of-discharge curves for these two are also practically identical for heads up to 20 feet. Above this point the variation is due to a difference in the degree of submergence. The crest elevation for all

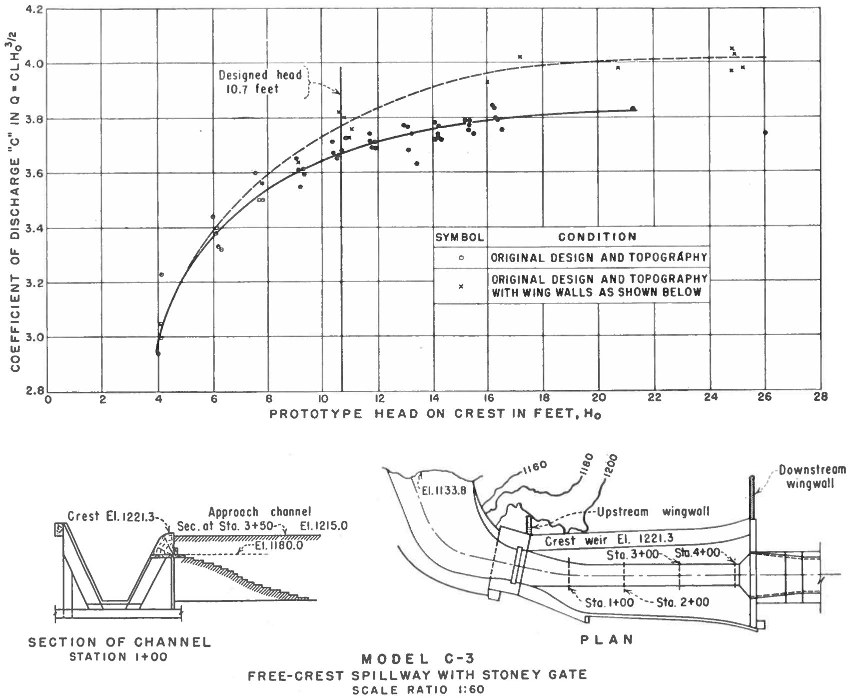

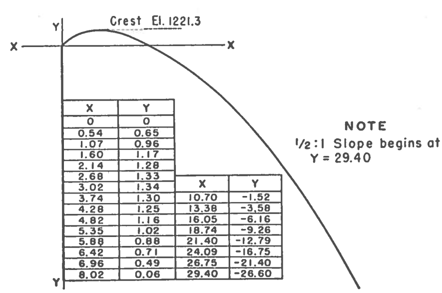

X	Y
0	0
0.54	0.65
1.07	0.96
1.60	1.17
2.14	1.28
2.68	1.33
3.02	1.34
3.74	1.30
4.28	1.25
4.82	1.16
5.35	1.02
5.88	0.88
6.42	0.71
6.96	0.49
8.02	0.06

X	Y
10.70	-1.52
13.38	-3.58
16.05	-6.16
18.74	-9.26
21.40	-12.79
24.09	-16.75
26.75	-21.40
29.40	-26.60

COORDINATES OF CREST

FIGURE 50.—COEFFICIENT-OF-DISCHARGE CURVES—MODEL C-3.

subsequent designs was fixed at 1205.4. Shape 4, model M–3, indicated by a dash line on the right profile in figure 51, was calibrated for five positions of the gates. The highest coefficient obtained with the gates in the lowest position is 3.65, which represents an improvement over the M–1 shape. The coefficient, however, drops to 3.62 at the designed head, due to submergence of flow from the side channel. The discharge coefficients for the gates in the raised positions are considerably higher than those for the gates in the lowered positions. It is true that the discharge for a given head should be greater for a jet springing free from the edge of a gate than for flow over the

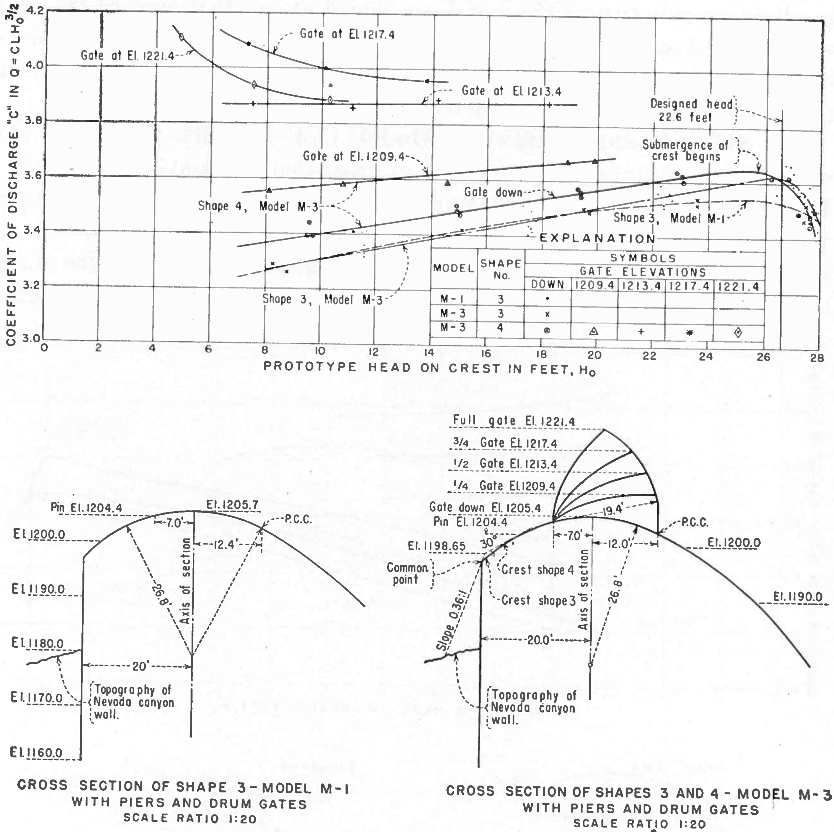

COORDINATES DOWNSTREAM FROM P.C.C.

ELEVATION	DIST. FROM AXIS	ELEVATION	DIST. FROM AXIS
1202.6 *	12.4 *	1160.0	52.4
1200.0	17.0	1155.0	55.1
1197.5	20.8	1150.0	57.8
1195.0	24.0	1140.0	63.1
1192.5	26.8	1130.0	67.8
1190.0	29.5	1120.0	72.4
1185.0	34.2	1110.0	76.7
1180.0	38.2	1100.0	80.8
1175.0	42.2	1090.0	84.9
1170.0	45.6	1080.0	88.8
1165.0	49.0	1070.0	92.4

* POINT OF TANGENCY WITH CIRCULAR CREST.

FIGURE 51.—COEFFICIENT-OF-DISCHARGE CURVES—SHAPES 3 AND 4, MODELS M-1 AND M-3.

broad overflow section. However, with the gate in the raised position the head is measured above the tip of the gate rather than above the high point of the nappe as with the gate in the lowered position. Computing the coefficients for raised positions of the gates on the basis of the head above the high point of the nappe would give even larger values than are shown in figure 51. As a matter of clarification, it should be stated that the abscissa of the graph in figure 51, in all cases constitutes the head measured above the crest of the spillway (1205.4 or 1205.7, whichever applies), while the ordinate or coefficient of discharge was computed using the head measured above the lip of the gate, which varies with each gate setting.

56. Side-Channel Spillway, Model C–4.—Model C–4 was constructed on a 1:60 scale with gates, as described on page 77 of Bulletin 1, Part VI. The downstream coordinates were the same as for the previous shape. Three different sections have been recorded for the upstream portion; namely, shapes 5, 6, and 7, all of which are shown in figure 52. Coefficient curves for these three shapes with the gates

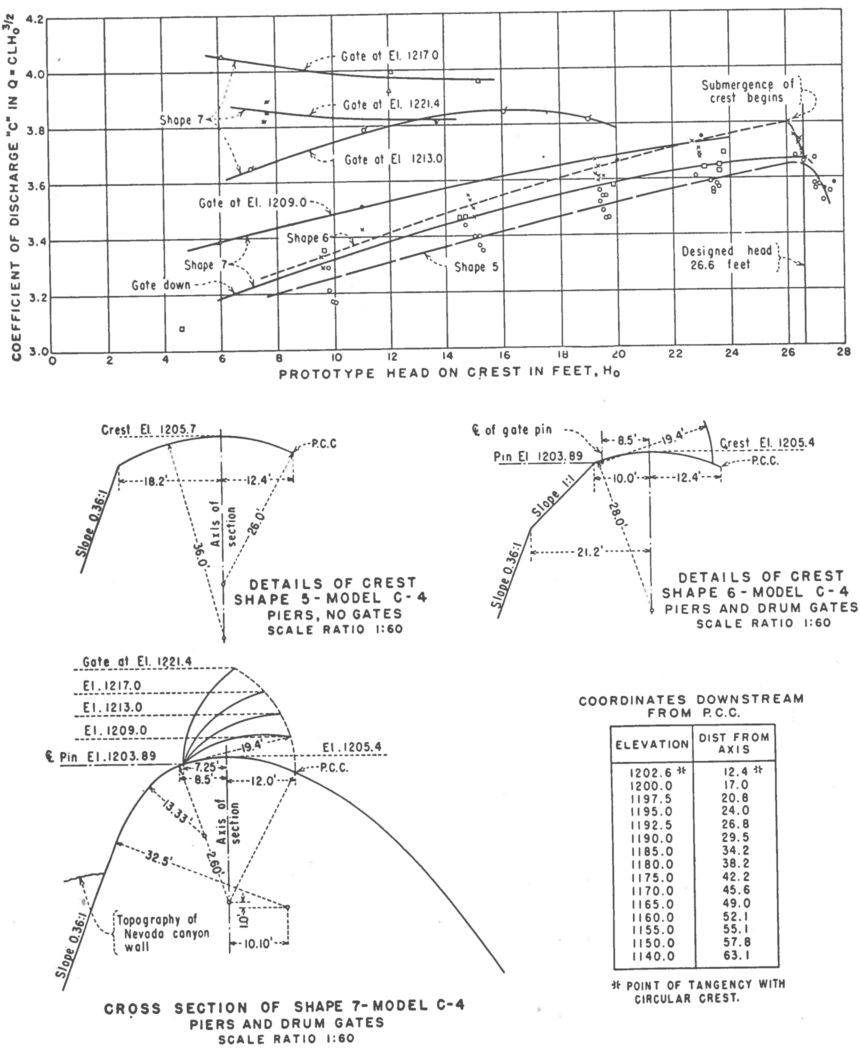

COORDINATES DOWNSTREAM FROM P.C.C.

ELEVATION	DIST FROM AXIS
1202.6 *	12.4 *
1200.0	17.0
1197.5	20.8
1195.0	24.0
1192.5	26.8
1190.0	29.5
1185.0	34.2
1180.0	38.2
1175.0	42.2
1170.0	45.6
1165.0	49.0
1160.0	52.1
1155.0	55.1
1150.0	57.8
1140.0	63.1

* POINT OF TANGENCY WITH CIRCULAR CREST.

FIGURE 52.—COEFFICIENT-OF-DISCHARGE CURVES—SHAPES 5, 6, AND 7, MODEL C–4.

in the down position have been plotted in the same figure. Shape 5 shows a maximum coefficient of 3.65, while shape 6 shows one of 3.80. Shape 7, which was calibrated for five positions of the gates, and appears offhand to represent the best design, shows a maximum coefficient of only 3.67 for the gates down. The discharge coefficients for the gates in the raised positions do not compare favorably with those for shape 4, model M–3, shown in figure 51. However, coefficient data for these positions are meager for both models.

During the work on shape 7, model C–4, a short study was made to determine the effect produced on the coefficient of discharge by changing the length of the nose on the piers. Four pier noses were tried and, as shown by the coefficient curves in figure 53, the effect of length of pier nose was practically negligible. The total spread in the coefficient of discharge amounts to only 0.5 percent. From an observer's standpoint, flow conditions around the piers with the longer noses are preferable; however, the length of the pier nose can be carried to an extreme. Of the four piers shown in figure 53, pier 3 is probably the most practical.

57. Side-Channel Spillway, Model C–7.—Model C–7 was constructed on a 1:60 scale for calibration purposes only. The section was constructed to conform to shape 7 and included piers but no drum gates. The side-channel portion was made larger than the scale ratio would dictate in order to eliminate submergence of the crest at the higher discharges, and the topography was made removable to various elevations. This model was constructed for the purposes of studying the effect of the upstream excavation on the coefficient of discharge. The results are plotted on figure 54 for five different depths of excavation. The maximum deviation in the coefficient for the designed head amounts to 3 percent for the two extreme elevations of cut; namely, 1,200 and 1,055. Some intermediate elevation of cut would no doubt prove the most economical design. The depth of approach excavation on the Nevada and the Arizona spillways was determined from these tests.

58. Comparison of Models M–5, C–5, and C–6, Final Design.—A section of the final design overflow shape, shape 8, which was used on the Hoover Dam spillways is shown in figure 55. The crest was located at elevation 1,205.4 and the drum gates had a lift of 16 feet to elevation 1,221.4. The upstream faces of the spillways varied from vertical to a slope of 1/2:1, depending on the topography at the site.

Three identical models were constructed with shape 8, to scale ratios of 1:20, 1:60, and 1:100. The first two were complete with gates and piers and the third included piers but not gates. These tests were made when hydraulic model testing was in its infancy and

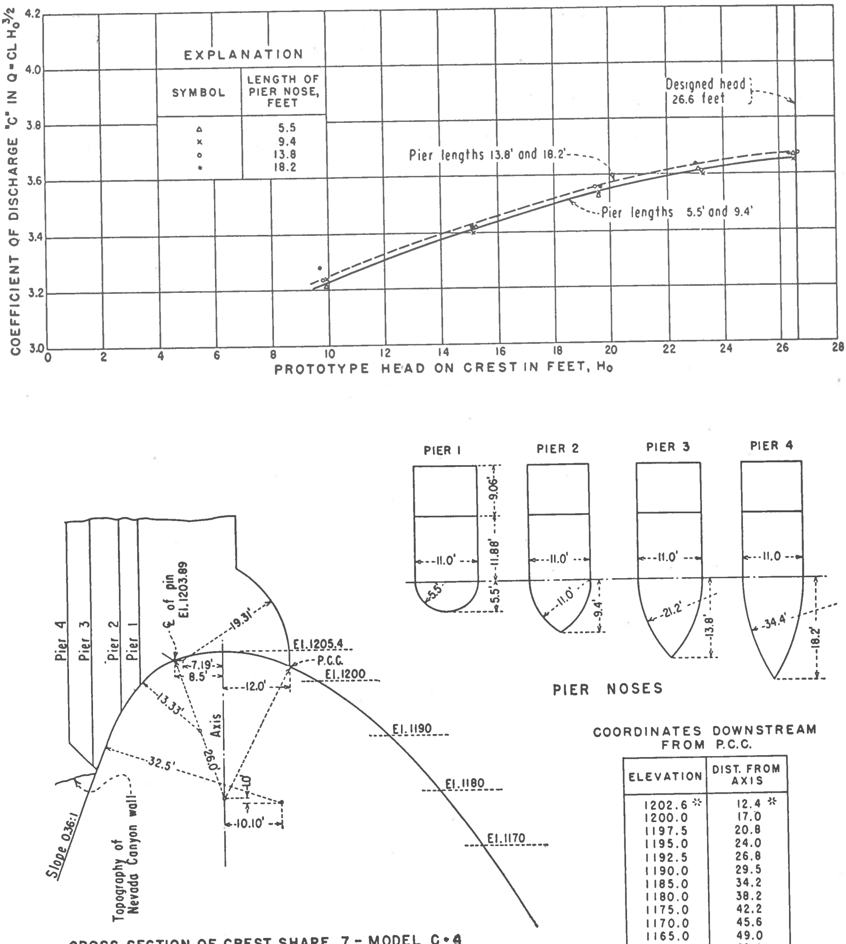

ELEVATION	DIST. FROM AXIS
1202.6 *	12.4 *
1200.0	17.0
1197.5	20.8
1195.0	24.0
1192.5	26.8
1190.0	29.5
1185.0	34.2
1180.0	38.2
1175.0	42.2
1170.0	45.6
1165.0	49.0
1160.0	62.1
1155.0	55.1
1150.0	57.8
1140.0	63.1

* POINT OF TANGENCY WITH CIRCULAR CREST.

FIGURE 53.—VARIATION OF DISCHARGE COEFFICIENT WITH SHAPE OF PIER NOSE—MODEL C-4.

it was desired to investigate the practicability of the similitude relationships. These three models and their behavior have been discussed on page 122 of Bulletin 1, Part VI. The discharge coefficients are compared in figure 55. For the gates in the down position, the coefficients for the three models were plotted against the head and an average curve drawn through the points. There is some spread in the points but, as a whole, the plot is as satisfactory as can be expected. For the raised positions of the gates, only two sets of points were available. These have been plotted for four gate positions in figure 55.

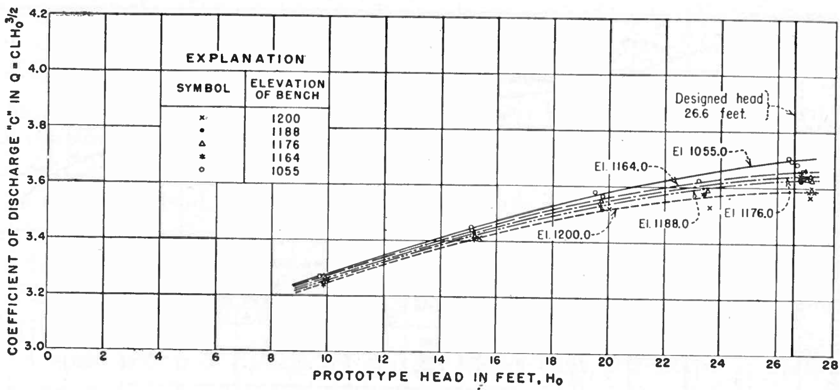

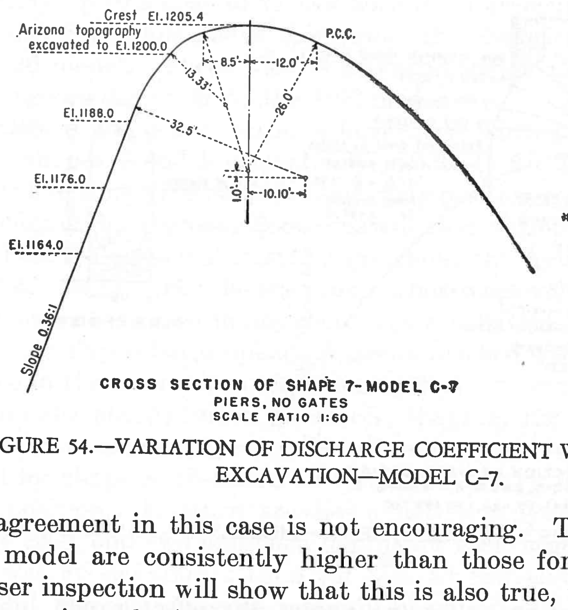

COORDINATES DOWNSTREAM FROM P.C.C.

ELEVATION	DIST. FROM AXIS
1202.6	12.4
1200.0	17.0
1197.5	20.8
1195.0	24.0
1192.5	26.8
1190.0	29.5
1185.0	34.2
1180.0	38.2
1175.0	42.2
1170.0	45.6
1165.0	49.0
1160.0	52.1
1155.0	55.1
1150.0	57.8
1140.0 *	63.1 *

* BEGINNING OF 1/2:1 SLOPE.

FIGURE 54.—VARIATION OF DISCHARGE COEFFICIENT WITH UPSTREAM EXCAVATION—MODEL C-7.

The agreement in this case is not encouraging. The points for the 1:60 model are consistently higher than those for the 1:20 model. A closer inspection will show that this is also true, to a lesser extent, for the points obtained with the gates fully down. The points for the 1:100 model are higher than those for the 1:60 model, but the order is not consistent; however, in general, the smallest scale model appears to have the highest coefficients and the largest scale model the lowest coefficients. To what extent experimental errors, such as may have been made in the discharge and head measurements, are involved, it is now difficult to surmise. However, it is known that there was considerably more turbulence present in the larger scale model than in the smaller two. Therefore, if any difficulty was en-

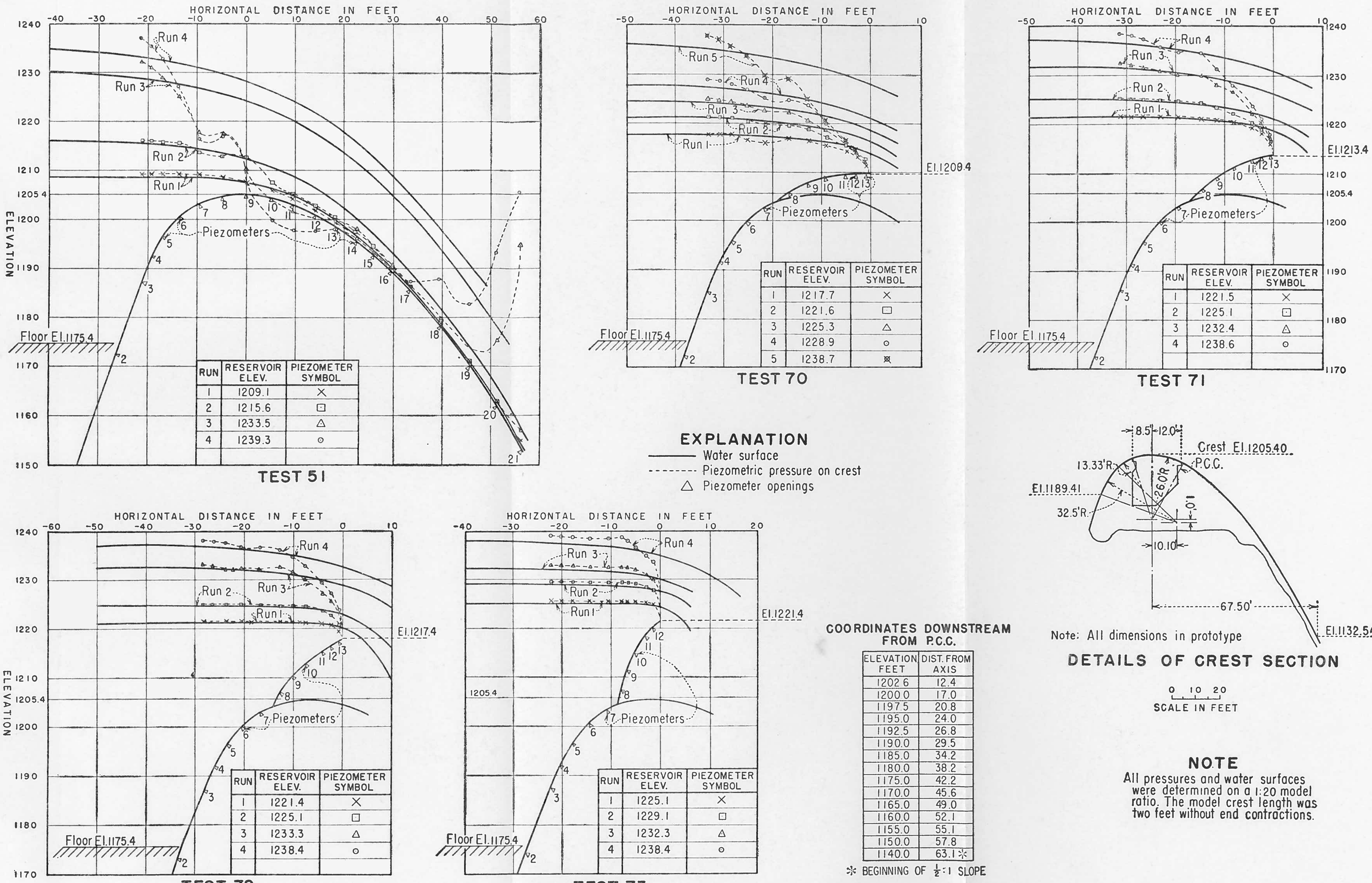

COORDINATES DOWNSTREAM FROM P.C.C.

ELEVATION FEET	DIST. FROM AXIS
1202.6	12.4
1200.0	17.0
1197.5	20.8
1195.0	24.0
1192.5	26.8
1190.0	29.5
1185.0	34.2
1180.0	38.2
1175.0	42.2
1170.0	45.6
1165.0	49.0
1160.0	52.1
1155.0	55.1
1150.0	57.8
1140.0	63.1 ✻

✻ BEGINNING OF $\frac{1}{2}$:1 SLOPE

NOTE

All pressures and water surfaces were determined on a 1:20 model ratio. The model crest length was two feet without end contractions.

FIGURE 57.—WATER SURFACES AND PIEZOMETRIC PRESSURES—SHAPE 7, MODEL C-8.

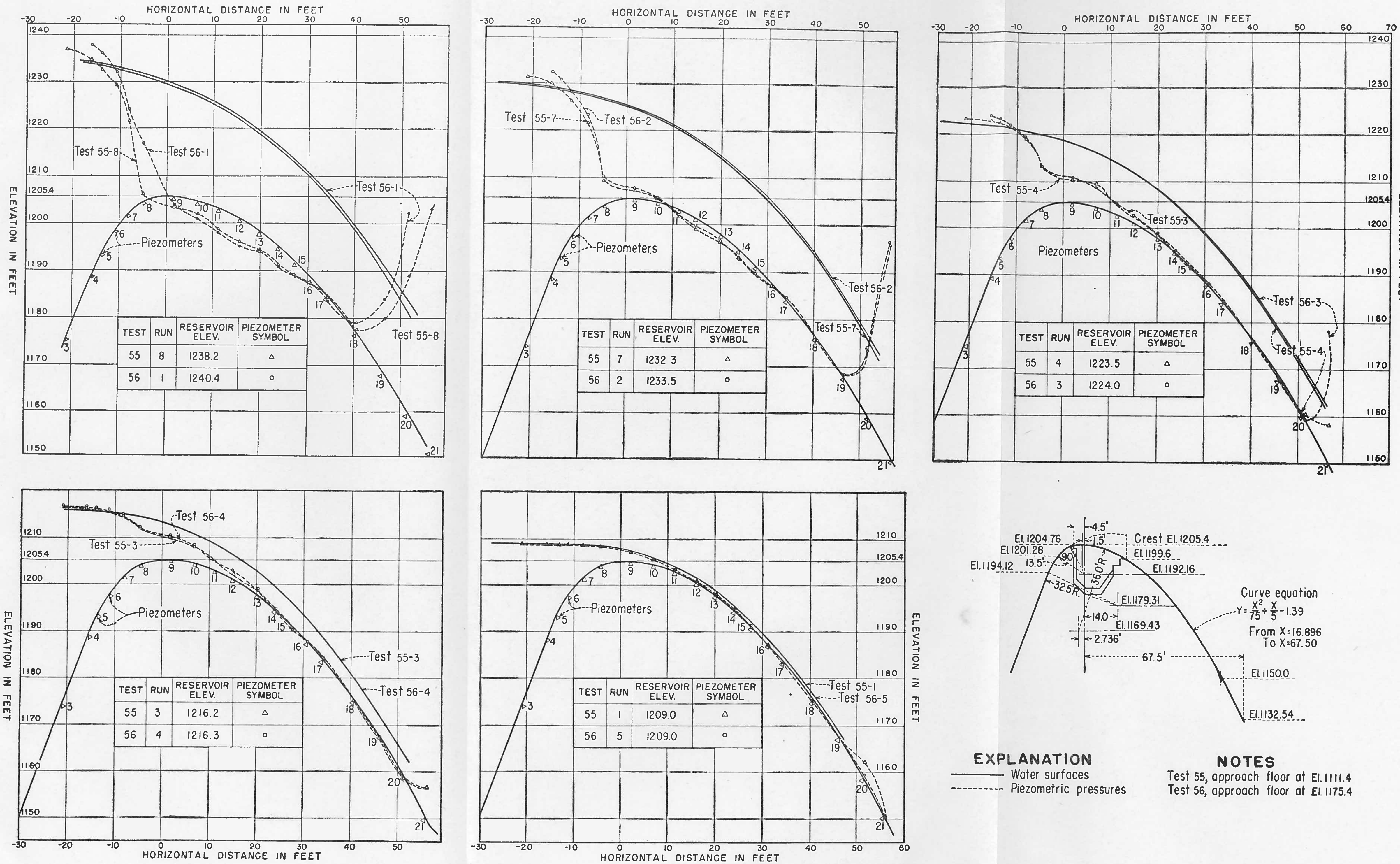

FIGURE 58.—WATER SURFACES AND PIEZOMETRIC PRESSURES—SHAPE 8, MODEL C-8.

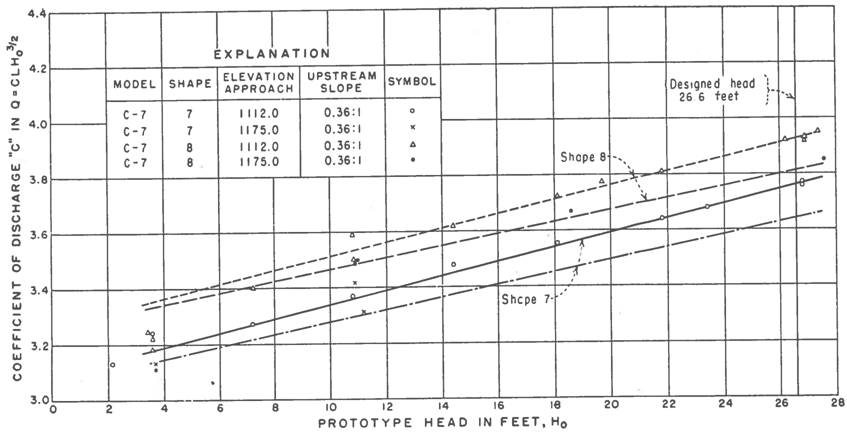

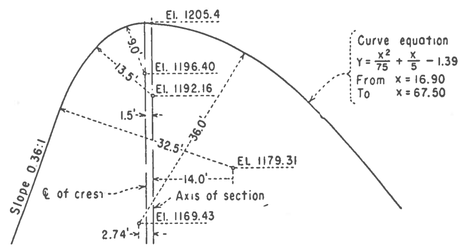

CROSS SECTION SHAPE 8 - MODEL C-8
(FINAL DESIGN)
NO GATES OR PIERS
SCALE RATIO 1:20

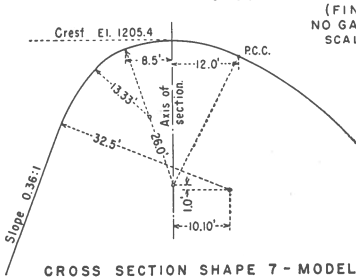

CROSS SECTION SHAPE 7 - MODEL C-8
GATE BUT NO PIERS
SCALE RATIO 1:20

NOTE: This model was 2 feet wide or 40 feet prototype.

COORDINATES DOWNSTREAM FROM P.C.C.

ELEVATION	DIST. FROM AXIS
1202.6 *	12.4 *
1200.0	17.0
1197.5	20.8
1195.0	24.0
1192.5	26.8
1190.0	29.5
1185.0	34.2
1180.0	38.2
1175.0	42.2
1170.0	45.6
1165.0	49.0
1160.0	52.1
1155.0	55.1
1150.0	57.8
1140.0	63.1

* POINT OF TANGENCY WITH CIRCULAR CREST.

FIGURE 56.—COEFFICIENT-OF-DISCHARGE CURVES—MODEL C-8.

An attempt was made to cover the field as completely as possible in the time available, yet much remains to be done. The field still remains open for research on low dams, which, in the majority of cases, involves the most difficult solutions. In addition, the value of the experimental information condensed in this bulletin will depend on the extent to which it proves to be practical and useful. This can only be determined by general practice, over a period of time.

This study does not include the design of overfall shapes with vacuum pressures on the face. Such designs are permissible for certain conditions, but require considerable judgment and experience on the part of the designer.

BIBLIOGRAPHIES

The following bibliographies include references to some of the more important published articles and reports on studies of overfall and submerged dams.

A list of the bulletins being published as Boulder Canyon Project Final Reports, with prices shown for those now available for distribution, is given at the end of this report.

61. Bibliography on Overflow Dams:

1. Anonymous.
Luftwiderstand des fallenden Wasserstrahles, (Air Resistance to Falling Jets of Water), Zentralblatt der Bauverwaltung, Vol. 30, 1910, pp. 481, 530 and 572.
2. Bharadwaj.
Theory of Broad-Crested Weir, Indian Engineering, Vol. 100, 1936, p. 202.
3. Borland, W. M.
Coefficients of Discharge for Rounded Crest Weirs, Thesis, Univ. of Colorado, 1938.
4. Boussinesq.
L'ecoulementen deversoir (The Flow over Spillways), Memoir de l'Academie, 1907.
5. Bradley, J. N.
Comparison of Discharge Coefficients for Various types of Overflow Spillway Sections, Bur. of Recl. Hyd. Lab. Report 208 (unpublished), Sept. 3, 1946.
6. Camp, C. S.
Determination of Shape of Nappe and Coefficient of Discharge of a Vertical Sharp-Crested Weir, Circular in Plan, with Radially Inward Flow, Thesis, Univ. of Iowa, June 1937.
7. Cragoe, C. S.
Changes in the Viscosity of Liquids with Temperature, Pressure and Composition, Proc. World Petroleum Cong., London, Vol. 11, 1933, p. 529.
8. Creager and Justin.
Design of Solid Gravity Dams, Hydroelectric Handbook, 1927, p. 208, John Wiley and Sons.
9. Dillman, O.
Untersuchungen an Neberfallen, Mitteilungen des hydraulischen Instituts der T. H. München, No. 7, Oldenbourg, Munich, 1933.
10. Du Pont, R. B.
Determination of the Under Nappe over a Sharp-Crested Weir Circular in Plan with Radial Approach, Thesis, Case School of Applied Science, 1937.
11. East, L. R.
Spillway Discharge Calculations, Civ. Eng., Vol. 2, 1932, p. 34.

12. Ehrenberger, R.
Versuche über die Verteilung der Drücke an Wehrrücken infolge des abstürzenden Wassers (Experiments on the Distribution of Pressures on the Downstream Faces of Spillway Crests Caused by the Overfalling Water), Die Wasserwirtschaft, Heft 5, 1929.

13. Eisner F.
Ueberfallversuche in verschiedener Modellgrösse, Preussische Versuchsanstalt für Wasserbau und Schiffbau, Berlin, 1933.

14. Escande, L.
Etude theorique et experimentale sur la similitude des fluides incompressible pesants, Toulouse, 1929.

15. ————.
Recherches sur les barrages-deversoirs (Research on Spillway Dams), Annales de l'Energie, Vol. 12, Nos. 11 and 12, 1929. See also Bulletin de la Suisse Romande, Vol. 56, No. 17.

16. ————.
Determination pratique du profil optimum d'un barrage-diversoir. Trace des piles par les methodes aerodynamiques. Application à un ouvrage determine (Practical Determination of the Best Profile of a Spillway Dam. Outline of the Piers by Aerodynamic Methods. Application to a Definite Project), Science et Industrie, Vol. 17, 1933, pp. 430 and 467.

17. Fischer, A., and A. Vitols.
Beitrag zur Ermittlung des vakuumlosen Dammprofiles nach dem Verfahren von A. Vitols (Contribution to Determining Vacuumless Spillway Profiles by the Method of A. Vitols), Wasserkraft und Wasserwirtschaft, Vol. 32, 1936, p. 283.

18. Fischer, H.
Die Beseitungen von Schwingungen an ubervund unterstromten Wehren und die Schwingungen am unterstromten Wehr and ihrer Beseitungen (The Elimination of Vibrations in Overflow and Sluiceway Dams and the Vibrations of Sluiceway Dams and their Prevention), Mitt. Forschung-Anst. G. H. H.-Konzern, Berlin, Vol. 5, Nos. 4 and 5, 1937.

19. Gabran, O.
Die Zahigkeit des Wassers unter dem Einfluss des Gasgehaltes (The Viscosity of Water under the Influence of its Gas Content), Wasserkraft und Wasserwirtschaft, Vol. 32, 1937, p. 212.

20. Gibson, A. H.
Flow over Notches and Weirs, Hydraulics and Its Applications, 1930, pp. 147–176, D. Van Nostrand Co.

21. Golaz, M.
Considerations theoriques sur le mouvement plan des liquides naturels et leur application au calcul du debit d'un deversoir à crete arrondie (Theoretical Considerations on the Laminar Flow of Natural Liquids and Their Application to the Calculation of the Discharge of Spillways with Rounded Crests), Science et Industrie, Vol. 17, 1933, p. 295.

22. Hailer, Rudolf.
Fehlerquellen bei der Überfallmessung (Sources of Error in Weir Measurements), Mitteilungen des hydraulischen Instituts der Technischen Hochschule, München, Heft 3, 1929. See also K. C. Reynolds' translation.

23. Harris, Chas. W.
Pressure Reduction on the Face of Orifice Plates and Weirs, Eng. Exp. Sta. Bull. No. 35, Univ. of Washington, Seattle.

24. Hasumi, M.
Ueber der Verteilung der Drücke am Wehrrücken (The Distribution of Pressure on Spillways), Die Wasserwirtschaft, Vol. 22, No. 5, 1929.

25. Hedberg, J.
Flow on Steep Slopes, Civ. Eng., Vol. 7, 1937, p. 633.

26. Herz, J.
Beitrag zur Abflussberechnung von Streichwehen (Calculation of the Discharge of Overfall Weirs), Die Wasserkraft, Vol. 20, 1925, pp. 41, 59, and 99.

27. Hill, E. P.
The Velocity of Water Flowing Down a Steep Slope, Selected Papers, Inst. C. E., Paper No. 3520.

28. Hinds, J.
Overflow Spillways, Bur. of Recl. Tech. Memo. No. 5, (unpublished), Feb. 24, 1917.

29. ————.
Flow of Water Over an Ogee Weir, Bur. Recl. Tech. Memo. No. 26, (unpublished), Sept. 1921.

30. Keutner, C.
Herleitung eines neuen Berechnungsverfahrens fur den Abfluss an Wehrens aus der Geschwindigkeits-verteilung des Wassers ueber Wehrkrone (Derivation of a New Procedure of Calculating the Discharge of Weirs from the Velocity Distribution of the Flow over the Weir Crest), Die Bautechnik, Vol. 7, 1929, p. 575.

31. ————.
Entstehung und Wasserabfuhrungsvermogen Verschiedener Strahlformer an Scharfkantigen Wehren (Origin and Possible Forms of Various Nappes of Sharp-Crested Weirs), Die Bautechnik, Vol. 9, 1931, p. 714.

32. ————.
Abfluss Untersuchungen und Berechnungen fur Ueberfalle an Scharfkantigen Wehren (Investigation of the Discharge and Calculations for the Overfall of Sharp-Crested Weirs), Willhelm Ernst & Sohns, Berlin, 1931.

33 Kirschmer, O.
Untersuchung der Ueberfallkoeffizienten für einige Wehre mit gerundeter Krone (Investigation of the Coefficients of Weirs with Rounded Crests), Mitteilungen des hydraulischen Instituts der Technischen Hochschule München, No. 2, 1928, p. 1.

34. Lauck, A.
Der Uberfall über ein Wehr (The Overfall of a Dam,) Zeits. f. ang. Math. u. Mech., 1925, S. 1.

35. Lauffer, Harold.
Druck, Energie und Fliesszustand in Gerinen mit Grossen Gefalle (Pressure, Energy and Flow Conditions in Channels with High Gradients), Wasserkraft and Wasserwirtschaft, Vol. 30, No. 7, 1935, pp. 78–82. Translated by D. P. Barnes in Bur. of Recl. Tech. Memo. No. 527, July 6, 1936.

36. Lyman, R. R.
Measurement of the Flow of Streams by Approved Forms of Weirs with New Formulas and Diagrams: Details and Summaries of the Results of Experiments by Francis, Bazin, Fteley, and Stearns and at the Hydraulic Laboratories of Cornell University and the University of Utah. Trans. Am. Soc. C. E., Vol. 77, 1914, p. 1189.

37. Marchi, G. de
Ricerche Sperimentali Sulle Dighe Tracimanti (Experimental Research on Broadcrested Weirs), Annali dei Lavori Pubblici Rome, 1928, Fasc. 7°, p. 581.

38. Mattiola, G. D.
Sopra l'Influenza della Viscosita del Fluido nei Regimi Turbolenti (The Influence of Viscosity of Fluids on Turbulent Flow), Atti della Reale Accad. Delle Scienze di Torino, 1935, p. 220.

39. Meyer, Adolph F.
High-Velocity Discharge of Overfall Dams and Forms of Spillway Profile, Eng. News-Rec., Vol. 94, April 9, 1925.

40. Mueller, H.
Beitrag zur Erforschung der Schwingungserscheinungen an uberstromten Wehren (Contribution to the Investigation of Oscillation Phenomena at Overflow Weirs), Wasserkraft und Wasserwirtschaft, Vol. 32, 1937, p. 61.

41. Musterle, Th.
Abflussberchnungen bei Wehren mit breiter Krone mit Hilfe des Impulssatzes (Discharge Calculations on Broad-crested Weirs with the Help of the Momentum Formula), Die Wasserwirtschaft, Jahrg. 1930, Heft 21.

42. Nelidov, I. M.
Importance of Study of Flow on Steep Slopes, Civ. Eng., Vol. 8, 1938, p. 121.

43. Olt, N. Enache de la
Contribution à la Theorie de l'Ecoulement sur les Deversoirs (Contribution to the Theory of the Flow over Spillways), Thesis, Paris, 1908.

44. Pajer, G.
Beitrag zur Theorie des Uberfalles (Contribution to the Theory of Spillways), Wasserkraft und Wasserwirtschaft, Heft 14, Vol. 31, July 16, 1936.

45. Pandit.
Determination of Water Profiles over Weirs and Flumes, Indian Engineering, Vol. 100, 1936, p. 192.

46. Poncin, H.
Sur la determination des elements d'un ecoulement en deversoir (On the Determination of the Flow Elements for a Spillway), Science et Industrie, Vol. 17, 1933, p. 560.

47. Rehbock, T.
Die Ausbildung der Ueberfalle beim Abfluss uber Wehre nebst Beschreibung der Anlage zur Beobachtung von Ueberfallen im Flussbaulaborborium zu Kerksruhe (Types of Overfalls for the Discharge of Water over Dams with Description of the Apparatus for Observing such Flows in the Hydraulic Laboratory at Karlsruhe), Fredericona Publication in Honor of the 52nd Birthday of the Grand Duke Frederick II, Karlsruhe, 1909.

48. Reynolds, K. C. (Translator).
Sources of Error in Weir Measurements (From Transactions of the Hydraulic Institute of the Munich Technical University, Bull. No. 3). Translation published in 1935 by the Am. Soc. of Mech. Eng. See also reference 22.

49. Ricco, G. Di
Equazione di Forma di Uno Stramazzo Dedotta Dalla Sua Equazione di Portata (Equation of the Form of the Nappe deduced from the Equation of Discharge), L'Energia Elettrica, Vol. 13, No. 10, 1936, p. 569.
50. Rouse, Hunter.
Verteilung der Hydraulischen Energie Bei einem Lotrechten Absturz (Distribution of Hydraulic Energy in Vertical Overfalls), R. Oldenbourg, Munich and Berlin, 1933.
51. ————.
Discharge Characteristics of the Free Overfall, Civ. Eng., April 1936.
52. ————.
Spillway Design, Fluid Mechanics for Hydraulic Engineers, 1938, p. 316, McGraw-Hill Book Co.
53. Schoder and Dawson.
Flow over Weirs and Dams other than Sharp-Crested, Hydraulics, 1927, p. 163, McGraw-Hill Book Co.
54. Schwartz, A. I.
Flow of Water in Channels Curved in Vertical Plane to an Arc of a Circle (From Trans. Sci. Res. Inst. of Hydrotechnics, Leningrad, Vol. 16, 1935, p. 129). Translated from the Russian at Univ. of Calif. as W. P. A. Project, No. 58.
55. Thorsen, Leroy A.
Effect of Vacuum on a Free Nappe, Thesis, Univ. of Iowa, June 1946.
56. Warnock, J. E.
Experiments Aid in Design at Grand Coulee, Civ. Eng., Vol. 6, No. 11, p. 737, November 1936.
57. Winkel, R.
Betrachtung zur Abflusstheorie der Überfallwehre (Consideration on the Discharge Theory of Overfall Dams), Die Bautechnik, Vol. 6, 1928, p. 721.
58. ————.
Die Geschwindigkeits-verteilung im Strahle über einer Wehrkröne (The Velocity Distribution in the Nappe over the Crest of a Spillway), Die Bautechnik, Vol. 7, 1929, p. 438.
59. Various authors.
Weir and Overfall Dam Experiments, Munich Technical University. Information Bulletins 1–7.

62. Bibliography on Submerged Dams:

60. Board of Engineers.
Report of the Board of Engineers on Deep Waterways, Part 1, 1900, p. 291.
61. Cox, Glen Nelson.
The Submerged Weir as a Measuring Device, Univ. of Wisconsin Eng. Exp. Sta. Bull. No. 67, 1928, p. 48–75.
62. Dominguez, Fco. Jovier
Experimental Results of Submerged Flow over Drops, Weirs, and Broad-Crested Weirs, Curso de Hidraulica, 1935, p. 191–219, Nascimento Publishing House, Santiago, Chile.
63. Horton, R. E.
Weir Experiments, Coefficients and Formulae, Water Supply and Irrigation Paper No. 200, U. S. Geol. Surv., 1907.

64. International Waterways Commission.
Experimental Coefficients of Submerged Weirs, 1905 to 1913.

65. National Resources Committee.
Submerged Dams, Low Dams, 1938, p. 64.

66. Soucek, Edward.
Meter Measurements of Discharge, University Dam, Trans. Am. Soc. C. E., Vol. 109, 1944.

67. Vennard, John K., and Roy F. Weston.
Submergence Effect on Sharp-Crested Weirs, Eng. News-Rec., June 3, 1943.

68. Voorduin, W. L.
Hydraulic Formulas, Davis Handbook of Hydraulics, 1942, p. 23.

69. Woodburn, James A.
Tests of Broad-Crested Weirs, Trans. Am. Soc. C. E., Vol. 96, 1932, p. 387.

70. Yarnell, D. L.
Flow of Flood Water over Railway and Highway Embankments, Public Roads, Vol. 11, No. 2, 1930, p. 30.

LIST OF BULLETINS

The following list shows tentative titles of final reports on the Boulder Canyon project, now being prepared for publication. During the work on the compilation of final reports, it has been found desirable to combine certain subjects which had originally been planned as separate bulletins. Consequently a few of the tentative titles given in bulletins heretofore published do not appear in the following list.

The following list also includes titles and prices of the bulletins which have been published and which are now available for distribution. Appropriate announcements will be made in engineering periodicals as additional bulletins become available.

PART I—INTRODUCTORY

General History and Description of Project
Legal and Financial Problems

PART II—HYDROLOGY

Stream Flow, Project Operation, and Utilization of Water

PART III—PREPARATORY EXAMINATIONS

Geologic Investigations

PART IV—DESIGN AND CONSTRUCTION

General Features*	(paper, $1.50; cloth, $2.00)
Boulder Dam*	(paper, $1.50; cloth, $2.00)
Diversion, Outlet, and Spillway Structures*	(paper, $2.50; cloth, $3.00)
Concrete Manufacture, Handling, and Control*	(paper, $2.50; cloth, $3.00)
Penstocks and Outlet Pipes	
Hydraulic Valves and Gates	
Power Plant Structure and Handling Facilities	
Power Plant Generating Equipment	
Imperial Dam and Desilting Works	
All-American Canal and Canal Structures	

PART V—TECHNICAL INVESTIGATIONS

Trial Load Method of Analyzing Arch Dams*	(paper, $1.50; cloth, $2.00)
Slab Analogy Experiments*	(paper, $1.00; cloth, $1.50)
Model Tests of Boulder Dam*	(paper, $1.50; cloth, $2.00)
Stress Studies for Boulder Dam*	(paper, $1.50; cloth, $2.00)
Penstock Analysis and Stiffener Design*	(paper, $1.00; cloth, $1.50)
Model Tests of Arch and Cantilever Elements*	(paper, $1.00; cloth, $1.50)

*For sale at offices of the Bureau of Reclamation in Boulder City, Nevada; Denver, Colorado; and Washington, D. C.

PART VI—HYDRAULIC INVESTIGATIONS

Model Studies of Spillways*	(paper, \$1.00; cloth, \$1.50)
Model Studies of Penstocks and Outlet Works*	(paper, \$1.00; cloth, \$1.50)
Studies of Crests for Overfall Dams*	(paper, \$2.00; cloth, \$2.50)
Model Studies of Imperial Dam, Desilting Works and All-American Canal Structures	

PART VII—CEMENT AND CONCRETE INVESTIGATIONS

Thermal Properties of Concrete*	(paper, \$1.00; cloth, \$1.50)
Investigations of Portland Cements	
Cooling of Concrete Dams	
Mass Concrete Investigations	
Contraction Joint Grouting	

*For sale at offices of the Bureau of Reclamation in Boulder City, Nevada: Denver, Colorado; and Washington, D. C.

O